J. Nat. & Phy. Sci. Vol. 19 2005 No. 1-2

ISSN 097-3799

प्राकृतिक एवं भौतिकीय विज्ञान शोध पत्रिका

JOURNAL OF NATURAL & PHYSICAL SCIENCES

खण्ड 19 अंक 1,2005
Vol.19 No. 1, 2005

गुरुकुल कांगड़ी विश्वविद्यालय, हरिद्वार
Gurukula Kangri Vishwavidyalaya, Haridwar

प्राकृतिक एवं भौतकीय विज्ञान शोध पत्रिका

Journal of Natural & Physical Scienes

REFERENCES

R.P. Bhardwaj: Origin of LF - VHF Radiations in lightning Spectra, Ph. D. Thesis, Gurukul Kangri University, Haridwar, 1995 .

R.F. Griffiths and C.T. Phelps: A model of lighting initiation arising from positive coroma streamers development. J. Geophys. Res. 81 (1976) 3671.

P.P. Pathak: Positive corona streamers as a source of high frequency radiation, J. Geophys. Res. 99D (1994) 10,843.

P.P. Pathak, J. Rai & N.C. Varshneya: VLF radiation from lighting, J. Roy. Astron. Soc. 69 (1982)197.

P.P. Pathak and S. Haziraka: Effect of ground conductivility on VLF radiation from lightning, Indian J. Radio & Space Phys. 14 (1985) 122.

M. Rao: Corona current after the return strokes and the mission of ELF waves in a lightning flash to earth. Radio Sci. 2 (1967) 241.

M. Rao and H. Bhattacharya: Lateral corona currents from return stroke channel and the slow field change after the return stroke in a lightning discharge, J. Geophys. Res. 71 (1967) 2811.

J. Rai: On the origion of VHF atmospherics, J. Atmos. & Terr. Phys. 40 (1978) 475.

J. Rai, M. Rao and B.A.P. Tantry: Bremsstrahllung as a possible source of VHF emission from lightning, Nature 238 (1972) 59.

B.F.J. Schonland, D.J. Malan and H. Callens: Progressive lighting Pt2. Proc. Roy. Soc. London 152 (1935) 595.

B.F.J. Schonland: The lightning discharge, in Handbuch der physik, edited by S Flugger Springer-Verlag, New York, 1956, 576.

R. Thottappillil and V.A. Rakov: Calculation of electromegnetic fields : A review Paper presented at XVIII General Assembly of URSI, New Delhi, Nov. 23-29 (2005).

C.D. Weidman and E.P. Krider: The amplitude of lightning radiation fields in the interval from 1 to 20 MHz. Radio Sci. 21 (1986) 964.

प्राकृतिक एवं भौतिकीय विज्ञान शोध पत्रिका

खण्ड 19 अंक (2) 2005

(1) प्रकाशन स्थान : गुरुकुल कांगड़ी विश्वविद्यालय, हरिद्वार

(2) प्रकाशन की अवधि : वर्ष में एक खण्ड, अधिकतम दो अंक

(3) मुद्रक का नाम : चन्द्र किरण सैनी

राष्ट्रीयता : भारतीय

व पता : किरण ऑफसेट प्रिंटिंग प्रेस
निकट गुरुकुल कांगड़ी फार्मेसी
कनखल, हरिद्वार – 249404 फोन नं0 245975

(4) प्रकाशक का नाम : प्रो0 आर. डी. शर्मा

राष्ट्रीयता : भारतीय

व पता : कुलसचिव,
गुरुकुल कांगड़ी विश्वविद्यालय
हरिद्वार – 249409

(5) प्रधान सम्पादक : प्रो0 ए. के. चोपड़ा

राष्ट्रीयता : भारतीय

व पता : जन्तु एवं पर्यावरण विज्ञान विभाग
गुरुकुल कांगड़ी विश्वविद्यालय
हरिद्वार – 249409

(6) प्रबन्ध सम्पादक : प्रो0 पी0 पी0 पाठक

राष्ट्रीयता : भारतीय

व पता : भौतिकी विभाग
गुरुकुल कांगड़ी विश्वविद्यालय
हरिद्वार – 249409

(7) स्वामित्व : गुरुकुल कांगड़ी विश्वविद्यालय
हरिद्वार – 249409

मैं प्रो0 आर. डी. शर्मा, कुलसचिव, गुरुकुल कांगड़ी विश्वविद्यालय, हरिद्वार, घोषित करता हूँ कि उपरिलिखित तथ्य मेरी जानकारी के अनुसार सही हैं।

हस्ताक्षर
प्रो0 आर. डी. शर्मा
कुलसचिव

Journal of Natural & Physical Sciences, Vol. 19 (1) (2005)

CONTENTS

Printed at : Kiran Printing Press, Kankhal-Hardwar, Phone: +91-1334-245975

INSTRUCTIONS FOR AUTHORS

The manuscript should be typed in double spacing on both sides of A4 size white paper leaving wide margins. The manuscripts should be arranged as follows: The first page should contain (in following order) Title, Abstract, Key-words & Phrases, Classification number, Author's names and Address. The back of this page should remain blank. Next page should start with usual headings of Introduction, Material and mathodes/Theoretical formulation, Results, Discussion, Acknowledgement (if any) and References etc. In the text the sentences like, "in prevous paper (ref) the authors, should not be used. References in the text are to be quoted by number in square brakets and are to be arranged alphabatically at the end. Thus the first reference appearing in the text would not necessarily be no. 1. They are to be written as follows:

S.A Naimpally and B.D. Warrack : Proximity Space, Cambridge Univ. Press, U.K., 1970 (for books)

B.E. Rhoades : A comparison of various definitions of contractive mappings, Trans. Amer. Math. Soc. 226(1977), 267-290 (For articles in journals, title of the articles are not essential in long review/survey articles.)

Reference should not be made to unpublished work like Ph. D thesis or papers communicated.

REPRINTS : Twenty five free reprints will be supplied. Additional reprints may be supplied at printer's cost.

EXCHANGE OF JOURNALS : Journals in exchange should be sent to the Chief Editor or Librarian, Gurukula Kangri Vishwavidyalaya, Hardwar 246404 INDIA

SUBSCRIPTION : Each volume of the journal is currently priced at Indian Rs. 500 in SAARC countries and US $ 100 elsewhere.

Journal of Natural & Physical Sciences, Vol. 19 (2) (2005)

CONTENTS

MATHEMATICS

PHYSICS

Printed at : Kiran Offset Printing Press, Kankhal, Haridwar, Phone : 01334-245975

INSTRUCTIONS FOR AUTHORS

The manuscript should be typed in double spacing on **both** sides of A4 size white paper leaving wide margins. The manuscripts should be arranged as follows: The first page should contain (in following order) Title, Abstract, Key-words & Phrases, Classification number, Author's names and Address. **The back of this** page **should remain** blank. Next page should start with usual headings of Introduction, Material and mathodes/Theoretical formulation, Results, Discussion, Acknowledgement (if any) and References etc. In the text the sentences like, "in previous paper [ref] the authors.....", should not be used as they discluse the identify of authors. References in the text are to be quoted by number in square brakets and are to be arranged alphabatically by authors' surname at the end. Thus the first reference appearing in the text would not necessarily be no. 1. They are to be written as follows:

S.A Naimpally and B.D. Warrack : Proximity Space, Cambridge Univ. Press, U.K., 1970 (for books)

B.E. Rhoades : A comparison of various definitions of contractive mappings, Trans. Amer. Math. Soc. 226(1977), 267-290 (For articles in journals, title of the articles are not essential in long review/survey articles.)

Reference should not be made to unpublished work like Ph. D. thesis or papers communicated.

REPRINTS : Twenty five free reprints will be supplied. Additional reprints may be supplied at printer's cost.

EXCHANGE OF JOURNALS : Journals in exchange should be sent to the Chief Editor or Librarian, Gurukula Kangri Vishwavidyalaya, Hardwar 246404 INDIA

SUBSCRIPTION : Each volume of the journal is currently priced at Indian Rs. 500 in SAARC countries and US $ 100 elsewhere.

Journal of Natural & Physical Sciences, Vol. 19 (1) (2005) 1-14

AN INVENTORY MODEL OF DETERIORATING ITEMS WITH NON - LINEAR FRACTIONAL OBJECTIVE

K. Das*, T. K. Roy, M. Maiti***

(Received 03. 03. 2003, Revised 30.07.2004)

ABSTRACT

A deterministic inventory model for deteriorating items over the finite time horizon is considered. Here, the demand is a function of time, selling price and the frequency of advertisement. Shortages are allowed and fully backlogged. Profitability i.e. the ratio of the net profit to the total cost is maximized under the restricted waste cost using non-linear fractional programming (NLFrP) technique. Model is illustrated with a numerical example.

Keywords: Non-linear Fractional programming, Profitability, Finite time horizon.

INTRODUCTION

In most of the classical deterministic inventory models, demand is considered to be constant, independent of time *t* and selling price *s*. However, in the case of certain types of inventory, particularly consumable goods (viz., foodgrains, oilseeds, etc.), the demand rate decreases with the increase of selling price and increases alongwith time. Cohen [7] first developed the joint pricing and ordering policy. Mukherjee [21], Das and Maiti [9] etc. developed their models with either price or both time and price dependent demand. Several researches (i.e. Wagner and within [32], Silver and Meal [26], Donaldson [11], Teng *et al* [30] and others) developed and solved the inventory models with time dependent demand.

In most of the earlier inventory models, life time of an item is assumed to be infinite while it is in storage. But, in reality, many physical goods deteriorate due to dryness, spoilage, vaporisation etc. and are damaged due to hoarding longer than their normal storage period. The deterioration also depends on preserving facilities and environmental conditions of warehouse/storage. So, due to the ill preservation conditions of some commonly used physical goods like paddy, wheat or any other type of foodgrains, vegetables, fruits, drugs, pharmaceuticals and radioactive substances etc. a certain protion of these goods are either damaged or decayed due to dryness, spoilage, vapourisation etc. and are not in a condition to satisfy the future demand of customers as fresh/good items. As a result, the loss due to this natural phenomenon (i.e. the deterioration effect) can't be ignored in the analysis of an inventory

*Department of Applied Mathematics with Oceanology and Computer Programming, Vidyasagar University, Midnapore- 721 102, India.
**Department of Mathematics, B.E. College (Deemed University), Howrah, India.

control system. Deterioration for such items is continuous and constant or time-dependent and/or dependent on the on-hand inventory. A number of research papers have already been published on the above type of items by Dave and Patel [10], Kang and Kim [19], Sachan [24], Bhunia and Maiti [3], Hariga et al. [16, 17, 18], Giri et al. [12,13] and others.

In the present age of advertisement, sale of a product upon the promotion of the product in public life. This may be done in the form of advertisement in modern electronic/ mass media or by decorative and attractive display in the showroom. According to Levin et al, [20]," it is a common belief that large piles of goods displayed in a supermarket will lead the customers to buy more" Recent marketing research also recognizes this relationship. Now-a-days, even in third world countries, to increase the sale, fashionable goods are glamorously displayed with the help of modern light and electrical arrangements. For this reason, several authors-Gupta and Vrat [14], Baker and Urban [1,2], Urban [31] and others presented some inventory models with stock-dependent demand.

Normally, duration of seasonal products is constant and these are available in the market every year for a fixed interval of time. Hence the time period for the business of seasonal goods is finite. Several researchers (Hariga and Benkherouf [15], Bhunia and Maiti [4], Chang and Dye [5] etc. have developed this type of inventory models with fixed time horizon.

Normally, in the case of decision making problems in inventory control system, average profit (cost) expression is maximized (minimized). This does not yield the relative picture about the cost involved and the profit made. For this reason, now-a-days, in the fields like transportation, resource allocation, production etc., profitability i.e. the ratio of total profit to the total cost over a fixed time period is maximized. It gives the maximum possible profit against a certain amount of expenditure over a fixed time period. It also leads to some kind of efficiency measure of the system and gives more insight into the system. This class of optimization method is termed as fractional programming. The ratio of the functions reveals the problem as a non-linear programming problem, even if the numerator and the denominator are linear. The first idea of fractional programming was given by J. Von Neumann [22, 23], where, in mathematical economics, an economic equilibrium model relating to the maximal growth rate of an expanding economy was introduced. Linear fractional programming was introduced by Charnes and Cooper [6]. There is a large number of research articles on fractional programming, which is listed in the bibliographies by Schaible [25] and Stancu-Minasian [27,28,29]. Till now, none has attempted to have such an analysis in inventory control system.

In this paper, a deterministic inventory model for deteriorating items over the finite time horizon is developed. Here, the demand is increasing linearly with time and decreasing linearly

with selling price. Also, the demand is influenced by the frequency of advertisement. Shortages are allowed and fully backlogged. Firstly, profitability i.e. the ratio of total profit to the total cost over the same time horizon is maximized under the restricted waste cost using fractional programming technique. Secondly, total profit is maximized as a single objective under the same constraint using a gradient based non-linear programming method and the corresponding profitability is also calculated for the same optimum decision values. Models are illustrated with numerical examples and the profitability obtained from two methods are compared. Lastly, in absence of shortages, profitability obtained from two methods are calculated and compared.

NOTATIONS AND ASSUMPTIONS

Deterministic inventory model for deteriorating item over the finite time horizon is developed under the following notations and assumptions.

c = cost per unit item,
h = holding cost per unit item per unit time,
g = shortage cost per unit item per unit time,
s = selling price per unit item (decision variable),
u = replenishment cost per cycle,
N = Frequency of advertisement per cycle,
θ = constant rate of deterioration $(0 < \theta < 1)$
H = prescribed time-horizon
m = total number of replenishment to be made during the prescribed time horizon H (an integer decision variable)
T = equal length of each time cycle, i.e., T = H/m
k = proportion of time in each time cycle T (i.e. shortage time index (STI) of the cycle) during which shortage occurs i.e., k be a real number in (0,1) (decision variable)
$D(t,s,N)$ = demand per unit time is a function of time, selling price and directly related to frequency of advertisement,
Wc = Maximum allowable waste cost

For j-th cycle, $j = 1,2,.....m$.

Q_j = maximum inventory level,
S_j = maximum shortage level,
$q_j(t)$ = inventory level at any time t,
$PF(s,k,m)$ = total profit over the time period
$TC(s,k,m)$ = total cost over the time period.

The basic assumptions about the model are:

(i) replenishment is instantaneous without lead time,

(ii) shortages are allowed and fully backlogged.

(iii) demand $D(t,s,N)$ per unit time is a function of time, selling price and directly related to frequency of advertisement in the form of.

$$D(t,s,N) = N^{\delta}(\alpha + \beta t - \gamma s)$$

Where, $\alpha, \beta, \gamma, \delta$ are non-negative number and N is a predetermined positive integer

(iv) advertisement cost is a fraction μ of the total selling price per cycle ($0 < \mu < 1$).

MODEL FORMULATION WITH SHORTAGES

In this inventory policy, shortages are met at the end of each cycle (cf. figure-1). In each j-th cycle, $[(j-1)T, jT]$, $(j = 1,2,\ldots\ldots, m)$ the procurement of $(Q_j + S_{j-1})$ (with $S_0 = 0$) units at $t = (j-1)T$ first satisfies the shortages (i.e. S_{j-1} units) of previous cycle and then the rest of the the procurement is kept in store where it undergoes the deterioration and the good units meet the demand during $[(j-1)T, (k+j-1)T]$. The inventory again falls back to zero at $t = (k+j-1)T$. At $t = H$, the amount is procured just to meet the shortage only. Thus, in the interval $[0, H]$, $(m+1)$ reorder points are at $t = (j-1)T$ and at $t = H$ and m shortage points are at $t = (k+j-1)T$, $(j = 1,2,\ldots\ldots,m)$.

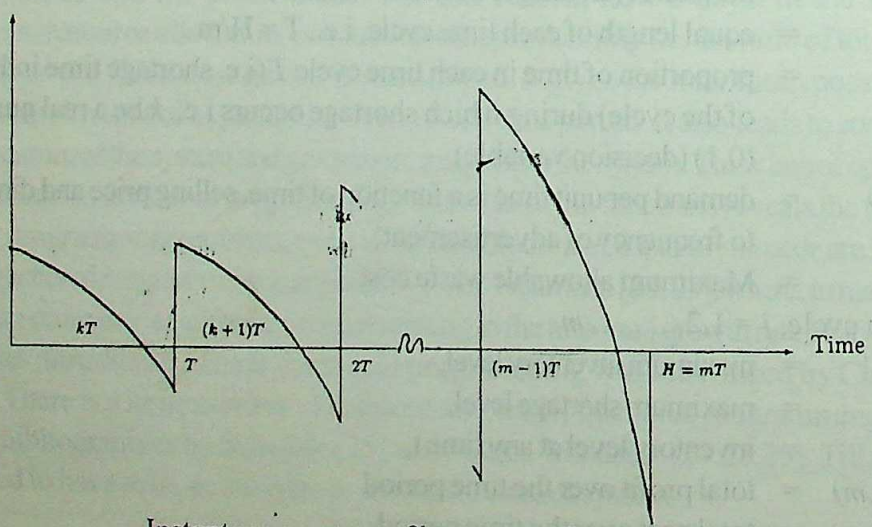

Instantaneous state of inventory of the model

Figure - 1

Therefore, if $q_j(t)$ be the inventory level at any time t, the differential equations describing the above system in the j - th cycle ($j = 1,2,\ldots\ldots, m$) are,

$$\frac{dq_j(t)}{dt} = \begin{cases} -D(t,s,N) - \theta qj(t), & (j-1)T \le t \le (k+j-1)T \\ -D(t,s,N), & (k+j-1)T \le t \le jT \end{cases} \quad (1)$$

with the boundary conditions,

$q_j(t) = 0$, at $t = (k + j - 1)\ T$ for $j = 1, \ldots\ldots, m$.

The solution of the equations in (1) is

$$q_j(t) = \begin{cases} \int_t^{(k+j-1)T} e^{\theta(x-t)} D(x,s,N)dx, & (j-1)T \le t \le (k+j-1)T \\ -\int_{(k+j-1)T}^{t} D(x,s,N)dx, & (k+j-1)T \le t \le jT \end{cases} \quad (2)$$

If Q_j be the inventory level at $t = (j\text{-}1)\ T$ and S_j be the shortage level at time $t = jT$, ($j = 1,\ldots\ldots m$), then

$$Q_j = \frac{N^\delta}{0} - \left[\left\{\alpha - \frac{\beta}{\theta} - \gamma s + \beta T(j-1)\right\}\{exp(\theta kT) - 1\} + \beta T exp(\theta kT)\right]$$

and $S_j = N^\delta T(1-k)\left\{\alpha - \frac{\beta}{\theta} - \gamma s + \frac{\beta T}{2}(k + 2j - 1\right\}$

In the interval $[(j - 1)\ T, jT]$, the holding cost is hV_j, shortage cost is gG_j and the number of deteriorated units is θV_j, where

$$V_j = \int_{(j-1)T}^{(k+j-1)T} q_j(t)dt = \frac{Q_j}{\theta} - \frac{N^\delta}{\theta^2} kT\left\{\alpha - \frac{\beta}{\theta} - \gamma s + \frac{1}{2}\beta T(k + 2j - 1)\right\}$$

$$G_j = \int_{(k+j-1)T}^{jT} q_j(t)dt = \frac{N^\delta}{2\theta}(1-k)^2 T^2\left\{\alpha - \frac{\beta}{\theta} - \gamma s + \frac{1}{3}\beta T(2k + 3j - 2)\right\}$$

Also in the j-th interval, the advertisement cost is $\mu s\ (Q_j + S_j - \theta V_j)$.

Therefore, if $PF(s, k, m)$ and $TC(s,k,m)$ be the total profit and the total cost over the time period $(0,H)$. Then

$$PF(s,k,m) = \{(1-\mu)\, s-c\}\,(Q+S) - \{h-(1-\mu)\,\theta\, s\}\,V - gG - mu \tag{3}$$

$$TC(s,k,m) = (\mu s + c)\,(Q+S) + (h-\theta\mu s)\,V + gG + mu \tag{4}$$

Where

$$Q = \frac{mN^{\delta}}{\theta}\left[\left\{\alpha - \frac{\beta}{\theta} - \gamma s + \frac{\beta H}{2m}(m-1)\right\}\left\{exp\left(\frac{\theta kH}{m}\right)-1\right\} + \frac{\beta Hk}{m}exp\left(\frac{\theta kH}{m}\right)\right] \tag{5}$$

$$S = \frac{m}{\theta}N^{\delta}H(1-k)\left\{\alpha - \frac{\beta}{\theta} - \gamma s + \frac{\beta H}{2m}(k+m)\right\} \tag{6}$$

$$V = \frac{mN^{\delta}}{\theta}\left[\left\{\alpha - \frac{\beta}{\theta} - \gamma s + \frac{\beta H}{2m}(m-1)\right\}\left\{exp\left(\frac{\theta kh}{m}\right) - \frac{\theta kH}{m} - 1\right\} - \frac{\theta k^2H^2}{2m^2}\right] \tag{7}$$

$$G = \frac{N^{\delta}}{2m}(1-k)^2H^2\left\{\alpha - \frac{\beta}{\theta} - \gamma s + \frac{\beta H}{6m}(4k+3m-1)\right\} \tag{8}$$

Here, $Q = \sum_{j=1}^{m} Q_j$ and similarly for S, V, G.

MATHEMATICAL ANALYSIS FOR FRACTIONAL PROGRAMMING

The non-linear fractional programming problem is stated as:

$$Max\ f(X) = \frac{NU(X)}{DE(X)} \tag{9}$$

subject to

$$gj(X) \le 0, \quad (j = 1,2,\ldots\ldots, l)$$

$$X \geq 0, X = (x_1, x_2, \ldots\ldots\ldots, x_n)^T$$

where, for real X, $DE(X) > 0$ and $NU(X)$ are non-linear functions, *If* $NU(X)$ is concave on $\Delta = \{X : g_j(X) \leq 0, X \geq 0\}$, with $NU(\xi) \geq 0$ for some $\xi \in \Delta$ and $DE(X) > 0$ is convex on Δ then the problem in (9) is known as concave-convex fractional programming problem.

Using the Schaible [25] transformation

$$Xy = R, \; y = \frac{1}{DE(X)}$$

and following Craven [8], problem (9) can be replaced as follows:

$$\text{Max } y\,NU\left(\frac{R}{y}\right) \tag{10}$$

subject to

$$yg_j\left(\frac{R}{y}\right) \leq 0, \quad (j = 1,2,\ldots\ldots l)$$

$$yDE\left(\frac{R}{y}\right) \leq 1,$$

$$y > 0, R = (r_1, r_2, \ldots\ldots, r_n)^T \geq 0.$$

Optimum values of the decision variable X^* of (9) can be obtained from the optimum values R^* and y^* of (10).

Following Craven [8], let, E be a convex set in $\Re^n$. If $NU(X)$ (≥ 0) be concave, differentiable and $DE(X)$ (>0) be convex, differentiable from E to $\Re$ then $f(X)$ is a pseudoconcave function. Again, if $f(X)$: $E \rightarrow \Re$ be a pseudoconcave function, then any local maximum X^* of $f(X)$ on E is a global maximum.

NLFrP AND NLP FORMULATION

NLFrP formulation

If $PR(s,k,m)$ be the profitability i.e. the ratio of total profit to the total cost and $WC(s,k,m)$ be the waste cost over the same time period, then the problem is to maximize

profitability subject to the restricted waste cost using fractional programming technique, i.e.

$$\text{Max } PR(s,k,m) \tag{11}$$

subject to

$$WC(s,k,m) \leq Wc,$$

where

$$PR(s,k,m) = \frac{\{(1-\mu)s - c\}(Q+S) - \{h - \mu\theta s\}V - gG - mu}{(\mu s - c)(Q+S) + (h - \theta\mu s)V + gG + mu} \tag{12}$$

$$WC(s,k,m) = \frac{cmN^{\delta}}{\theta}\left[\left\{\alpha - \frac{\beta}{\theta} - \gamma s + \frac{\beta H}{2m}(m-1)\right\}\right.$$

$$\left.\left\{exp\left(\frac{\theta kH}{m}\right) - \frac{\theta kH}{m} - 1\right\} - \frac{\theta k^2 H^2}{2m^2}\right] \tag{13}$$

m is a positive integer and $k \in (0,1)$

Using Schaible transformation as,

$$\left.\begin{aligned} ys &= x_1, \\ yk &= x_2 \\ y &= \frac{1}{(\mu s - c)(Q+S) + (h - \theta\mu s)V + gG + mu} \end{aligned}\right\} \tag{14}$$

problem (11) is transformed as follows:

$$\text{Max } TPR(x_1, x_2, y, m) \tag{15}$$

subject to

$$\frac{cmN^{\delta}}{\theta}\left[\left\{\alpha - \frac{\beta}{\theta} - \frac{\gamma x_1}{y} + \frac{\beta H}{2m}(m-1)\right\}\left\{exp\left(\frac{\theta H x_2}{my}\right) - \frac{\theta H x_2}{my} - 1\right\} - \frac{\theta x_2^2 H^2}{2m^2 y^2}\right] \leq Wc$$

$$y\left[\left\{\mu\frac{x_1}{y}+c\right\}(Q_T+S_T)+\left(h-\theta\mu\frac{x_1}{y}\right)V_T+gG_T+m\mu\right]\le 1$$

where,

TPR, (x_1, x_2, y, m)

$$= y\left[\left\{(1-\mu)\frac{x_1}{y}-c\right\}(Q_T+S_T)-\left(h-(1-\mu)\frac{x_1}{y}\right)V_T-gG_T-m\mu\right]$$

Q_T, S_T, V_T, G_T are obtained from (5), (6), (7) and (8) respectively, replacing s by x_1/y and k by x_2/y.

NLP FORMULATION

In this problem, total profit is directly maximized subject to the sameconstraint as in (11), i.e.

$$\text{Max} \quad PF(s, k, m) \tag{16}$$

Subject to

$$\frac{cmN^{\delta}}{\theta}\left[\left\{\alpha-\frac{\beta}{\theta}-\gamma s+\frac{\beta H}{2m}(m-1)\right\}\left\{\exp\left(\frac{\theta kH}{m}\right)-\frac{\theta kH}{m}-1\right\}-\frac{\theta k^2H^2}{2m^2}\right]\le W_e$$

where m is a positive integer and $k \in (0,1)$.

Above two mixed integer non-linear optimization problems in (15) and (16) are solved by the computer optimization package, LINGO.

Once the optimum solutions are obtained, the optimum profitability for NLFrP model is directly obtained whereas for NLP formulation, optimum probability is calculated from the expression $PF(s^*,k^*,m^*) / TC(s^*,k^*,m^*)$, where '*' indicates the optimum values of the corresponding variables.

MODEL WITHOUT SHORTAGES

So far, results have been derived allowing the backlogged shortages. If k is assumed to be 1 (one) in the above expressions the shortage point coincides with the reorder point i.e. stock is exhausted just at time, $t = jT$, $(j=1,2,.....m)$. Hence, the results for the model without shortages are easily obtained just putting k=1 in the derived expressions of model with shortages.

NUMERICAL RESULTS

To point out the advantages of NLFr formulation over the NLP formulation of an inventory model, the results of the models with and without shortage are presented for some data. To illustrate the above model, the following parametric values are considered.

$\alpha = 80$, $\beta = 0.50$, $\gamma = 2.50$, $\mu = 0.05$, $\theta = 0.02$, $c = \$10$, $h = \$0.80$, $g = \$1.75$, $u = \$70$, $Wc = \$60$,, $H = 18$ *hours*, $N = 2$, $\delta = 0.50$.

The optimum values, with shortage and without shortage obtained from two different method are shown in Table - 1 and Table - 2 respectively.

Table - 1

Optimum values for two methods with shortage

Methods	Profitability	m	k	s (in \$)	Q	S	profit (in \$)	waste
NLFrP	1.09627	4	0.62978	30.03	128.2853	80.6745	3224.34	36.76
NLP	0.76362	8	0.61597	22.29	433.6566	270.4731	6737.80	60.00

Table - 2

Optimum values for two mthods without shortage

Methods	Profitability	m	s (in \$)	Q	Profit (in \$)	Waste Cost (in \$)
NLFrP	0.98254	7	29.72	231.4993	3321.03	60.00
NLP	0.66751	20	22.87	667.3322	9069.45	60.00

DISCUSSION

From both Tables -1 and - 2, it is established that non-linear fractional programming technique gives better profitability than the non-linear programming method. Though, in both cases, NLP method yields more profit than that of fractional programming method, it involves more investment and incurs more waste cost on the material. This may not be allowed in the case of very costly and / or scarcely available materials. On the other hand, fractional

programming method presents the better profitability with less investment and obviously it is more acceptable to the retailers. Only for this reason, fractional programming technique is very useful to the decision makers (DMs).

Moreover, comparing Tables - 1 and -2, it is concluded that the DMs or retailers should allow fully backlogged shortages in the inventory system as both fractional programming and non-linear programming methods yields better profitability for the system with shortages than the system without shortages. Of course, here it is assumed that loss of good-will not affect the business.

CONCLUSION

In this paper, a realistic inventory model has been considered and the methodology of deriving highest profitability has been established. Normally, demand of consumable seasonal products like rice, potato, etc. increases with time. In the case of rice, its price becomes lowest just when the farmers harvests their products from the fields. But, in the developing countries like India, Bangladesh, etc., there are a lot of marginal farmers who start buying the foodgrains more in amount as the time passes. Hence, the demand of rice increases with time. Again, due to poor yields of a particular year of some other reasons like artificial crisis etc., if the price of rice is more i.e. beyond the reach of the common people, then the said marginal farmers try to have a substitute (wheat, maize, etc.) for rice fully or partially. Therefore, in this case, demand decreases as price increases. It is well known fact that rice,etc. get dried up with time. Moreover, in the age of information technology, the sale of each item depends upon the advertisement in the different media electronic or non electronic. Hence, a realistic inventory model has been considered taking the items to be deteriorating and its demand to be price and time dependent.

For the first time, fractional programming has been successfully applied to an inventory control problem. This methodology is very important as it reveals to the decision maker the highest possible profitability to be achieved in a particular system with/without constraints. Though, the NLFrP method has been applied to the inventory model with fixed time horizon, deterioration and variable demand in crisp environment, it can be easily extended to the other inventory models with price discount, inflation, etc. formulated in different environments like fuzzy, stochastic, fuzzy-stochastic, etc.

REFRENCES

(1) R.C. Baker and T. L. Urban: A dependent deterministic inventory system with an inventory level-dependent demand rate, Journal of Operational Research Society, 39 (1988), 1823-1831.

(2) R.C. Baker and T.L. Urban : A deterministic inventory system with an inentory-level-dependent demand rate, Journal of Operational Research Society, 40 (1989), 75-81.

(3) A.K. Bhunia and M. Maiti: A Two Warehouse Inventory Model for a Linear Trend in Demand, OPSEARCH, 31 (1994), 318-329.

(4) A.K. Bhunia and M. Maiti : A deterministic Inventory Replenishment Problem for Deteriorating Item with Time-Dependent Demand and Shortages for the finite Time Horizon, OPESEARCH, 34(1997), 51-61.

(5) H. J. Chang and C.Y. Dye: An EOQ model for deteriorating items with time varying demand and partial backlogging, Journal of Operational Research Society, 50(1999), 1176-1182.

(6) A.Charnes and W. W. Cooper: Programming with linear fractional functions, Naval Research Logistics Quarterly, 9 (1962), 181-186.

(7) M.A. Cohen: Joint pricing and ordering policy for exponentially decaying inventory with known demand, Naval Research Logistic Quarterly, 24 (1977), 257-268.

(8) B.D. Craven: Fractional Programming, Heldermann Verlag, Berlin 1988.

(9) K. Das, A. K. Bhunia and M. Maiti: An inventory model for deteriorating items with shortages and selling-price-dependent demand, IAPQR Transactions, 24 (1999), 55-65.

(10) U.Dave and L.K. Patel: ($T.S_i$) policy inventory model for deteriorating items with time proportional demand, journal of Operational Research Society, 32 (1981), 137-142.

(11) W.A. Donaldson: Inventory replenishment policy for a linear trend in demand - an analytical solution, Operational Research Quarterly, 28 (1977), 663-670.

(12) B.C. Giri, A. Goswami and K.S. Chaudhuri: An EOQ Model for Deteriorating Items with Time Varying Demand and Costs, Journal of Operational Research Society, 47 (1996), 1398-1405.

(13) B.C. Giri, T. Chakrabarty and K. S. Chaudhuri: A Note on a Lot Sizinig Heuristic for Deteriorating Items with Time-Varying Demands and Shortages, Computers & Operations Research, 27(2000), 495-505.

(14) R. Gupta and P. Vrat: An EOQ model for stock dependent consumtion rate, OPSEARCH, 23 (1986), 19-24.

(15) M.A. Hariga and L. Benkherouf: Optimal and heuristic inventory replenishment models for deteriorating items with exponential time-varying demand, European Journal of Operational Research, 79 (1994), 123-137.

(16) M. Hariga: An EOQ model for deteriorating items with shortages an time-varying demand, Journal of Operational Research Society, 46 (1995), 398-404.

(17) M. Hariga: Optimal EOQ Models for Deteriorating items with Time-Varying demand, Journal of Operational Research Society, 47 (1996), 1228-1246.

(18) M. Hariga and A. Al-Alyan: A lot Sizing Heuristic for Deteriorating Items with Shortages in Growing and Declining Markets, Computers & Operations Research, 24 (1997), 1075-1083.

(19) S. Kang and A. Kim: A study on the price and production level of the deteriorating inventory system, International Journal of Production Research, 21 (1983), 899-908.

(20) R.I. Levin, C.P. Mclaughlin, R.P. Lamone and J.F. Kottas: Production/Operations management: contemporary policy for managing operating systems, McGraw-Hill, New York, 1972, 373.

(21) S.P. Mukherjee: Optimum ordering interval for time varying decay rate of inventory, (OPESEARCH), 24 (1987), 1924.

(22) Von J. Neumamm: Ueber ein oknomischer Gleichgewichtssystem undeine verallgemeinerung des Brouwerschen Fixpunktsatzes, Ergebnisse eines Mathematisehen Kolloquiums, Hrsq. V.K. Menger Leirig-Wien, Heft, 8 (1937), 73-83.

(23) Von J. Neumann: A model of general economic equlibrium, Review of Economic Studies, 13 (1945), 1-9.

(24) R.S. Sachan: (T,Si) Inventory policy model for deteriorating items with time proportional demand, Journal of Operational Research Society, 35 (1991), 1013-1019.

(25) S. Schaible: Bibliography in fractional programming, Zeitschrift for Operational Research, 26 (1982), 211-241.

(26) E.A. Silver and H.C. Meal: A huristic for selecting lot size quantities for the case of a deterministic time varying demand rate and discrete opportunities for replenishment, Production Inventory Management, 14 (1973), 64-74.

(27) I. M. Stancu-Minasian: A second Bibliography of fractional programming 1960-1976, Pure and Applied Mathematical Sciences, 13 (1981), 35-69.

(28) I.M. Stancu-Minasian: A second Bibliography of fractional programming 1977-1981, Pure and Applied Mathematical Sciences, 17 (1981), 35-69.

(29) I. M. Stancu-Minasian: A third Bibliography of fractional programming 1977-1985, Pure and Applied Mathematical Sciences, 22 (1981), 109-122.

(30) J.T. Teng, M.S. Chern and H.L. Yang: An Optimal Recursive Method for various Inventory Replenishment Models with Increasing Demand and Shortages, Naval Research Logistics, 44 (1997), 791-806.

(31) T. L. Urban: Inventory models with demand rate dependent on stock and shortage levels, International Journal of Production Economics, 22 (1995), 85-93.

(32) H. M. Wagner and T. M. Within: Dynamic version of the economic lost size model, Management Science, 5 (1958), 89-96.

Journal of Natural & Physical Sciences, Vol. 19 (1) (2005) 15-18

A NOTE ON TESTS FOR DIVISIBILITY

V. P. PANDE*

(Received 10.11.2004)

In the present paper we obtain general tests for divisibility of numbers as well as the generalization of the recent result due to Pant [2].

INTRODUCTION

Finding special criteria under which a given integer is divisible by another integer has been of abiding interest to the number theorists and decomposition of large numbers in canonical forms has assumed perennial importance. The related problem is that of finding the prime factors of numbers and thus the need arises for the tests for divisibility. Some tests of divisibility by particular numbers are available e.g. those by the integers 2^h, 3, 5, 7, 9, 11, 13, 37 and 101 are known [1, 3]. However, general tests for divisibility are not available. In a recent work, Pant [2] has obtained some tests of divisibility. The theorem of Pant [2] is the following:

Theorem 1.1: If $a, b, p, q,$ are non-negative integers and p, q are relatively prime, then

$$(10p+q)\big|(10a+b) \Leftrightarrow (10p+q)\big|(qa-pb)$$

where the notation $x|y$ is used to show that the integer x divides the integer y.

GENERALIZATION

We now obtain the generalization of the above result by considering the dividend and the divisor in various forms. We do this by considering general representation of numbers in place of decimal representaion.

Theorem 2.1: If a, b, p, q, N are non-negative integers and p, q are relatively prime, then

$$(Np+q)\big|(Na+b) \Leftrightarrow (Np+q)\big|(qa-pb)$$

Proof. Let $(Np+q)\big|(Na+pb)$. Then $Na+b=k(Np+q)$ for some integer k. This means $qa - pb = (a - pk)(Np + q)$ that is $Np + q \mid qa - pb$ since $a - pk$ is an integer.

Conversely, let $Np + q \mid qa - pb$. Then there exists some integer k such that $qa - pb = k(Np + q)$. Then $q(a - k) = p(Nk + b)$. This implies that p/q (a - k), that is $p| a - k$ since p, q are relatively prime. Moreover, $Na + b = (a - k)(Np + q)/p$. This means that $Np + q \mid Na + b$ since

*Department of Mathematics, Kumaon University S.S.J. Campus, Almora-263601(U.A.)

$(a - k) / p$ is an integer. This proves the theorem.

We now generalize the above theorem to make it applicable when the dividend is considered in the form $N^2a + Nb + c$ in place of $Na + b$.

Theorem 2.2: If a, b, c, p, q, N are non-negative integers and p,q are relatively prime, then

$$(Np+q)\Big|\left(N^2a+Nb+c\right) \Leftrightarrow (Np+q)\Big|\left(q^2a - qpb + p^2c\right)$$

Proof. Since p,q are relatively prime, from the above theorem we get

$$(Np+q)\Big|\left(N^2a+Nb+c\right) \Leftrightarrow (Np+q)\Big|\left(N(Na+b)+c\right)$$

$$\Leftrightarrow (Np+q)\Big|\left(q(Na+b)-pc\right)$$

$$\Leftrightarrow (Np+q)\Big|\left(Nqa+(qb-pc)\right)$$

$$\Leftrightarrow (Np+q)\Big|\left(q.qa-p(qb-pc)\right)$$

$$\Leftrightarrow (Np+q)\Big|\left(q^2a-pqb+p^2c\right)$$ This proves the theorem.

In a similar manner, using mathematical induction we can establish the following :

Theorem 2.3: If $a_0, a_1, a_2, \ldots\ldots\ldots a_n, p, q, N$ are non-negative integers and p, q are relatively prime, then

$$(Np+q)\Big|\left(N^n a_0 + N^{n-1}a_1 + N^{n-2}a_2 \ldots\ldots\ldots\ldots + Na_{n-1} + a_n\right)$$

$$\Leftrightarrow (Np+q)\Big|\left(q^n a_0 - p^{n-1}pa_1 + q^{n-2}p^2a_2 \ldots\ldots\ldots\ldots + (-1)^n p^n a_n\right)$$

By writing the divisor $Np + q$ in the from $N(p + 1) - (N - q)$, we can prove the following analogues of the above theorems 2.1 to 2.3.

Theorem 2.4: If a, b, p, q, N are non-negative integers and p, q are relatively prime, then

$$(Np-q)\Big|(Na+b) \Leftrightarrow (Np-q)\Big|(qa+pb)$$

Theorem 2.5: If a,b,c,p,q,N are non-negative integers and p, q are relatively prime, then

$$(Np-q)\Big|(N^2a+Nb+c) \Leftrightarrow (Np-q)\Big|(q^2a+qpb+p^2c).$$

Theorem 2.6: If $a_0,a_1,a_2,.....a_n, p,q, N$ are non-negative integers and p,q are relatively prime, then

$$(Np-q)\Big|(N^n a_0+N^{n-1}a_1+N^{n-2}a_2.....+Na_{n-1}+a_n)$$

$$\Leftrightarrow (Np-q)\Big|(q^n a_0+p^{n-1}pa_1+q^{n-2}p^2a_2.....+p^n a_n)$$

Remark 1: Very useful tests for divisibility can be obtained from the above results by giving special values to N,e.g. $N = 8, 10, 100, 1000$ etc. The case $N = 8$ may be useful for implementation on digital computers since digital computers generally use octal representation of integers. Several tests, which are available for the decimal system of representation, are special cases of the above mentioned theorems. For example, taking $p = q = 1, N = 1000$ in theorem 2.5 we get

$$999\Big|(N^2a+Nb+c) \Leftrightarrow 999\Big|(a+b+c)$$

Let,

$$999\Big|1110888 = 1.1000^2+110.1000+888 \Leftrightarrow 999\Big|(1+110+888) = 999$$

which is similar to the test for divisibility by 37 (Since 37 | 999) as given on page 372 in [3].

Similarly taking $p = q = 1, N = 100$ in Theorem 2.3

$101|(100^n a_0+100^{n-1}.a_1+.....+100\ a_{n-1}+a_n)$

$101|(a_0-a_1+a_2-.....)$ for example $101|432334534546$ since

$101|(43-23+34-53+45-46) = 0$ as discussed in [3].

Remark 2: If we take $N = 10$, we get the result due to Pant [2].

Acknowledgement: I thank Prof. R.P. Pant for providing me a preprint of his paper [2].

REFERENCE

1. David M. Burton: Elementary Number Theory, Universal Book Stall, New Delhi, 1993.
2. R.P. Pant: Fixed point theorems and dynamics of functions, J.Indian Math. Soc.70 (2003) in press.
3. S.G. Telang: Number Theory (edited by Nadkarni and Dani), Tata McGraw Hill, 1996.

Journal of Natural & Physical Sciences, Vol. 19 (1) (2005) 19-27

Mn(II) CATALYSED PERIODATE OXIDATION OF ANILINE IN ACETONE-WATER MEDIUM - A KINETIC-MECHANISTIC STUDY

R.D. Kaushik*, Prabha Singh and Surekha Kannaujia***

(Received 10. 08. 2004 and Revised 17.11.04)

ABSTRACT

Results of kinetic-mechanistic studies on the Mn (II) catalysed periodate oxidation of aniline (ANIL) in acetone-water medium have been presented and discussed. Reaction has been found to be first order in each reactant and catalyst. Effect of dielectric constant of the medium, ionic strength, free radical scavengers and pH on the reaction rate have been discussed. Stoichiometry (1 mol ANIL: 2 mol periodate) and thermodynamic parameters have been evaluated. The main product identified (2, 5-dianilino-p-benzoquinoneimine) and the kinetic studies have been used to propose a suitable mechanism.

Key words: Kinetic-mechanistic study, Periodate oxidation, Aniline, Mn (II) catalysed.

INTRODUCTION

Reports on kinetic-mechanistic studies on the Mn (II) catalysed periodate oxidation of aromatic amines are very few [3-8]. Kinetic and mechanistic studies on uncatalysed periodate oxidation of few aromatic amines[9-14] and Mn (II) catalysed oxidation of 4-chloro-2-methylaniline[15] and o-toluidine[16] have been investigated earlier. In the present paper, we are reporting the kinetic-mechanistic studies on Mn (II) catalysed periodate oxidation of aniline (ANIL) in acetone-water medium.

MATERIALS AND METHODS

Chemicals of E.Merck/CDH A.R. grade were used after distillation/recrystallization. Triply distilled water was used for preparation of the solutions. The progress of the reaction was followed spectrophotometrically by recording the absorbance at 360 nm i.e. the λ_{max} of reaction mixture in the duration in which the λ_{max} did not change. The pH was maintained at 6.0 by using Thiel, Schultz and Koch buffer [1] in all kinetic runs except when the effect of pH was studied. NaCl solutions were used for maintaining the ionic strength (μ) in the kinetic runs. Plane mirror method and Guggenheim's method were used for evaluation of initial rates [$(dA/dt)_i$] and pseudo first order rate constant k_1 (or second order rate constant k_2) respectively.

*Department of Chemistry, Gurukul Kangri University, Haridwar-249404 (India)

**Department of Chemistry, D.A.V. (P.G.) College, Muzaffarnagar (U.P.)

RESULTS AND DISCUSSION

Initially the reaction mixture was yellow in which changed into red in about 40 minutes. On standing overnight, it changed to brown color followed by precipitation. The reaction mixture was prepared by taking periodate in excess and kept overnight. After precipitation, the supernatant liquid was extracted with petroleum ether (40-60^{0}C).

On evaporation of the solvent, a yellowish-red colored compound with melting point 243^{0}C (d) {Lit. [2] 245^{0}C (d) for 2, 5-dianilino-p-benzoquinoneimine} was obtained. This compound responded positively to the test for quinone. The values of absorption maxima obtained in UV-VIS spectrum in dioxane were 280nm, 385nm and 535nm (values reported for 2, 5-dianilino-p-benzoquinoneimine[19] are 280nm, 370nm and 470nm in dioxane). I. R. spectrum in KBr, showed bands at 1290 cm^{-1} and 3270 cm^{-1} which indicates the presence of secondary aromatic amine group. A band at 1340 cm^{-1} was found due to the presence of C-N stretching vibrations of tertiary aromatic amine. Peaks at 2840 and 2920 cm^{-1} were due to the aromatic =C-H stretching vibrations. Considerable enhancement in the intensity of the band at 1580 cm^{-1} indicated that the benzene ring is conjugated with a carbonyl group. A band at 1170 cm^{-1} represented the vibrations for an aryl ketone. Further a band at 1630 cm^{-1} was due to >C = N and >C = O stretching vibrations of imines. Peaks in the region 1000-600 cm^{-1}, indicated the pattern of substitution in the benzene ring.

On the basis of the melting point and UV-VIS spectrum which matched with that available in literature for 2, 5-dianilino-p-benzoquinoneimine [2,19] and expected IR spectrum of the same [20], this reaction product was identified as 2,5-dianilino-p-benzoquinoneimine. Its structure is shown in the chart. This compound has also been reported by Tanabe[2] as one of the oxidation products of oxidation of aniline by HIO_4 at different pH values and by Srivastava *et al.* for the oxidation of aniline by sodium meta periodate in acetone-water medium [23].

1 mol ANIL consumed 2 moles of periodate as determined iodometrically. The data (table-1) indicated 2nd order for the reaction, being first order in each reactant. Linear relation between concentration of the reactants and rate supported the 2nd order kinetics. In pseudo first order condifions (table-2), the $[(dA/dt)]^{-1}$ or k_1^{-1} vs $[S]^{-1}$ plots were linear with almost negligible intercept, suggesting the Michaelis-Menten type kinetics being followed with respect to both reactants with the possibility of formation of a fast decaying intermediate complex between reactants [15-17].

Data in table-3 established the first order in catalyst. Rate-pH profile showed a maxima at pH = 6.0 (table-4, Fig. 1). A linear relation between log $(dA/dt)_i$ or log k_2 and 1/D with negative slope (where D is the dielectric constant of the medium) and a primary linear type plot between log $(dA/dt)_i$ or log k_2 vs ionic strength (μ) that were obtained from the data in table-

5, indicated an ion-dipole interaction in this reaction. This is supported by our observation that free radical scavengers like acryl amide and allyl alcohol exerted no effect on reaction rate.

Arrhenius plot was drawn by varying the temperature between 35 ± 0.1°C to 50 ± 0.1°C taking [ANIL] = 6.0 x 10^{-3} M, [$NaIO_4$] = 6.0 x 10^{-4} M, [Mn^{++}] = 2.0 x 10^{-6} M and acetone = 10.0% (v/v). The values of different thermodynamic parameters were: Ea = 5.27 k. Cal. mol^{-1}; A = 4.21 x 10^3 lit. mol^{-1}. sec^{-1}; $\Delta S^{\ddagger}$ = - 44.1 e. u.; $\Delta F^{\ddagger}$ = 18.54 k. Cal.mol^{-1} and $\Delta H^{\ddagger}$ = 4.64 k.Cal.mol^{-1}. A large negative value of $\Delta S^{\ddagger}$ suggests the formation of strongly solvated, charged and rigid transition state.

Table-1. ***Determination of order w. r. t. reactants.***

λ_{max} = 360nm; Acetone = 10.0% (v/v); Temp = 35 ± 0.1°C; [Mn^{++}] = 1.456 x 10^{-7} M.

[ANIL] x 10^6M	4.0	6.0	8.0	10	12	14	12	12	12	12	12	12
[$NaIO_4$] x 10^4M	50	50	50	50	50	50	1.2	1.4	1.6	1.8	2.0	2.2
$(dA/dt)_i$ x10^3(min^{-1})	4.0	5.9	7.8	9.7	11.7	13.6	5.0	5.8	6.65	7.4	8.25	9.15

Table-2. ***Variation of OMA and periodate.***

λ_{max} = 360nm; Acetone = 10.0% (v/v); Temp = 35±0.1°C; [Mn^{++}] = 2.912x10^{-7} M; [Mn^{++}]*2x10^{-6}

[ANIL] x 10^6M	1.2*	1.4*	1.6*	1.8*	2.0*	0.5	0.5	0.5	0.5	0.5
[$NaIO_4$] x 10^4M	1.2	1.2	1.2	1.2	1.2	50	55	60	65	70
$(dA/dt)_i$ x10^3(min^{-1})	12	14	16	18	20	6.5	7.0	7.7	8.1	8.7
k_1x10^3(sec^{-1})	2.3	2.69	3.15	3.53	3.84	1.44	1.6	1.78	1.96	2.13
k_2(L. mol^{-1}.sec^{-1})	1.92	1.92	1.97	1.97	1.91	0.29	0.29	0.30	0.30	0.30

Table-3. ***Determination of order w.r.t. Mn^{++}.***

λ_{max} = 360nm; [$NaIO_4$]=6.0 x 10^{-4}M;[ANIL]=6.0x10^{-3}M;Temp.=35.0±0.1°C;Acetone=10%(v/v)

[Mn^{++}] x 10^7M	8.0	12.0	16.0	20.0	24.0	28.0
$(dA/dt)_i$x10^3(min^{-1})	11.5	17.0	23.0	28.2	34.0	39.6

Table-4. ***Effect of pH on reaction rate.***

λ_{max} = 360nm; [ANIL] = 6.0 x 10^{-3}M; [$NaIO_4$] = 61.0x10^{-4}M; Acetone=10%(v/v); Temp.=35.0±0.1°C; [Mn^{++}] = 2.912x10^{-7}M

pH	3.0	3.5	4.0	4.5	5.0	5.5	6.0	6.5	7.0	7.5	8.0
$(dA/dt)_i x10^3 (min^{-1})$	1.2	1.4	1.6	1.8	2.2	2.6	6.4	2.8	2.4	2.0	1.0

Table-5. ***Effect of Dielectric constant of medium (D) and ionic strength (μ) on the reaction rate.***

λ_{max} = 360nm; [ANIL] = 6.0 x 10^{-3}M; [$NaIO_4$] = 61.0 x 10^{-4}M; ** Acetone = 10%(v/v); Temp. = 35.0±0.1°C; [Mn^{++}] = 1.456 x 10^{-7} M or 2.912 x 10^{-7} M*

D*	72.4	71.0	69.7	68.4	66.8	--	--	--	--	--
**μx10^5	100	100	100	100	100	2.0	8.0	16	24	32
$(dA/dt)_i 10^3 (min^{-1})$	15	14.3	13.9	13.1	11.2	15.5	16.0	17.0	18.0	19.0
$k_1 x10^4$ (sec^{-1})	25.7	23.0	21.1	18.4	15.4	21.11	23.03	24.94	26.86	30.32
$k_2 x10^2 (L.mol^{-1}sec^{-1})$	42.9	38.4	35.2	30.1	25.6	35.18	38.38	41.58	44.78	50.53

The increase in the rate from pH 3.0 to 6.0 may be due to the decrease in the protonation of ANIL from pH 3.0 to 6.0 (table-4, fig-1), which makes greater concentrations of ANIL available for the reaction. This leads to the assumption that unprotonated ANIL is the reactive species in the present case. Second part of this profile suggests that out of various species in which periodate exists, periodate monoanion [IO_4^-] is the reactive species in present investigation [18]. Pavolva et al.[18] established that [IO_4^-] goes on decreasing with increase in pH beyond the value 6.0, which thereby reduces the rate of reaction beyond pH 6.0. We have reported similar rate - pH profiles in case of periodate oxidation of some other aromatic amines [9-15,21].

Based on these results, the proposed mechanism (Chart) might involve the lone pair of electrons on nitrogen atom of ANIL for the co-ordinate bond formation between ANIL and Mn^{++} species in a reversible step to form complex C_1 in step (i). C_1, in turn, interacts with IO_4^- in slow and rate determining step (ii) to give C_2 which changes by fast hydrolysis in to C_3. The formation of a charged intermediate complex C_2 by the attack of IO_4^- on the nitrogen of anilino group and stabilization of positive charge on nitrogen of this group, has already been established and supported by LFER studies for the uncatalysed periodate oxidation of few aromatic amines

[22]. In addition, a high negative value of entropy of activation and the effect of dielectric constant on the reaction rate support the involvement of solvation effects in this reaction.

It should also be noted that the initial part of the reaction is significant in the present case and the second molecule of IO_4^- reacting later to give C_4 is not significant. C_4 may change by using further steps involving IO_4^- and aniline molecules to give C_5, i.e. the main product of reaction that has been isolated, separated and characterized in this case as 2, 5-dianilino-p-benzoquinoneimine. The overall process may be represented as follows:

$$ANIL + Mn^{++} \underset{k_2}{\overset{k_1}{\rightleftharpoons}} C_1 \qquad \text{---(i)}$$

$$C_1 + [IO_4^-] \xrightarrow[Slow]{k_3} C_2 + Mn^{++} \qquad \text{--- (ii)}$$

$$C_2 \xrightarrow[Fast]{+H^+,\ H_2O} C_3 + H_2O + HIO_3 \qquad \text{--- (iii)}$$

$$C_3 + IO_4^- \xrightarrow{+H^+} C_4 + H_2O + HIO_3 \qquad \text{--- (iv)}$$

$$C_4 \xrightarrow[Fast]{+2ANIL+IO_4^-+H_2O} C_5\ (2,5\text{-dianilino-p-benzoquinoneimine}) \text{--- (v)}$$

On applying steady state treament to C_1, the rate law in terms of rate of loss of $[IO_4^-]$ may be derived as follows:

Rate of loss of $[IO_4^-]$ or $-d[IO_4^-]/dt = k_3 [C_1] [IO_4^-]$ = Rate of loss of C_1 or $-d[C_1]/dt$ (1)

Rate of formation of $C_1 = + d[C_1]/dt = k_1[ANIL] [Mn^{++}] - k_2 [C_1]$

At steady state, $-d[C_1]/dt = + d[C_1]/dt$

Therefore, $k_3[C_1] [IO_4^-] = k_1 [ANIL] [Mn^{++}] - k_2[C_1]$

Or $[C_1] \{k_3[IO_4^-]+k_2\} = k_1 [ANIL] [Mn^{++}]$

$$\text{Or } [C_1] = \frac{k_1[ANIL][Mn^{++}]}{k_3[IO_4^-] + k_2} \qquad (2)$$

From, (1) and (2), $-d[IO_4^-]/dt = \dfrac{k_3 k_1 [ANIL][Mn^{++}][IO_4^-]}{k_2 + k_3[IO_4^-]}$ (3)

Since step (ii) is slow and rate determining step, hence $k_3 [IO_4^-] << k_2$ may be assumed. Therefore, the rate law (3), may be written as rate law (4) which explains all of the observed kinetic data.

$-d[IO_4^-]/dt = k_{obs}.[ANIL] [Mn^{++}] [IO_4^-]$ (4)

where, $k_{obs} = k_3.k_1/k_2$

Acknowledgements : Financial assistance from U.G.C. for undertaking this research work is gratefully acknowledged.

Figure-1. RATE - pH PROFILE

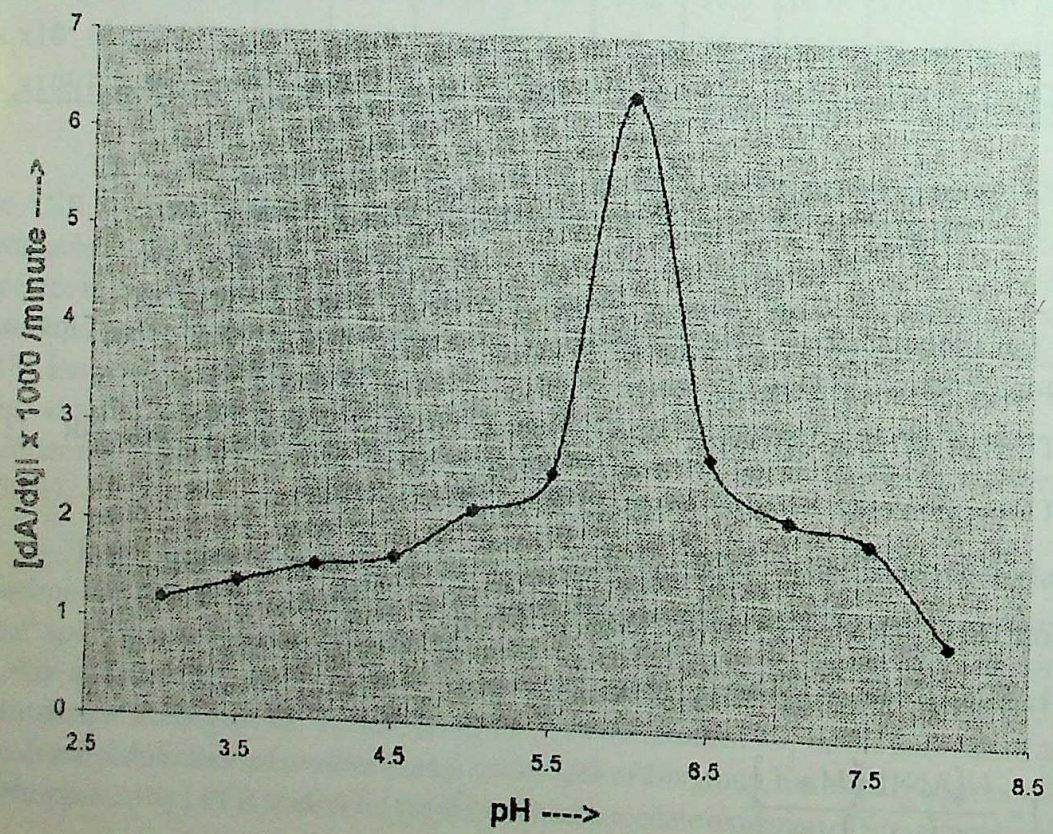

CHART - I

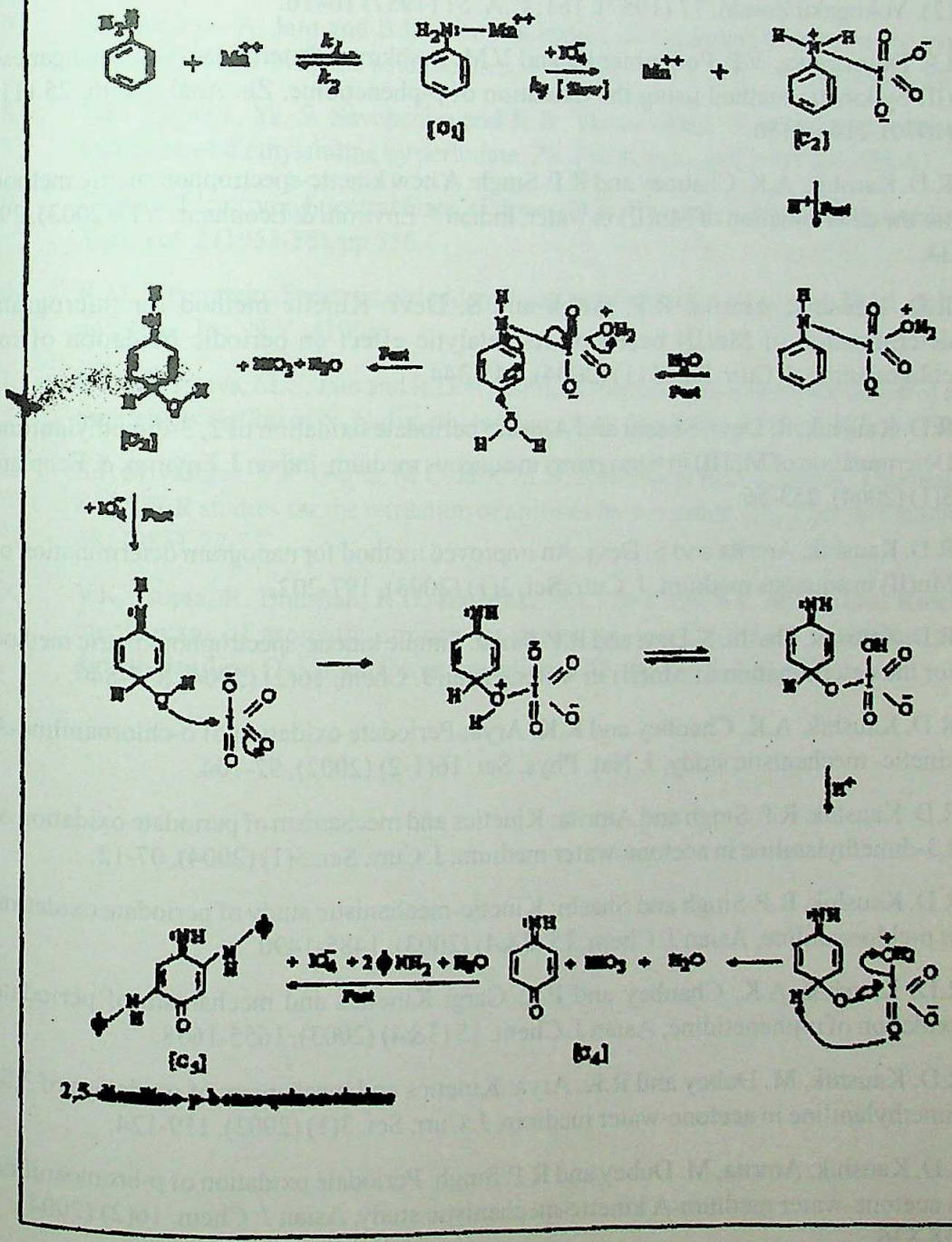

REFERENCES

1. H.T.S. Britton: Hydrogen ions. D.Von Nostrand Co. (1956), 354.
2. H. Tanabe: Periodic acid oxidation of N-glycosides IX--Periodic acid oxidation of anilines (2), Yokugaku Zasshi. 77 (1957), 161; C.A. 51 (1957) 10416.
3. I.F. Dolmanova, V.P. Poddubienko and V.M. Peshkova: Determination of manganese (II) by kinetic method using the oxidation of p-phenetidine, Zh. Anal. Khim. 25 (11) (1970), 2146-2150.
4. R.D. Kaushik, A.K. Chaubey and R.P. Singh: A new kinetic-spectrophotometric method for the determination of Mn(II) in water, Indian J. Environ. & Ecoplann. 7(1) (2003), 29-34.
5. R.D. Kaushik, Amrita, R.P. Singh and S. Devi: Kinetic method for microgram determination of Mn(II) based on its catalytic effect on periodic oxidation of m-chloroaniline, J. Curr. Sci. 5 (1) (2004), 341-344.
6. R.D. Kaushik, S. Devi, Shashi and Amrita: periodate oxidation of 2, 3-dimethylaniline Determination of Mn(II) in nanograms in aqueous medium, Indian J. Environ. & Ecoplan. 8(1) (2004), 253-56.
7. R.D. Kaushik, Amrita and S. Devi: An improved method for nanogram determination of Mn(II) in aqueous medium, J. Curr. Sci. 3(1) (2003), 197-202.
8. R.D. Kaushik, Shashi, S. Devi and R.P. Singh: Simple kinetic-spectrophotometric method for the determination of Mn(II) in water, Asian J. Chem. 16(2) (2004) 837-840.
9. R.D. Kaushik, A.K. Chaubey and R.K. Arya: Periodate oxidation of o-chloroaniline-A kinetic- mechanistic study, J. Nat. Phys. Sci. 16(1-2) (2002), 97-104.
10. R.D. Kaushik, R.P. Singh and Amrita: Kinetics and mechanism of periodate oxidation of 2,3-dimethylaniline in acetone-water medium, J. Curr. Sci. 5(1) (2004), 07-12.
11. R.D. Kaushik, R.P. Singh and Shashi: Kinetic-mechanistic study of periodate oxidation of p-chloroaniline, Asian J. Chem. 15 (3&4) (2003), 1485-1490.
12. R.D. Kaushik, A.K. Chaubey and P.K. Garg: Kinetics and mechanism of periodate oxidation of p-phenetidine, Asian J. Chem. 15 (3&4) (2003), 1655-1658.
13. R.D. Kaushik, M. Dubey and R.K. Arya: Kinetics and mechanism of oxidation of 3,5-dimethylaniline in acetone-water medium, J. Curr. Sci. 3(1) (2003), 119-124.
14. R.D. Kaushik, Amrita, M. Dubey and R.P. Singh: Periodate oxidation of p-bromoaniline in acetone-water medium-A kinetic-mechanistic study, Asian J. Chem. 16(2) (2004), 818-836.

15. R.D. Kaushik, Shashi, Amrita and S. Devi: Kinetics and mechanism of Mn(II) catalyzed periodate oxidation of 4-chloro-2-methylaniline, Asian J. Chem. 16(2) (2004), 818-822.

16. R.D. Kaushik, S. Kannaujia and Shashi: Kinetics and mechanism of Mn(II) catalyzed periodate oxidation of o-toluidine, J. Nat. Phys. Sciences, 18(1) (2004), 115-124.

17. N. Nalwaya, A. Jain and B.L. Hiran: Kinetics of oxidation of glycine by pyridinium bromochromate in acetic acid medium, J. Indian Chem. Soc. 79 (7) (2002), 587-589.

18. V.K. Pavolva, Ya. S. Sevchenko and K.B. Yatsmiriskii : Kinetics and mechanism of oxidation of diethylaniline by periodate, Zh. Fiz. Khim., 44 (3) (1970), 658-63.

19. Organic Electronic Spectral Data, (Editor - H.E. Ungnade), Interscience publishers, N. York Vol. 2 (1953-55), pp 556.

20. R.M. Silverstein: Spectrometric identification of organic compunds, 5th ed., John Wiley and sons. Inc. N.Y., (1991).

21. S.P. Srivastava, M.C. Jain and R.D. Kaushik: Kinetics of periodeate oxidation of aromatic amines-Oxidation of N, N-dimethylaniline, Nat. Acad. Sci. Letters, 2(2) (1979), 63-64.

22. S.P. Srivastava, V.K. Gupta, M.C. Jain, M.N. Ansari and R.D. Kaushik: Thermodynamic and LFER studies for the oxidation of anilines by periodate ion, Thermo Chimica Acta, 68 (1983), 27-33.

23. V.K. Gupta, R. Bhushan, R.D. Kaushik, M.C. Jain and S.P. Srivastava: Kinetics and mechanism of aromatic amines by periodate ion-Oxidation of aniline and N,N dimethylaniline, Oxidation Communications, 7(3-4) (1984), 420-423.

Journal of Natural & Physical Sciences, Vol. 19 (1) (2005) 29-37

SOME COMMON FIXED POINT THEOREMS FOR COMMUTING MAPPINGS IN MENGER SPACES

B.D. Pant* and Suneel Kumar*

(Received 04.08.2004 Revised 07.01.2005)

ABSTRACT

In this paper we prove some common fixed point theorems for triplet of commuting mappings satisfying a new contraction condition in Menger spaces.

Key words: Probabilistic metric space, Menger space, Contraction mappings, Fixed point.

Mathematics Subject Classifications (2000): 54H 25, 47H 10.

INTRODUCTION

Sehgal and Bharucha-Reid [8] initiated the study of fixed points of contraction mappings in probabilistic metric spaces (PM-spaces). Ciric [3] introduced the notion of 'generalized contraction' on a PM-space. Jungck [5] generalized the Banach contraction principle by introducing a contraction condition for a pair of commuting mappings on a metric space. Some fixed point theorems for a pair of commuting mappings in PM-spaces have been proved in ([2], [4], [11]). Singh and Pant [9] introduced the notion of 'generalized contraction triplet' in PM-spaces in which one of the mappings commutes with the other two (also see [10]). Chamola [1] and Vasuki [12] have proved some fixed point theorems for mappings satisfying a new contraction condition.

In this paper, we prove some common fixed point theorems for a triplet of mappings satisfying a new contraction type condition in Menger spaces. In our results one of the mappings commutes with either of the two. Thus the present results are obtained under the condition weaker than those in [9].

PRELIMINARIES

Definiton 1. A PM-space is an ordered pair (X,F) where X is a non-empty set of elements and F is a mapping from $X \times X$ to £, the collection of all distribution functions. The value of F at $(u, v) \in X \times X$ is represented by $F_{u,v}$. The function $F_{u,v}$ are assumed to satisfy the following conditions:

*Department of Mathematics, R.H. Govt. Postgraduate College, Kashipur 244 713, India.
E-mail address: matsuneel@yahoo.co.in

(a) $F_{u,v}(x) = 1$ *for all* $x > 0$ iff $u = v$;

(b) $F_{u,v}(0) = 0$;

(c) $F_{u,v}(x) = F_{v,u}(x)$;

(d) If $F_{u,v}(x) = 1$ and $F_{v,w}(y) = 1$ then $F_{u,w}(x+y) = 1$.

A mapping t : $[0,1] \times [0,1] \to [0,1]$ is called a t-norm if it satisfies

(e) $t(0,0) = 0$, $t(a,1) = a$;

(f) $t(a,b) \leq t(c,d)$ for $a \leq c$, $b \leq d$;

(g) $t(a,b) = t(b,a)$;

(h) $t\{t(a,b),c\} = t\{a, t(b,c)\}$

for all a, b, c, d in $[0,1]$.

A Menger space is a triplet (X, F, t), where (X, F) is a PM-space and t-norm t is such that the inequality

(d) $F_{u,w}(x+y) \geq t\{F_{u,v}(x), F_{v,w}(y)\}$

holds for all $u, v, w \in X$ and all $x \geq 0, y \geq 0$.

For details of topological preliminaries, we refer to Schweizer and Sklar [6, 7].

Definiton 2[9]: Three mappings P, Q, T on a PM-space (X, F) will be called a generalized contraction triplet $(P, Q; T)$ if there exists a constant h $\in (0,1)$ such that for every $u, v \in X$

$$F_{Pu,Qv}(hx) \geq \min\{F_{Tu,Tv}(x), F_{Pu,Tu}(x), F_{Qv,Tv}(x), F_{Pu,Tv}(2x), F_{Qv,Tu}(2x)\}$$

holds for all $x > 0$.

Definiton 3[9]: Let P, Q and T be mappings from X to itself. If there exists a point u_0 in X and a sequence $\{u_n\}$ in X such that

$$Tu_{2n+1} = Pu_{2n},\ Tu_{2n+2} = Qu_{2n+1} \text{ for n} = 0,1,2.....$$

then the space X will be called $(P, Q; T)$-orbitally complete with respect to u_0 or simply $(P, Q; T(u_0))$-orbitally complete if the closure of $\{Tu_n : n = 1,2...\}$ is complete.

Definiton 4[9]: T will be called $(P, Q; T(u_0))$-orbitally continuous if the restriction of T on the closure of $\{Tu_n : n = 1,2....\}$ is continuous.

Lemma [10]: Let $\{y_n\}$ be a sequence in a Menger space (X, F, t), where t is continuous and

satisfies $t(x, x) \geq x$ for every $x \in [0,1]$. If there exists a constant $h \in (0,1)$ such that

$$F_{y_n, y_{n+1}}(hx) \geq F_{y_{n-1}, y_n}(x), \; n = 1,2,3...$$

then $\{y_n\}$ is a Cauchy sequence in X.

RESULTS

Theorem 1: Let (X, F, t) be a Menger space, where t is continuous and satisfies $t(x, x) \geq x$ for every $x \in [0,1]$. Let $P, Q\, T : X \to X$ satisfy the following condition

$$(F_{Pu, Qv}(hx))^2 \geq \min\{F_{Tu, Tv}(x),\, F_{Tu, Pv}(x),\, F_{Tu, Tv}(x)\, F_{Tu, Qv}(x)\, F_{Tu, Pu}(x)$$
$$F_{Tv, Qv}(x),\, F_{Tu, Qv}(2x) F_{Tv, Pu}(2x)\} \qquad (1)$$

for all $u, v \in X$ and $h \in (0,1)$. Further, assume that either $PT = TP$ or $QT = TQ$. If there exists a point u_0 in X such that X is $(P, Q; T(u_0))$-orbitally complete and T is $(P, Q : T(u_0))$-orbitally continuous, then P, Q and T have a unique common fixed point and $\{Tu_n\}$ converges to the common fixed point.

PROOF: Let $u_0 \in X$. Define $\{u_n\}$ as follows:

$$Tu_{2n+1} = Pu_{2n},\; Tu_{2n+2} = Qu_{2n+1} \text{ for } n = 0, 1, 2... \qquad (2)$$

By (1)

$$(F_{Tu_{2n+1},\, Tu_{2n+2}}(hx))^2 = F_{Pu_{2n},\, Qu_{2n+1}}(hx))^2 \geq \min\{F_{Tu_{2n},\, Tu_{2n+1}}(x) F_{Tu_{2n},\, Tu_{2n+1}}(x),$$
$$F_{Tu_{2n},\, Tu_{2n+1}}(x) F_{Tu_{2n+1},\, Tu_{2n+2}}(x),\; F_{Tu_{2n},\, Tu_{2n+1}}(x) F_{Tu_{2n+1},\, Tu_{2n+2}}(x),$$
$$F_{Tu_{2n},\, Tu_{2n+2}}(2x),\; F_{Tu_{2n+1},\, Tu_{2n+1}}(2x)\},$$

giving

$$\geq \min\{(F_{Tu_{2n},\, Tu_{2n+1}}(x))^2,\, F_{Tu_{2n},\, Tu_{2n+1}}(x) F_{Tu_{2n+1},\, Tu_{2n+2}}(x)\}.$$

since $F_{Tu_{2n},\, Tu_{2n+2}}(2x) \geq \min\{F_{Tu_{2n},\, Tu_{2n+}}(x),\, F_{Tu_{2n+1},\, Tu_{2n+2}}(x)\}$.

Now, suppose that

$$(F_{Tu_{2n+1},\, Tu_{2n+2}}(hx))^2 \geq (F_{Tu_{2n},\, Tu_{2n+1}}(x))^2$$

then

$$F_{Tu_{2n+1},\, Tu_{2n+2}}(hx) \geq F_{Tu_{2n},\, Tu_{2n+1}}(x).$$

Again suppose that

$$(F_{Tu_{2n+1},\, Tu_{2n+2}}(hx))^2 \geq F_{Tu_{2n},\, Tu_{2n+1}}(x) F_{Tu_{2n+1},\, Tu_{2n+2}}(x)$$

then

$$F_{Tu_{2n+1},\, Tu_{2n+2}}(hx) \geq F_{Tu_{2n},\, Tu_{2n+1}}(x).$$

So in both the cases, we have

$$F_{Tu_{2n+1},\, Tu_{2n+2}}(hx) \geq F_{Tu_{2n},\, Tu_{2n+1}}(x).$$

Similarly

$$F_{Tu_{2n+2},\, Tu_{2n+3}}(hx) \geq F_{Tu_{2n+1},\, Tu_{2n+2}}(x).$$

In general

$$F_{Tu_{n+1},\, Tu_{n+2}}(hx) \geq F_{Tu_n,\, Tu_{n+1}}(x)$$

By lemma [10], $\{Tu_n\}$ is a Cauchy sequence in X. Since X is $(P, Q; T(u_0))$-orbitally complete, then $\{Tu_n\}$ converges to a point z in X.

Now we prove that $Qz = Tz$.

Let $U_{Qz}(\varepsilon,\lambda)$ be an (ε, λ)-neighbourhood of Qz. By the continuity condition on T, $TTu_{2n} \to Tz$ and $TTu_{2n+1} \to Tz$. So there exists an integer $k = k(\varepsilon,\lambda)$ such that

$$n \geq k \text{ implies } F_{Tu_{2n},\, Tz}\left(\frac{1-h}{2h}\varepsilon\right) > 1-\lambda \text{ and } F_{Tu_{2n+1},\, Tz}\left(\frac{1-h}{2h}\varepsilon\right) > 1-\lambda \tag{3}$$

Suppose $PT = TP$, then by (1),

$$(F_{TTu_{2n+1},\, Qz}(\varepsilon))^2 = (F_{TPu_{2n},\, Qz}(\varepsilon))^2 = (F_{PTu_{2n},\, Qz}(\varepsilon))^2$$

$$\geq \min\{F_{TTu_{2n},\, Tz}(\varepsilon/h) F_{TTu_{2n},\, TTu_{2n+1}}(\varepsilon/h),\ F_{TTu_{2n},\, Tz}(\varepsilon/h) F_{Tz,\, Qz}(\varepsilon/h),$$
$$F_{TTu_{2n},\, TTu_{2n+1}}(\varepsilon/h) F_{Tz,\, Qz}(\varepsilon/h),\ F_{TTu_{2n},\, Qz}(2\varepsilon/h) F_{Tz,\, TTu_{2n+1}}(2\varepsilon/h)\}$$

$$\geq \min\{F_{TTu_{2n},\, Tz}(\varepsilon/h)\{F_{TTu_{2n},\, Tz}\left(\frac{1-h}{2h}\varepsilon\right),\ F_{Tz,\, TTu_{2n+1}}\left(\frac{1+h}{2h}\varepsilon\right)\},$$

$$F_{TTu_{2n},\, Tz}(\varepsilon/h)\ \{F_{Tz,\, TTu_{2n}}\left(\frac{1-h}{2h}\varepsilon\right),\ F_{TTu_{2n},\, Qz}\left(\frac{1+h}{2h}\varepsilon\right)\},$$

$$\{F_{TTu_{2n},\,Tz}\left(\frac{1-h}{2h}\varepsilon\right), F_{Tz,\,TTu_{2n+1}}\left(\frac{1+h}{2h}\varepsilon\right)\}\ \{F_{Tz,\,TTu_{2n}}\left(\frac{1-h}{2h}\varepsilon\right), F_{TTu_{2n},\,Qz}\left(\frac{1+h}{2h}\varepsilon\right)\},$$

$$\{F_{TTu_{2n},\,Tz}(\varepsilon/h), F_{Tz,\,Qz}(\varepsilon/h)\}\ \{F_{Tz,\,TTu_{2n}}(\varepsilon/h), F_{TTu_{2n},\,TTu_{2n+1}}(\varepsilon/h)\}$$

$$\geq \min\{F_{TTu_{2n},\,Tz}(\varepsilon/h)F_{TTu_{2n},\,Tz}\left(\frac{1-h}{2h}\varepsilon\right), F_{TTu_{2n},\,Tz}(\varepsilon/h)F_{Tz,\,TTu_{2n}}\left(\frac{1-h}{2h}\varepsilon\right),$$

$$(F_{TTu_{2n},\,Tz}\left(\frac{1-h}{2h}\varepsilon\right))^2, (F_{TTu_{2n},\,Tz}(\varepsilon/h))^2, F_{TTu_{2n},\,Tz}(\varepsilon/h)F_{TTu_{2n},\,TTu_{2n+1}}(\varepsilon/h),$$

$$F_{Tz,\,Qz}(\varepsilon/h)F_{Tz,\,TTu_{2n}}(\varepsilon/h), F_{Tz,\,Qz}(\varepsilon/h)F_{TTu_{2n},\,TTu_{2n+1}}(\varepsilon/h)\}$$

$$> (1-\lambda)^2 \qquad \text{by (3)}$$

giving, $F_{TTu_{2n+1},\,Qz}(\varepsilon) > 1-\lambda$ for all $n \geq k$.

Consequently $Tz = Qz$.

To prove $Tz = z$, let $U_{Tz}(\varepsilon, \lambda)$ be a neighbourhood of Tz. Since $\{Tu_n\}$ is a Cauchy sequence, there exists an integer $k = k(\varepsilon, \lambda)$ such that

$$F_{Tu_{2n},\,Tu_{2n+1}}\left(\frac{1-h}{2h}\varepsilon\right) > 1-\lambda \text{ for all } n \geq k. \tag{4}$$

By (1), we have

$$(F_{Tu_{2n+1},\,Tz}(\varepsilon))^2 = (F_{Pu_{2n},\,Qz}(\varepsilon))^2$$

$$\geq \min\{F_{Tu_{2n},\,Tz}(\varepsilon/h)F_{Tu_{2n},\,Tu_{2n+1}}(\varepsilon/h), F_{Tu_{2n},\,Tz}(\varepsilon/h)F_{Tz,\,Tz}(\varepsilon/h),$$

$$F_{Tu_{2n},\,Tu_{2n+1}}(\varepsilon/h)F_{Tz,\,Tz}(\varepsilon/h),\ F_{Tu_{2n},\,Tz}(2\varepsilon/h)F_{Tz,\,Tu_{2n+1}}(2\varepsilon/h)\}$$

$$\geq \min\{\{F_{Tu_{2n},\,Tu_{2n+1}}\left(\frac{1-h}{2h}\varepsilon\right), F_{Tu_{2n+1},Tz}\left(\frac{1+h}{2h}\varepsilon\right)\}\ F_{Tu_{2n},\,Tu_{2n+1}}(\varepsilon/h),$$

$$F_{Tu_{2n},\,Tz}(\varepsilon/h), F_{Tu_{2n},\,Tu_{2n+1}}(\varepsilon/h),$$

$$\{F_{Tu_{2n},\,Tu_{2n+1}}(\varepsilon/h), F_{Tu_{2n+1},\,Tz}(\varepsilon/h)\}\ \{F_{Tz,\,Tu_{2n}}(\varepsilon/h), F_{Tu_{2n},\,Tu_{2n+1}}(\varepsilon/h)\}\}$$

$$\geq \min\{F_{Tu_{2n},\,Tu_{2n+1}}\left(\frac{1-h}{2h}\varepsilon\right)F_{Tu_{2n},\,Tu_{2n+1}}(\varepsilon/h), F_{Tu_{2n},\,Tz}(\varepsilon/h),$$

$$F_{Tu_{2n},\,Tu_{2n+1}}(\varepsilon/h),\ F_{Tu_{2n},\,Tu_{2n+1}}(\varepsilon/h)F_{Tz,\,Tu_{2n}}(\varepsilon/h),$$
$$(F_{Tu_{2n},\,Tu_{2n+1}}(\varepsilon/h))^2,\ F_{Tu_{2n+1},\,Tz}(\varepsilon/h)F_{Tz,\,Tu_{2n}}(\varepsilon/h),$$
$$F_{Tu_{2n+1},\,Tz}(\varepsilon/h)F_{Tu_{2n},\,Tu_{2n+1}}(\varepsilon/h)\}$$

$$\geq (F_{Tu_{2n},\,Tu_{2n+1}}\left(\frac{1-h}{2h}\varepsilon\right))^2$$

$$> (1-\lambda)^2 \qquad \text{by (4)},$$

giving

$F_{Tu_{2n+1},\,Tz}(\varepsilon) > 1 - \lambda$ for all $n \geq k$

So $z = Tz$ since $Tu_{2n+1} \to z$.

So far we have proved that $Qz = Tz = z$.

Now we have to prove that z is also a fixed point of P. For this, let $Pz \neq z$.

By (1),

$$(F_{Pz,\,z}(x))^2 = (F_{Pz,\,Qz}(x))^2$$
$$\geq \min\{F_{Tz,\,Tz}(x)F_{Tz,\,Pz}(x),\ F_{Tz,\,Tz}(x)F_{Tz,\,Qz}(x),$$
$$F_{Tz,\,Pz}(x)F_{Tz,\,Qz}(x),\ F_{Tz,\,Qz}(2x)F_{Tz,\,Pz}(2x)\}$$
$$\geq \min\{F_{z,\,Pz}(x),\ 1,\ F_{z,\,Pz}(x),\ F_{Tz,\,Pz}(2x)\}$$

giving

$(F_{Pz,\,z}(x))^2 = F_{z,\,Pz}(x)$, a contradiction.

Therefore, $Pz = z$.

Thus $Pz = Qz = Tz = z$.

Similarly, if $QT = TQ$, we can prove $Pz = Qz = Tz = z$.

To prove the uniqueness of z as a common fixed point of P, Q and T, let y $(\neq z)$ be another common fixed point.

By (1).

$$(F_{y,z}(x))^2 = (F_{Py,\,Qz}(x))^2$$

$$\geq \min \{F_{Ty,\,Tz}(x)F_{Ty,\,Py}(x),\ F_{Ty,\,Tz}(x)\,F_{Tz,\,Qz}(x),$$
$$F_{Ty,\,Py}(x)F_{Tz,\,Qz}(x)F_{Ty,\,Qz}(2x)F_{Tz,\,Py}(2x)\}$$
$$\geq \min \{F_{y,\,z}(x),\ F_{y,\,z}(x),\ 1,\ (F_{y,\,z}(2x))^2\}$$

$$(F_{y,\,z}(x))^2 = F_{y,\,z}(x)$$

This is impossible, since $y \neq z$.

Therefore, $y = z$ and hence z is a unique common fixed point of P, Q and T.

This completes the proof.

The result in [9] for a contraction triplet has been proved by taking one of the mappings commuting with both of the other two mappings. But in the present result, one of the mappings commutes with either of the two. Hence our result improves the result in [9] and a number of other results as well.

COROLLARY 1: Let X, P, Q, T be as in Theorem 1. If the mappings P, Q and T satisfy the following condition

$$(F_{Pu,\,Qv}(hx))^2 \geq \min \{F_{Tu,\,Pu}(x)F_{Tv,\,Qv}(x),\ F_{Tu,\,Pu}(x)F_{Tu,\,Qv}(2x)$$
$$F_{Tv,\,Pu}(2x)F_{Tv,\,Qv}(x),\ F_{Tv,\,Pu}(2x)F_{Tu,\,Qv}(2x)\} \tag{5}$$

for all u, $v \in X$ and $h \in (0,1)$. Then the conclusion of Theorem 1 holds.

PROOF: By (5) and (2), we have

$$(F_{Tu_{2n+1},\,Tu_{2n+2}}(hx))^2 = (F_{Pu_{2n},\,Qu_{2n+1}}(hx))^2$$
$$\geq \min \{F_{Tu_{2n},\,Tu_{2n+1}}(x)F_{Tu_{2n+1},\,Tu_{2n+2}}(x),$$
$$F_{Tu_{2n},\,Tu_{2n+1}}(x)F_{Tu_{2n},\,Tu_{2n+2}}(2x),\ F_{Tu_{2n+1},\,Tu_{2n+1}}(2x)F_{Tu_{2n+1},\,Tu_{2n+2}}(x),$$
$$F_{Tu_{2n+1},\,Tu_{2n+1}}(2x)F_{Tu_{2n},\,Tu_{2n+2}}(2x)\}$$

giving

$$\geq \min \{F_{Tu_{2n},\,Tu_{2n+1}}(2x)F_{Tu_{2n+1},\,Tu_{2n+2}}(x),\ (F_{Tu_{2n},\,Tu_{2n+1}}(x))^2\}.$$

since

$$F_{Tu_{2n},\,Tu_{2n+2}}(2x) \geq \min \{F_{Tu_{2n},\,Tu_{2n+1}}(x),\ F_{Tu_{2n+1},\,Tu_{2n+2}}(x)\}.$$

Now, suppose that

$$(F_{Tu_{2n+1},\, Tu_{2n+2}}(hx))^2 \geq F_{Tu_{2n},\, Tu_{2n+1}}(x) F_{Tu_{2n+1},\, Tu_{2n+2}}(x)$$

then

$$F_{Tu_{2n+1},\, Tu_{2n+2}}(hx) \geq F_{Tu_{2n},\, Tu_{2n+1}}(x).$$

Again suppose

$$(F_{Tu_{2n+1},\, Tu_{2n+2}}(hx))^2 \geq (F_{Tu_{2n},\, Tu_{2n+1}}(x))^2$$

then

$$F_{Tu_{2n+1},\, Tu_{2n+2}}(hx) \geq F_{Tu_{2n},\, Tu_{2n+1}}(x).$$

So in both the cases, we have

$$F_{Tu_{2n+1},\, Tu_{2n+2}}(hx) \geq F_{Tu_{2n},\, Tu_{2n+1}}(x).$$

Similarly

$$F_{Tu_{2n+2},\, Tu_{2n+3}}(hx) \geq F_{Tu_{2n+1},\, Tu_{2n+2}}(x).$$

In general

$$F_{Tu_{n+1},\, Tu_{n+2}}(hx) \geq F_{Tu_n,\, Tu_{n+1}}(x)$$

By lemma [10], $\{Tu_n\}$ is a Caucy sequence in X. Since X is $(P, Q; T(u_0))$-orbitally complete, $\{Tu_n\}$ converges to a point z in X. Now, it can be easily proved, as in Theorem-1 that z is a unique common fixed point.

THEOREM 2: Let (X, F, t) be a complete Menger space, where t is continuous and satisfies $t(x, x) \geq x$ for every $x \in [0,1]$. Let $P, Q, T : X \to X$ satisfy the condition (1) for all u, v in X and $h \in (0,1)$. Further, suppose that either $PT = TP$ or $QT = TQ$ and $P(X) \cup Q(X) \subseteq T(X)$. If T is continuous, then P, Q and T have a unique common fixed point.

PROOF: Let $u_0 \in X$. Define sequence $\{u_n\}$ in X given by the rule

$$Tu_{2n+1} = Pu_{2n}, \quad Tu_{2n+2} = Qu_{2n+1} \qquad \text{for n} = 0, 1, 2...$$

This can be done by virtue of $P(X) \cup Q(X) \subseteq T(X)$. Now the proof of Theorem 1 works.

COROLLARY 2: Let X be as in Theorem 2. Let $P, Q, T : X \to X$ satisfy the condition (5) for all u, v, in X and $h \in (0,1)$. Further, suppose that either $PT = TP$ or $QT = TQ$ and $P(X) \cup Q(X) \subseteq T(X)$. If T is continuous, then the conclusion of Theorem 2 holds.

Acknowledgement: The authors thank the referee for the critical reading of the paper and the valuable suggestions to improve the paper.

REFERENCES

1. K. P. Chamola : Fixed points of mappings satisfying a new contraction condition in random normed spaces, Math. Japon. 33 (1988) 821-825.

2. K. P. Chamola, R.C. Dimri and B.D. Pant : On nonlinear contractions on Menger spaces, Ganita, 39 (1988) 49-54.

3. Lj. B. Ciric: On fixed points of generalized contraction on probabilistic metric spaces, Publ. Inst. Math. (Beograd) (N.S.) 18 (32) (1975) 71-78.

4. R. Dedeic and N. Sarapa : On common fixed point theorems for commuting mappings on Menger spaces, Radovi Mat. 4(1988) 269-278.

5. G. Jungck : Commuting mappings and fixed points, Amer. Math. Monthly 83 (1976) 261-263.

6. B. Schweizer and A. Sklar : Statistical metric space, Pacific J. Math. 10 (1960)313-334.

7. B. Schweizer and A. Sklar : Probabilistic Metric Spaces, North Holland Series 1983.

8. V. M. Sehgal and A. T. Bharucha-Reid : Fixed points of contraction mappings on probabilistic metric spaces, Math. Systems Theory 6 (1972) 97-102.

9. S.L. Singh and B.D. Pant : Common fixed point theorems for commuting mappings in probabilistic metric spaces, Honam Math. J. 5 (1983) 139-150.

10. S.L. Singh and B.D. Pant : Common fixed point theorems in probabilistic metric spaces and extension to uniform spaces, Honam Math. J. 6 (1984) 1-12.

11. B.M.L. Tivari and B.D. Pant : Fixed points of a pair of mappings in probabilistic metric spaces, Jnanabha 13 (1983) 13-25.

12. R. Vasuki : A fixed point theorem for a sequence of maps satisfying a new contractive type condition in Menger spaces, Math. Japon. 35 (1990) 1099-1102.

Journal of Natural & Physical Sciences, Vol. 19 (1) (2005) 39-58

DISTANCE BETWEEN FUZZY MATRICES AND ITS APPLICATIONS-I

Madhumangal Pal* and Amiya K. Shyamal

(Received 27.09.2004 and Revised 31.01.05)

ABSTRACT

Two basic distances, Hamming distance and Euclidean distance between two fuzzy matrices are defined in this paper and a lot of algebraic properties are investigated using these two distances. Two applications 'recognition of character' and 'analysis of crowdness of a network', using Hamming distance, are presented here.

Keywords: Fuzzy matrix, fuzzy operators, Hamming and Euclidean distances.

INTRODUCTION

In real life situation, matrices play an important role in different branches of science and technology. But, due to presence of various types of uncertainties, the traditional classical matrices may not be sufficient for the precise description of the characteristics of any system, pattern, etc. To measure the different kinds of uncertainties, fuzzy sets [18, 27, 28], intuituinistic fuzzy sets [1,2], interval mathematics [2,4], rough sets [17], etc. are used as mathematical tools. Fuzzy matrices are used for cluster analysis of many pattern classification problems [3, 7, 13, 21]. Fuzzy matrices has attracted the attention of many authors and they have presented a number of results on the convergence of power sequence of fuzzy matrices [5, 8, 12, 14, 22]. Several authors [5, 6, 10, 11] studied the canonical form of different fuzzy matrices. Xin [25, 26] studied controllable fuzzy matrices. Ragab et al. [19] presented some properties on determinant and adjoint of a square fuzzy matrix. Pal [16] introduced intuitionistic fuzzy determinant. Pal et al. [9] introduced intuitionistic fuzzy matrices. Shyamal and Pal [20] introduced two new operators on fuzzy matrices.

In this paper, we define two basic distances Hamming distance, Euclidean distance and we have investigated a lot of properties for Hamming distance and Euclidean distance. Two real life problems have been solved using Hamming distance.

The first problem is "recognition of character" using Hamming distance. In the age of automation, men having the natural propensity of performing all types of work automatically instead of human interference, the character recognition is one of the most successful and

*Department of Applied Mathematics with Oceanology and Computer Programming, Vidyasagar University, Midnapore-721 102, INDIA. e-mail: madhumangal@lycos.com

epoch-making application of automatic pattern recognition. The objective of chatacter recognition system is to recognise a character automatically by machine without typing or human interaction. There are various types of optical character recognition system in different languages. Several works on optical character recognition system are available in lliterature [15, 23, 24]. Here we discuss and analyze a new system of character recognition. In this process recognition of character is possible by measuring the Hamming distance. In the second application, we study the crowdness of a network and measures the fluctuation of crowdness of the network.

DEFINITIONS

In this section, fuzzy matrix and boolean fuzzy matrix are defined and some operations on fuzzy matrices are also introduced.

Definition 1 Fuzzy Matrix: A fuzzy matrix (FM) A of order $m \times n$ is defined as $A = [<a_{ij}, a_{ij\mu}>]_{m \times n}$ where $a_{ij\mu}$ is the membership value of the element a_{ij} in A. For simplicity, we write A as $A = [a_{ij\mu}]$.

Definition 2 Boolean Fuzzy Matrix: A fuzzy matrix $A = [a_{ij}]_{m \times n}$ is said to be a boolean fuzzy matrix of order $m \times n$ if all the elements of A are either 0 or 1.

Let $A = [a_{ij}]$ and $B = [b_{ij}]$ be any two fuzzy matrices of order $m \times n$. The following operations are defined for any two elements x and y of a fuzzy matrix.

(i) $x \vee y = max\ (x, y)$

(ii) $x \wedge y = min\ (x, y)$

(iii) $x \oplus y = x + y - x.y$

(iv) $x \odot y = x.y$

(v) $x \Theta y = \begin{cases} x, \text{ if } x > y \\ 0, \text{ if } x \leq y \end{cases}$

(iv) $x^{(\alpha)} = \begin{cases} 1, \text{ if } x \geq \alpha \\ 0, \text{ if } x < \alpha \end{cases}$.

The following operations are defined for any two fuzzy matrices $A = [a_{ij}]$ and $B = [b_{ij}]$ of order $m \times n$ as follows:

(i) $A \oplus B = [a_{ij} + b_{ij} - a_{ij}.b_{ij}]$

(ii) $A \odot B = [a_{ij}.b_{ij}]$

(iii) $A \vee B = [a_{ij} \vee b_{ij}]$

(iv) $A \wedge B = [a_{ij} \wedge b_{ij}]$

(v) $A \ominus B = [a_{ij} \ominus b_{ij}]$

(vi) $A^{[k+1]} = A[k] \odot A,\ A^{[1]} = A,\ k = 1, 2,...$

(vii) $[k+1]A = [k]\ A \oplus A,\ [1]A = A,\ k = 1, 2, ...$

(viii) $A@B = \left[\frac{a_{ij} + b_{ij}}{2}\right]$

(ix) $A\$B = \left[\sqrt{a_{ij}.b_{ij}}\right]$

(x) $A^{(\alpha)} = \left[\alpha_{ij}^{(\alpha)}\right]$

(xi) $A' = [a_{ji}]$ (the transpose of A)

(xii) $A^c = [1\text{-}a_{ij}]$ (the complement of A)

(xiii) $A \leq B$ if and only if $a_{ij} \leq b_{ij}$ for all i, j

(xiv) For any two fuzzy matrices A and B, $\min(A,B) = \begin{cases} A, \text{if } A \leq B \\ B, \text{ if } B \leq A. \end{cases}$

The operators '+', '-', '.' are ordinary addition, subtraction and multiplication.

For an $m \times n$ fuzzy matrix $A = [a_{ij}]$ we have,

(i) A is reflexive if and only if $a_{ii} = 1$ for all $i = 1, 2, ..., n$.

(ii) A is irreflexive if and only if $a_{ii} = 0$ for all $i = 1, 2, ..., n$.

(iii) A is nearly irreflexive if and only if $a_{ii} \leq a_{ij}$ for all $i, j = 1, 2, ..., n$.

(iv) A is symmetric if and only if $A' = A$.

(v) A is identity if and only if $a_{ii} = 1$ and $a_{ij} = 0$ for all $i \neq j$, for all i, j. The identity matrix of order $n \times n$ is generally denoted by I_n.

(vi) A is weakly reflexive if $a_{ii} \geq a_{ij}$ for all i, j.

(vii) A is diagonal if $a_{ii} \geq 0$ and $a_{ij} = 0$, $i \neq j$ for all i, j.

DISTANCES BETWEEN FMs

In this section, we defined two basic distances between FMs. The distance δ between FMs A and B is a mapping from the set of FMs (M) to the set of real numbers (R)

i.e., $$\delta : M \times M \to R.$$

Hamming distance: The Hamming distance between two FMs A and B of order $m \times n$ is

$$H(A,B) = \sum_{i=1}^{m}\sum_{j=1}^{n}\left|a_{ij} - b_{ij}\right|.$$

It is obvious that $0 \leq H(A, B) \leq m.n.$

If $a_{ij} = 1$ and $b_{ij} = 0$ for all i,j or $a_{ij} = 0$ and $b_{ij} = 1$ for all i, j (1)

then $H(A, B) = m.n.$

If $a_{ij} = b_{ij}$ for all i, j (2)

then $H(A, B) = 0.$

The Hamming distance $H : M \times M \to R$ satisfies the following conditions:

(i) $H(A, B) \geq 0$ for all $A, B \in M$,

(ii) $H(A, B) = 0$ iff $A = B$ for all $A, B \in M$,

(iii) $H(A, B) = H(B, A)$ for all $A, B \in M$ (symmetry),

(iv) $H(A, B) \leq H(A, C) + H(C, B)$ for all $A, B, C \in M$ (triangular inequality).

Thus the distance function H is a metric on M.

Normalised Hamming distance: The normalised Hamming distance between two FMs A and B is denoted by $H^*(A, B)$ and is defined as

$$H^*(A,B) = \frac{H(A,B)}{m.n}.$$

It may be noted that $0 \leq H^*(A, B) \leq 1.$

Euclidean distance: The Euclidean distance between two FMs A and B of order $m \times n$ is defined as

$$E(A,B)=\sqrt{\sum_{i=1}^{m}\sum_{i=1}^{n}\left(a_{ij}-b_{ij}\right)^2}\ .$$

It is also obvious that $0 \le E(A, B) \le \sqrt{mn}$. The sign of equality holds when (1) and (2) are satisfied. The Euclidean distance E also a metric on M.

Normalised Euclidean distance: The Normalised Euclidean distance between two FMs A and B is denoted by $E^*(A, B)$ and is defined as

$$E^*(A,B)=\frac{E(A,B)}{\sqrt{m.n}}.$$

Here also $0 \le E^*(A, B) \le 1$.

The maximum Hamming distance between two boolean fuzzy matrices A and B of order $m \times n$ is $m.n$. It is possible only when one of the following conditions hold. $a_{ij}=1$ and $b_{ij}=0$ or $a_{ij}=0$ and $b_{ij}=1$. Again if $a_{ij}=b_{ij}$ then distance will be zero, it is the minimum distance between two matrices.

Depending on the values of $H^*(A, B)$ or $E^*(A, B)$ we can define the following terms.

(i) If $H^*(A, B)=1$ or $E^*(A, B)=1$ then A and B are *totally opposite.*

(ii) If $H^*(A, B)=0.5$ or $E^*(A, B)=0.5$ then A and B are *nearly equal.*

(iii) If $H^*(A, B)=0.25$ or $E^*(A, B)=0.25$ then A and B are *almost equal.*

(iv) If $H^*(A, B)=0$ or $E^*(A, B)=0$ then A and B are *exactly equal.*

PROPERTIES OF DISTANCES

A large number of properties for Hamming distance and Euclidean distance are investigated in this section, which are presented below.

Property 1: For any fuzzy matrix A,

(i) $H(A, A^{[2]}) \le H(A, A^{[k]})$; $k = 2, 3, \ldots$

(ii) $H(A, [2]A) \le H(A, [k]A)$; $k = 2, 3, \ldots$

(iii) $E(A, A^{[2]}) \le E(A, A^{[k]})$; $k = 2, 3, \ldots$

(iv) $E(A, [2]A) \le E(A, [k]A)$; $k = 2, 3, \ldots$

(v) $H(A, A^{[2]}) = H(A, [2]A)$

(vi) $E(A, A^{[2]}) = E(A, [2]A)$

Proof: (i) Let $A = [a_{ij}]$.

Then, $A^{[2]} = A \odot A = [a^2_{ij}]$. For any positive integer k, $A^{[k]} = [a^k_{ij}]$. Since $0 \le a_{ij} \le 1$ then, $a^2_{ij} \ge a^3_{ij} \ge .... \ge a^k_{ij}$, for any positive integer k. Hence, $H(A, A^{[2]}) \le H(A, A^{[k]})$, $k = 2, 3,...$

(ii) Let $A = [a_{ij}]$.

Then, $[2]A = A \oplus A = [2a_{ij} - a^2_{ij}] = [1 - (1 - a_{ij})^2]$. For any positive inteher k, we have $[k]A = [1-(1 - a_{ij})^k]$. Now, $H(A,[2]A) = \sum_{i=1}^{n} \sum_{j=1}^{n} \left| a_{ij} - 1 + \left(1 - a_{ij}\right)^2 \right|$.

and $H(A, [k]A) = \sum_{i=1}^{n} \sum_{j=1}^{n} \left| a_{ij} - 1 + \left(1 - a_{ij}\right)^k \right|$.

Since, $1 - a - (1-a)^2 \le 1 - a - (1 - a)^k$ for $k \ge 2$

Therefore, $\left| a - 1 + (1 - a)^2 \right| \ge \left| a - 1 + (1 - a)k \right|$

Since, $0 \le a_{ij} \le 1$ we have, $(1-a_{ij})^2 \ge (1-a_{ij})k$, for any positive integer k.

Hence, $H(A, [2]A) \le H(A, [k]A)$.

Proofs of (iii), (iv) are similar to (i).

(v) $H(A, A^{[2]}) = \sum_{i=1}^{n} \sum_{j=1}^{n} \left| a_{ij} - a^2_{ij} \right|$ and

$H(A, [2]A) = \sum_{i=1}^{n} \sum_{j=1}^{n} \left| a_{ij} - 1 + \left(1 - a_{ij}\right)^2 \right|$. We have, $(a - 1) + (1 - a)^2 = a(a - 1)$ and $a - a^2 = a(1 - a)$.

Therefore, $\left| a_{ij} - a^2_{ij} \right| = \left| a_{ij} - 1 + \left(1 - a_{ij}\right)^2 \right|$.

Hence, $H(A, A^{[2]}) = H(A, [2]A)$.

Proofs of (vi) is similar to (v).

Property 2: Let I_n be the identity fuzzy matrix of order n x n and $A = [a_{ij}]$ be any FM of the same order. Then,

(i) I^c_n and $A \ominus I_n$ are irreflexive FMs.

(ii) $I_n \vee A$ and $I_n \oplus A$ are relexive FMs.

(iii) $I_n \wedge A$, $I_n \odot A$ and $I_n \$ A$ are diagonal FMs.

(iv) $I_n @ A$ is weakly reflexive FM.

(v) $I_n \oplus (A \oplus A')$ is reflexive and symmetric FM.

Property 3: Let I_n be the identity FM of order $n \times n$ and $A = [a_{ij}]$ be any FM of the same order. Then,

(i) $H(I_n \odot A, I_n \wedge A) = 0$.

(ii) $H(I_n \oplus A, I_n \vee A) = 0$.

(iii) $H(I_n \odot A, I_n \$ A) \leq n$.

(iv) $H(I_n, I_n \odot A) \leq n$.

(v) $H(I_n, I_n \wedge A) \leq n$.

(vi) $H(I_n, I_n \$ A) \leq n$.

(vii) $H(I_n, I^c_n) = n^2$.

(viii) $H(I_n \oplus (A \oplus A'), I_n \oplus A) \leq n^2 - n$.

(ix) $H(I^c_n, A \ominus I_n) \leq n^2 - n$.

(x) $H(I_n, I_n \oplus A) \leq n^2 - n$.

(xi) $H(I_n, I_n \vee A) \leq n^2 - n$.

Proof: Proofs of (i) and (ii) are trivial.

(iii) Since both the FMs $I_n \odot A$ and $I_n \$ A$ are diagonal FMs, then all the non-diagonal elements of both the FMs are same, in particular they are zero. The diagonal elements of $I_n \odot A$ and $I_n \$ A$ are different. Here the number of diagonal elements is 'n'.

Hence, $H(I_n \odot A, I_n \$ A) \leq n$.

Again if all the diagonal elements of A are either 1 or 0, then all the diagonal elements of $I_n \odot A$ and $I_n \$ A$ are same, they are either 1 or 0 respectively.

Therefore, $H(I_n \odot A, I_n \$ A) = 0$.

The proofs of (iv), (v) and (vi) are similar to (iii).

(iv) In this case I_n is identity FM of order $n \times n$, then it is obvious that all the diagonal elements of I_n are 1 and all the non-diagonal elements are 0. I^c_n is irreflexive FM of the same order whose all the diagonal elements are 0 all the non-diagonal elements are 1.

Hence, $H(I_n, I^c_n) = n^2$.

(viii) Here all the diagonal elements ('n' in number) of $I_n \oplus (A \oplus A')$ and $I_n \oplus A$ are same, they are 1, since both the FMs $I_n \oplus (A \oplus A')$ and $I_n \oplus A$ are reflexive FMs of order $n \times n$. But the non-diagonal elements of both the FMs are different from each other. The number of non-diagonal elements of FMs $I_n \oplus (A \oplus A')$ and $I_n \oplus A$ are $n^2 - n$.

Therefore, $H(I_n \oplus (A \oplus A'), I_n \oplus A) \leq n^2 - n$.

The proofs of (ix), (x) and (xi) are similar to (viii).

Property 4: For any two fuzzy matrices $A = [a_{ij}]$ *and* $B = [b_{ij}]$ *of the same order,*

(*i*) $H(A, A \wedge B) = H(B, A \vee B)$.

(*ii*) $H(A, A \vee B) = H(B, A \wedge B)$.

(*iii*) $H(A, A \oplus B) = H(B, A \odot B)$.

(*iv*) $H(A, A \odot B) = H(B, A \oplus B)$.

(*v*) $H(A \oplus B, A \vee B) = H(A \odot B, A \wedge B)$.

(*vi*) $H(A, B) = H(A \vee B, A \wedge B)$.

(*vii*) $H(A \odot B, A \vee B) = H(A \oplus B, A \wedge B)$.

(*viii*) $H(A, A @ B) = H(B, A @ B)$.

(*ix*) $H(A @ B, A \vee B) = H(A @ B, A \wedge B)$.

(*x*) $H(A \oplus B, A @ B) = H(A \odot B, A @ B)$.

(*xi*) $H(A, A @ B) = H(A @ B, A \wedge B)$.

(*xii*) $H(A^c \oplus B^c, (A \oplus B)^c) = H(A^c \odot B^c, (A \odot B)^c)$.

(*xiii*) $H(A^c \oplus B^c, (A \odot B)^c) = H((A \oplus B)^c, A^c \odot B^c)$.

Proof (vii): We have,

$$H(A \odot B, A \vee B) = \sum_{i=1}^{n} \sum_{j=1}^{n} \left| a_{ij}.b_{ij} - \max\{a_{ij}, b_{ij}\} \right| \text{ and}$$

$$H(A \odot B, A \vee B) = \sum_{i=1}^{n} \sum_{j=1}^{n} \left| a_{ij} + b_{ij} - a_{ij}.b_{ij} - \max\{a_{ij}, b_{ij}\} \right|$$

Two cases will arise:

Case-I When $a_{ij} \geq b_{ij}$ then $H(A \odot B, A \vee B) = \sum_{i=1}^{n} \sum_{j=1}^{n} \left| a_{ij}.b_{ij} - a_{ij} \right|$ and also

$H(A \oplus B, A \wedge B) = \sum_{i=1}^{n} \sum_{j=1}^{n} \left| a_{ij} - a_{ij}.b_{ij} \right|$.

Case-II. When $b_{ij} \geq a_{ij}$ then $H(A \odot B, A \vee B) = \sum_{i=1}^{n} \sum_{j=1}^{n} \left| a_{ij}b_{ij} - b_{ij} \right|$ and

$H(A \oplus B, A \wedge B) = \sum_{i=1}^{n} \sum_{j=1}^{n} \left| b_{ij} - a_{ij}.b_{ij} \right|$.

Hence, from both the cases we have, $H(A \odot B, A \vee B) = H(A \oplus B, A \wedge B)$.

(xiii) We have $A^c = [1 - a_{ij}]$ and $B^c = [1 - b_{ij}]$.

Similarly, $(A \odot B)^c = [1 - a_{ij}.b_{ij}]$ and $(A \oplus B)^c = [1 - (a_{ij} + b_{ij} - a_{ij}.b_{ij})]$.

Now, $H(A^c \oplus B^c, (A \odot B)^c) = \sum\sum \left| 1 - a_{ij} + 1 - b_{ij} - \left(1 - a_{ij}\right).\left(1 - b_{ij}\right) - 1 + a_{ij}.b_{ij} \right|$

$= \sum\sum \left| 1 - \left(a_{ij} + b_{ij} - a_{ij}.b_{ij}\right) - \left(1 - a_{ij}\right).\left(1 - b_{ij}\right) \right|$.

$H((A \oplus B)^c, A^c \odot B^c) = \sum\sum \left| 1 - \left(a_{ij} + b_{ij} - a_{ij}.b_{ij}\right) - \left(1 - a_{ij}\right).\left(1 - b_{ij}\right) \right|$.

Hence, $H(A^c \oplus B^c, (A \odot B)^c) = H((A \oplus B)^c, A^c \odot B^c)$.

Remaining all other proofs are same as (vii).

Property 5: For any two fuzzy matrices $A = [a_{ij}]$ and $B = [b_{ij}]$ of the same order,

(*i*) $E(A, A \wedge B) = E(B, A \vee B)$.

(*ii*) $E(A, A \vee B) = E(B, A \wedge B)$.

(*iii*) $E(A, A \oplus B) = E(B, A \odot B)$.

(*iv*) $E(A, A \odot B) = E(B, A \oplus B)$.

(*v*) $E(A \oplus B, A \vee B) = E(A \odot B, A \wedge B)$.

(*vi*) $E(A, B) = E(A \vee B, A \wedge B)$.

(*vii*) $E(A \odot B, A \vee B) = E(A \oplus B, A \wedge B)$.

(*viii*) $E(A, A @ B) = E(B, A @ B)$.

(*ix*) $E(A @ B, A \vee B) = E(A @ B, A \wedge B)$.

(*x*) $E(A \oplus B, A @ B) = E(A \odot B, A @ B)$.

(*xi*) $E(A, A @ B) = E(A @ B, A \wedge B)$.

(*xii*) $E(A^c \oplus B^c, (A \oplus B)^c) = E(A^c \odot B^c, (A \odot B)^c)$.

(*xiii*) $E(A^c \oplus B^c, (A \odot B)^c) = E((A \oplus B)^c, A^c \odot B^c)$.

Property 6: For any two fuzzy matrices $A = [a_{ij}]$ and $B = [b_{ij}]$ of same order,

(*i*) $H(A, A \odot B) \geq H(A, A \wedge B)$.

(*ii*) $H(A, A \odot B) \geq H(A \oplus B, A \vee B)$.

(*iii*) $H(A, A \oplus B) \geq H(A, A \vee B)$.

(*iv*) $H(A, A \oplus B) \geq H(A \oplus B, A \vee B)$.

(*v*) $H(A \odot B, A \vee B) \geq H(A \vee B, A \wedge B)$.

(*vi*) $H(A \vee B, A \wedge B) \geq H(A @ B, A \vee B)$.

(*vii*) $H(A \oplus B, A @ B) \geq H(A @ B, A \vee B)$.

(*viii*) $H(A \odot B, A \vee B) \geq H(A \oplus B, A @ B)$.

(*ix*) $H(A \oplus B, A \odot B) \geq H(A \oplus B, A @ B)$.

(*x*) $H(A \oplus B, A \wedge B) \geq H(A \oplus B, A \vee B)$.

(*xi*) $H(A \oplus B, A \ominus B) \geq H(A \oplus B, A \vee B)$.

(*xii*) $H(A \odot B, A \vee B) \geq H(A' \oplus B, A \vee B)$.

(*xiii*) $H(A \oplus B, A \wedge B) \geq H(A \vee B, A @ B)$.

(*xiv*) $H(A \vee B, A \$ B) \geq H(A \vee B, A \wedge B)$.

(*xv*) $H(A \vee B, A \$ B) \geq H(A \wedge B, A \$ B)$.

(*xvi*) $H(A \oplus B, A \$ B) \geq H(A \vee B, A \$ B)$.

(*xvii*) $H(A \oplus B, A \wedge B) \geq H(A \vee B, A \wedge B)$.

(*xviii*) $H(A \ominus B, A \oplus B) \geq H(A \ominus B, A \vee B)$.

Proof: Proofs of (i) to (iv) are trivial.

(v) We have,

$$H(A \odot B, A \vee B) = \sum_{i=1}^{n} \sum_{j=1}^{n} \left| a_{ij} . b_{ij} - max\{a_{ij}, b_{ij}\} \right| \text{ and}$$

$$H(A \vee B, A \wedge B) = \sum_{i=1}^{n} \sum_{j=1}^{n} \left| max\{a_{ij}, b_{ij}\} - min\{a_{ij}, b_{ij}\} \right|.$$

Two cases will arise.

Case-I. When $a_{ij} \geq b_{ij}$ then, $H(A \odot B, A \vee B) = \sum_{i=1}^{n} \sum_{j=1}^{n} \left| a_{ij} . b_{ij} - a_{ij} \right|$ and

$H(A \vee B, A \wedge B) = \sum_{i=1}^{n} \sum_{j=1}^{n} \left| a_{ij} - b_{ij} \right|$.

Since $b_{ij} \geq a_{ij}$, b_{ij} as $0 \leq a_{ij}, b_{ij} \leq 1$ therefore $|a_{ij}.b_{ij} - a_{ij}| \geq |a_{ij} - b_{ij}|$.

Hence, $H(A \odot B, A \vee B) \geq H(A \vee B, A \wedge B)$.

Case-II. When $b_{ij} \geq a_{ij}$ we have

$H(A \odot B, A \vee B) = \sum_{i=1}^{n} \sum_{j=1}^{n} \left| a_{ij}.b_{ij} - b_{ij} \right|$ and

$H(A \vee B, A \wedge B) = \sum_{i=1}^{n} \sum_{j=1}^{n} \left| b_{ij} - a_{ij} \right|$.

Hence, from both the cases we have,

$H(A \odot B, A \vee B) \geq H(A \vee B, A \wedge B)$.

Remaining all the proofs are similar to (v).

Property 7: For any two fuzzy matrices $A = [a_{ij}]$ and $B = [b_{ij}]$ of same order,

(*i*) $E(A, A \odot B) \geq E(A, A \wedge B)$.

(*ii*) $E(A, A \odot B) \geq E(A \oplus B, A \vee B)$.

(*iii*) $E(A, A \oplus B) \geq E(A, A \vee B)$.

(*iv*) $E(A, A \oplus B) \geq E(A \oplus B, A \vee B)$.

(*v*) $E(A \odot B, A \vee B) \geq E(A \vee B, A \wedge B)$.

(*vi*) $E(A \vee B, A \wedge B) \geq E(A @ B, A \vee B)$.

(*vii*) $E(A \oplus B, A @ B) \geq E(A @ B, A \vee B)$.

(*viii*) $E(A \odot B, A \vee B) \geq E(A \oplus B, A @ B)$.

(*ix*) $E(A \oplus B, A \odot B) \geq E(A \oplus B, A @ B)$.

(*x*) $E(A \oplus B, A \wedge B) \geq E(A \oplus B, A \vee B)$.

(*xi*) $E(A \oplus B, A \ominus B) \geq E(A \oplus B, A \vee B)$.

(*xii*) $E(A \odot B, A \vee B) \geq E(A \oplus B, A \vee B)$.

(*xiii*) $E(A \oplus B, A \wedge B) \geq E(A \vee B, A @B)$.

(*xiv*) $E(A \vee B, A \$ B) \geq E(A \vee B, A \wedge B)$.

(*xv*) $E(A \vee B, A \$ B) \geq E(A \wedge B, A \$ B)$.

(*xvi*) $E(A \oplus B, A \$ B) \geq E(A \vee B, A \$ B)$.

(*xvii*) $E(A \oplus B, A \wedge B) \geq E(A \vee B, A \wedge B)$.

(*xviii*) $E(A \ominus B, A \oplus B) \geq E(A \ominus B, A \vee B)$.

Propery 8: for any two fuzzy matrices $A = [a_{ij}]$ and $B = [b_{ij}]$ of same order,

(*i*) $H((A \wedge B) \wedge (A \ominus B), (A \wedge B \vee (A \ominus B)) \geq H((A \wedge B) \wedge (A \ominus B), (A \vee B) \vee (A \ominus B))$.

(*ii*) $H((A \wedge B) \wedge (A \ominus B), (A \vee B \vee (A \ominus B)) \geq H((A \wedge B) \wedge (A \ominus B), (A \vee B) \wedge (A \ominus B))$.

(*iii*) $H((A \wedge B) \wedge (A \ominus B), (A \vee B \vee (A \ominus B)) \geq H((A \vee B) \wedge (A \ominus B), (A \wedge B) \vee (A \ominus B))$.

(*iv*) $H((A \vee B) \vee (A \ominus B), (A \vee B \wedge (A \ominus B)) \geq H((A \vee B) \wedge (A \ominus B), (A \wedge B) \vee (A \ominus B))$.

(*v*) $H((A \vee B) \vee (A \ominus B), (A \vee B \wedge (A \ominus B)) \geq H((A \vee B) \vee (A \ominus B), (A \wedge B) \vee (A \ominus B))$.

Propery 9: for any two fuzzy matrices $A = [a_{ij}]$ and $B = [b_{ij}]$ of same order,

(*i*) $E((A \wedge B) \wedge (A \ominus B), (A \wedge B \vee (A \ominus B)) \geq E((A \wedge B) \wedge (A \ominus B), (A \vee B) \vee (A \ominus B))$.

(*ii*) $E((A \wedge B) \wedge (A \ominus B), (A \vee B \vee (A \ominus B)) \geq E((A \wedge B) \wedge (A \ominus B), (A \vee B) \wedge (A \ominus B))$.

(*iii*) $E((A \wedge B) \wedge (A \ominus B), (A \vee B \vee (A \ominus B)) \geq E((A \vee B) \wedge (A \ominus B), (A \wedge B) \vee (A \ominus B))$.

(*iv*) $E((A \vee B) \vee (A \ominus B), (A \vee B \wedge (A \ominus B)) \geq E((A \vee B) \wedge (A \ominus B), (A \wedge B) \vee (A \ominus B))$.

(*v*) $E((A \vee B) \vee (A \ominus B), (A \vee B \wedge (A \ominus B)) \geq E((A \vee B) \vee (A \ominus B), (A \wedge B) \vee (A \ominus B))$.

APPLICATION TO CHARACTER RECOGNITION

For a long time human being tried to perform all types of work automatically instead of manual procedures. The character (alphabet) recognition is one of them. Several conventional methods are available to recognise the characters. But recognition of a character gets easier by measuring the Hamming distance. Here we discuss about the recognition of a character (printed only) by the help of Hamming distance. The recognition of hand written characters is a challenging task for computer scientist due to the large variability of style of the hand written characters. Specially, in the case of hand written character variation of shape occurs due to writing habit, style, mood, etc. Which will differ from man to man and also some other factors such as the writing instruments, writing surface, etc. Now we shall illustrate how character recognition is possible by this process. There are 52 fixed printed English alphabets in binary matrix form including upper case and lower case alphabets. Now a printed manuscript of same font, same size and shape (length, width etc.) is taken to serve the purpose. A scanner which is placed on the top of the printed manuscript and scanner scanned each of the character. As a scanning process the scanner will draw a horizontal scan line when it will find black pixels of the character at the time of its top-down movement from the top of the manuscript. It will draw another horizontal scan line i.e., parallel to the first horizontal line at the fag-end of that

character. After completion of downwards movement the scanner will starts its horizontal movement and it will draw two parallel vertical scan lines touching at least one black pixel in the left and right side of the same character. Thus we formed a minimum sized rectangular box called *bounding box* which is needed to enclose the character. The black pixels of the character within the bounding box are filled up by 1 and white pixels are filled up by 0. It is nothing but a binary matrix of the character is formed. Now we measure the Hamming distance between the worked out binary matrix and the former binary matrix representation of 52 given characters. For which specific binary matrix of 52 former given characters the Hamming distance is zero, the worked out character will be the same specific character. In this case, there are some limitations. The characters have same font, same size and shape. Here for example, we consider two printed characters, say, 'h' and 'g'. Every pixel of both the characters (tracing path of the character) is filled up by 1 and the other pixels (back ground of the character) is filled up by 0. The boolean matrices of these two characters are shown in Figure 1. The boolean matrices for the characters 'h' and 'g' are respectively by X and Y.

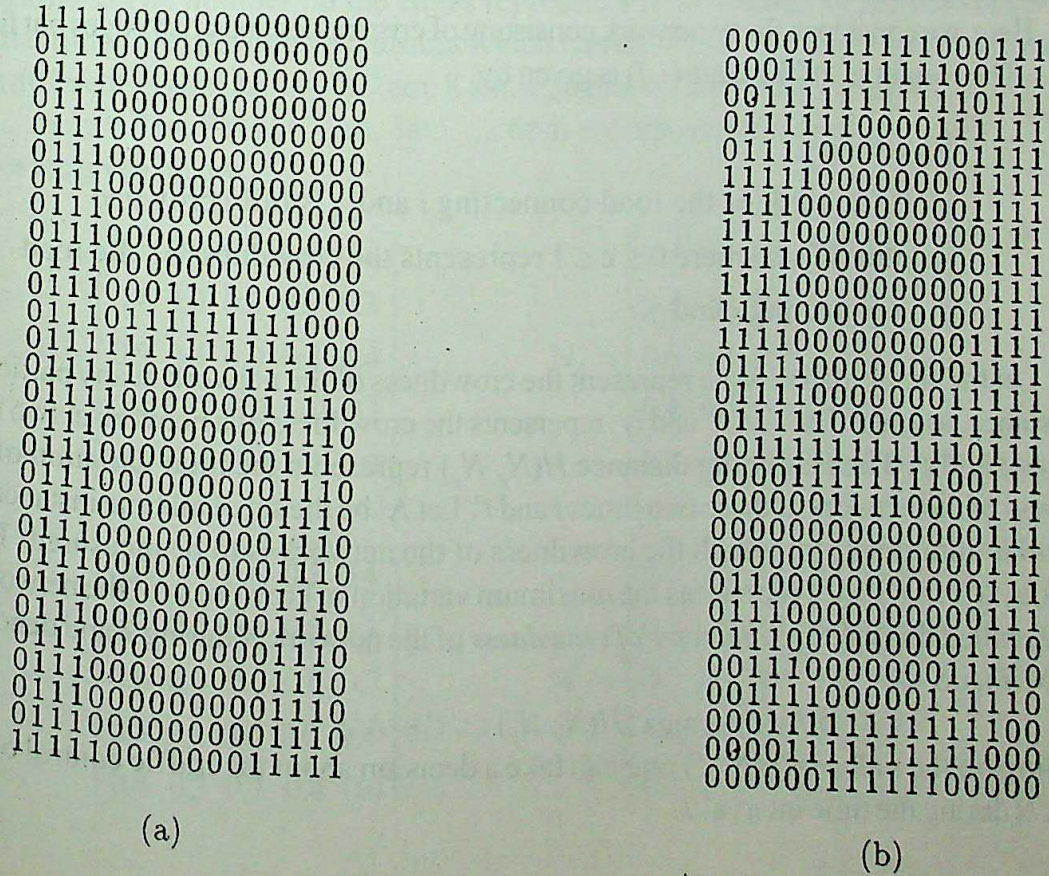

Figure 1: Binary matrices (a) for 'h' and (b) for 'g'

The Hamming distance between the matrices X and Y is $H(X, Y) = 215$.

This imply that the characters 'h' and 'g' for the matrices X and Y are not same, i.e., they are different from each other. But $H(X, X) = 0$ and $H(Y, Y) = 0$. Here Hamming distance in both the cases are zero. These implies that both the characters are same in each of the cases. Becuse same character have the same font, same size and shape, therefore the boolean matrix representation of a particular character will be exactly same. Hence all the time Hamming distance will be zero, if we measure the distance between the same characters.

ANALYSIS OF CROWDNESS OF A NETWORK

In this section, another application of distances between matrices is presented. We consider a network $N = (V, E)$ consisting of $|V| = n$ nodes and $|E| = m$ edges where $V = \{v_1, v_2, ..., v_n\}$ and $E = \{e_1, e, ..., e_m\}$ represent the set of nodes and set of edges of the network N. For example, $v_1, v_2, ..., v_n$ may represent the important places of a city and $e_1, e_2, ..., e_m$ represent the roads connecting the places. The weight of each edge represents the crowdness of the road connecting the places. The crowdness of a road can not be represented as crisp value, it should be a fuzzy quantity. The network of this type called the *fuzzy network* (or *graph*). So, a special investigation is required to study these type of problems.

Here, we consider a fuzzy network consisting of crisp nodes and crisp edges but fuzzy weights. The weight w_{ij} of the edge (i, j) is given by

$$w_{ij} = \begin{cases} 0, \text{ for } i = j \\ 1, \text{ if } (i, j) \notin E \text{ or the road connecting } i \text{ and } j \text{ is fully crowded} \\ c, \text{ otherwise, where } 0 \le c \le 1 \text{ represents the crowdness of the road} \\ \quad \text{connecting } i \text{ and } j. \end{cases}$$

Let the fuzzy matrix N_t be represent the crowdness of the network at any particular time instance, say, at t. The FM N_t and $N_{t'}$ repersents the crowdness of a network at two time instances t and t'. The Hamming distance $H(N_t, N_{t'})$ represents the total variation of the crowdness of the network at these two times t and t'. Let Λ^T be the set of all time instances of a particular duration T, for which the crowdness of the network is to be measured. Then $\max\{H(N_t, N_{t'}) : t, t' \in \Lambda^T\}$ represents the maximum variation of crowdness of the network N during T, called this value as *diameter of crowdness* of the network N during T and denoting it by $\delta(N, T)$, i.e.

$$\delta(N, T) = \max\{H(N_t, N_{t'}) : t, t' \in \Lambda^T\}.$$

Depending on the value of $\delta(N, T)$ one can take a decision about the traffic control of the network N during the time interval T.

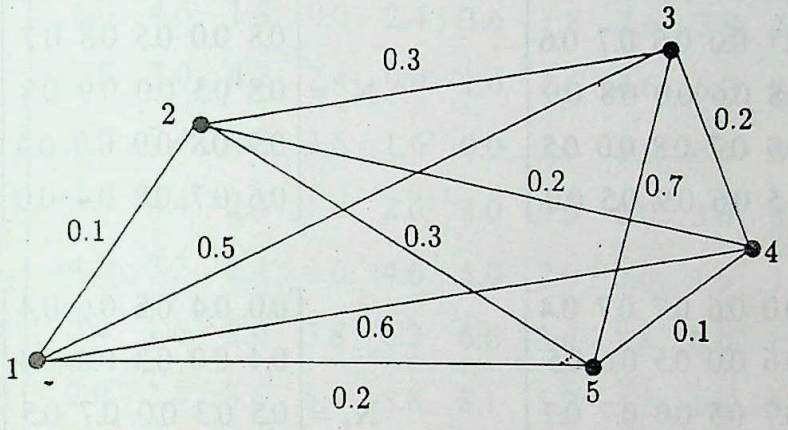

Figure 2: A fuzzy network

To illustrate our problem we consider a network N of Figure 2 consisting five places and ten edges. The number on the edges represent the crowdness of the network N at a particular time. We take twelve matrices which represent the crowdness of the network at twelve different instances, say, at 7 am, 8 am, ..., 6 pm. So $T = [7\text{ am}, 6\text{pm}]$ and $\Lambda^T = \{7\text{ am}, 8\text{ am}, ..., 6\text{pm}\}$. The FMs at 7 am, 8am, ..., 6pm are represented by $N_1, N_2, ..., N_{12}$. These matrices are given below.

$$N_1 = \begin{bmatrix} 0.0 & 0.1 & 0.5 & 0.4 & 0.2 \\ 0.1 & 0.0 & 0.3 & 0.2 & 0.3 \\ 0.5 & 0.3 & 0.0 & 0.2 & 0.4 \\ 0.4 & 0.2 & 0.2 & 0.0 & 0.1 \\ 0.2 & 0.3 & 0.4 & 0.1 & 0.0 \end{bmatrix} \qquad N_2 = \begin{bmatrix} 0.0 & 0.3 & 0.6 & 0.4 & 0.3 \\ 0.3 & 0.0 & 0.4 & 0.3 & 0.2 \\ 0.6 & 0.4 & 0.0 & 0.3 & 0.5 \\ 0.4 & 0.3 & 0.3 & 0.0 & 0.2 \\ 0.3 & 0.2 & 0.5 & 0.2 & 0.0 \end{bmatrix}$$

$$N_3 = \begin{bmatrix} 0.0 & 0.3 & 0.6 & 0.5 & 0.4 \\ 0.3 & 0.0 & 0.6 & 0.5 & 0.3 \\ 0.6 & 0.6 & 0.0 & 0.6 & 0.7 \\ 0.5 & 0.5 & 0.6 & 0.0 & 0.4 \\ 0.4 & 0.3 & 0.7 & 0.4 & 0.0 \end{bmatrix} \qquad N_4 = \begin{bmatrix} 0.0 & 0.5 & 0.7 & 0.6 & 0.4 \\ 0.5 & 0.0 & 0.6 & 0.5 & 0.4 \\ 0.7 & 0.6 & 0.0 & 0.8 & 0.8 \\ 0.6 & 0.5 & 0.8 & 0.0 & 0.5 \\ 0.4 & 0.4 & 0.8 & 0.5 & 0.0 \end{bmatrix}$$

$$N_5 = \begin{bmatrix} 0.0 & 0.7 & 0.8 & 0.9 & 0.5 \\ 0.7 & 0.0 & 0.6 & 0.7 & 0.6 \\ 0.8 & 0.6 & 0.0 & 0.8 & 0.9 \\ 0.9 & 0.7 & 0.8 & 0.0 & 0.5 \\ 0.5 & 0.6 & 0.9 & 0.5 & 0.0 \end{bmatrix} \qquad N_6 = \begin{bmatrix} 0.0 & 0.8 & 0.8 & 0.9 & 0.6 \\ 0.8 & 0.0 & 0.5 & 0.8 & 0.7 \\ 0.8 & 0.5 & 0.0 & 0.9 & 0.8 \\ 0.9 & 0.8 & 0.9 & 0.0 & 0.4 \\ 0.6 & 0.7 & 0.8 & 0.4 & 0.0 \end{bmatrix}$$

$$N_7 = \begin{bmatrix} 0.0 & 0.6 & 0.7 & 0.7 & 0.4 \\ 0.6 & 0.0 & 0.5 & 0.6 & 0.5 \\ 0.7 & 0.5 & 0.0 & 0.7 & 0.7 \\ 0.7 & 0.6 & 0.7 & 0.0 & 0.3 \\ 0.4 & 0.5 & 0.7 & 0.3 & 0.0 \end{bmatrix} \qquad N_8 = \begin{bmatrix} 0.0 & 0.4 & 0.5 & 0.6 & 0.4 \\ 0.4 & 0.0 & 0.3 & 0.6 & 0.4 \\ 0.5 & 0.3 & 0.0 & 0.7 & 0.5 \\ 0.6 & 0.6 & 0.7 & 0.0 & 0.3 \\ 0.4 & 0.4 & 0.5 & 0.3 & 0.0 \end{bmatrix}$$

$$N_9 = \begin{bmatrix} 0.0 & 0.3 & 0.5 & 0.4 & 0.3 \\ 0.3 & 0.0 & 0.3 & 0.5 & 0.3 \\ 0.5 & 0.3 & 0.0 & 0.6 & 0.5 \\ 0.4 & 0.5 & 0.6 & 0.0 & 0.2 \\ 0.3 & 0.3 & 0.5 & 0.2 & 0.0 \end{bmatrix} \qquad N_{10} = \begin{bmatrix} 0.0 & 0.2 & 0.4 & 0.3 & 0.2 \\ 0.2 & 0.0 & 0.2 & 0.4 & 0.3 \\ 0.4 & 0.2 & 0.0 & 0.5 & 0.4 \\ 0.3 & 0.4 & 0.5 & 0.0 & 0.2 \\ 0.2 & 0.3 & 0.4 & 0.2 & 0.0 \end{bmatrix}$$

$$N_{11} = \begin{bmatrix} 0.0 & 0.3 & 0.4 & 0.3 & 0.3 \\ 0.3 & 0.0 & 0.3 & 0.4 & 0.3 \\ 0.4 & 0.3 & 0.0 & 0.6 & 0.4 \\ 0.3 & 0.4 & 0.6 & 0.0 & 0.3 \\ 0.3 & 0.3 & 0.4 & 0.3 & 0.0 \end{bmatrix} \qquad N_{12} = \begin{bmatrix} 0.0 & 0.2 & 0.4 & 0.4 & 0.3 \\ 0.2 & 0.0 & 0.3 & 0.5 & 0.4 \\ 0.4 & 0.3 & 0.0 & 0.5 & 0.3 \\ 0.4 & 0.5 & 0.5 & 0.0 & 0.3 \\ 0.3 & 0.4 & 0.3 & 0.3 & 0.0 \end{bmatrix}$$

Let N_Λ be the set of all above matrices. The Hamming distances between any two matrices are given in the following table:

	N_1	N_2	N_3	N_4	N_5	N_6	N_7	N_8	N_9	N_{10}	N_{11}	N_{12}
N_1	0.0	2.0	4.4	6.0	8.6	9.0	6.0	4.0	2.4	2.0	2.6	2.6
N_2	2.0	0.0	2.8	4.6	7.0	7.4	4.4	3.2	1.6	2.4	2.2	2.6

N_3	4.4	2.8	0.0	1.8	4.2	4.8	2.4	2.4	2.0	3.6	2.6	3.0
N_4	6.0	4.6	1.8	0.0	2.4	3.6	1.8	2.6	3.8	5.4	4.0	4.4
N_5	8.6	7.0	4.2	2.4	0.0	1.6	2.6	4.6	6.2	8.8	6.8	6.8
N_6	9.0	7.4	4.8	3.6	1.6	0.0	3.0	5.0	6.6	8.1	7.2	7.2
N_7	6.0	4.4	2.4	1.8	2.6	3.0	0.0	2.0	3.6	5.2	4.2	4.2
N_8	4.0	3.2	2.4	2.6	4.6	5.0	2.0	0.0	1.6	3.2	2.2	2.2
N_9	2.4	1.6	2.0	3.8	6.2	6.6	3.6	1.6	0.0	1.6	1.0	1.4
N_{10}	2.0	2.4	3.6	5.4	8.8	8.1	5.2	3.2	1.6	0.0	1.0	1.4
N_{11}	2.6	2.2	2.6	4.0	6.8	7.2	4.2	2.2	1.0	1.0	0.0	1.2
N_{12}	2.6	2.6	3.0	4.4	6.8	7.2	4.2	2.2	1.4	1.4	1.2	0.0

Here the diameter of N_A^* is, $\delta(N, T) = 9.0$. From the table we see that the maximum and the minimum distance is 9.0 and 1.0 respectively. Since the difference of these two values is large, then it is clear that the fluctuation of the crowdness of the network is high. From this we come to a conclusion that some necessary action should be taken to control the dense traffic when the network is highly busy. Otherwise no action is required when the network is not so busy.

If the difference of these two distances is small then it implies that crowdness of the network does not fluctuate. There are two reasons behind it. Firstly, it implies that all the time the network is not so busy. It is possible if most of the elements of the matrices are small. Then the difference between two corresponding elements of different matrices are more or less same, then it produces nearly equal distances. Automatically, the difference between the largest and the smallest distance will be small. Hence in this case no action is required.

Secondly, it may be all the time network is highly crowded. Due to crowdness of the network all the elemants of different matrices will be large. Naturally the difference of the corresponding elements of different matrices will be small. Accordingly, the difference between any two Hamming distance will be small. In this case i.e., when all the time the network is highly crowded, the traffic density or frequent traffic jam can be controlled with the help of new roads or bypass system.

CONCLUSION

In this paper, we have investigated a number of properties using Hamming and Euclidean distance. The main objective of this paper is to recognise a character automatically and to measure the fluctuation of crowdness of a network with the help of Hamming distance. The whole discussion is based on only with printed character having same font, same size and shape. In the case of hand written character the proposed method is also equally effective if it is modified. Here the fluctuation of crowdness of a network has been discussed and some decisions have been made depending on the value of Hamming distance. This conception may be useful and acceptable in tele-network system and also in many other network systems. Therefore it can be emphatically concluded that both the proposed methods serve the purpose of achieving the goal successfully.

Acknowledgement : The authors are greatly acknowledge to the referee for his valuable comments to prepare the paper.

REFERENCES

1. K. Atanassov: Intuitionistic fuzzy sets, Fuzzy Sets and Systems, 20 (1986) 87-96.
2. K. Atanassov: Operations over interval valued intuitionstic fuzzy sets, Fuzzy Sets and Systems, 64 (1994) 159-174.
3. J.C. Dunn: A graph theoretic analysis of pattern classification via Tamura's fuzzy relation, IEEE Trans. Syst. Man Cybern, SMC, 4(3) (1974) 310-313.
4. M.B. Gorzalzany: A method of inference in approximation reasoning based on interval-valued fuzzy sets, Fuzzy Sets and Systems, 21 (1987) 1-17.
5. H. Hashimoto: Convergence of powers of a fuzzy transitive matrix, Fuzzy Sets and Systems, 9 (1983) 153-160.
6. H. Hashimoto: Canonical form of a transitive matrix, Fuzzy Sets and Systems, 11 (1983) 157-162.
7. A. Kandel and L. Yelouwitz: Fuzzy chains, IEEE Trans. Syst. Man Cybern, SMC, 4(5) (1974) 472-475.
8. A. Kandel: Fuzzy mathematical Techniques with Applications (Addison-Wesley, Tokyo, 1986).
9. M. Pal, S.K. Khan and A.K. Shyamal: Intuitionistic fuzzy matrices, Notes on Intuitionistic Fuzzy Sets, 8(2) (2002) 51-62.

10. K.H. Kim and F.W. Roush: Generalised fuzzy matrices, Fuzzy Sets and Systems, 4 (1980) 293-315.

11. W. Kolodziejczyk: Canonical form of a strongly transitive fuzzy matrix, Fuzzy Sets and Systems, 22(1987) 292-302.

12. W. Kolodziejczyk: Convergence of powers of s-transitive fuzzy matrices, Fuzzy Sets and Systems, 26 (1988) 127-130.

13. H.L. Larsen and R.R. Yager: Efficient computation transitive closures, Fuzzy Sets and Systems, 38 (1990) 81-90.

14. J. X. Li: Convergence of powers of controllable fuzzy matrices, Fuzzy Sets and Systems, 62 (1994) 83-99.

15. Mantas: An overview of character recognition methodologies, Pattern Recognition, 19 (1986) 425-430.

16. M. Pal: Intuitionistic fuzzy determinant, V.U.J. Physical Sciences, 7 (2001) 87-93.

17. Z. Pawlak, Rough Sets: International J. Information and Computer Sciences, 11 (1982) 341-356.

18. H. Prade and D. Dubois: Fuzzy Sets and Systems : Theory and Applications, (Academic Press London, 1980).

19. M.Z. Ragab and E.G. Eman: The determinant and adjoint of a square fuzzy matrix, Fuzzy Sets and Systems, 61 (1994) 297-307.

20. A.K. Shyamal and M. Pal: Two new operators on fuzzy matrices, Journal of Applied Mathematics and Computing, 15 (2004) 91-107.

21. S. Tamura, S. Higuchi and K. Tanaka: Pattern classification based on fuzzy relations, IEEE Trans. Syst. Man Cybern, SMC, 1(1) (1971) 61-66.

22. M.G. Thomason: Convergence pf power of a fuzzy matrix, J. Math Anal. Appl., 57 (1977) 476-480.

23. K.Y. Wang, R.G. Casey and F.M. Wahl: Document analysis system, IBJM. Res. Dev. 26 (1982) 647-656.

24. P.S.P. Wang: Character and Handwrittenh Recognition, (World Scientific, Singapore, 1991).

25. L.J. Xin: Controllable fuzzy matrices, Fuzzy Sets and Systems, 45 (1992) 313-319.

26. L.J. Xin: Convergence of powers of controllable fuzzy matrices, Fuzzy Sets and Systems, 62 (1994) 83-88.

27. L.A. Zadeh: Fuzzy Sets, Information and Control, 8 (1965) 338-353.

28. H. J. Zimmerman: Fuzzy Set Theory and its Applications, (Kluwer Academic Publishers Boston, 1996).

Journal of Natural & Physical Sciences, Vol. 19 (1) (2005) 59-66

NON-EQUILIBRIUM THERMODYNAMIC MODEL OF TEMPERATURE-DEPENDENT BIOLOBICAL GROWTH

N. G. Sarkar

(Received 13.10.2004 Revied 25.02.2005)

ABSTRACT

The first part of the paper deals with the modification of the Gompertz equation for biological growth for temperature dependent growth rate and its solution for state near the reference value of temperature. The graphical picture for numerical solution has been presented. The second part deals with a nonequilibrium thermodynamical modelling of the growth process with temperature dependent phenomenological coefficient which requires further investigation.

Mathematics Subject Classification (2000) : 92A17

Keywords: Gompertz Equation, Characteristic value, Thermodynamic force and flux, Reference Temperature, Temperature Dependent Growth, Development Paramenter, Phenomenological Coefficient.

INTRODUTION

The study of growth, development and aging of living system is one of the fundamental problems of biological sciences. There are many equations describing the growth processes [1,2]. In most of the existing models the parmeters appearing in the model equations are taken to be constant or temperature independent. Every living organism survives with in a certain temperature range, it dies down when the temperature corsses the boundary of tolerance limit. The temperature is an important factor, which greatly influences the growth and development of the living organism. So, for a realistic picture of growth process the model equaltion should be temperature dependent [6,7]. In the present paper we have made an attempt to study the growth of a living organism on the basis of Gompertz equation with time and temperature dependent growth rate. This includes the non-equilibrium thermodynamic model and analysis of growth processes near the reference temperature of the living organism.

GOMPERTZ GROWTH EQUATION : TEMPERATURE DEPENDENT GROWTH RATE

A basic model equation describing a wide range of the growth of living systems is the Gompertz equation written in the form [3].

$$\frac{dm}{dt} = \mu e^{-Dt} m, \qquad \mu, D > 0 \tag{2.1}$$

*Department of Mathematics, Maulana Azad College, 8, Rafi Ahmed Kidwai Road, Kolkata - 700 013, India

where $m = m(t)$ is the mass (or weight) of an organism at any time t, μ is the growth rate at $t = 0$ and D is the development parameter. When m is temperature independent and depends only on time t, then the solution (2.1) is given by

$$m = m(t) = \mu_0 e^{\frac{\mu}{D}\left(1-e^{-Dt}\right)} \tag{2.2}$$

with condition

$$m(0) = m_0 > 0, \quad m(\infty) = M > m_0 \tag{2.2a}$$

where m_0 is the initial mass of an organism and M is the final mass. We now assume that growth rate μ depends on temperature T and following Arrhenius law [2,3] we take the growth rate μ as

$$\mu = \mu(T) = \mu_0 e^{-K\left[\frac{1}{T}-\frac{1}{T_c}\right]} \tag{2.3}$$

where $K = E/R$ is a constant characteristic value of the organism and T_c is the reference temperature [7].

with conditions

$$\mu_0 = \mu(T_c) > 0 \tag{2.3a}$$

where T_c is the reference temperature. Using equation (2.3) in equation (2.1) we get modified growth equation.

$$\frac{dm}{dt} = \mu_0 m e^{-\left[K\left(\frac{1}{T}-\frac{1}{T_c}\right)+Dt\right]} \equiv f\ (T,t,m), \text{ (say)} \tag{2.4}$$

At $T = T_c$ the solution of equation (2.4) becomes

$$m(t) = m(T_c,t) = m_0 e^{\frac{\mu_c}{D}\left(1-e^{-Dt}\right)} \tag{2.5}$$

The equation (2.4) is the first order non-homogeneous differential equation for Gompertzian growth model with temperature dependent growth rate.

Let us now investigate the solution of the equation (2.4) near the reference value $T = T_c$.

The mass m is now both time t and temperature T dependent. The solution of equation (2.4) at any time t for $T = T_c$ is known and given by equation (2.5). Now we seek the approximate solution for T sufficiently near T_c and for this we use Taylor's series expansion [5].

$$m(T, t) = m(T_c, t) + (T - T_c)\, y(t), y(0) = 0 \tag{2.6}$$

where
$$y(t) = \frac{\partial m(T,t)}{\partial T} \tag{2.7}$$

In equation (2.4) f is continuously differentiable with respect to T. Using equation (2.6) in equation (2.4) shows that $y(t)$ satisfies the equation

$$y(t) = A(t)\, y(t) + B(t), y(0) = 0 \tag{2.8}$$

where
$$A(t) = \frac{\partial f}{\partial m} \quad \text{at } T = T_c, \quad m = m(T_c, t)$$

and
$$B(t) = \frac{\partial f}{\partial T} \quad \text{at } T = T_c, \quad m = m(T_c, t)$$

here
$$A(t) = \mu_0 e^{-Dt} \quad \text{and} \quad B(t) = \alpha e^{\frac{\mu_0}{D}\left(1 - e^{-Dt}\right)} \tag{2.9}$$

where
$$a = \frac{K \mu_0 m_0}{T_c^2} \tag{2.10}$$

The complete solution of the equation (2.8) is given by

$$y(t) = \frac{a}{D}\left(1 - e^{-Dt}\right) e^{\frac{\mu_0}{D}\left(1 - e^{-Dt}\right)} \tag{2.11}$$

putting the value of $y(t)$ from equation (2.11) in equation (2.6) we get finally the solution of equation (2.4) for T near T_c as

$$m(T,t) = m_0 e^{a\left(1 - e^{-Dt}\right)} + \frac{m_0 K (T - T_c) a}{T_c^2}\left(1 - e^{-Dt}\right) e^{a\left(1 - e^{-Dt}\right)} \tag{2.12}$$

with the initial condition

$$m(T, 0) = m(T_c, 0) = m_o > 0, \quad a = \mu_0 / D \tag{2.13}$$

which determines the mass of an organism or an animal at any time t for temperature T near reference value T_c. For our present numerical experiments we shall assume $T = 27^0$C, lower reference $T_c = 25^0$C, upper reference $T_c = 29^0$C, $m_o = 10$, $D = 0.01$, $\mu_o = 0.02$, $\alpha = 2$, $K = 210$ and $0 \leq t < \infty$. Then the growth patterns of the organism given by the equation (2.12) for the fixed temperature $T = 27^0$C has been shown for both reference temperature $T_c = 25^0$C and 29^0C in Fig.1 and Fig.2 respectively.

TEMPERATURE-DEPENDENT GROWTH : NON-EQUILIBRIUM THERMODYNAMIC MODEL

The growth of a living system is the consequence of the process of metabolism, which is the result of a number of complex chemical reaction. So a realistic theory of growth should be based on the physico-chemical analysis of the process. The first attempt to such a physico-chemical theory of growth on irreversible thermodynamics is due to Prigogine and Weamme [8]. This theory was later modified by Zotin and Zotina [9,10], Lurrie and Wagensberg [11,12].

Let us now develop a non-equilibrium thermodynamic model of temperature dependent biological growth on the basis of the modified Gometzian model equation (2.8) or on the basis of the approximate solution (2.12) valid for temperature near its reference value T_c.

The fundamental problem connected with non-equilibrium thermodynamic model is to define properly the fluxes and force. For simplicity we take a simple thermodynamic flux J and a thermodynamic force X to represent the growth process. We take the flux J as the specific rate of change of mass of an organism.

$$J = \frac{1}{m}\frac{dm}{dt}, \quad m = m(T,t) \tag{3.1}$$

Equation (2.4) and (2.5) show that the stationary or steady state of growth of an organism is reached after an infinitely large time. This is practically impossible due to limited growth and finite life span of an organism. It shows that for growth and development there must be some restriction on the order of the exponential Dt. We assume that

$$|Dt| << 1 \tag{3.2}$$

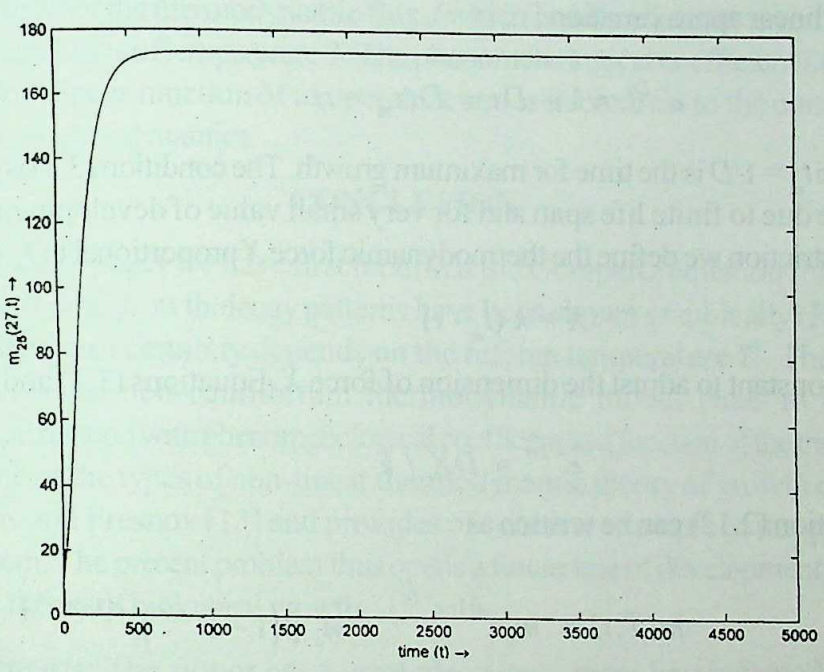

Fig.1: Graphical representation of growth pattern for reference temperature T_c = 25°C.

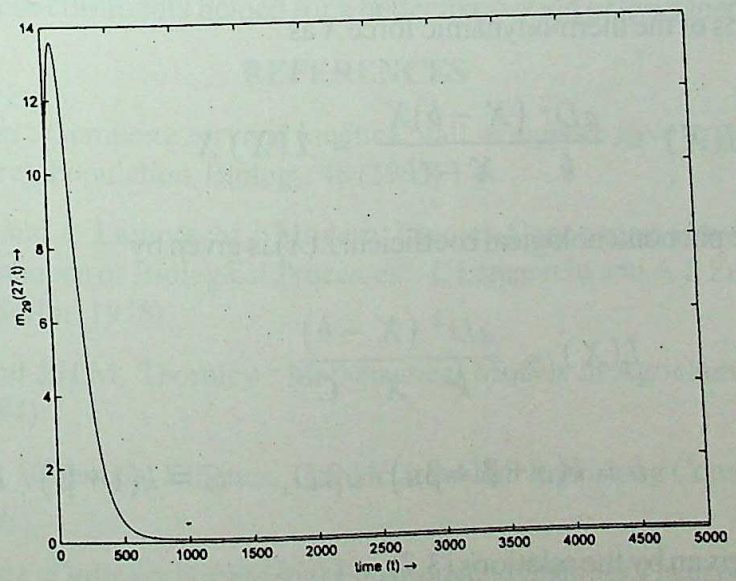

Fig. 2 : Graphical representation of growth patten for reference temperature T_c = 29°C.

and hence the linear approximation :

$$e^{-Dt} \approx 1 - Dt = D(t_m - t) \tag{3.3}$$

where $t_m = 1/D$ is the time for maximum growth. The condition (3.2) is possible for the time t is finite due to finite life span and for very small value of development parameter D. Under this restriction we define the thermodynamic force X proportional to $t_m - t$, and we write

$$X = k\,(t_m - t) \tag{3.4}$$

where k is a constant to adjust the dimension of force X. Equations (3.3) and (3.4) the give

$$e^{-Dt} \approx DX / k \tag{3.5}$$

Equation (2.12) can be written as

$$m(T,t) = m_o e^{a\left(1-e^{-Dt}\right)} + m_o\,\beta\left(1-e^{-Dt}\right)e^{a\left(1-e^{-Dt}\right)} \tag{3.6}$$

where

$$\beta = \frac{Ka\left(T - T_c\right)}{T_c^2} \geq 0; \qquad a = \mu_0 / D \tag{3.7}$$

Using equations (3.5) and (3.6) in equation (3.1), the thermodynamic flux J can be expressed in terms of the thermodynamic force X as

$$J(X) = \frac{aD^2}{k}\frac{(X-b)X}{X-C} = L(X)\,X \tag{3.8}$$

where the phenomenological coefficient $L(X)$ is given by

$$L(X) = \frac{aD^2}{k}\frac{(X-b)}{X-C} \tag{3.9}$$

with

$$b = k(a + \beta + \beta a) / a\beta D, \qquad C = k(1+\beta) / D\beta \tag{3.10}$$

and β and a are given by the relations (3.7).

We thus see that the thermodynamic flux $J(X)$ is non-linear function of thermodynamic force X. The equation (3.8) shows that $J(X) \to 0$ as $X \to 0$ as it should be. From (3.8) and

(3.10), we also see that the thermodynamic flux J which is defined as the specific growth rate is a non-linear funcations of temperature T. The phenomenological coefficient $L(X)$ defined by (3.9) is also a non-linear function of temperature and is in contrast to the constant value in linear irreversible thermodynamics.

CONCLUSION

In the present paper we have first modified the Gompertz equation for temperature dependent growth. The growth/decay patterns have been shown graphically (Fig. 1 and Fig. 2.). The growth pattern certainty depends on the referen temperature T_c. The second part which deals with the non-equilibrium thermodynamic model leads to a non-linear phenomenological relation with phenomenological coefficent as a function of the thermodynamic force. This is one of the types of non-linear thermodynamic theory of growth developed by Zotin, Konoplev and Presnov [13] and provides of concrete example of the general theory developed by them. The present problem thus opens a future line of development of non-linear thermodynamic theory of biological growth.

Acknowledgements: The author has a great pleasure in recording indebtedness to Prof. C.G. Chakrabarti, S.N. Bose Professor of Theoretical Physics, Department of Applied Mathematics, Calcutta University for his constant encouragement and valuable suggestions in the preparation of the paper. The author whishes to thank Mr. Malay Banerjee, Scottish Church College, Kolkata for the preparation of Computer Graph. The author also thanks the learned referee whose comments helped for a better exposition of the paper.

REFERENCES

1. D.M. Euston : Gompertz survival kinetics : fall in number alive or growth in number dead? Theoret. Population. Biology, 48 (1995) 1-6

2. R. Walter, and I, Lamprecht : Modern Theoies Concerning Growth Equation. In "Thermodynamics of Biological Processes". I. Lamprecht and A.I. Zotin (Eds) Walter de Gruyte, Berlin (1978).

3. J. France and J.H.M. Thornley : Mathematical Models in Agriclture : Butterworths, London (1984).

4. K. J. Laidler : Chemical Kinetics, Tata McGraw-Hill Publishing Company Ltd., New Delhi (1978).

5. D. A. Sanchez : Ordinary Differential Equations and Stability Theory- An lntroduction Dover Publications Inc. New York (1968).

6. S. A. L. M. Kooijman : The Von Bertalanffy Growth rate as a function of physiological parameters of Comparative Analysis in "Mathematical Ecology" (eds.) T.G. Hallan and S.A. Levin : World Scientific, Singapore (1988).

7. C.G. Chakrabarti and S. Bhadra : Non-equilibrium Thermodynamics and Stochastics of Gompertzian Growth : J. Biol. Systems, 4 (2), (1996) 151-157.

8. I. Prigogine and J.N. Weamme : Biologie et thermodynamique des' Phenomenes irreverssibles. Experimentia, 2 (1946) 451.

9. A. l. Zotin and R. S. Zotina : Thermodynamic aspects of Development Biology, J. Theor. Biol., 19 (1967) 57.

10. A. I. Zotin and R.S. Zotina : In "Thermodynamics and Kinetics of Biological Processes". I. Lamprecht and A.I. Zotin (eds.), Walter de Gruyter, Berlin (1983).

11. D. Lurric and J. Wagensberg : Entropy Balance in Biological Development and Heat Dissipation in Embryogenesis. Non-equilibrium Thermodynamics, 4 (1979) 127.

12. D. Lurrie and J. Wagensberg : Non-equilibrium Thermodynamics and Biological Growth and Development. J. Theoretical Biology, 78 (1979) 241.

13. A. I. Zotin, V. A. Konoplev and E. V. Presnov : In "Thermodynamics of Biological Processess" I. Lampretch and A.I. Zotin (eds.). Walter de Gruyter, Berlin (1978).

Journal of Natural & Physical Sciences, Vol. 19 (1) (2005) 67-73

THERMODYNAMIC AND STOCHASTIC APPROACHES TO A PREDATOR-PREY MODEL WITH PREDATOR INTERFERENCE

Syamali Bhadra*

(Received 03.07.2004 Revised 22.05.2005)

ABSTRACT

The paper deals with the non-equilibrium thermodynamic and stochastic modelling and stability analysis of a prey-predator system with predator interference.

Keywords: Predator interference, non-equibilibrium, thermodynamic stability, fluctuating enviroment, stochastic stability.

Mathematics Subject Classification (2000) : 92A17

INTRODUCTION

An interesting association of two species is that of predator and prey relationship Here, we consider an interesting model due to De Angelis [3] consisting of one prey and one predator species population interference on the trophic function. The stability of the system is tested in three different cases viz. the dynamic, the thermodynamic and the stochastic. The results obtained mathematically in this paper agree with the results obtained experimentally by Leo Luckinbill [5] in case of Paramecium Aurelia growing together with its predator Didinun Nastum.

Let the sizes of prey and predator species be denoted by $N(t)$ and $P(t)$ respectively. The model is given by

$$\left.\begin{aligned} \frac{dN}{dt} &= rN\left(1-\frac{N}{K}\right)-\frac{aNP}{(1+\alpha N+bP)} \\ \frac{dP}{dt} &= P\left[-\mu+\frac{bN}{1+\alpha N+\beta P}\right] \end{aligned}\right\} \tag{1.1}$$

where K is the carrying capacity of the prey species, r is its growth rate, a is the uptake rate, α, β are the interference rate, μ is the mortality rate of the predator, b is food conversion efficiency of the predator, all the parameters are assumed to be positive.

*(Department of Mathematics, Bidhannagar college) AK 207, Sector II, Salt Lake city, Kolkata 700091

A fundamental characteristic of a biological system is the property of stability. A biological community is considered to be stable, when the number of component populations do not undergo sharp fluctuation. This definition is close to the physical or rather thermodynamical concept of stability, which considers a system as being stable when large fluctuations which can destroy equilibrium are unlikely. The non-equilibrium modelling of any ecosystem supplemented by the stochastic theory of fluctuation is playing a significant role in the development of theoretical biology [1,2,7].

Here we analyse the non-equilibrium thermodynamic model and the stochastic model of the given system.

BACKGROUND : BASIC EQUATIONS

Let us first consider the deterministic analysis of stability of the system of equations (1.1). The steady state solution is given by

$$\frac{dN^*}{dt} = 0 \qquad \frac{dP^*}{dt} = 0 \tag{2.1}$$

where $$N^* = \frac{1}{2}\left\{K \pm \sqrt{\left(K^2 - \frac{4a\mu K}{rb}\right)}\right\}$$

$$P^* = \frac{1}{\mu\beta}\left[(b - \mu\alpha)N^* - \mu\right] \tag{2.2}$$

The steady state population exists provided $K > \frac{4a\mu}{br}$ (2.3)

Now we study the local stability analysis of the system by giving small perturbations to (N^*, P^*) such that

$$N = N^* + x, \qquad P = P^* + y$$

where (x, y) are infinitesimally small quantities.

The linearized system is given by,

$$\left.\begin{aligned}\frac{dx}{dt} &= a_{11}x + a_{12}y\\ \frac{dy}{dt} &= a_{21}x + a_{22}y\end{aligned}\right\} \tag{2.4}$$

where

$$\left.\begin{aligned}a_{11} &= K - 2N^*\\ a_{12} &= 0\\ a_{21} &= bP^* - \mu\alpha\\ a_{22} &= bN^* - \mu\beta\end{aligned}\right\} \tag{2.5}$$

The system is locally stable provided $K < 2N^*$ and $K > \frac{4a\mu}{br}$ (2.6)

THERMODYNAMIC MODEL AND STABILITY

Form the thermodynamic point of view an ecosystem is an open system exchanging nutrient, biomass and energy with the environment. In an ecosystem the energy is stored exclusively with itself and assuming that the internal energy is additive with respect to the population sizes of the ecosystem species, the transfer of energy is governed by the same equations (1.1) [6].

However, to develop the non-equilibrium thermodynamic model we transform the system of equations (2.4) to the following form

$$\left.\begin{aligned}J_1 &= L_{11}X_1 + L_{12}X_2\\ J_2 &= L_{21}X_1 + L_{22}X_2\end{aligned}\right\} \tag{3.1}$$

where

$$\left.\begin{aligned}J_1 &= \frac{dx}{dt}\\ J_2 &= \frac{dy}{dt}\end{aligned}\right\}$$ are the thermodynamic fluxes

$$\left.\begin{aligned} X_1 &= N - N^* \\ X_2 &= P - P^* \end{aligned}\right\} \tag{3.2}$$

are the thermodynamic forces.

where

$$\left.\begin{aligned} L_{11} &= K - 2N^* \\ L_{12} &= 0 \\ L_{21} &= bP^* - \mu\alpha \\ L_{22} &= bN^* - \mu\beta \end{aligned}\right\} \tag{3.3}$$

The above relations are linear phenomenological relations of irreversible thermodynamics [9]. The model is stable in the stationary state (N^*, P^*) under the followings conditions [6,9]:

$$\left(\frac{1}{2}\delta^2 S\right)\Big|_{st} = -\sum_{i=1}^{2} \delta x_i \delta J_i > 0 ,$$

where S is the entropy of the system

or $\quad L_{11}(\delta x_1)^2 + (L_{12}+L_{21})\ \delta x_1\ \delta x_2 + L_{22}(\delta x_2)^2 < 0$

which implies $K < 2N^*$ and $bN^* < \mu\beta$ or $K > \dfrac{4a\mu}{br}$ (3.4)

We thus see that conditions for the thermodynamic stability of the ecosystem governed by (2.1) are the same as that obtained by the deterministic dynamical analysis of the system.

STOCHASTIC MODEL AND STABILITY

Since the natural environment for any population are uncertain and stochastic, so here we consider small fluctuation in the population size casued by the random disturbance of the environment [4]. In order to consider the effect of randomly changing environment we add small fluctuating term $\phi(t)$ to both the equations of the linearized form (2.4).

The system of the stochastic differential equations is given by,

$$\left.\begin{aligned}\frac{dx}{d\tau} &= (K - 2N^*)x + O.y + \phi_1(\tau)\\ \frac{dy}{d\tau} &= (bp^* + \mu\alpha)x + (bN^* + \mu\beta)y + \phi_2(\tau)\end{aligned}\right\} \quad (4.1)$$

Taking Fourier transform of (4.1), we get [8]

$$\left.\begin{aligned}(K - 2N^* + i\omega)\tilde{x}(\omega) + O.\tilde{y}(\omega) + \tilde{\phi}_1(\omega)\\ (bP^* - \mu\alpha)\tilde{x}(\omega) + (bN^* - \mu\beta + i\omega)\tilde{y}(\omega) + \tilde{\phi}_2(\omega) = 0\end{aligned}\right\} \quad (4.2)$$

where the transfer functions $T_1(\omega)$ and $T_2(\omega)$ for the two populations are given by [8],

$$\left.\begin{aligned}T_1(\omega) &= \frac{\tilde{x}(\omega)}{\tilde{\varphi}_1(\omega)} = \frac{\{(bP^* - \mu\alpha) - (bN^* - \mu\beta + i\omega)\}}{\{(K - 2N^* + i\omega)(bN^* - \mu\beta + i\omega)\}}\\ T_2(\omega) &= \frac{\tilde{y}(\omega)}{\tilde{\varphi}(\omega)} = \frac{\{(bP^* - \mu\beta) - (K - 2N^* + i\omega)\}}{\{(K - 2N^* + i\omega)(bN^* - \mu\beta + i\omega)\}}\end{aligned}\right\} \quad (4.3).$$

Let us now calculate the auto covariance function ACF for the two types of species assuming the random variable $\phi_i(\tau)$ to be a white noise with spectral density D_i $(i = 1,2)$.

The ACF will be given by [8]

$$\rho_i(\tau) = \langle x_i(t)\, x_i(t+\tau)\rangle$$

$$= \frac{1}{2\pi}\int_{-\infty}^{\infty} S_i(\omega)\cos\tau\omega\, d\omega \quad (4.4a)$$

where $S_i(\omega) = |T_i(\omega)|^2 D_i \quad (i = 1,2)$ (4.4b)

Using (4.3), we have

$$\rho_i(\tau) = B_i e^{-\lambda_1|\tau|} + C_i e^{-\lambda_2|\tau|} \qquad (i = 1,2) \quad (4.5)$$

where B_i, C_i are constants and

$$-\lambda_{1,2} = \frac{1}{2}\left[-\beta \pm \sqrt{\beta^2 - 4\omega_D^2}\right] \tag{4.6}$$

$$\beta = -\left[(K - 2N^*) + (bN^* - \mu\beta)\right]$$

$$\omega_0^2 = (K - 2N^*)(bN^* - \mu\beta)$$

The stochastic stability in the sense of second-order moment requires the finiteness of ACF [8] which requires the conditions $\beta \geq 4\omega^2_0$ or equivalently

$$K < 2N^* \text{ and } K > \frac{4a\mu}{br} \tag{4.7}$$

These are the same conditions as obtained earlier from the dynamical and thermodynamic models of the system.

BIOLOGICAL VIEW OF THE MODEL

The auto correlation function states that the relationship between the two species will exist for a certain time. When the time becomes large the relationship will terminate at once. This event depends on the environment of the prey-predator's habitat. The termination of the relationship depends on the change of the atmosphere where they grow. We test our model on such a prey-predator system where Leo-Luckinbill grew Paramecium Aurelia together with its predator Didinum Nastum in 6 ml of standard cerophyl medium. The Didinum consumed all the prey in a few hours. When the medium was thickened with methyl cellulose, the populations went through two or three diverging oscillations lasting several days before becoming extinct. The results obtained from this experiment helps to test the validity of the predator-prey model used here. So that the stochastic model used here is valid for this particular predator-prey system.

CONCLUSION

The present paper is an attempt in the direction of non-equilibrium thermodynamic and stochastic dynamic modelling of a two-species predator-prey system and to investigate the criteria of stability of the system. Both the models have led to the same criteria of stability identical to that based on the deterministic differential equation method by local stability analysis. The validity of the model is tested by comparison with the Luckinbill's experiment with Didinum and Paramecium.

Acknowledgement: The author wishes to thank Dr. D. Kesh, Department of Mathematics. Jadavpur University, for his constant co-operation to prepare this paper.

REFERENCES

1. C.G. Chakrabarti, Sutapa Ghosh and Syamali Bhadra: Non-equilibrium Thermodynamics of Lotka - Volterra Ecosystems : Stability and Evaluation; J. Biological Physics, 21 (1995) 273-284.

2. C.G. Chakrabatri and Syamali Bhadra Non-equilibrium Thermodynamics and Stochastic of Gompertzian Growth; J. Biological System, 4 (1996) 151-157.

3. D.L. DeAngelis : Dynamics of Nutrient Cycling and food webs; Chapman and Hall London (1992).

4. C.W. Gardiner: Handbook of stochastic methods, springer-verlag, Berlin (1983).

5. W. Harrison, Gary : Comparing Predator-Prey Models etc.; Ecology, 76(1995)357-374.

6. P. Glansdroff and I. Prigogine : Thermodynamics Theory of Structure, Stability and Fluctuation, Wiely-Intenscience, New-York (1971).

7. I. Lamprecht and A.I., Zotin : Thermodynamics and Kinetics of Biological Processes, Walter-de-gruyter, Berlin (1983).

8. R.M. Nisbet and W.S.C. Gurney : Modelling fluctuating populations, John Wiely and Sons. New-York (1982).

9. I. Progogine : Introduction to Thermodynamics of Irreversible Processes, Interscience Publishers, New-York (1962).

Journal of Natural & Physical Sciences, Vol. 19 (1) (2005) 75-80

RADIATION FROM DART LEADER IN LF-VHF RANGE

P.P. Pathak* and Shelly Rajput*

(Received 06. 06. 2005)

ABSTRACT

The magnitude of electromagnetic radiation emitted by dart leader in LF-VHF range is not explained so far theoretically. For this explaination the electric field radiated by a corona streamer is integrated throughtout the dart leader channel. The magnitude of radiation in LF-VHF range is calculated and it is found that the computed values are higher than observed values during stepped leader.

INTRODUCTION

Lightning discharges emit electromagnetic radiation which cover a wide frequency range from few Hertz in ELF to ultraviolet rergion[4]. In VLF range the observed power is accounted for the radiation from a variable dipole constituted by the propagating lightning channel and its image in finitely conducting ground [5,6]. ELF power is accounted for lateral corona current flowing towards return stroke channel within the stepped leader sheath [9,10]. The UHF power is attributed to the Bremsstrahlung radiation arising due to coulomb field interaction in the lightning channel [7,8]. Brook and Kitagawa [1], Horner and Bradley [3] in their observations of radiation in LF-VHF band concluded that stepped leader, dart leader and K-change are strong source of radiation in this frequency range. But none of the mechanisms given above for ELF, VLF or UHF radiation could give the radiation observed in LF-VHF range. In this paper an attempt is made to explain the magnitude of observed radiation in this range during the dart leader.

THEORY

As dart leader propagates in a perviously ionised column of air, it should consist of a very large number of positive corona streamers simultaneously. All such streamers emit radiation. For calculation of radiated field from a streamer, we use streamer propagation model of Griffiths and Phelps [2]. Because of propagation in perviously ionised air column, corona streamer propagation should be vigorous, we can assume (+ve) tip charge Q to be increasing as z^2, i.e.,

$$Q = Q_0 z^2 \tag{1}$$

Now, a system of positive and negative charge density will make a variable dipole moment,

*Department of Physics, Gurukul Kangri University, Haridwar-249404

$$\vec{p}(t) = \int \vec{r}\rho(\vec{r},t)dV \tag{2}$$

$\rho(\vec{r},t)$ being charge density at position $\vec{r}$ and time t. For propagation of streamer in z-direction, Pathak [4] derived value of dipole moment using above expression as

$$\vec{p}(t) = \frac{Q}{4} z\hat{k}$$

With Q from Eq. (1) the magnitude of dipole moment becomes

$$p(t) = \frac{Q_0}{4} z^3 = \frac{Q_0}{4} v_s^3 t^3 \tag{3}$$

where v_s is the streamer velocity. Differentiating Eq. (3) twice we get

$$\frac{d^2p}{dt^2} = \frac{3}{2} Q_0 v_s^3 t \tag{4}$$

The radiated field due to a dipole is given by,

$$E_1 = \frac{1}{4\pi\varepsilon_0 c^2 r} \frac{d^2p}{dt^2} \tag{5}$$

So, using equation (4) we get,

$$E_1 = \frac{1}{4\pi\varepsilon_0 c^2 r} \frac{3}{2} Q_0 v_s^3 t \tag{6}$$

If n be the corona streamer density, the expression of electric field due to element of thickness dx at height $(H - x)$ from the ground (H being height of cloud base) is

$$dE = E_1 n\pi a^2 dx$$

$$= \frac{1}{4\pi\varepsilon_0 c^2} \frac{3}{2} \frac{n\pi a^2 Q_0 v_s^3 t dx}{\sqrt{(H-x)^2 + D^2}} \tag{7}$$

where, a is the radius of dart leader channel and D, is the distance of observation point from the foot of leader channel.

The electric field due to whole channel is given by the intergal of Eq. (7) with $dx = v\,dt$ i.e.,

$$E = \int_0^t \frac{1}{4\pi\varepsilon_0 c^2}\frac{3}{2}\frac{n\pi a^2 Q_0 v_s^3 t v dt}{\sqrt{(H - vt)^2 + D^2}}$$

$$= \frac{1}{4\pi\varepsilon_0 c^2}\frac{3}{2} n\pi a^2 Q_0 v_s^3 v \int_0^t \frac{t dt}{\sqrt{(H - vt)^2 + D^2}}$$

$$= E_0 I$$

where, v is the velocity of dart leader,

$$E_0 = \frac{1}{4\pi\varepsilon_0 c^2}\frac{3}{2} n\pi a^2 Q_0 v_s^3 v$$

$$I = \int_0^t \frac{t dt}{\sqrt{(H - vt)^2 + D^2}}$$

On solving the above integral, we get

$$I = \frac{1}{v^2}\left[\sqrt{(H - vt)^2 + D^2} - \sqrt{H^2 + D^2}\right]$$

$$- \frac{H}{v^2}\left[\ln\left\{(H - vt) + \sqrt{(H - vt)^2 + D^2}\right\} - \ln\left(H + \sqrt{H^2 + D^2}\right)\right]$$

CALCULATION AND RESULTS

As mentioned above that after the first set of stepped leader and return stroke consecutive leader steps use to be much larger than the first one, so much so that whole distance from cloud to ground is covered in one or two steps. This is known as dart leader. We

consider a dart leader, which covers a height of 4 km moving downward from cloud to ground in a single step. The radius of dart leader is of the order of few :neters in the range 1 to 10 m (same as of stepped leader). An average value of 3m can be taken for calculations. Dart leader moving in a previously ionised air column, sweeps down with speed in the range of 10^6 to 2.3×10^7 m/s[11]. For calculation it is taken as 5×10^7 m/s. We have calculated the electric field from dart leader at a distance 50 km on the ground from the foot of channel. The velocity of corona streamer is taken as 5×10^5 m/s and the initial charge on th tip of the corona streamer is taken 4.61×10^{-7}C[2]. As dart leader moves in previously ionised air left by stepped leader and return stroke, so the number of corona streamers is expected to be very large. The number of corona streamers is taken 75 m^{-3} for calculation.

With these values the electric field from dart leader of height 4 km at a distance of 50 km from the foot of leader channel is calculated. The values of electric field are plotted with propagation time. These values are fitted to a parabolic curve $A + Bt + Ct^2$ and the values of constant A, B and C are evaluated. Then by Foreier transform $E(t)$ is converted into $E(w)$ and $20\log E(f)$ is evaluated and plotted with log f. The calculated values for the electric field from dart leader are higher as compared to observations during stepped leader[12].

DISCUSSION AND CONCLUSION

The values of electric field from dart leader by positive corona streamer mechanism are plotted in the frequency range 200kHz - 300 MHz. However this is not the range in whole of which, the dart leader may radiate by this mechanism. The radiation from stepped leader can be understood by visualizing the propagation of corona streamer system over the distance of about 100 m as shown by Griffiths and Phelps[2] at velocities of the order of 10^5 m/s. A dipole of this dimension would radiate around $\lambda \geq 100$ m, i.e., $f \leq 3$ MHz. But smaller duration is available for propagation time in which the stepped leader reaches the ground and return stroke strarts i.e. less than 100μs. In this duration corona streamers can propagate upto distance of 50m only, so it can radiate around $\lambda \geq 50$m or $f \leq 6$ MHz. In case of dart leader as there are no small steps, possibility of smaller wavelength does not exist. We have full time for streamers to propagate and radiate at $\lambda \geq 50$m of $f \leq 6$ MHz. As the air column in which the dart leader propagates is already partially ionized, streamer propagation will also be vigorous and faster. The effect of this is seen in higher values of fields.

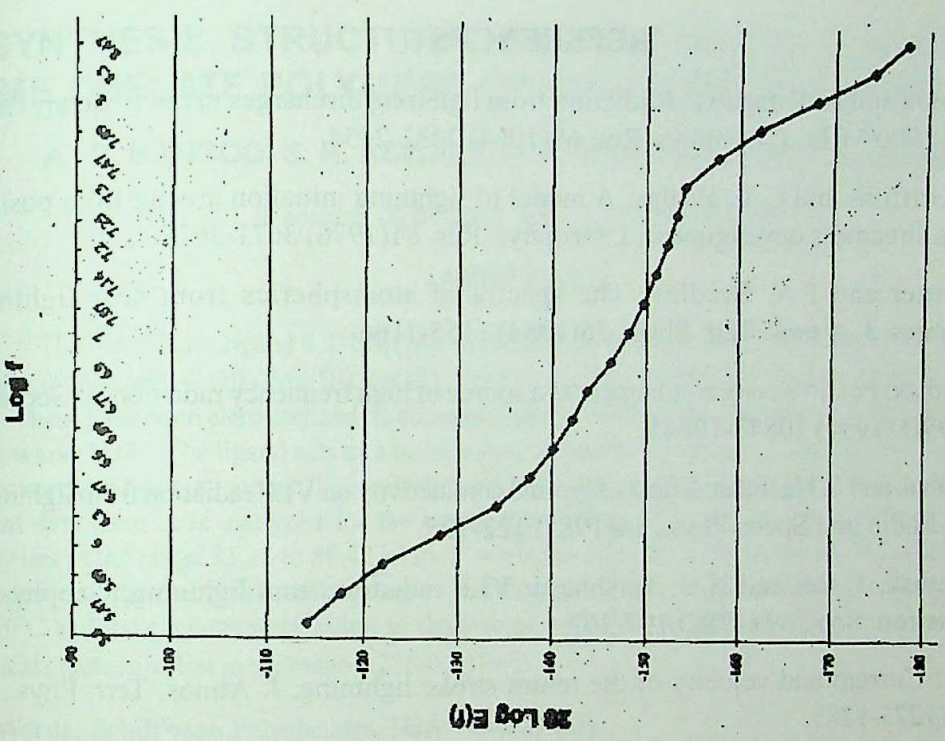

The graph showing computed values of electric field radiated during dart leader at a distance of 50 km.

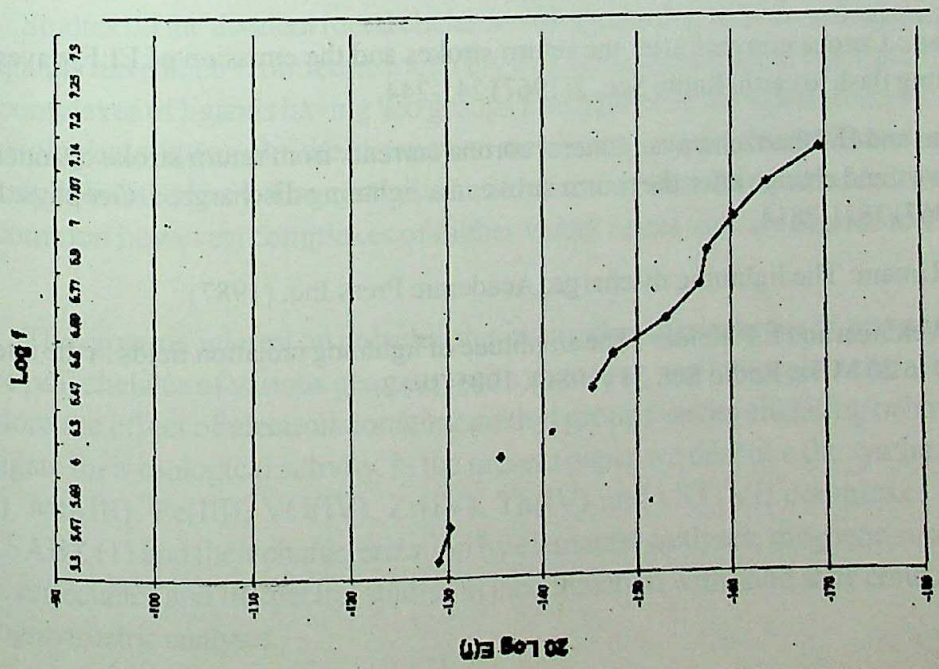

The graph showing computed values of electric field radiated during stepped leader at a distance of 50 km.

REFERENCES

1. M. Brook and N. Kitagawa: Radiation from lightning discharges in the frequeny range 400 to 1000 MHz, J. Geophys. Res. 69(1964) 2431-2434.
2. R.F., Griffiths and C.T., Phelps: A model of lightning initiation arising from positive corona streamers development, J. Geophys. Res. 81(1976) 3671-3676.
3. F. Horner and P.A. Bradley: The spectra of atomspherics from near lightning discharges, J. Atmos. Terr. Phys., 26(1964) 1155-1166.
4. P.P. Pathak: Positive corona streamers as a source of high frequency radiation, J. Geophys. Res., 99D (1994) 10843-10845.
5. P.P. Pathak and S. Haziraka: Effect of ground conductivity on VLF radiation from lightning, Ind. J. Radio and Space Phys., 14(1985) 122-125.
6. P.P. Pathak, J. Rai and N.C. Varshneya: VLF radiation from lightning, Geophys. J. Roy. Astron. Soc., 69 (1982) 197-207.
7. J. Rai : Current and velocity of the return stroke lightning, J. Atmos. Terr. Phys., 40 (1978) 1275-1285.
8. J. Rai, M. Rao and B.A.P. Tantry : Bremsstrahlung as a possible source of UHF emissions from lightning, Nature, 238 (1972) 59-60.
9. M. Rao : Corona currents after the return strokes and the emission of ELF waves in a lightning flash to earth, Radio Sci., 2(1967) 241-244.
10. M. Rao and H. Bhattacharaya : Lateral corona currents from return stroke channel and the slow field change after the return stroke in a lightning discharge, J. Geophys. Res., 71 (1967) 2811-2814.
11. M.A. Umam: The lightning discharge, Academic Press Inc. (1987).
12. C.D. Weidman and E.P. Krider : The amplitude of lightning radiation fields in the interval from 1 to 20 MHz, Radio Sci. 21 (1986). 1905-1912.

Journal of Natural & Physical Sciences, Vol. 19 (1) (2005) 81-90

SYNTHESIS, STRUCTURAL AND ELECRICAL STUDIES OF SOME CHELATE POLYMERS OF BIS-BIDENTATE SCHIFF BASE

A . D. BANSOD, S. R. ASWALE, P. R. MANDLIK AND A. S. ASWAR*

(Received 09.08.2005 and revised 29.09.2005)

ABSTRACT

The Schiff base ligand 4,4'-bis[(N-o-toluylsalicylaldimine-5)-azo] biphenyl (H_2BTSAB) and its chelate polymers with Cr(III), Mn(III), Fe(III), VO(IV), Zr(IV), Th(IV), Ti(III) and UO_2(VI) have been prepared. These have been characterized by elemental analyses, IR and reflectance spectra, magnetic susceptibilities and TGA. The ligand acts as a bisbidentate molecule coordinating through the phenolic oxygen and azomethine nitrogen atoms. The polychelates were found to be quite stable up to about 300°C. The thermal data have been analyzed for the kinetic parameters by using Broido's method and activation energy lies in the range 33.18 to 80.42 kJ mol^{-1} while the decomposition follows first order kinetics. The dependence of the electrical conductivity on the temperature has been studied in the temperature range 40-220°C and the chelates were found to show semiconducting behaviour. The activation energy of the electrical conduction lies in the range 1.233-0.127 eV.

Key Words: Schiff base, Polychelates, TGA, Conductivity.

INTRODUCTION

Studies on the divalent metal chelates with symmetric as well as unsymmetric Schiff base ligands have been reported extensively due to their biological relevance [1-4]. Even metal complexes of ligands having azo groups find a place in the literature due to their use as model biological systems. But the literature on metal complexes with Schiff base ligands having azo group is limited [5,6]. The synthesis and characterization of divalent metal chelates are quite common however; complexes of higher valent metal ions are limited to a few reports [7,8].

The growing interest on polychelates inspired us to use the bis bidentate ligand (1) to prepare polychelates of various geometry with tri-, tetra-, and hexavalent metal ions in order to explore the effect of electron donating methyl groups on the chelating behaviour and to investigate their biological activity. In the present paper we describe the synthesis of Ti(III), Cr(III), Mn(III), Fe(III), VO(IV), Zr(IV), Th(IV) and UO_2(VI) complexes with ligand H2BTSABZ (1) and their characterization by elemental analyses, magnetic susceptibilities, diffuse reflectance and IR spectral studies in inconjunction with solid state conductivities and thermogravimetric analyses.

*Department of Chemistry, S. G. B. Amravati University, Amravati, 444 602. E-mail: - aswar2341@rediffmail.com

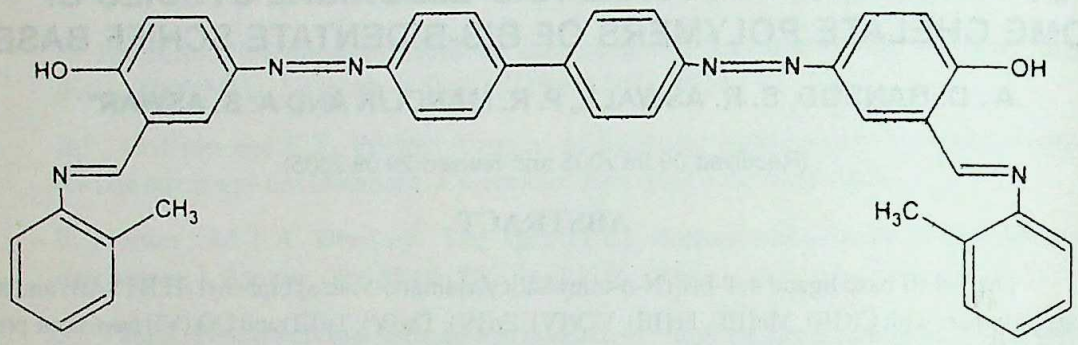

Scheme (I)

EXPERIMENTAL

All chemicals used were of AR grade and the solvents were used after distillation. Microanalyses of C, H and N were carried out at the Regional Sophisticated Instrumentation Center (*RSIC*), Punjab University, Chandigarh, India. The metal contents were determined by standard methods [9,10], after decomposing the chelates with conc. HNO_3.^{1}H NMR spectra of the ligand was taken using TMS as the internal standard on a 90 MHz Perkin-Elmer R-32 spectrometer. The IR spectra (KBr) were recorded on a Perkin Elmer-842 spectrophotometer in the region 400-4000 cm^{-1} at *RSIC*, Punjab University, Chandigarh. Magnetic measurements were carried out at room temperature by the Gouy method using Hg $[Co(SCN)_4]$ as calibrant. The reflectance spectra of the solid compounds, suitably diluted with MgO, were recorded on a Carl-Zeiss DMR-21 spectrophotometer at *RSIC*, Indian Institute of Technology, Chennai, India. Thermogravimetric analyses of the complexes were carried out on a simple manually operated thermobalance fabricated in our laboratory. The instrument was calibrated using crystalline copper sulfate pentahydrate. Samples were run in air atmosphere with a heating rate of 10^0C min^{-1}. The electrical conductivity was measured in pellets using a dc micro voltmeter [11-17].

Synthesis of 4,4'-bis[(N-o-toluylsalicylaldimine-5-)-azo] biphenyl

The ligand was prepared by the method reported in literature with slight modifications. The dye 4,4'-bis[(salicylaldehyde-5)-azo] biphenyl was prepared by diazotization [12]. The dye (2.5 g, 0.005 mol) was dissolved in 25 mL methanol. A solution of o-toluidene (1.1 g, 0.01 mol) in 25mL ethanol was added to it (mole ratio 1:2), with constant stirring. A drop of conc. H_2SO_4 was added as a catalyst and the reaction mixture was refluxed in a water bath for about 3 h. The Schiff base ligand 4,4'-bis[(N-o-toluylsalicylaldimine-5)-azo] biphenyl (H_2BTSAB) was obtained as a greenish brown product. It was crystallized from 1:1 DMF-

ethanol mixture, yield, 2.5 g, (80%); m.p. 235°C.

Synthesis of Polychelates

The polychelates were prepared by reaction of the metal salts; $CrCl_3.6H_2O$, $Mn(OAc)_3.2H_2O$, $FeCl_3$, $VOSO_4.5H_2O$, $ZrOCl_2.8H_2O$, $Th(NO_3)_4.5H_2O$, $TiCl_3$ and $UO_2(NO_3)_2.6H_2O$; with the Schiff base ligand. To a solution of the ligand (3.2 g, 0.005 mol) in DMF (25 mL), a solution of the metal salt (0.005 mol) in ethanol (25 mL) was added with constant stirring. The mixture was refluxed on an oil bath for 2-3 h. The resulting polychelates were filtered, washed several times with hot water, hot DMF, ethanol and finally with acetone to remove unreacted reactants, and dried at 100°C in an electric oven for 45 minutes; yields, 60-65% (Table 1).

RESULTS AND DISCUSSION

The reaction of 4,4'-bis[(salicylaldehyde-5)-azo] biphenyl with o-toluidenein DMF-ethanol mixture yields the Schiff base (H_2BTSAB) (1), the formulation of which is supported by analytical and spectral data. Its 1H NMR spectrum in DMSO-d_6 shows signals at 7.16-8.10, 8.25 and 8.74 ppm (δ) corresponding to phenyl-C=N and phenolic protons, respectively [18]. The signals due to CH_3 protons observed at 1.27 ppm (δ). The IR spectrum of the Schiff base shows bands at 1616, 1483, 1282 and 3030 cm^{-1} corresponding to n(C=N), n(N=N), n(C-O) and n(OH) frequencies, respectively[19].

The ligand H_2BTSAB reacts with metal salts in a 1:1 mol ratio resulting in the formation of polychelates according to the general equation (1). The elemental analyses (Table-1) indicate 1:1 (metal: ligand) stoichiometry. The resulting polychelates are coloured solids and insoluble in water and most of the organic solvents, but are sparingly soluble in DMF and DMSO only.

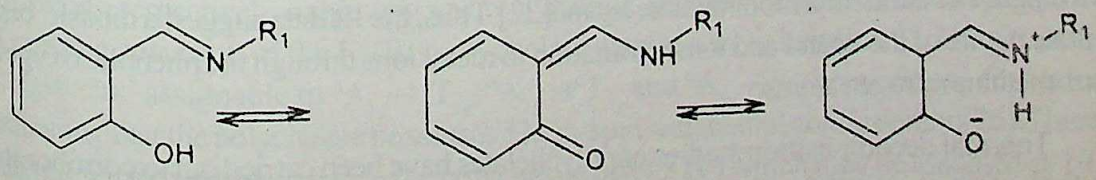

H_2BTSAB - (II)

For M = Cr(III), Fe(III), Zr(IV), Th(IV), Ti(III) : X=Y=H_2O;

VO (IV): X= H_2O and Y= O

Mn (III): X= OAc and Y = Nil;

UO_2(VI): X= Y= O

The ligand H_2BTSAB shows a broad intense band at 3030 cm^{-1} assignable tointramolecular, H-bonded phenolic OH stretching vibrations, which are absent in the spectra of the polychelates, indicating the coordination of the ligand with the metal ion through the phenolic oxygen atom [20]. This is further supported by the shift to higher frequency (26-38 cm^{-1}) of υ(C-O) vibrations from 1282 cm^{-1} in ligand to 1308-1320 cm^{-1} in the polychelates, and also confirmed by the appearance of a new, low-intensity band at 517-558 cm^{-1} in the spectra of the polychelates due to υ(M-O) vibrations. A strong and sharp band at 1616 cm^{-1} in the spectrum of the ligand due to υ(C=N), shows a shift to lower frequency by ~20 cm^{-1} in the spectra of the polychelates, thereby indicating the coordination to the metal ions by the azomethine nitrogen [21]. This is again supported by the appearance of a new, low-intensity band at 400-466 cm^{-1} due to u(M-N) vibrations owing to the formation of a new metal ligand bond. Strong and sharp bands at 972 and 905 cm^{-1} in the spectra of the oxovanadium and dioxouranium polychelates, may be attributed to υ (V=O) and υ_{as}(U=O) modes, respectively. A moderately sharp band occurs at 1483 cm^{-1} in the spectra of the ligand and the polychelates due to u (N=N), and no change in its position shows the indifferent nature of the azo group towards coordination.

A broad and strong band in the polychelates of Cr(III), Fe(III), VO(IV), Zr(IV), Th(IV) and Ti(III), in the region 3367-3400 cm^{-1} due to υ(O-H) and a sharp shoulder at 1650-1656 cm^{-1} due to υ(H_2O) indicate the presence of water molecules and a strong sharp band at 830 cm^{-1} due to the δ(H_2O) rocking mode suggests these water molecules as coordinated ones. Two additional bands are observed at 1522 and 1391 cm^{-1} in Mn(III) polychelate, which may be assigned to uas(OCO) and us(OCO) vibrations of the acetato group. The difference between uas and us of 131 cm^{-1} indicates that the acetato group is coordinated as a monodentate ligand, it further exhibits a band at 666 cm^{-1} due to d(OCO), which is considered a diagnostic band for a monodentate ligand[22]. Thus, the IR data suggest a dibasic bisbidentate nature of the ligand and its coordination to metal ions through the phenolic oxygen and azomethine nitrogen atoms.

Thermal decomposition studies of polychelates have been carried out to corroborate the information obtained from the IR spectral studies about the status of water molecules present in some of these polychelates as well as to know their decomposition pattern. In the case of the Cr(III), Fe(III), Zr(IV), Th(IV) and Ti(III) polychelates, elimination of two water molecules takes place between 140-230°C, indicating the presence of two coordinated water molecules, while the VO(IV) polychelate loses one coordinated water molecule in this range. The polychelates of Mn(III) and UO_2(VI) show negligible weight-loss up to ~300°C indicat-

ing the absence of any water molecules. The second stage of the decomposition is fast and proceeds at 400-600°C leading to the formation of the respective metal oxides. The thermal stability order of the polychelates, on the basis of the procedural decomposition temperature, is Ti > Cr > UO_2 > Mn = Zr > VO > Th > Fe (Table 1).

The order of thermal decomposition and the corresponding activation energies have been evaluated from the figures generated using Broido's equation [23]. The plots of $\ln[\ln(1/y)]$ *vs.* $1/T$ are linear corresponding to first order kinetics where the fraction not yet decomposed (i.e. residual weight fraction), $y = (w_t - w_\infty)/(w_0 - w_\infty)$, where w_t is the weight of the substance at temperature t^0C, w_0 is the weight of the substance at initial state and w_∞ is the weight of the residue at the end of the decomposition. The slopes of the plots yield the thermal activation energy (E_a) of decomposition, which lies between 33.18 and 80.42 kJ mol^{-1}.

The magnetic moments of the polychelates are given in Table 1. The observed value for the Cr(III) polychelate is 4.01 B.M., in accordance with the spin-only value for three unpaired electrons corresponding to high-spin octahedral Cr(III) complexes[24]. The Mn(III) polychelate has a magnetic moment of 4.94 B.M., indicating the presence of four unpaired electrons, and that of Fe(III), 5.90 B.M., indicating the high-spin state of Fe(III). The magnetic moments of 1.73 and 1.81 B.M. of the VO(IV) and Ti(III) polychelates, respectively, suggest the presence of one unpaired electron, the higher value may be due to orbital contributions.

The diffuse reflectance spectrum of the Cr(III) polychelate exhibits three bands at 16,720, 22,420 and 28,090 cm^{-1} which may be assigned to $^4A_{2g} \rightarrow {}^4T_{2g}(F)$, $^4A_{2g} \rightarrow {}^4T_{1g}(F)$ and $^4A_{2g} \rightarrow {}^4T_{1g}(P)$ transitions, respectively, for an octahedral stereochemistry[25]. The Mn(III) polychelate shows an intense band at 27,780 cm^{-1} which may be due to a ligand to metal charge transfer transition. In the second region three moderate to weak d-d bands are observed at 13,420, 16,390 and 18,180 cm^{-1}, assigned to $^5B_1 \rightarrow {}^5B_2$, $^5B_1 \rightarrow {}^5A_1$ and $^5B_1 \rightarrow {}^5E$ transitions, respectively, suggesting square-pyramidal geometry around the Mn(III) ion[26]. The electronic spectrum of the Fe(III) polychelate displays three bands at 11,300, 21,505 and 27,030 cm^{-1} assignable to $^6A_{1g} \rightarrow {}^4T_{1g}$, $^6A_{1g} \rightarrow {}^4T_{2g}$ and $^6A_{1g} \rightarrow {}^4E_g$ transitions, respectively, indicating that the polychelate possesses a high-spin, octahedral configuration[26]. Three d-d transition bands are observed in the polychelate of VO(IV) which may be assigned as 10,200 cm^{-1} $d_{xy}(b_2) \rightarrow d_{xz}$, $d_{yz}(e^*)$, 18,870 cm^{-1} $d_{xy}(b_2) \rightarrow d_{x^2-y^2}(b_1^*)$ and 26,450 cm^{-1} $d_{xy}(b_2) \rightarrow d_{z^2}(a_1^*)$, towards octahedral geometry. Only one band has been observed at 18, 660 cm^{-1}, derived from the transition $^2T_{2g} \rightarrow {}^2E_g$ for an octahedral symmetry in the Ti(III) polychelate. The broad and double-hump nature of the spectrum indicates the presence of Jahn Teller distortion. The Zr(IV), Th(IV) and UO_2(VI) polychelates, as expected, are diamagnetic . Their

electronic spectra do not exhibit any characteristic d-d transitions except charge transfer bands.

The measurement of the solid state electrical conductance of the Schiff base ligand and its polychelates was carried out in their pellet form, from room temperature to about 493K. The results of the electrical conductivity and activation energy are incorporated in Table 2. The room temperature electrical conductivity lies in the range 3.82×10^{-11} to $1.05 \times 10^{-12}\ \Omega^{-1}\ cm^{-1}$, indicating their semiconducting nature [27] and decreases in the order Zr > VO > Cr > Th > BTSAB > Ti > Mn > Fe > UO_2. The electrical conductivity (σ) varies exponentially with the absolute temperature according to the relationship $\sigma = \sigma_0 \exp(-E_a / kT)$, where σ_0 is a constant, E_a the activation energy of conduction process, T the absolute temperature and k the Boltzman constant. When log σ is plotted against $1/T$, a linear dependance was observed, also suggesting the semiconducting behaviour of the ligand and it's polychelates. Here, the lower temperature region has lower slopes with lower activation energies and the higher temperature region has higher slopes with higher E_a values. This break observed in plots i.e., phase transition, in case of the ligand, may be attributed to two molecular structures having keto and enol forms which exchange the conduction at different thermal stabilities. [Eq (2)].

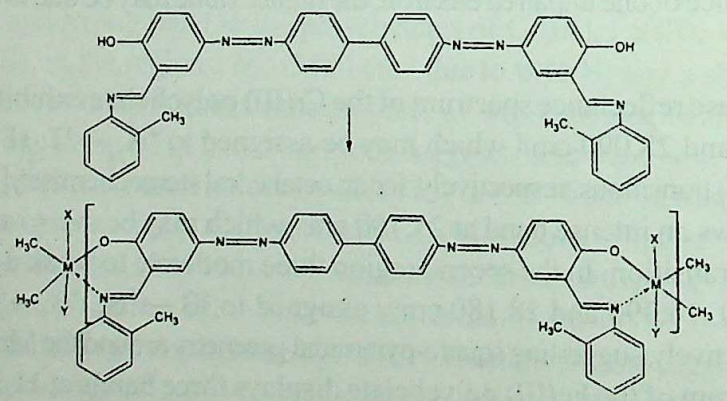

Scheme- (III)

In the case of the polychelates the lower values of logσ in the low temperature region may be attributed to extrinsic conduction present in them, where the conduction is due to excitation of carriers from the donor localized level to the conduction band. Whereas at higher temperatures these may behave as intrinsic semiconductors in which the carriers are thermally activated from the valence band to the conduction band. This may be because of the interaction between the electrons of d-orbital of the metal and π orbital of the ligand at higher temperature, which leads to localized action of the π electronic charge on ligand that tends to

increase the activation energy [28]. The activation energy of electrical conduction is calculated from the slopes of these plots in the high temperature region, which lies in the range between 1.233 and 0.127 eV.

TABLE: 1 ANALYTICAL AND PHYSICAL DATA OF THE POLYCHELATES

Sr. No.	Compound (Colour)	Formula Weight	μ_{eff}	Decomp. Temp.(°C)	Ea (kJ mol^{-1})	Yield (%)	Elemental analysis (%) C	H	N	M
1	H_2BTSAB (Greenish brown)	628.00	------	360	33.18	80	76.00 (76.43)	5.00 (5.10)	13.00 (13.38)	------
2	[Cr(BTSAB)(H_2O)$_2$]Cl (Light brown)	713.99	4.01	340	52.04	65	66.00 (66.47)	4.25 (4.37)	12.00 (12.24)	7.02 (7.28)
3	[Mn(BTSAB)(OAC)] (Light brown)	716.94	4.94	310	80.36	60	67.67 (68.11)	4.34 (4.46)	12.00 (11.35)	7.11 (7.42)
4	[Fe(BTSAB)(H_2O)]Cl (Brown)	717.85	5.90	270	80.42	65	67.57 (11.8)	4.53 (7.78)	11.53 (11.70)	7.49 (7.78)
5	[VO(BTSAB)(H_2O)] (Light brown)	692.94	1.73	290	58.85	60	67.25 (67.52)	4.25 (4.50)	11.28 (11.82)	6.91 (7.17)
6	[Zr(BTSAB)(H_2O)$_2$] (Yellowish brown)	753.22	dia.	310	34.96	62	63.59 (63.73)	4.34 (4.51)	10.80 (11.15)	11.79 (12.11)
7	[Th(BTSAB)(H_2O)$_2$](NO_3)$_2$ (Golden brown)	894.04	dia.	280	40.35	63	53.33 (53.69)	3.49 (3.80)	9.03 (9.40)	25.63 (25.95)
8	[Ti(BTSAB)(H_2O)$_2$]Cl (Yellowish brown)	709.88	1.81	390	46.76	60	67.22 (67.62)	4.37 (4.74)	11.69 (11.83)	6.53 (6.74)
9	[UO_2(BTSAB)] (Maroon)	896.03	dia	320	39.75	60	53.17 (53.57)	3.04 (3.35)	8.73 (9.37)	26.26 (26.58)

TABLE: 2 ELECTRICAL CONDUCTIVITY DATA OF BTSAB AND ITS POLYCHELATES

Sr.	Compound	ElectricalConductivity $(\Omega^{-1}\ cm)^{-1}$	Temperature (K)	Activation energy (eV)
1	H_2BTSAB	5.45×10^{-12} 3.47×10^{-10}	40 220	0.512
2	$Cr(BTSAB)(H_2O)_2]Cl$	1.69×10^{-11} 1.85×10^{9}	40 220	0.0445
3	[Mn(BTSAB)(OAc)]	3.47×10^{-12}	40 220	0.902
4	$[Fe(BTSAB)(H_2O)_2]Cl$	1.27×10^{-12} 2.85×10^{-11}	40 220	0.687
5	$[VO(BTSAB)(H_2O)]$	3.15×10^{-11} 8.80×10^{-11}	40 220	1.233
6	$[Zr(BTSAB)(H_2O)_2]$	3.82×10^{-12} 8.80×10^{-11}	40 220	1.233
7	$[Th(BTSAB)(H_2O)_2](NO_3)_2$	1.05×10^{-12} 1.96×10^{-11}	40 220	0.990
8	$[Ti(BTSAB)(H_2O)_2]Cl$	3.52×10^{-12} 2.40×10^{-10}	40 220	0.349
9	$[UO_2(BTSAB)]$	1.05×10^{-12} 1.96×10^{-11}	40 220	0.219

Acknowledgement: The authors wish to thank the University authorities for providing laboratory facilities. One of us (S.R.A) is grateful to the University Grants Commission, Western Regional Office, Pune, for the award of a Teachers' Fellowship

REFRENCES

1. A. F. Shoair, A. A. El-Bindary, A. Z. El-Sonbati, and R. M. Younes: Stereochemistry of new nitrogen containing hetrocyclic aldehydes III novel bis bidentate azodye compounds, Polish. J.Chem, 74 (2000), 1047.

2. M. R. Maurya: Development of the coordination chemistry of vanadium through biscathylacetonato oxovanadium (IV), Coord.Chem.Rev. 237 (2003), 163.

3. M. R. Maurya, S. Khurana, W. Zhangal and D. Rehder Eur.J.Inorg.Chem: Synthesis, characterization and antibiotic studies of dioxovanadium (IV) complexes containing ONS donor ligands derived from S-benzylidihiocarbazate Eur.J. Inor. Chem. (2002), 1749.

4. A. P. Mishra, M. Khare and S. K. Gautam: Synthesis, physico-chemical

characterization and antimicrobial studies of some bioactive Schiff bases and their metal chelates, Synth. React.Inorg.Met-Org. Chem. 32(8) (2002), 1485.

5. M. N. Patel, S. H. Patil: Synthesis and stereochemistry characterization of some new coordination compounds, Synth.React. Inorg Met-Org Chem. 12 (1982), 203.

6. F. A. El-Saied, M. A. Ayad, R. M. Issa and S. A. Aly: 4- azomalonitrile antipyridine complex of some first row transition metal, Polish J. Chem. 74 (2000), 919.

7. A.K.Rana, N R Shah, M S Patil, A M Karampurwala and J R Shah: Polychelates derived from 4,4'-(4,4'-biphenylenebisaze) di (salicylaldehyde oxime), Makromol Chem. 182 (1981), 3387.

8. M. N. Patel and S. H. Patil: Studies on polyazo methine chelate polymers, J Makromol Sci Chem., 17 (1982), 675.

9. B. T. Thaker, I. Patel, P. Patel and S. Goldsmith: Synthesis and characterisation of manganese (III) hetrochelates, Indian J Chem. 42A (2003), 2487.

10. M. R. Maurya, C. Khuranas, Schulzke and D.Rehder Eur.J.Inorg.Chem: Dioxo and oxovanadium (V) complex of biometric hydrazone ONO donor ligand J. Inorg Chem., (2001), 719.

11. Vogel A.I.A Text Book of Organic Chemistry, 4th Edn, E.L.B .S., Longman, London,(1978), 748.

12. M. R. Maurya, N. Agarwal and S. Khurana: Synthesis and charactersation of metal complex of methylene bridged hexadentate tetranoinic ligands, Ind.J.Chem, 39A (2000), 1093.

13. D. H., Sutariya, J. R. Patel and M. N. Patel: Magnetic, spectral, thermal and electrical properties of new coordination polymers, J. Indian Chem. Soc, 73(1996), 309.

14. H. B. Pancholi and M .M. Patel: Charactersation and antimicrobial activities of some new coordination polymers, J.Polym. Mater, 13 (1994), 261.

15. A. M. Karampurwala, A. Ray and R. P. Patel: Polychelates of bissemicarbazone of 5,5'methylene bis-salicylaldehyde with VO (II), Mn (II), Cr(III) ,Fe(III) and Zn(II), Synth. React.Inorg.Met. Org. Chem., 19 (3) (1989), 219.

17. R. C. Maurya P. Patel and S. Rajput: Synthesis and characterization of mixed ligand complex of Cu(II) ,Ni(II),Co(II),Zn(II),Sm(II)and UO2(VI) with Schiff base derived from the surfa drug sulfamerazine and 2,2'-bipyridine, Synth. React Inorg. Met-Org Chem. 33(8) (2003), 801.

16. R. C.Maurya and S. Rajput: Oxovanadium (IV) complex of bioinorganic and medicinal relevance: synthesis, characterization and 3D molecules modeling and analysis of some

oxovanadium (IV) complex involving O-O donor environment, J. Mol. Stru, 687 (2004), 35

17. A. A. Broids, J Polym Sci, 7 (1964), 1761.

18. P. K. Rai and R. N. Prasad: Electrical and structural studies of Cr(III) ,Fe(III) and Co(II) complex of two novel 12-membered terazamacrocycles, Synth. React Inorg. Met-Org. 24(5) (1994), 749.

19. B. T. Thaker and I.A. Patel: Manganese (III) complex with hexadentate Stiff base derived from hetrocyclic b-diketones and triethylene tetramine, Indian J. Chem., 38A (1992), 423.

20. B. T. Thaker, I. A. Patel and P. B. Thaker: Manganese (III) complex with Schiff base derived from hetrocyclic b-diketone and some diamines, Indian J.Chem.37A (1998), 429.

21. L. J. Paliwal and R. B. Kharat: Magnetic spectral and thermal properties of coordination polymers derived from terephthaaldehydebis benzyldithiocarbazate), Makromol Chem. 160 (1998), 67.

22. R. C. Maurya, D.D. Mishra and V. Pillai: Studies of mixed ligand complex of oxavanadium (IV) complex involving acetylacetone and nitrogen or oxygen donor organic compound, Synth. React. Inorg. Met. Org. Chem., 25 (7) (1995), 1127.

23. M. S. Islam and M. A. Alam: Studies on mixed ligand complex of oxavanadium (IV) and Ti(III)with organic dibasic acid and hetrocyclic amines , J. Indian Chem. Soc., 76 (1999), 255.

24. M. R. Maurya and N. Bharti: Synthesis, thermal and spectral studies of oxoperoxo and dioxo comples of vanadium (V) molybdenum (VI) and tungsten (VI) with 2(a-hydoxyalkyl/ aryl) benzimidazakic, Trans.Chem, 24 (1999), 389

25. K. A. El -Manakhly: Electrical and magnetic properties of some anthraquinone o-car boxylic phenylhydrazone metal complexes, J.Indian Chem.Soc, 75 (1998), 315.

26. H. A. Hammand H A, O. M. Yassin and K. A. El-Manakhly: Spectroscopic studies on the ligand field strength of some chelating agents, J. Indian Chem.Soc.76 (1996), 253.

27. K.K. Narag, T.K. Rao S.Shresha anS. Shresha: Synthesis, chractersation, thermal and electrical properties of Ytirium (III) and Lanthanide (III) complex of salicyaldehyde benroylhydrozone, Synth. React.Inorg.Met. Org. Chem., 30(5) (2000), 931.

28. M. N. Patel, D. H Sutariya, and J.R.Patel: Struture, semicomducting and thermal studies of some Schiff base coordination polymers, Synth. React.Inorg.Met. Org. Chem. 24(3)(1994), 401.

Journal of Natural & Physical Sciences, Vol. 19 (1) (2005) 91-98

THREE DIMENSIONAL MATHEMATICAL MODEL FOR PRIMARY POLLUTANTS

Ajendra Kumar*, Virendra Arora* and Prabhakar Pradhan*

(Revised 14.10.2005)

ABSTRACT

A three dimensional problem with time independent situation at point source is considered to evaluate the concentration distribution of pollutants emitted. In this model three cases including constant, linear and oscillatory emitting emission profiles have been considered. This model being three dimensional in nature is more suitable for impact of point source emission.

Keywords: Point source, eddy diffusivities and Pollutants.

INTRODUCTION

Air pollution has emerged as one of the most ominous problem of twentieth century. Developing countries, like India, and its neighboring countries are facing a much serious air pollution compared to their western counterparts. Rapid advancement in industry led to heavy and noticeable pollution of air. The atmosphere is not infinite but extends up to certain height above the surface of the earth form the various characteristic layers called troposphere, mesosphere and thermosphere. Khan [7] has given a three dimensional model of atmospheric dispersion of pollutant in a stable boundary layer. Trivedi and Arya [5, 6] has given the information about the atmospheric pollutants and meteorological parameters. To reduce the spread of pollution originating from industry operations, planting of a green belt surrounding the industry had been suggested by Schnelle [2]. A model of chemically reactive pollutant is given by Goyal[4]. In this paper Mathematical modeling and solution procedures of dispersion model have been discussed.

MATHEMATICAL MODEL

Consider 3-D Diffusion equation of a point source at $(0, 0, h_s)$ emitting chemically reactive atmospheric pollutant (C). Several removal mechanisms like rainout / washout and ground absorption are associated with the life cycle of pollutants[1]. Under these assumptions, the PDEs governing the concentration of the pollutant with the boundary conditions can be written as

$$U\frac{\partial C}{\partial x} = K_y\frac{\partial^2 C}{\partial y^2} + K_z\frac{\partial^2 C}{\partial z^2} - \left(K + K_g\right)C \qquad (1)$$

*Department of Mathematics & Statistics, Gurukula Kangri Vishwavidyalaya, Haridwar-249 404

Where, U is the mean velocity of pollutant along x-direction, K_y and K_z are the diffusivities in y and z direction respectively, K is the rate of conversion of primary pollutant to secondary product, K_g is the rate of removal of C by means of rainout/washout and other quatities have the same usual meanings.

$$\frac{\partial C}{\partial x} = \alpha \frac{\partial^2 C}{\partial y^2} + \beta \frac{\partial^2 C}{\partial z^2} - \gamma C \tag{2}$$

Here, $\alpha = \frac{K_y}{U}$, $\beta = \frac{K_z}{U}$ and $\gamma = \frac{\left(K + K_g\right)}{U}$

The Boundary condition for C are

$$C(x, y, z) = Q\delta(y)\delta(z - h_s) \qquad \text{at } x = 0$$

Where Q is the emission strength of source and δ is Dirac delta function.

$$C(x, y, z) = 0 \qquad y \to \pm\infty \qquad \text{for every } y, z.$$

$$\frac{\partial C}{\partial z}(x, y, z) = 0 \qquad z \to \pm\infty \qquad \text{for every } x, y.$$

METHOD OF SOLUTION

We can solve the Eq. (1) by MSV [3]

$$C = (X_{(x)}\, Y_{(y)}\, Z_{(z)})$$
$$= XYZ \tag{3}$$

If $$\frac{\partial C^{(1)}}{\partial x} = \alpha \frac{\partial^2 C^{(1)}}{\partial y^2} \tag{4}$$

$$\frac{\partial C^{(2)}}{\partial x} = \beta \frac{\partial^2 C^{(2)}}{\partial y^2} \tag{5}$$

$$\frac{\partial C^{(3)}}{\partial x} = -\gamma \frac{\partial^2 C^{(3)}}{\partial y^2} \tag{6}$$

Equation (4) $\Rightarrow \frac{\partial C^{(1)}}{\partial x} = \alpha \frac{\partial^2 C^{(1)}}{\partial y^2}$

$C^{(1)} = (X.Y)$

$$\frac{\partial C^{(1)}}{\partial x} = \frac{\partial}{\partial x}(X.Y)$$

$$= X^1 Y$$

Similarly

$$\frac{\partial C^{(1)}}{\partial y} = Y^1 X$$

$$\frac{\partial^2 C^{(1)}}{\partial y^2} = Y^{11} X$$

$\Rightarrow \quad X^1 Y = \alpha Y^{11} X$

$\Rightarrow \quad \frac{X^1}{\alpha X} = \frac{Y^{11}}{Y} = K$

$\Rightarrow \quad X^1 = \alpha K X, \; Y^{11} = YK$

Case I $(K = 0)$:

$X^1 = 0$ $\qquad$ $Y^{11} = 0$

$X = C_1$ (constant) $\qquad$ $Y = C_2 + C_3 y$

where C_1, C_2 and C_3 are arbitrary constants.

Hence $C^{(1)} = C_1 (C_2 + C_3 y)$

$= A + Bx$

Where A and B is also constant.

Case II. $(K<0) \Rightarrow K = -p^2 < 0$ $\qquad$ for all $p \in R$ (set of reals)

$X^1 = -\alpha p^2 X$ $\qquad$ $Y^{11} = -p^2 Y$

$$X = C_4 e^{-\alpha p^2 X} \qquad Y = C_5 \cos py + C_6 \sin py$$

$$C^{(1)} = C_4 e^{-\alpha p^2 X} \ (C_5 \cos py + C_6 \sin py)$$

Case III. $(K>0)$ => $K = p^2 > 0 \qquad \forall\, p \in R$

$$X^{1} = \alpha p^2 X \qquad Y^{11} = p^2 Y$$

$$X = C_7 e^{\alpha p^2 X} \qquad Y = C_8 e^{py} + C_9 e^{-py}$$

$$C^{(1)} = C_7 e^{\alpha p^2 X} (C_8 e^{py} + C_9 e^{-py})$$

$$(B) => \frac{\partial C^{(2)}}{\partial x} = \beta \frac{\partial^2 C^{(2)}}{\partial y^2}$$

$$C^{(2)} = (X.Z)$$

$$\frac{\partial C^{(2)}}{\partial x} = \frac{\partial}{\partial x}(X.Z)$$

$$= X^{1} Z$$

Similarly

$$\frac{\partial C^{(2)}}{\partial z} = Z^{1} X$$

$$\frac{\partial^2 C^{(2)}}{\partial z^2} = Z^{11} X$$

$$=> \quad X^{1} Z = \beta Z^{11} X$$

$$=> \quad \frac{X^{1}}{\beta X} = \frac{Z^{11}}{Z} = L$$

$$=> \quad X^{1} = \beta L X, \ Z^{11} = ZK$$

Case I $(K = 0)$:

$$X^{1} = 0 \qquad Z^{11} = 0$$

$$X = C_{10} \text{ (constant)} \qquad Z = C_{11} + C_{12} x$$

Where C_{10}, C_{11} and C_{12} are arbitrary constants.

Hence $C^{(2)} = C_{10}(C_{11} + C_{12}x)$

$= D + Ex$

Where D and E is also constant.

Case II. $(K < 0) \Rightarrow K = -p^2 < 0 \qquad \forall\, p \in R$

$X^1 = -\beta p^2 X \qquad Z^{11} = -p^2 Z$

$X = C_{13}\, e^{-\beta p^2 X} \qquad Z = C_{14} \cos pZ + C_{15} \sin pZ$

$C^{(2)} = C_{13} e^{-\beta p^2 X}(C_{14} \cos pZ + C_{15} \sin pZ)$

Case III. $(K>0) \Rightarrow K = p^2 > 0 \qquad \forall\, p \in R$

$X^1 = \beta p^2 X \qquad Z^{11} = p^2 Z$

$X = C_{15}\, e^{\beta p^2 X} \qquad Z = C_{16} e^{pZ} + C_{17} e^{-pZ}$

$C^{(2)} = C_{15} e^{\beta p^2 X}(C_{16} e^{pZ} + C_{17} e^{-pZ})$

$$(C) \Rightarrow \qquad \frac{dC^{(3)}}{dx} = -\gamma C^{(3)}$$

$$\frac{dy}{C} = -\gamma dx$$

$$\Rightarrow \qquad \log_e C^{(3)} = -\gamma x + C_{18}$$

$C^{(3)} = e^{-\gamma x} . e^{C_{18}}$

$C^{(3)} = Me^{-\gamma x}$, where $M = e^{C_{18}}$

By the boundary conditions:

$C^{(2)} = C^{13} e^{\beta p^2 X}(C_{14} e^{pZ} + C_{15} e^{-pZ})$

$$C^{(2)} = \sum_{n=0}^{\infty} a_n^2 \; e^{\beta p^2 X} \; e^{pZ} + \sum_{n=0}^{\infty} b_n^2 \; e^{\beta p^2 X} \; e^{-pZ}$$

$$\frac{dC^{(2)}}{dz} = \sum_{n=0}^{\infty} a_n^2 \; e^{\beta p^2 X} \; e^{pZ} + \sum_{n=0}^{\infty} b_n^2 e^{\beta p^2 X} \; e^{-pZ}$$

$$z \to +\infty, \qquad \frac{\partial C}{\partial z} = 0 \,,\; a_n^2 = 0$$

$$\Rightarrow \qquad C^{(2)} = \sum_{n=0}^{\infty} b_n^2 \; e^{\beta p^2 X} \; e^{-pZ}$$

$$z \to -\infty, \qquad \frac{\partial C}{\partial z} = 0 \,,\; b_n^2 = 0$$

$$\Rightarrow \qquad C^{(2)} = \sum_{n=0}^{\infty} a_n^2 \; e^{\beta p^2 X} \; e^{pZ}$$

$$C^{(1)} = C_7 e^{\alpha p^2 X} \left(C_8 e^{pY} + C_9 e^{-pY}\right)$$

$$= \sum_{n=0}^{\infty} a_n^1 \; e^{\alpha p^2 X} \; e^{pZ} + \sum_{n=0}^{\infty} b_n^1 \; e^{\alpha p^2 X} \; e^{-pY}$$

By the boundary conditions:

$$y \to -\infty, \qquad C = 0 \Rightarrow b^1{}_n = 0 \Rightarrow C^{(1)} = \sum_{n=0}^{\infty} a_n^1 \; e^{\alpha p^2 X} \; e^{pZ}$$

$$y \to +\infty, \qquad C = 0 \Rightarrow a^1{}_n = 0 \Rightarrow C^{(1)} = \sum_{n=0}^{\infty} b_n^1 \; e^{\alpha p^2 X} \; e^{-pZ}$$

$$C = (C^{(1)}, C^{(2)}, C^{(3)})$$

$$C = \frac{\|C^1\|}{n}$$

where $\|C^1\| = \alpha_1 C^1 + \alpha_2 C^2 + \alpha_2 C^3$

$$\Rightarrow C = \frac{\alpha_1 C^1 + \alpha_2 C^2 + \alpha_3 C^3}{3}$$

By the boundary conditions:

Case 1: $(y, z) \to (\infty, \infty)$

$$\left\{\alpha_1^{(1)} \sum b_n^{(1)} e^{\alpha p^2 x} e^{-py} + \alpha_2^{(1)} \sum b_n^{(2)} e^{p^2 \beta x} e^{-pz} + \alpha_3^{(1)} \sum \alpha_n^{(3)} e^{-\gamma x}\right\}/3$$

Case 2: $(y, z) \to (-\infty, -\infty)$

$$\left\{\alpha_1^{(2)} \sum a_n^{(1)} e^{\alpha p^2 x} e^{py} + \alpha_2^{(2)} \sum a_n^{(2)} e^{p^2 \beta x} e^{pz} + \alpha_3^{(2)} \sum \alpha_n^{(3)} e^{-\gamma x}\right\}/3$$

Case 3: $(y, z) \to (-\infty, \infty)$

$$\left\{\alpha_1^{(3)} \sum a_n^{(1)} e^{\alpha p^2 x} e^{py} + \alpha_2^{(3)} \sum b_n^{(2)} e^{p^2 \beta x} e^{pz} + \alpha_3^{(3)} \sum \alpha_n^{(3)} e^{-\gamma x}\right\}/3$$

Case 4: $(y, z) \to (\infty, -\infty)$

$$\left\{\alpha_1^{(4)} \sum b_n^{(1)} e^{\alpha p^2 x} e^{-py} + \alpha_2^{(4)} \sum a_n^{(2)} e^{p^2 \beta x} e^{pz} + \alpha_3^{(4)} \sum \alpha_n^{(3)} e^{-\gamma x}\right\}/3$$

RESULT AND DISCUSSION

1. Solution to a three-dimensional dispersion model for an elevated point source is developed and some of the features of the solution were illustrated above. Diffusivities and its effects on rain/wash out has been incorporated in equations to reduce the concentration of the pollutants in various circumstances. Limiting cases have also been considered for validation with realistic situations.

2. This model can also be used to investigate the effects artificially introduced sinks in the removal of the contaminant from the atmosphere.

3. The above model can brought to reality by introducing nonlinearity, and to solve those equations requires numerical simulation techniques, hence Matlab is suitable software to give clear graphs with numerical results.

REFERENCES

1. F. Pasquill & F. B. Smith: Atmospheric Diffusion. 3rd edition. Van Nostrand, London, 1983.

2. B. Karl Schnelle, Jr. & Charles A. Brown : Air Pollution Control Technology Handbook, CRC Press, Boca Raton, 2001.

3. P.P.Gupta, G.S.Malik: Numerical Techniques, Science and Engineering 29th Edition, Krishna Prakashan Media, Meerut, 2002.

4. Pramila Goyal: Modelling of chemical reactive pollutants, Proc. of First DST-SERC school on "Mathematical Modelling of Atmospheric Pollutants", Bangalore, 2001, 387-398.

5. R.K. Trivedi & P.K.Goel: An introduction to air pollution, ABD Publishers, Jaipur,2003.

6. S. P. Arya : Air Pollution Meteorology and Dispersion, Oxford University Press, New York , 1999.

7. Sujit Kumar Khan, M. Venkatachalappa & Dulal Pal: Three dimensional analytical model of atmospheric dispersion of pollutant in a stable boundary layer, Inter. J. Environmental Studies, 41(1992) 133-149.

Journal of Natural & Physical Sciences, Vol. 19 (1) (2005) 99-109

A MODEL OF β-CELL MASS, INSULIN, GLUCOSE, RECEPTOR AND SOMATOSTATIN DYNAMICS

Somna Mishra, V. Arora* and V.K. Katiyar**

(Received 14.10.2005)

ABSTRACT

Existing mathematical models of β-cell mass, Insulin, Glucose and Receptor dynamics contribute to the study of the disease describing different pathways to diabetes. But Somatostatin dynamics has not been considered in modeling the Glucose-Insulin regulatory system. In our model, we focus our study on Somatostatin dynamics to whole glucoregulatory system. We incorporate the dynamics of somatostatin into an existing mathematical model, resulting in a system of five non-linear differential equations that we use to find out the behavior of glucoregulatory system. Our model describes the levels of β-cell mass, Insulin, Glucose, Insulin receptor and Somatostatin under physiological and pathological steady states and a saddle point.

Keywords: somatostatin, diabetes mellitus, insulin.

Mathematics Classification No.: 92C50

INTRODUCTION

Diabetes mellitus is a chronic metabolic disease characterized by the uncoupling of blood glucose levels and insulin secretion, causing abnormal glycemic excursions. Type1 diabetes is characterized by a complete insulin deficiency. Treatment consists of attempting to match exogenous insulin delivery to the metabolic needs of the patient during meals, exercise and sleep. The body regulates the processes that control the production and storage of glucose by secreting the endocrine hormone, insulin from the pancreatic β-cells insulin facilitates anabolic metabolism throughout the body. An increase in insulin above basal concentration will decrease the release of glucose from the liver and increase glucose uptake into insulin-receptive tissues. There are many substances in the body that promote and inhibit insulin secretion, refining the detail to which the β - *cells* react to changes in the body's metabolic state. One such hormone is somatostatin, which is secreted in *D*-cells.

Somatostatin is a gastrointestinal hormone closely related to the function of gastrointestinal system [8]. Somatostatin is a 14 amino peptide. It also has several kinds of molecules and distributes vastly in the body.

The somatostatin in gastrointestinal system is secreted in *D*-cells. It is mainly in intes-

*Gurukula Kangri Vishwavidyalaya, Hardwar, India, *E-mail:mishra_somna@yahoo.com
**Indian Institute of Technology, Roorkee, India

tinal nerve plexus, stomach and pancreas, and it is also in gastric and intestinal fluid. In the antrum, there are many *D*-cells, most of which belong to the open type endocrine cells that can directly secrete somatostatin into gastric fluid [8, 9]. Somatostatin also has the role of regulating pancreatic hormones such as glucagons and insulin. The stomach is comprised of many histologically distinct regions, but only two main compartments are taken in account, the antrum (lower) and corpus (upper) regions. It is found that antral somatostatin (S_A) is more effective than corpus somatostatin (S_C) [8]. So we have considered the dynamics of antral somatostatin to develop our model.

Topp et al. [12] suggested their model of β-cell mass, Insulin and Glucose kinetics consisting of three nonlinear ordinary differential equations. The model presented by them is as follows: -

$$\frac{dG}{dt} = \gamma - (\mu + \xi I)G \tag{1}$$

$$\frac{dI}{dt} = \frac{\sigma \beta G^2}{\alpha + G^2} - \psi I \tag{2}$$

$$\frac{d\beta}{dt} = \left(-\omega + uG - yG^2\right)\beta \tag{3}$$

Later Harnandez et al.[7] presented the extension of the model of Topp et al [12]. which describes the β-cell mass, Insulin, Glucose and Receptor dynamics resulting in four dimensional system of nonlinear ordinary differential equations: -

$$\frac{dG}{dt} = \gamma - (\mu + \xi RI)G \tag{4}$$

$$\frac{dI}{dt} = \frac{\sigma \beta G^2}{(1+R)(\alpha + G^2)} - \psi I - \psi RI \tag{5}$$

$$\frac{d\beta}{dt} = \left(-\omega + uG - yG^2\right)\beta \tag{6}$$

$$\frac{dR}{dt} = \rho(1-R) - kIR - \zeta R \tag{7}$$

Here a mathematical model has been developed for coupled β-cell mass, insulin, glucose, receptor and somatostatin dynamics. This model permits to describe the normal behavior of the system and to find out the effects of different defects on the whole system behavior.

METHODS

Model Development

In present model of the glucose regulatory system, the fasting plasma glucose, insulin and somatostatin concentration, β-cell mass, surface insulin receptor dynamics and somatostatin dynamics have been studied. The form of the system is as follows: -

$$\frac{dG}{dt} = \gamma - (\mu + \xi RI)G - \left(\frac{S_A}{k_{SS}}\right)G \tag{8}$$

$$\frac{dI}{dt} = \frac{\sigma\beta G^2}{(1+R)(\alpha + G^2)} - \psi I - \psi RI - \left(\frac{S_A}{k_{SS}}\right)I \tag{9}$$

$$\frac{d\beta}{dt} = (-\omega + uG - yG^2)\beta \tag{10}$$

$$\frac{dR}{dt} = \rho(1-R) - kIR - \zeta R \tag{11}$$

Antral Somatostatin

$$\frac{d[S_A(t)]}{dt} = D_A(t)\left(\frac{K_{AS}[A_A(t)]}{([A_A(t)]+\alpha_{AS})\left(1+\frac{[S_A(t)]}{k_{SS}}\right)\left(1+\frac{[N_C(t)]}{k_{NS}}\right)}\right)$$

$$+ D_A(t)\left(\frac{K_{NS1}[N_E(t)]}{([N_E(t)]+\alpha_{NS1})\left(1+\frac{[S_A(t)]}{k_{SS}}\right)\left(1+\frac{[N_C(t)]}{k_{NS}}\right)}\right) - \tau_S[S_A(t)] \quad (12)$$

Corpus Somatostatin

$$\frac{d[S_C(t)]}{dt} = D_C(t)\left(\frac{K_{NS2}[N_E(t)]}{([N_E(t)]+\alpha_{NS2})\left(1+\frac{[S_C(t)]}{k_{SS}}\right)\left(1+\frac{[N_C(t)]}{k_{NS}}\right)}\right)$$

$$+ D_C(t)\left(\frac{K_{GS}[Gtn_C(t)]}{([Gtn_C(t)]+\alpha_{GS})\left(1+\frac{[S_C(t)]}{k_{SS}}\right)\left(1+\frac{[N_C(t)]}{k_{NS}}\right)}\right) - \tau_S[S_C(t)] \quad (13)$$

Where G is the concentration of blood glucose (in mg/dl), I is the concentration of blood insulin (in $\mu U/ml$), β is the β-cell mass (in mg), R is the fraction of insulin receptors on the surface of the muscle cells and S_A is the concentration of antral somatostatin (in pM).

In equation (8), it is assumed that a person eats regularly [3], therefore at fasting condition, glucose is secreted at a constant rate by liver and kidneys. The glucose dynamics is represented by

$$\frac{dG}{dt} = \gamma - (\mu + \xi RI)G - \left(\frac{S_A}{k_{SS}}\right)G$$

Where $\left(\frac{S_A}{k_{SS}}\right)G$ represents the decrease in the concentration of glucose due to the release of somatostatin, if the concentration of glucose in blood increases above the requirement of the body. Somatostatin inhibits the excessive secretion of glucagons and gastrin and further regulates the level of glucose in blood [9].

Similarly somatostatin also regulates the level of insulin in blood. The following nonlinear ordinary differential equation represents insulin dynamics:

$$\frac{dI}{dt} = \frac{\sigma\beta G^2}{(1+R)(\alpha + G^2)} - \psi I - \psi RI - \left(\frac{S_A}{k_{SS}}\right)I$$

Where $\frac{G^2}{\alpha + G^2}$ represents the sigmoidal relationship between plasma glucose concentration and insulin secretion [12]. $\frac{d}{1+R}$ is the rate at which a single β-cell will secrete insulin and d is the maximal β-cell insulin secretory rate [7].

The β-cell mass dynamics does not depend directly on concentration of somatostatin and fraction of insulin receptors. Therefore, we use the same equation in our model as described by Topp et al [12], as shown below:

$$\frac{d\beta}{dt} = \left(-\omega + uG - yG^2\right)\beta$$

Also the fraction of insulin receptors on the surface of muscle cells does not depend upon concentration of somatostatin, so this equation is also used as derived by Hernandez et al [7].

$$\frac{dR}{dt} = \rho(1-R) - kIR - \zeta R$$

As described previously that antral somatostatin has a much greater effect than somatostatin produced in the corpus [8]. So in our model we have taken in account the dynamics of antral somatostatin (S_A). Since the secretion of somatostatin is inhibited by both somatostatin itself and the CNS (central nervous system) neurotransmitter acetylcholine [8], it is assumed that the product of the inhibitory terms $\left(1+\frac{S_A(t)}{k_{SS}}\right)\left(1+\frac{N_C(t)}{k_{NS}}\right)$ captures the desired inhibitory dynamics. It is also found that antral somatostatin secretion is also proportional to the antral acid concentration $A_A(t)$ and ENS (enteric nervous system) effector concentration $N_E(t)$ and the term τ_s describes the clearance rate of somatostatin. Thus the equation for antral somatostatin dynamics is as follows:

$$\frac{d[S_A(t)]}{dt} = D_A(t)\left(\frac{K_{AS}[A_A(t)]}{([A_A(t)]+\alpha_{AS})\left(1+\frac{[S_A(t)]}{k_{SS}}\right)\left(1+\frac{[N_C(t)]}{k_{NS}}\right)}\right)$$

$$+ D_A(t)\left(\frac{K_{NS1}[N_E(t)]}{([N_E(t)]+\alpha_{NS1})\left(1+\frac{[S_A(t)]}{k_{SS}}\right)\left(1+\frac{[N_C(t)]}{k_{NS}}\right)}\right) - \tau_S[S_A(t)]$$

The parameters values are presented in Table 1.

Table 1#

Parameter	Value	Units	Biologic Interpretation
γ	864	*mg/dl d*	Glucose production rate by liver when $G=0$
μ	1.44	*1/d*	Glucose clearance rate independent of insulin
ξ	0.85	*ml/μU d*	Insulin induced glucose uptake rate
σ	43.2	*μU/ml d mg*	β-cell maximum insulin secretory rate
α	20,000	*mg² /dl²*	Gives inflection point of sigmoidal function

ψ	216	$1/d$	Whole body insulin clearance rate
ω	0.03	$1/d$	β-cell natural death rate
u	0.614285e-3	$dl/mg\ d$	Determines β-cell glucose tolerance range
y	0.2857e-5	$dl^2/mg^2\ d$	Determines β-cell glucose tolerance range
ρ	2.64	$1/d$	Insulin receptor recycling rate
k	0.02	$ml/\mu U\ d$	Insulin dependent receptor endocytosis rate
ζ	0.24	$1/d$	Insulin independent receptor endocytosis rate
k_{ss}	9.0e-11	M	Dissociation constant of somatostatin from so matostatin receptor on *D*-cells
K_{AS}	8.04e-15	$Mh^{-1}\ cell^{-1}$	Maximal somatostatin secretion rate due to stimulation with antrum acid
K_{NSI}	1.14e-15	$Mh^{-1}cell^{-1}$	Maximal rate of secretion of antral somatostatin due to enteric nervous stimulus
k_{NS}	1.0e-9	M	Dissociation constant of GRP from receptors on *D*-cells
α_{AS}	0.05	M	Acid concentration at which the rate of somatostatin secretion is half maximal
α_{NSI}	6.28e-7	M	Concentration of the ENS stimulant at which the rate of antral somatostatin secretion is half maximal
τ_S	13.86	$h^{-1}\ cell^{-1}$	Clearance rate of somatostatin

The above parameter values are taken from the literature [1, 2, 3].

RESULTS

Model Behavior

The behavior of these subsystems is examined independently and then the whole system is analyzed.

Analyzing the system as a whole, the $\beta IGRS_A$ model has three steady-state solutions

in (β, I, G, R, S_A) : a physiological point (862.515, 12.7, 81.5, 0.84, 8.4084), a saddle point (202.8369, 6.04, 145, 0.855, 11.61) and a pathological point (0, 0, 550, 0.91, 11.7818). The physiological point and pathological point can also be termed as stable node.

The model can be divided into fast (G, I, S_A) and slow (β, R) subsystems. The change in glucose and insulin levels of fast subsystem has been described on a time-scale of minutes and somatostatin levels of fast subsystem has been described on a time-scale of hours while the slow subsystem describes the β-cell mass dynamics and receptor dynamics on the time-scale of days.

It is to be taken in account the study of the effects of changes in certain parameter values on steady states. It can be calculated (from equation (10)) that the values of glucose at the physiological and saddle equilibria are given by the expression $\frac{u \pm \sqrt{u^2 - 4y\omega}}{2\omega}$. The values of ω, u and y can be altered in such a way that all three equilibria lie in the solution space [7].

Analyzing the fast subsystem, β-cell mass will be treated as a parameter due to its slow dynamics [12]. By the study of steady state solutions and from the nullclines $\left(\frac{dG}{dt} = 0 and \frac{dI}{dt} = 0\right)$ for given β-cell mass (862.515 mg) [Fig.1], it is observed that there is a single globally attracting fixed point and this fixed point is shifted to the lower glucose and higher insulin as β-cell mass value increases [Fig. 2], which is consistent with the results showed by Topp et al. [12]. In Fig. 2, graph (1), (2) and (3) are for $\beta = 400$, 862.5 and 1200 respectively.

The β-cell mass predicted by our model is 862.515 mg at physiological point for a healthy person which is consistent with the observed value of 850 mg [3]. By the β-cell mass dynamics, there are three β-cell mass null surfaces $\beta = 0\ mg$, $G = 81.5\ mg/dl$ and $G = 145\ mg/dl$ and it is observed that β-cell mass decreases below $G = 81.5\ mg/dl$ and above $G = 145\ mg/dl$ and it increases for all points between $G = 81.5\ mg/dl$ and $G = 145\ mg/dl$ [Fig. 3], which is consistent with the result shown by Topp et al. [12]. If a defect in the β-cell mass results at the point where death rate exceeds the replication rate for all levels of glucose then only steady state solution is the pathological state with zero β-cell mass i.e. the state of severe hyperglycemia.

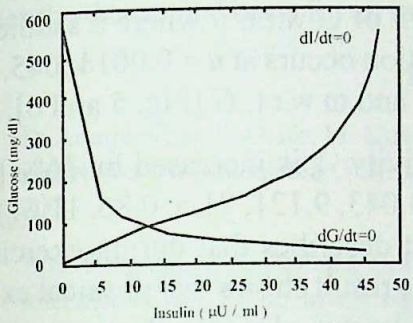

Fig. 1: The β-cell mass is fixed at 862.5 mg and glucose nullcline and insulin nullcline are shown. This shows that there is a globally attracting fixed point which occurs at the intersection of the glucose and insulin nullclines.

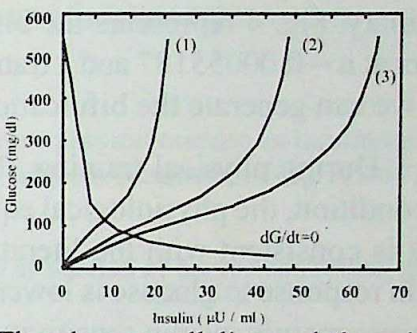

Fig. 2: The glucose nullcline and three insulin nullclines are represented for (1) β=400 mg, (2) β=862.5 mg and (3) β=1200 mg and it is found that the fixed point is shifted to lower glucose and higher insulin as β-cell mass value increases.

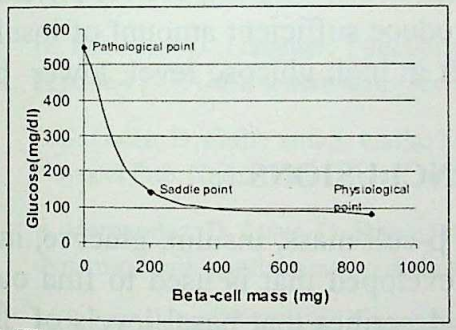

Fig. 3: The system has three steady-states: a physiological point, a saddle point and a pathological point. The fixed point having glucose level greater than 550 mg/dl has not been taken into consideration because it is not physiologically interesting due to negative β-cell mass.

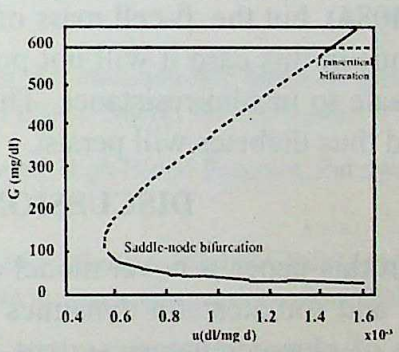

Fig. 4: It represents the bifurcation diagram G vs. u. The dashed line (----) represents the saddle point while the solid line (—) represents two stable fixed points. Figure shows that a saddle node bifurcation occurs at u=0.00055187 and a transcritical bifurcation occurs at u=0.00145045

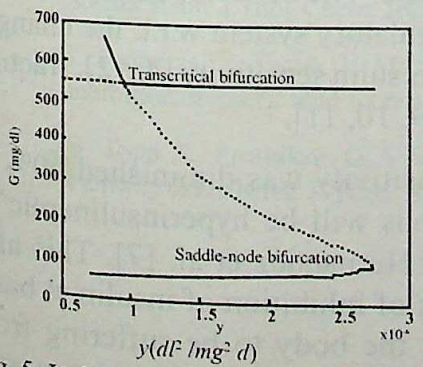

Fig. 5: It shows that bifurcation diagram of G vs. y vs. , where a saddle node bifurcation occurs at y=0.00000275515 and a transcritical bifurcation occurs at y=0.000000945.

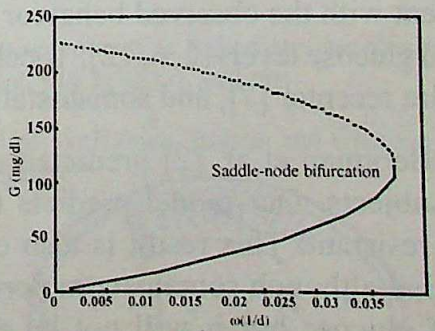

Fig. 6: It represents the bifurcation diagram of G vs. ω, where a saddle node bifurcation occurs at ω= 0.0325668 and a transcritical bifurcation occurs at ω<0.

Also the changes in the value of ω, u and y cause the equilibrium values to become imaginary. Fig. 4 represents the bifurcation diagram of G w.r.t. u where a saddle node occurs at $u = 0.00055187$ and a transcritical bifurcation occurs at $u = 0.00145045$. Similarly we can generate the bifurcation diagram for y and ω w.r.t. G [Fig. 5 and 6].

During physical training, the insulin sensitivity ξ is increased by 36% [1]. In this condition, the physiological equilibrium is (633.043, 9.121, 81.5, 0.86, 11.61). This result is consistent with the literature [1, 6, 8] that describes that during exercise the insulin response to glucose is lower than at rest. This result shows that physical exercise improves mainly insulin sensitivity, and to a lesser degree, glucose effectiveness. Thus insulin resistance can be prevented with physical exercise.

The insulin sensitivity ξ in insulin resistant, low tolerant obese subjects is decreased by 60% [2]. In this state the physiologic equilibrium is (2180.54, 35.092, 81.5, 0.76, 8.4084), but the β-cell mass of 2180.54 mg is obviously impossible physiologically. Thus in this case it will not possible to produce sufficient amount of insulin to compensate to insulin resistance. This will result in high glucose level, lower β-cell mass and thus diabetes will persist.

DISCUSSION AND CONCLUSIONS

In this paper, a novel model of coupled β-cell mass, insulin, glucose, insulin receptor and somatostatin dynamics has been developed that is used to find out the behavior of glucoregulatory system. The model describes that basal levels of β-cell mass, insulin, glucose, insulin receptor and somatostatin will approach the physiological steady state of $\beta = 862.515$, $I = 12.7$, $G = 81.5$, $R = 0.84$, $S_A = 8.4084$ under normal conditions. Also it is observed that the β-cell mass moves towards zero (i.e. death rate of β-cell exceeds the replication rate) at glucose levels greater than 145 *mg/dl* which derive the system towards pathological equilibrium state. The behavior of the model is consistent with the observed behavior of the glucoregulatory system w.r.t. the changes in blood glucose levels [2, 6, 12], β-cell mass [7, 12], insulin sensitivity [4, 12], fraction of insulin receptor [7], and somatostatin levels [5, 8, 9, 10, 11].

Bergman et al. [2] predicted that insulin sensitivity was diminished 60% in obese subjects. Our model predicts that such persons will be hyperinsulinemic or insulin resistant. This result is also consistent with Hernandez et al. [7]. This also shows that although somatostatin performs the work of inhibition of insulin at basal level of glucose but it will not be able to prevent the body to be suffering from hyperinsulinemia. Thus insulin sensitivity plays a key role in the glucoregulatory system. Although previous studies have not considered somatostatin dynamics with β-cell mass, insulin, glucose and receptor dynamics, the present model predicts a natural explanation for this quantitative behavior somatostatin. Finally, the $\beta IGRS_A$ model

provides the theoretical basis for an indirect measurement of somatostatin *in vivo*.

REFERENCES

1 D. Araujo-Vilar, E. Osifo, M. Kirk: Influence of Moderate physical exercise on Insulin-mediated and Non-insulin-mediated Glucose uptake in Healthy subjects. Metabolism. 46(2) (1997); 203-209.

2 R.N. Bergman, L.S. Phillips, C. Cobelli: Physiologic evaluation of factors controlling glucose tolerance in man. J. Clin. Invest. 68 (1981); 1456-1467.

3 F. Dela, J. Mikines, M.V. Listow: Twenty-four hour profile of plasma glucose and glucoregulatory hormones during normal living conditions in trained and untrained men. J. Clin. Meta. 73 (1991); 982-989.

4 M. Derouich, A. Boutayeb: The effect of physical exercise on the dynamics of Glucose and Insulin. J. Biomechanics. 35 (2002); 911-917.

5 H. Fehmann, J. Habener: Functional receptors for the insulinotropic hormone glucagon like peptide-I (737) on a somatostatin secreting cell line. FEBS. 279(2) (1991); 335-340.

6 D.S. Galla, D. Galla and S. Galla: Diabetes. Diabetes, High Blood Pressure, Put away forever. Navneet Pub. (India) Ltd. (2004); 36-58.

7 R. Hernandez, D. Lyles, D. Rubin, et al.: A Model of -cell mass, Insulin, Glucose and Receptor dynamics with applications to diabetes. (2001); <www.csupompna.edu/~swirkus/Diabetes.pdf>

8 M.P. Joseph Ian, Y. Zavros, J. Merchant, et al.: A model for integrative study of human gastric acid secretion. J. Appl. Physiol. 8 (2002); 8.

9 S. Marino, S. Ganguli, M.P. Joseph Ian, et al.: The importance of an Inter-compartmental Delay in a model for Human Gastric Acid Secretion. Bull. Math. Biol. (2003).

10 J. Park, T. Chiba, T.Yamada: Mechanism for Direct inhibition of Canine Gastric Parietal cells by Somatostatin. J. Biol. Chem. 262(29) (1987); 14190-14196.

11 L. Piqueras, Y. Tache, V. Martinez: Somatostatin receptor type 2 mediates bombesin induced inhibition of gastric acid secretion in mice. J. Physiol. 549.3 (2003); 889-901.

12 B. Topp, K. Promilow, G. Vries, et al.: A Model of -cell mass, Insulin and Glucose Kinetics: Pathway to Diabetes. J. Theo. Biol. 206 (2000); 605-619.

प्राकृतिक एवं भौतिकीय विज्ञान शोध पत्रिका

खण्ड 19 अंक (1) 2005

(1)	प्रकाशन स्थान	:	गुरुकुल कांगड़ी विश्वविद्यालय, हरिद्वार
(2)	प्रकाशन की अवधि	:	वर्ष में एक खण्ड, अधिकतम दो अंक
(3)	मुद्रक का नाम	:	चन्द्र किरण सैनी
	राष्ट्रीयता	:	भारतीय
	व पता	:	किरण ऑफसेट प्रिंटिंग प्रेस निकट गुरुकुल कांगड़ी फार्मेसी कनखल, हरिद्वार – 249404 फोन नं0 245975
(4)	प्रकाशक का नाम	:	प्रो0 ए0 के0 चोपड़ा
	राष्ट्रीयता	:	भारतीय
	व पता	:	कुलसचिव, गुरुकुल कांगड़ी विश्वविद्यालय हरिद्वार – 249409
(5)	प्रधान सम्पादक	:	प्रो0 वीरेन्द्र अरोड़ा
	राष्ट्रीयता	:	भारतीय
	व पता	:	गणित विभाग गुरुकुल कांगड़ी विश्वविद्यालय हरिद्वार – 249409
(6)	प्रबन्ध सम्पादक	:	डॉ0 पी0 पी0 पाठक
	राष्ट्रीयता	:	भारतीय
	व पता	:	भौतिकी विभाग गुरुकुल कांगड़ी विश्वविद्यालय हरिद्वार – 249409
(7)	स्वामित्व	:	गुरुकुल कांगड़ी विश्वविद्यालय हरिद्वार – 249409

मैं प्रो0 ए.के. चोपड़ा, कुलसचिव, गुरुकुल कांगड़ी विश्वविद्यालय, हरिद्वार, घोषित करता हूँ कि उपरिलिखित तथ्य मेरी जानकारी के अनुसार सही हैं।

हस्ताक्षर

प्रो0 ए. के. चोपड़ा

कुलसचिव

ISSN 097-3799

प्राकृतिक एवं भौतिकीय विज्ञान शोध पत्रिका

JOURNAL OF NATURAL & PHYSICAL SCIENCES

खण्ड 19 अंक 2, 2005
Vol. 19 No. 2, 2005

गुरुकुल कांगड़ी विश्वविद्यालय, हरिद्वार

Gurukula Kangri Vishwavidyalaya, Haridwar

प्राकृतिक एवं भौतकीय विज्ञान शोध पत्रिका
Journal of Natural & Physical Scienes

Journal of Natural & Physical Sciences, Vol. 19 (2) (2005) 111-135

SPECIAL SOLUTIONS, HIROTA FORM, LAX PAIR AND SIMILARITY REDUCTIONS OF THE CMKDV-II EQUATION

Abulgassim A. Mohammad* and M. Can.**

(Received 16. 05. 2005)

ABSTRACT

In this paper firstly the Painleve analysis developed by Weiss *et al.* for nonlinear partial differential equations is applied to the CMKdV-II equation and the data obtained by the truncation technique is used to obtain some analytical solutions, infinite dimensional Lie symmetries, the Hirota bilinear form, and a Lax pair of the equation.

Secondly combining group theory and singularity analysis we obtained some information about the similarity solutions of the CMKdV-II equation.

It has been shown that this equation possess a four dimensional solvable Lie algebra of the point symmetries and the similarity reductions due to these symmetries have the Painleve property.

INTRODUCTION

Quasilinear parabolic equations, or nonlinear reaction-diffusion systems arise in the modelling of phenomena in physics, chemistry, biology and other applied sciences. The complex modified Korteweg-de Vries-I equation (CMKdV-I)

$$\omega_t + \alpha\left(|\omega|^2\omega\right)_x + \beta\,\omega_{xxx} = 0 \tag{1}$$

and the complex modified Korteweg-de Vries-II equation (CMKdV-II)

$$\omega_t - 6|\omega|^2\omega_x + \omega_{xxx} = 0 \tag{2}$$

are amoung them. The CMKdV-I equation (1) is studied elsewhere [5]. In this work we are going to investigate the CMKdV-II equation (2).

Since the formulation of the Painleve tests, there has been considerable interest in using the Painleve property as a means of determining whether given equations, both partial and ordinary differential equations, are integrable. To apply the test to a partial differential equation we use the theory of complex functions with several complex variables.

The major difference between analytic functions of one complex variable and several complex variables is that, in general, the singularities of a function of several complex variables can not be isolated if $f = f(z_1,\ldots,z_n)$ is a meromorphic function of n complex variables ($2n$ real variables), the singularities of f occur along analytic manifolds of (real) dimension $2n$-2. These manifolds are determined by conditions of the form $\phi(z_1,\ldots,z_n)$, where ϕ is an analytic function of $(z_1,\ldots,z_n)$ in a neighborhood of the manifold.

* Garyunis University, Mathematics Department Benghazi-Libya P.O. Box 9480 Tell & Fax: +218612229617
** Istanbul Technical University, Mathematics Department Maslak 80626 Istanbul Turkiye

With reference to the above, we say that a *partial differential equation has the Painleve property when the solutions of the PDE are single valued about the movable, singularity manifolds.* For partial differential equations we require that the solution be a *single-valued functional* of the data, i.e. *arbitrary functions*[9]. This is a formal property and not a restriction on the data itself.

To verify if a PDE has the Painleve property we introduce a method for expanding a solution of a nonlinear PDE about a movable, singular manifold.

Let $u = u(z_1,\ldots,z_n)$ be a solution of the PDE and assume that

$$u = \phi^p \sum_{j=0}^{\infty} u_j \phi^j \tag{3}$$

where ϕ and

$$u_j = u_j(z_1,\ldots,z_n) \tag{4}$$

are analytic functions of $(z_1,\ldots,z_n)$ in a neighborhood of manifold. Substitution of (3) into the PDE determines the possible values of p and defines the recursion relations for u_j, $j = 0,1,2,\ldots$. When p is a negative integer and (3) is a valid and general expansion about the manifold, then the solution has a single valued representation about the singularity manifold. If this representation is valid for all allowed movable singularity manifolds, then the PDE has the Painleve property. For a specific PDE it is necessary to identify all possible values for p and then find the form of the resulting *phi* series [2].

A point that will emphasize is that the *phi* series for nonlinear PDE contain a lot of information about the PDE. For the equations which have the Painleve property a method has been developed for finding Lie symmetries, Lax pairs and Backlund transformations [1,7,9,11,12]. An outline and an application of the *singular manifold method* is presented in the next section. For equations that do not have the Painleve property it is still possible to obtain single valued expansions by specializing the arbitrary functions that appear in the *phi* series expansions. This specialization leads to a system of partial differential equations for the formally arbitrary data. For specific systems, and conjectured in general, these equations are integrable. The form of the resulting reduction enables the identification of integrable reductions of the original systems.

Now we are going to illustrate the nature of the Painleve test on the complex modified Korteweg-de Vries-II equation (2).

PAINLEVE ANALYSIS FOR CMKdV-II EQUATION

Since the absolute value $|\cdot|$ in (2) brings some difficulty in the calculations, we first let $\omega = u + iv$ and separate the real and imaginary parts in (2) and obtain the system

$$\begin{aligned} u_t - 6(u^2+v^2)u_x + u_{xxx} &= 0 \\ v_t - 6(u^2+v^2)v_x + v_{xxx} &= 0 \end{aligned} \tag{5}$$

Now we modify the method of Weiss *et. al.*[9] for the system of partial differential equations and follow the four steps of the algorithm.

***Step 1:* Dominant behaviours:**

Let $\phi(x,t)=0$ be the solution singularity manifold of (5) and substitute

$$u(t,x)=u_0(t,x)\phi(t,x)^p$$
$$v(t,x)=v_0(t,x)\phi(t,x)^p \tag{6}$$

in the system of partial differential equations (5), where p is real and $\phi(t,x)$ is arbitrary. To balance the nonlinear terms with the third order terms one must take $p=-1$.

***Step 2*: Branches**

Now we substitute

$$u=\sum_{j=0}^{\infty}u_j\phi^{j-1}, \qquad v=\sum_{j=0}^{\infty}v_j\phi^{j-1} \tag{7}$$

in (5), and arranging terms with respect to the ascending powers or the arbitrary function $\phi(t,x)$ we get:

For $j=0$: The two equations are

$$u_0\left(u_0^2+v_0^2-\phi_x^2\right)=0, \text{ and } v_0\left(u_0^2+v_0^2-\phi_x^2\right)=0.$$

They are linearly dependent and yield only the relation

$$u_0^2+v_0^2=\phi_x^2. \tag{8}$$

between $u_0(t,x)$ and $v_0(t,x)$. Hence for nonzero values of $u_0(t,x), v_0(t,x)$ we have only one branch in which one of the $u_0(t,x)$ and $v_0(t,x)$ is arbitrary.

For $j=1$: The two equations are the same and we have the relation

$$u_0u_1+v_0v_1=-\frac{1}{2}\phi_{xx} \tag{9}$$

For $j=2$:

$$\begin{aligned}
&6\phi_x\left[u_0\left(u_1^2-v_1^2\right)+u_2\left(u_0^2-v_0^2\right)+2u_0v_0v_2\right)\\
&-3u_{0x}\left(4u_0u_1+4v_0v_1+\phi_{xx}\right)-6\left(u_0^2+v_0^2\right)u_{1x}-3\phi_xu_{0xx}-u_0\left(\phi_{xxx}+\phi_t\right)=0,\\
&-6\phi_x\left[u_0\left(u_1^2-v_1^2\right)-u_2\left(u_0^2-v_0^2\right)+2u_0v_0u_2\right]\\
&-3v_{0x}\left(4u_0u_1+4v_0v_1+\phi_{xx}\right)-6\left(u_0^2+v_0^2\right)v_{1x}-3\phi_xv_{0xx}-v_0\left(\phi_{xxx}+\phi_t\right)=0,
\end{aligned} \tag{10}$$

For $j\geq 3$:

$$\phi_x\left[(j-1)(j-2)(j-3)\phi_x^2-6(j-1)\left(u_0^2+v_0^2\right)+12u_0^2\right]u_j+12u_0v_0\phi_xv_j$$

$$= Q_1\left(u_0, u_1, \ldots, u_{j-1}, \phi\right), \quad j = 0,1,2,\ldots$$

$$12u_0v_0\phi_x u_j + \phi_x\left[(j-1)(j-2)(j-3)\phi_x^2 - 6(j-1)\left(u_0^2 + v_0^2\right) + 12v_0^2\right]v_j$$

$$= Q_2\left(u_0, u_1, \ldots, u_{j-1}, \phi\right), \quad j = 0,1,2,\ldots . \tag{11}$$

where

$$Q_1 = -u_{j-3,t} - u_{j-3,xxx} - (j-3)\left(\phi_t u_{j-2} + 3\phi_x u_{j-2,xx} + 3\phi_{xx}u_{j-2,x} + \phi_{xxx}u_{j-2}\right)$$
$$-3(j-2)(j-3)\left(\phi_x^2 u_{j-1,x} + \phi_x\phi_{xx}u_{j-1}\right)$$
$$-6\sum_{k=0}^{j-1}\left[\sum_{j=0}^{k}\left(u_i u_{k-i} + v_i v_{k-i}\right)\right]u_{j-k-1,x}$$
$$-6\phi_x\sum_{k=0}^{j-1}\left[\sum_{j=0}^{k}\left(u_i u_{k-i} + v_i v_{k-i}\right)\right](j-k-1)u_{j-k}$$
$$+6\phi_x u_0\sum_{i=1}^{j-1}\left(u_i u_{j-1} + u_i u_{j-1}\right), \tag{12}$$

and

$$Q_2 = -v_{j-3,t} - v_{j-3,xxx} - (j-3)\left(\phi_t v_{j-2} + 3\phi_x v_{j-2,xx} + 3\phi_{xx}v_{j-2,x} + \phi_{xxx}v_{j-2}\right)$$
$$-3(j-2)(j-3)\left(\phi_x^2 v_{j-1,x} + \phi_x\phi_{xx}v_{j-1}\right)$$
$$-6\sum_{k=0}^{j-1}\left[\sum_{j=0}^{k}\left(u_i u_{k-i} + v_i v_{k-i}\right)\right]v_{j-k-1,x}$$
$$-6\phi_x\sum_{k=0}^{j-1}\left[\sum_{j=0}^{k}\left(u_i u_{k-i} + v_i v_{k-i}\right)\right](j-k-1)v_{j-k}$$
$$+6\phi_x v_0\sum_{i=1}^{j-1}\left(u_i u_{j-1} + v_i v_{j-1}\right). \tag{13}$$

Step3: **Resonances**

By virtue of the relation (8) the determinant of the coefficient matrix of the unknowns u_j, v_j in the system of linear algebraic equations (11) is

$$\Lambda = (j+1)j(j-1)(j-3)(j-4)(j-5)\phi_x^4 \tag{14}$$

The values of j for which $u_j(t,x), v_j(t,x)$ can not be determined from the system uniquely are -1,0,1,3,4 and 5. These are the resonaces of the system (5).

***Step 4:* Compatibility conditions at the resonances**

At resonance points the rank of the coefficient matrix is one. Hence for the system to be consistent, after substitution in (11) of the previously computed $u_i(t,x)$, $u_i(t,x)$, $i \le j-1$, the rank of the augmented matrix must also be one. Clearly the resonance point $j=-1$ corresponds to the free singularity manifold function $\phi(x,t)$. At the resonance $j=0$, we have only the relation (8) between u_0 and v_0. Hence one of them is arbitrary. For $j=1$ the two equations of the system are the same and we have only the relation (9) between u_1 and v_1. Therefore one of them is taken arbitrary. For $j=2$ we have a system of two linear algebraic equations (10) in u_2, v_2 with a nonsingular coefficient matrix. Hence u_2, v_2 are solved uniquely in u_1, v_1, u_0, v_0 and ϕ. For $j=3$ the system of two linear algebraic equations in u_3, v_3 has a coefficient matrix with rank 1. The rank of the augmented matrix is also 1.

Hence one u_3 of v_3 or remains arbitrary. At $j=4$ and $j=5$ we have the same, hence u_4 and u_5 are taken arbitrary.

To show that the rank of the augmented matrices are 1, we used computer algebra package Mathematica[10]. For the augmented matrix at the resonance $j=5$, the computation took around 48 hours nonstop running of a personnel computer with a 486 CPU and a 16 MB ram. However another PC with a Pentium CPU finished it in 12 hours.

To write a general solution to this system, one needs six arbitrary functions. u_5, u_4, u_3, u_1, u_0 and ϕ are arbitrary functions in the series (7). Therefore the system (5) passes the Painleve test for PDE's.

Since the CMKdV-II Equation (2) has the Painleve property, it has a more rich structure compared to the one of the CMKdV-I equation [5]. Now using the data obtained from this analysis we are going to find some exact solutions, and infinite Lie symmetry, a Hirota bilinear form and a Lax pair of the CMKdV-II Equation.

EXACT SOLUTIONS

Let us truncate the series in (7) at the second term and assume that $u_j = 0$, $j \ge 2$. Then we are going to find a truncated series solution to the system (5) of the form

$$u = \frac{u_0}{\phi} + u_1$$

$$v = \frac{v_0}{\phi} + v_1 \qquad (15)$$

After the throughout substitution of $u_0u_1 + v_0v_1 = -\frac{1}{2}\phi_{xx}$ if we let $u_2 = v_2 = 0$ in the system of algebraic equations (10) we get

$$C_1 = 6\phi_x u_0\left(u_1^2 + v_1^2\right) - 6\phi_x^2 u_{1x} + 3\phi_{xx}u_{0x} - 3\phi_x u_{0xx} - \phi_{xxx}u_0 - \phi_t u_0 = 0$$

$$C_2 = 6\phi_x v_0\left(u_1^2 + v_1^2\right) - 6\phi_x^2 v_{1x} + 3\phi_{xx}v_{0x} - 3\phi_x v_{0xx} - \phi_{xxx}v_0 - \phi_t v_0 = 0 \qquad (16)$$

Similarly letting $u_2 = v_2 = u_3 = v_3 = 0$ in the system of algebraic equations for u_3, v_3 one obtains

$$C_3 = 6\phi_x u_0 u_{0x}\left(u_1^2 + v_1^2\right) + 6\phi_x\phi_{xx}u_0u_{1x} + \phi_x u_0 u_{0xxx} + \phi_x u_0 u_{0t} = 0,$$

$$C_4 = -6\phi_x u_0 u_{0x}\left(u_1^2 + v_1^2\right) + 6\phi_x\phi_{xx}v_0v_{1x} + \phi_x v_0 v_{0xxx} + \phi_x v_0 v_{0t} = 0, \qquad (17)$$

while for $u_2 = v_2 = u_3 = u_3 = v_4 = 0$ the system of algebraic equations for u_4, v_4 yields

$$C_5 = u_{1t} - 6\left(u_1^2 + v_1^2\right)u_{1x} + u_{1xxx} = 0,$$

$$C_6 = v_{1t} - 6\left(u_1^2 + v_1^2\right)v_{1x} + v_{1xxx} = 0, \qquad (18)$$

i.e. u_1, v_1 must be a solution of the original system of PDE's (7). Therefore the relation (15) can be taken as an auto-Backlnd transformation that relates two solutions u,v and u_1, v_1 of (5) if u_0, v_0 and u_1, v_1 interrelated by (12) and (13) satisfy (16) and (17).

$C_1 = 0$ and $C_3 = 0$ in (16) and (17) form an algebraic system of linear equations in $u_1^2 + v_1^2$ and u_{1x}. Solving these unknowns from these equations one obtains

$$u_{1x} = \frac{u_{0x}\left(3\phi_{xx}u_{0x} - 3\phi_x u_{0xx} - \phi_{xxx}u_0 - \phi_t u_0\right) + \phi_x u_0\left(u_{0xxx} + u_{0t}\right)}{6\phi_x\left(\phi_x u_{0x} - \phi_{xx}u_0\right)},$$

$$u_1^2 + v_1^2 = \frac{\phi_{xx}\left(3\phi_{xx}u_{0x} - 3\phi_x u_{0xx} - \phi_{xxx}u_0 - \phi_t u_0\right) + \phi_x^2\left(u_{0xxx} + u_{0t}\right)}{6\phi_x\left(\phi_x u_{0x} - \phi_{xx}u_0\right)}. \qquad (19)$$

Similarly $C_2 = 0$ and $C_4 = 0$ in (16) and (17) form another system of algebraic linear equations in $u_1^2 + v_1^2$ and v_{1x} whose solution gives

$$v_{1x} = \frac{v_{0x}\left(3\phi_{xx}v_{0x} - 3\phi_x v_{0xx} - \phi_{xxx}v_0 - \phi_t v_0\right) + \phi_x v_0\left(v_{0xxx} + v_{0t}\right)}{6\phi_x\left(\phi_x v_{0x} - \phi_{xx}v_0\right)},$$

$$u_1^2 + v_1^2 = \frac{\phi_{xx}\left(3\phi_{xx}v_{0x} - 3\phi_x v_{0xx} - \phi_{xxx}v_0 - \phi_t v_0\right) + \phi_x^2\left(v_{0xxx} + u_{0t}\right)}{6\phi_x\left(\phi_x v_{0x} - \phi_{xx}v_0\right)}. \qquad (20)$$

On the other hand eliminating $u_1^2 + v_1^2$ between $C_1 = 0$, $C_2 = 0$ in (16) and between $C_3 = 0$, $C_4 = 0$

in (17), one obtains an algebraic system of two linear equations in u_{1x} v_{1x} and. Solving these unknowns from these equations one obtains

$$u_{1x} = \frac{3u_{0x}\phi_{xx}\left[\phi_{xx}\left(u_{0x}v_0 - v_{0x}u_0\right) - \phi_x\left(u_0v_{0xx} - v_0u_{0xx}\right)\right]}{6\phi_x\left(\phi_x u_{0x} - \phi_{xx}u_0\right)}$$

$$- \frac{u_0\phi_x^2\left(u_{0xxx}v_{0x} - u_x v_{0xxx} + v_{0x}u_{0t} - u_{0x}v_{0t}\right)}{6\phi_x\left(\phi_x u_{0x} - \phi_{xx}u_0\right)},$$

$$u_{1x} = \frac{3v_{0x}\phi_{xx}\left[\phi_{xx}\left(v_{0x}u_0 - u_{0x}u_0\right) - \phi_x\left(v_0u_{0xx} - u_0v_{0xx}\right)\right]}{6\phi_x\left(\phi_x v_{0x} - \phi_{xx}v_0\right)}$$

$$- \frac{v_0\phi_x^2\left(v_{0xxx}u_{0x} - v_x u_{0xxx} + u_{0x}v_{0t} - v_{0x}u_{0t}\right)}{6\phi_x\left(\phi_x v_{0x} - \phi_{xx}v_0\right)}. \tag{21}$$

The values of $u_1^2 + v_1^2$ in (19) and (20) must be the same. This leads to the compatibility condition

$$\frac{\partial}{\partial x}\left(-\frac{u_{0x}^2 + v_{0x}^2}{\phi_x^2} + \frac{2}{3}\frac{\phi_{xxx} + \phi_t}{\phi_t}\right) = 0,$$

and hence

$$-\frac{u_{0x}^2 + v_{0x}^2}{\phi_x^2} + \frac{2}{3}\frac{\phi_{xxx} + \phi_t}{\phi_t} = \gamma(t), \tag{22}$$

where $\gamma(t)$ is an arbitrary smooth function of t. Again using the values of u_{1x}, v_{1x} in (19) and (20) one also finds

$$2\left(v_0u_{1x} - u_0v_{1x}\right) = \frac{\partial}{\partial x}\left(\frac{u_0v_{0x} - v_0u_{0x}}{\phi_x}\right) \tag{23}$$

Differentiating (12) with respect to x one gets

$$u_0u_{0x} + v_0v_{0x} = \phi_x\phi_{xx} \tag{24}$$

Rearranging terms and taking the squares of both sides of the resulting equation one gets

$$u_0^2u_{0x}^2 - 2u_0u_{0x}\phi_x\phi_{xx} + \phi_x^2\phi_{xx}^2 = v_0^2v_{0x}^2 \tag{25}$$

subtituting the values of u_{0x}^2 and ϕ_x^2 computed from (12) into (25) we get

$$\phi_x^2u_{0x}^2 - 2u_0u_{0x}\phi_x\phi_{xx} + \phi_{xx}^2u_0^2 = v_0^2\left(u_{0x}^2 + v_{0x}^2 - \phi_{xx}^2\right) \tag{26}$$

or equivalently

$$\phi_x u_{0x} = \phi_{xx} u_0 \pm v_0 \left(u_{0x}^2 + v_{0x}^2 - \phi_{xx}^2\right)^{\frac{1}{2}} \tag{27}$$

Following the same procedure one also gets

$$\phi_x v_{0x} = \phi_{xx} v_0 \pm u_0 \left(u_{0x}^2 + v_{0x}^2 - \phi_{xx}^2\right)^{\frac{1}{2}} \tag{28}$$

Now taking the squares of the both sides of (27) and (28) and summing up the results we finally obtain

$$\phi_x^2 \left(v_{0x}^2 + u_{0x}^2 - \phi_{xx}^2\right) = \pm 4 \phi_{xx} u_0 v_0 \left(v_{0x}^2 + u_{0x}^2 - \phi_{xx}^2\right)^{\frac{1}{2}} + \phi_x^2 \left(v_{0x}^2 + u_{0x}^2 - \phi_{xx}^2\right) \tag{29}$$

where parallel signs of $\pm$'s are used in both equations. Hence we have shown that

$$u_{0x}^2 + v_{0x}^2 - \phi_{xx}^2 = 0 \tag{30}$$

Using the compatibility condition (22) in (30) one gets a partial differential equation in the singularity manifold function $\phi(t, x)$:

$$\frac{\phi_t}{\phi_x} + \frac{\phi_{xxx}}{\phi_x} - \frac{3}{2} \frac{\phi_{xx}^2}{\phi_x^2} = \gamma(t) \tag{31}$$

The ϕ equation (31) is invariant under the group II of homographic transformations

$$\phi \rightarrow \frac{a\phi + b}{c\phi + d} \quad ad - bc \neq 0 ; \tag{32}$$

hence it can be written in terms of two homographic invariant functions

$$S = \{\phi, x\} = \frac{\phi_{xxx}}{\phi_x} - \frac{3}{2} \left(\frac{\phi_{xx}}{\phi_x}\right)^2 \tag{33}$$

called the Schwarzian derivative, and

$$C = -\frac{\phi_t}{\phi_x} \tag{34}$$

which has the dimension of a velocity.

In terms of the invariant derivatives C and S, the PDE (31) can be summarized as

$$S - C = \gamma \tag{35}$$

By the compatibility condition $(\phi_t)_{xxx} = (\phi_{xxx})_t$ one also has

$$S_t + C_{xxx} + 2C_x S + C S_x = 0 .$$

Therefore the Schwarzian derivative S must satisfy the Korteweg-de Vries like equation

$$S_t + 3SS_x + S_{xxx} = \gamma S_x \tag{36}$$

In the special case of $\gamma(t) \equiv 0$, this equation reduces to the Korteweg-de Vries equation

$$S_t + 3SS_x + S_{xxx} = 0.$$

On the other hand in the view of (30), the expression (27) reduces to

$$\phi_x u_{0x} - \phi_{xx} u_0 = 0 \tag{27}$$

which leads to

$$\frac{\partial}{\partial x}\left(\frac{u_0}{\phi_x}\right) = 0 \quad \text{or } u_0 = \alpha\,\phi_x \tag{38}$$

Therefore the relation (12) implies that

$$v_0 = \beta\,\phi_x, \qquad \alpha^2 + \beta^2 = 1 \tag{39}$$

In the view of (14) and (22 one also finds that

$$u_1 = \alpha L\,, v_1 = \beta L\,, \quad L = -\frac{\phi_{xx}}{2\phi_x} \tag{40}$$

To satisfy the conditions to C_1, C_6, α and β must be constants. To find exact solutions to the CMKdV-II equation in (2) we must take solutions $S = S(t,x)$ of the Korteweg-de Vries-like equation (36) and substitute in (33) to find $\phi(t,x)$. The solutions of the ϕ equation (31) is obtained by the help of the following two lemmas about the differential equations written in terms of the Schwarzian derivatives[9].

LEMMA 1. Let ψ_1 and ψ_2 be two linearly independent solutions of the equation

$$\frac{d^2\psi}{dz^2} + P(z)\psi = 0 \tag{41}$$

which are defined and holomorphic on some simply connected domain D in complex plane. Then $W(z) = \psi_1(z)/\psi_2(z)$ satisfies the equation

$$\{W : z\} = 2P(z) \tag{42}$$

at all points of D where $\psi_2(z) \neq 0$. Conversely if $W(z)$ is a solution of (42), holomorphic in some neighborhood of $z_0 \in D$, then one can find two linearly independent solutions $\psi_1(z)$ and $\psi_2(z)$ of (41) such that $W(z) = \psi_1(z)/\psi_2(z)$.

LEMMA 2. The Schwarzian derivative is invariant under fractional linear transformation acting on the first argument, namely,

$$\left\{\frac{aW+b}{cW+d}; z\right\} = \{W; z\} \qquad ad - bc \neq 0 \tag{43}$$

where a, b, c, d are constants.

Solutions for Constant S

The constant functions $S = \pm 2\lambda^2$ with λ a constant are solutions of the Korteweg-de Vries-like equation (36).

For $S = -2\lambda^2$: we have

$$S = \{\phi : x\} = -2\lambda^2 . \tag{44}$$

Hence $P(x) = -\lambda^2$ in (41), and two linearly independent solutions are

$$\psi_1 = E(t)e^{\lambda x} + F(t)e^{-\lambda x}, \quad \psi_2 = G(t)e^{\lambda x} + H(t)e^{-\lambda x}. \tag{45}$$

Therefore by Lemma 1. And Lemma 2., one obtains

$$\phi(t,x) = \frac{E(t)e^{\lambda x} + F(t)e^{-\lambda x}}{G(t)e^{\lambda x} + H(t)e^{-\lambda x}}, \quad EH - FG \neq 0 \tag{46}$$

To determine the t-dependence of $\phi(t,x)$ let us recall from (33) with $\gamma \equiv 0$ that

$$C = S = -2\lambda^2 = -\frac{\phi_t}{\phi_x}. \tag{47}$$

This leads to a system of nonlinear ordinary differential equations in coefficients E, F, G and H:

$$\begin{cases} EG' - E'G = 0 \\ FH' - F'H = 0 \\ 4\lambda^3 GH = G'H' - GH'. \end{cases} \tag{48}$$

A particular solution of (48) is

$$\frac{H(t)}{G(t)} = e^{-4\lambda^3 t}, \quad E(t) = BG(t), \quad F(t) = AH(t) \tag{49}$$

where A, B $(A \neq B)$ are real arbitrary constants. This solution of (48) leads to

$$\phi(t,x) = A + Be^{-\lambda\zeta} Sech\lambda\zeta, \qquad \zeta = x + 2\lambda^2 t. \tag{50}$$

With this $\phi(t,x)$ one gets

$$u_0(t,x) = -\lambda\alpha\, Be^{-\lambda\zeta} Sech\lambda\zeta(1 + Tanh\lambda\zeta) \tag{51}$$

and

$$u_1(t,x) = \lambda\alpha\, Tanh\lambda\zeta, \tag{52}$$

$$u(t,x) = \lambda\alpha\left(1 - \frac{2}{1 + Me^{2\lambda\zeta}}\right). \tag{53}$$

Where M is an arbitrary constant. For $M = 1$ one gets as a special case

$$u(t,x) = \lambda\alpha \; Coth\lambda\zeta \,. \tag{54}$$

Hence $u(t,x)$ and $u_1(t,x)$ in the above are exact solutions for the usual MKdV equation

$$\omega_t - 6\omega^2\omega_x + \omega_{xxx} = 0 \tag{55}$$

which are not new, and the corresponding exact solutions of the CMKdV-II equation (2) are

$$\omega(t,x) = u_1(t,x) + iu_1(t,x) \tag{56}$$

and

$$\omega(t,x) = u(t,x) + iu(t,x) \tag{57}$$

For $S = 2\lambda^2$: we have

$$S(\phi : x) = 2\lambda^2 . \tag{58}$$

Hence $P(x) = \lambda^2$ in (41), and two linearly independent solutions are

$$V_1 = E(t)e^{\lambda ix} + F(t)e^{-\lambda ix}, \quad V_2 = G(t)e^{\lambda ix} + H(t)e^{-\lambda ix} . \tag{59}$$

By Lemma 1. and Lemma 2. one gets

$$\phi(t,x) = \frac{E(t)e^{\lambda ix} + F(t)e^{-\lambda ix}}{G(t)e^{\lambda ix} + H(t)e^{-\lambda ix}}, \qquad EH - FG \neq 0 . \tag{60}$$

To determine the t-dependence of $\phi(t,x)$ we use (35) with $\gamma \equiv 0$ and obtain

$$\phi(t,x) = A\tan\lambda\zeta, \qquad \zeta = x + 2\lambda^2 t \tag{61}$$

where A is an arbitrary constant. With this $\phi(t,x)$ one gets

$$u_0(t,x) = \lambda\alpha A\sec^2\lambda\zeta \;, \tag{62}$$

$$u_1(t,x) = -\lambda\alpha\tan\lambda\zeta \;,$$

$$v_1(t,x) = -\lambda\beta\tan\lambda\zeta \,, \tag{63}$$

and

$$u(t,x) = \lambda\alpha\cot\lambda\zeta \;,$$

$$v(t,x) = \lambda\beta\cot\lambda\zeta \,. \tag{64}$$

where λ, α, β, are arbitrary constants provided that $\alpha^2 + \beta^2 = 1$.

The functions $u_1(t,x)$, $u(t,x)$ are well known solutions of the modified Korteweg de-Vries equation (55) and the corresponding solutions of the complex modified Korteweg de-Vries-II equation (2) are of the form

$$\omega(t,x)=u_1(t,x)+i\,v_1(t,x), \tag{65}$$

and

$$\omega(t,x)=u(t,x)+i\,v(t,x). \tag{66}$$

Solutions for $S=-4/x^2$:

The function $S=-4/x^2$ is also a solution of the Korteweg-de Vries-like equation in (36) with $\gamma\equiv 0$.

With $S=-4/x^2$ one has

$$S=\{\phi:x\}=-\frac{4}{x^2}. \tag{67}$$

Hence $P(z)=-2/x^2$ in equation (41), and two linearly independent solutions are $1/x$ and x^2. Therefore by Lemma 1. and Lemma 2. one obtains

$$\phi(t,x)=\frac{E(t)x^3+F(t)}{G(t)x^3+H(t)},\ EH-FG\neq 0. \tag{68}$$

To determine the t-dependence of $\phi(t,x)$ let us recall from (35) with $\gamma\equiv 0$ that

$$C=S=-\frac{4}{x^2}=-\frac{\phi_t}{\phi_x}. \tag{69}$$

This leads to a system of nonlinear ordinary differential equations.

$$\begin{cases} EF'-E'F=0 \\ EH'-E'H+FG'-F'G=0 \\ -12(EH-FG')=FH'-F'H. \end{cases} \tag{70}$$

A particular solution of (70) can be found by inspection. Let E and G be constants then one has

$$F(t)=12Et+M,\qquad H(t)=12Gt+N \tag{71}$$

where M and N are arbitrary constants. Hence one obtains

$$\phi(t,x)=1+\frac{A}{x^3+12t+B},$$

$$u_0(t,x)=-\frac{3\alpha A x^2}{(x^3+12t+B)^2},$$

$$v_0(t,x) = -\frac{3\beta A x^2}{\left(x^3 + 12t + B\right)^2},$$

$$u_1(t,x) = \alpha \frac{2x^3 - 12t - B}{\left(x^3 + 12t + B\right)x},$$

$$v_1(t,x) = \beta \frac{2x^3 - 12t - B}{\left(x^3 + 12t + B\right)x}, \tag{72}$$

where A and B are arbitrary constants.

Using (72) in (15) one finally obtains an exact solution for the CMKdV-II equation (2) as

$$\omega(t,x) = u(t,x) + iv(t,x) \tag{73}$$

with

$$\omega(t,x) = \alpha\left(\frac{3x^2}{x^3 + 12\beta t + K} - \frac{1}{x}\right),$$

$$v(t,x) = \beta\left(\frac{3x^2}{x^3 + 12\beta t + K} - \frac{1}{x}\right). \tag{74}$$

where K is an arbitrary constant.

Another Special Solution

In the special case of $u_1 = v_1 = 0$, the conditions $C_1 = 0$ and $C_2 = 0$ in (16) reduces to

$$\begin{aligned} u_{0xxx} + u_{0t} &= 0, \\ v_{0xxx} + v_{0t} &= 0. \end{aligned} \tag{75}$$

The functions

$$\begin{aligned} u_0(t,x) &= A\cos\left(\delta x + \delta^3 t\right) \\ v_0(t,x) &= A\sin\left(\delta x + \delta^3 t\right) \end{aligned} \tag{76}$$

where A and δ are two arbitrary constants, satisfy the system (75). Hence in this case

$$\phi_x^2 = u_0(t,x)^2 + v_0^2(t,x) = A^2 \tag{77}$$

is a constant. Therefore we must have

$$\phi(t,x) = Ax + B(t) \tag{78}$$

where $B(t)$ is an arbitrary function.

With this $\phi(t,x)$ the truncated solution in (15) becomes

$$u(t,x)=\frac{A}{Ax+B(t)}\cos\left(\delta x+\delta^3 t\right),$$

$$v(t,x)=\frac{A}{Ax+B(t)}\sin\left(\delta x+\delta^3 t\right) \quad . \tag{79}$$

Two functions in (79) satisfy the original system (5) if

$$B(t)=3\delta^2 At+A\delta_1$$

where δ_1 is another arbitrary constant. Hence

$$\omega(t,x)=\frac{e^{i\left(\delta x+\delta^3 t\right)}}{x+3\delta^2 t+\delta_1} \tag{80}$$

is a special solution of the CMKdV-II equation for arbitrary constants δ and δ_1.

Infinite Symmetries by Truncated Expansions

Let us write the system (5) in the form

$$u_t=F(u,v)=-u_{xxx}+6\left(u^2+v^2\right)u_x,$$

$$v_t=G(u,v)=-v_{xxx}+6\left(u^2+v^2\right)v_x. \tag{81}$$

To find the infinite symmetries, we linearize (81) about a solution u, v;

$$\omega_{1t}=\frac{\partial}{\partial\varepsilon}F(u+\varepsilon\omega_1,v+\varepsilon\omega_2)\Big|_{\varepsilon=0}$$

$$=-\omega_{1xxx}+12(u\omega_1+v\omega_2)u_x+6\left(u^2+v^2\right)\omega_{1x} \tag{82}$$

$$\omega_{2t}=\frac{\partial}{\partial\varepsilon}G(u+\varepsilon\omega_1,v+\varepsilon\omega_2)\Big|_{\varepsilon=0}$$

$$=-\omega_{2xxx}+12(u\omega_1+v\omega_2)u_x+6\left(u^2+v^2\right)\omega_{2x}.$$

Any solution ω_1,ω_2 of (82) yields a symmetry or infinitesimal transformation about u,v. That is the transformation

$$u^*=u+\varepsilon\omega_1$$

$$v^*=v+\varepsilon\omega_2 \tag{83}$$

leaves the system (5) form-invariant[12].

Considering equations in (16) we observe that u_0, v_0 is the solution of the linearized system (82) about the solution u_1, v_1 of the original system (5).

Since for each of the infinitely many solutions ϕ one has a transformation

$$u^* = u_1 + \varepsilon u_0,$$

$$v^* = v_1 + \varepsilon v_0 \tag{84}$$

which is admitted by the system (5), we obtain another evidence for the integrability of the CMKdV-II equation (2).

Hirota's Bilinear form and Solutions of the CMKdV-II Equation

Hirota's method requires the transformation of the CMKdV-II equation

$$\omega_t - 6|\omega|^2\omega_x + \omega_{xxx} = 0 \tag{85}$$

into a homogeneous bilinear form of degree two. If this bilinear equation can be solved, then an N-parameter solution can be obtained as series which self-truncates at a finite length. Series expansions which self-truncate in this way are then automatically exact solutions. However self-truncation does not occur for all bilinear equations; if it does occur then the equation in question possesses multiple soliton solutions.

To transform the CMKdV-II equation into a homogeneous bilinear form, let

$$\omega = \frac{g}{f}, \text{ and } |g|^2 = -ff_{xx} + f_x^2 \tag{86}$$

Substitution into (85) leads to

$$fg_t - f_t g + 3(f_{xx}g_x - f_x g_{xx}) + fg_{xxx} - f_{xxx}g = 0. \tag{87}$$

This can be written as

$$\left[\left(\frac{\partial}{\partial x} - \frac{\partial}{\partial x'}\right)^3 + \left(\frac{\partial}{\partial t} - \frac{\partial}{\partial t'}\right)\right] g(x,t) f(x',t')\Big|_{\substack{x'=x \\ t'=t}} = 0 \tag{88}$$

Or in Hirota's more elegant formalism

$$\left(D_x^3 + D_t\right) g \cdot f = 0. \tag{89}$$

Now let us consider the truncated solution

$$\omega = \frac{\omega_0}{\phi} + \omega_1 \tag{90}$$

where

$$\omega_0 = u_0 + iv_0\,, \quad \omega_1 = u_1 + iv_1\,, \tag{91}$$

$$u_0 = \alpha\,\phi_x, \quad v_0 = \beta\,\phi_x, \quad \alpha^2 + \beta^2 = 1\,, \tag{92}$$

$$u_1 = \alpha\,L, \quad v_1 = \beta\,L, \quad L = \frac{\phi_{xx}}{2\phi_x}\,, \tag{93}$$

$$\frac{\phi_t}{\phi_x} + \frac{\phi_{xxx}}{\phi_x} - \frac{3}{3}\frac{\phi_{xx}^2}{\phi_x^2} = \gamma(t)\,. \tag{94}$$

Here ω and ω_1 are both separate solutions of the CMKdV-II equation. To show the equivalence of these results with the Hirota form (89), we start from one solution $\omega = g/f$ and another solution $\omega_1 = g^{(1)}/f^{(1)}$. Since from (86) $|\omega|^2 = -(\log f)_{xx}$, we find from (90-94) that

$$|\omega|^2 = -\frac{\partial^2}{\partial x^2}\log\phi + |\omega_1|^2\,. \tag{95}$$

We can now see that

$$f = \phi\, f^{(1)}\,, \tag{96}$$

and then (90) immediately gives

$$g = \omega_0 f^{(1)} + \phi\, g^{(1)}\,. \tag{97}$$

renaming g as $g^{(n)}, f$ as $f^{(n)}, \omega$ as $\omega^{(n)}$ and $g^{(1)}, f^{(1)}, \omega_1$ as $g^{(n-1)}, f^{(n-1)}$ and $\omega^{(n-1)}$, we have

THEOREM 1. If $f^{(n)}$ and $g^{(n)}$ satisfy

$$\left(D_x^3 + D_t\right) g^{(n)} \cdot f^{(n)} = 0, \quad \left|g^{(n)}\right|^2 = f^{(n)} f_{xx}^{(n)} - f_x^{(n)2} = 0 \tag{98}$$

and if

$$f^{(n)} = \phi_{(n-1)} f^{(n-1)}\,,$$

$$g^{(n)} = \omega_0 f^{(n-1)} + \phi_{(n-1)} g^{(n-1)}\,, \tag{99}$$

then the resulting equations in ϕ_{n-1}, ω_0 and $\omega^{(n-1)}$ are satisfied by the Painleve relations (9-94). Furthermore

$$f^{(n)} = \prod_{i=1}^{n-1} \phi_i\,. \tag{100}$$

Proof. If we substitute (99) in (98) demand $f^{(n-1)}$ and $g^{(n-1)}$ also satisfy (98), and use (94) when necessary, we see that the assertion of the theorem is correct. (100) follows from the repeated application of (99) with $f^{(0)} = 1$.

It is clear that at each iteration of the Backlund transformation (99), a new singularity manifold ϕ_i is produced. These can be built up in product form to give $f^{(n)}$ in the form of (100).

The Painleve Analysis and the Lax Pairs

The singular manifold method of Painleve analysis has been applied successfully to CMKdV-II equation in order to find its Lax par only by considerations arising from Painleve analysis[1,10].

The goal of this subsection is to demonstrate a connection between the Painleve property and the occurrence of Lax pair from Painleve analysis to the Korteweg-de Vries equation.

The KdV equation

$$u_t + uu_x + \delta u_{xxx} = 0 \tag{101}$$

posses the Painleve property[12]. The expansion about the singularity manifold has the form

$$u = \phi^{-2} \sum_{j=0}^{\infty} u_j \phi^j \quad . \tag{102}$$

The resonances are at $j = -1,4$ and 6. From recursion relations one finds

$$j = 0: \quad u_0 = -12\delta \phi_x^2 \; ; \tag{103}$$

$$j = 1: \quad u_1 = -12\delta \phi_{xx} \; ; \tag{104}$$

$$j = 2: \quad \phi_x \phi_t + \phi_x^2 u_2 + 4\delta \phi_x \phi_{xxx} - \delta \phi_{xx}^2 = 0 \; . \tag{105}$$

The truncated series solution to the KdV equation (101) is of the form

$$u = \frac{u_0}{\phi^2} + \frac{u_1}{\phi} + u_2 \tag{106}$$

if

$$u_{2t} + u_2 u_{2x} + \delta u_{2xxx} = 0 \; . \tag{107}$$

Hence one obtains the following Backlund transformation

$$u = 12\delta \frac{\partial^2}{\partial x^2} \ln \phi + u_2 \; , \tag{107}$$

where u and u_2 satisfy (101) and

$$\phi_x \phi_t + \phi_x^2 u_2 + 4\delta \phi_x \phi_{xxx} - 3\delta \phi_{xx}^2 = 0 \; , \tag{108}$$

$$\phi_{xt}\phi_{xx}u_2 + \delta\,\phi_{xxxx} = 0\ . \tag{109}$$

Eliminating u_2 between (108) and (109) we find that

$$\frac{\partial}{\partial x}\left[\frac{\phi_t}{\phi_x} + \left\{\frac{\partial}{\partial x}\left(\frac{\phi_{xx}}{\phi_x}\right) - \frac{1}{2}\left(\frac{\phi_{xx}}{\phi_x}\right)^2\right\}\right] = 0\ . \tag{110}$$

or

$$\frac{\phi_t}{\phi_x} + \delta\,\{\phi; x\} = \lambda \tag{111}$$

where

$$\{\phi; x\} = \frac{\partial}{\partial x}\left(\frac{\phi_{xx}}{\phi_x}\right) - \frac{1}{2}\left(\frac{\phi_{xx}}{\phi_x}\right)^2 \tag{112}$$

is the Schwarzian derivative of ϕ . Equation (111) is invariant under the Mobius group H of homographic transformations acting on ϕ . This invariance and other well-known properties of the Schwarzian derivative suggest that the substitution

$$\phi = \frac{v_1}{v_2} \tag{113}$$

where (v_1, v_2) satisfy the same system of linear equations,

$$v_{xx} = av\ , \tag{114}$$

$$v_t = bv_x + cv\ , \tag{115}$$

might be of use. With the notation

$$\theta_x = v_2 v_{1x} - v_1 v_{2x}\ , \tag{116}$$

$$\psi_x = v_2 v_{1t} - v_1 v_{2t}\ , \tag{117}$$

it is found that

$$\frac{\psi_t}{\theta_x} + \delta\left(\{\phi; x\} - 2\frac{v_{2xx}}{v_2} + 2\frac{\theta_{2xx}}{\theta_x}\frac{v_{2x}}{v_2}\right) = \lambda\ . \tag{118}$$

If v_1, v_2 satisfy

$$v_{xx} = av\ , \tag{119}$$

$$v_t = bv_x + cv\ , \tag{120}$$

then

$$\theta_{xx} = 0 \ , \tag{121}$$

and

$$\psi_t = b\theta_x \ . \tag{122}$$

We find from (117) that

$$b = 2\delta a + \lambda \ . \tag{123}$$

By requiring

$$v_{xxt} = v_{txx} \ , \tag{124}$$

it is found that

$$a_t = 6\delta a a_x - \delta a_{xxx} + \lambda a_x \ , \tag{125}$$

$$c_x = -\delta a_{xx} \ , \tag{126}$$

$$b_{xx} = -c_x \ . \tag{127}$$

Hence (119) and (120) are just the Lax pair for the KdV equation.

For the complex modified Kortewef-de Vries equation

$$\omega_t - 6|\omega|^2 \omega_x + \omega_{xxx} = 0 \tag{128}$$

the Backlund transformation reads

$$\omega = e^{i\Theta} \frac{\phi_x}{\phi} + \omega_1, \quad \Theta = \tan^{-1} \frac{\beta}{\alpha} \tag{129}$$

where Θ is an arbitrary constant and

$$\omega_1 = -e^{i\Theta} \frac{\phi_{xx}}{2\phi_x} \tag{130}$$

and from (31) for $\gamma(t) = \lambda$ a constant, one has

$$\frac{\phi_t}{\phi_x} + \{\phi; x\} = \lambda \ . \tag{131}$$

On the other hand for the modified Kortewef-de Vries equation [12]

$$\omega_t + \delta \frac{\partial}{\partial x}\left(\omega_{xx} - \frac{\omega^3}{2}\right) = \lambda \omega_x \tag{132}$$

the Backlund transformation becomes

$$\omega = \frac{2\phi_x}{\phi} + \omega_1 \ , \tag{133}$$

where

$$\omega_1 = \frac{\phi_{xx}}{2\phi_x} \tag{134}$$

and

$$\frac{\phi_t}{\phi_x} + \{\phi; x\} = \lambda \,. \tag{135}$$

Now identifying equations (111), (131) and (135) we find that

CMKdV-II: , $\omega - \omega_1 = e^{i\Theta\frac{\phi_x}{\phi}}$

MKdV: $\omega - \omega_1 = \frac{2\phi_x}{\phi}$,

KdV: $u - u_2 = 12\delta \frac{\partial}{\partial x}\left(\frac{\phi_x}{\phi}\right)$,

and

$$u - u_2 = 6\delta \frac{\partial}{\partial x}(\omega - \omega_1) = 12\delta e^{-i\Theta} \frac{\partial}{\partial x}(\omega - \omega_1) \,. \tag{136}$$

Furthermore, using (105) we find

$$u_2 + \lambda = 3\delta\left(\omega_{1x} - \frac{1}{2}\omega_1^2\right) = 3\delta\, e^{-i\Theta}\left(\omega_{1x} - \frac{1}{2}\omega_1^2\right), \tag{137}$$

$$u + \lambda = 3\delta\left(\omega_x - \frac{1}{2}\omega^2\right) = 12\delta\, e^{-i\Theta}\left(\omega_x - \frac{1}{2}\omega^2\right). \tag{138}$$

(137) and (138) are Miura transformations, mapping solutions of the three equations into each others. Equation (136) may be used to invert the Miura transformations.

CLASSICAL LIE SYMMETRIES AND SIMILARITY REDUCTIONS

In this section we firstly study the classical Lie symmetries of the CMKdV-II equation which can be obtained through the Lie group method of infinitesimal transformations, originally developed by S. Kie[13]. Secondly using the classical symmetries of the equation, similarity reductions will be obtained and it will be shown that these reductions have the Painleve property. Though the method is entirely algorithmic, it often involves a large amount of tedious algebra and auxiliary calculations which are virtually unmanageable manually. Recently symbolic manipulation programs have been developed, especially in Mathematica, Macsyma and Reduce. In order to facilitate the determination of the classical Lie symmetries we used SPDE package in the computer algebra software REDUCE [6]. Then to investigate the Painleve property of the associated similarity reductions we interacted with Mathematica[14].

Classical Lie Symmetries of the CMKdV-II Equation

We consider the one parameter (ε) Lie point transformations of (x,t,u,v) given by

$$\begin{aligned} x^* &= x+\varepsilon\zeta_1(x,t,u)+O(\varepsilon^2),\\ t^* &= t+\varepsilon\zeta_2(x,t,u)+O(\varepsilon^2),\\ u^* &= u+\varepsilon\eta_1(x,t,u)+O(\varepsilon^2),\\ v^* &= v+\varepsilon\eta_2(x,t,u)+O(\varepsilon^2). \end{aligned} \tag{139}$$

The system in (5) is invariant under this transformation if it is invariant under the operator

$$X=\xi_1\frac{\partial}{\partial x}+\xi_2\frac{\partial}{\partial t}+\eta_1\frac{\partial}{\partial u}+\eta_2\frac{\partial}{\partial v}\,.$$

$$+\zeta_1\frac{\partial}{\partial u_x}+\zeta_2\frac{\partial}{\partial u_t}+\gamma_1\frac{\partial}{\partial v_t}+\zeta_{111}\frac{\partial}{\partial u_{xxx}}+\gamma_{111}\frac{\partial}{\partial v_{xxx}} \tag{140}$$

Hence $\zeta_1,\zeta_2,\eta_1,\eta_2$ are found from the determining equations derived from this invariancy condition[4].

By the use of the REDUCE program

```
Load spde;
out "c:/abul/ab.son";
deq (1):=u(1,2)-6*(u(1)2+u(2)2)*u(1,1)+u(1,1,1,1);
deq (2):=u(2,2)-6*(u(1)2+u(2)2)*u(2,1)+u(2,1,1,1);
sder (1):=u(1,1,1,1);
sder (2):=u(2,1,1,1);
cresys ();
prsys ();
simpsys ();
result ();
shut "c:/abul/ab.son";
```

we called the package SPDE in the computer algebra system REDUCE[4] to find the generators of the Lie group which that system (5) admits. The overdetermined system of the determining equations consists of 60 partial differential equations.

The package automatically solves it and gives the symmetry generators:

$$X_1=\frac{\partial}{\partial x},\quad X_2=\frac{\partial}{\partial t},$$

$$X_3=v\frac{\partial}{\partial u}-u\frac{\partial}{\partial v},\quad X_4=x\frac{\partial}{\partial x}+3t\frac{\partial}{\partial t}-u\frac{\partial}{\partial u}-v\frac{\partial}{\partial v}\,. \tag{141}$$

The nonvanishing commutators are

$$[X_1,X_4]=X_1,\quad [X_2,X_4]=3X_2\,. \tag{142}$$

Hence a commutator table can be formed as follows:

$$\begin{array}{cccccc} & X_1 & X_2 & X_3 & X_4 \\ X_1 & 0 & 0 & 0 & X_1 \\ X_2 & 0 & 0 & 0 & 3X_2 \\ X_3 & 0 & 0 & 0 & 0 \\ X_4 & -X_1 & -3X_2 & 0 & 0. \end{array} \tag{143}$$

The linear space $\{X_1, X_2, X_3, X_4\}$ spanned by X_1, X_2, X_3, X_4 is a Lie algebra with the skew symmetric operator in the table. The subspaces $L_3 = \{X_1, X_2, X_3\}$, $L_2 = \{X_1, X_2\}$ and $L_1 = \{X_1\}$ are 3,2,1 dimensional subalgebras of $L_4 = \{X_1, X_2, X_3, X_4\}$ accordingly. Furthermore these subalgebras have the inclusion property

$$L_1 \subset L_2 \subset L_3 \subset L_4 \,. \tag{144}$$

and hence L_4 is a solvable Lie algebra.

Similarity Reductions of the CMKdV-II Equation

Similarity reduction corresponding to the symmetry generator $X_1 + CX_2$ then obtained by solving the characteristic equations

$$\frac{dx}{1} = \frac{dt}{C} = \frac{du}{0} = \frac{dv}{0} \,. \tag{145}$$

Integration of these ordinary differential equations yields the travelling wave reduction

$$u = f(\zeta), \quad v = g(\zeta), \quad \zeta = x - Ct \tag{146}$$

and $W(\zeta) = f(\zeta) + ig(\zeta)$ satisfies the complex ordinary differential equation

$$-W''' + CW' + 6|W|^2 W' = 0, \qquad ' = \frac{d}{d\zeta} \tag{147}$$

where C, the speed of the traveling wave is an arbitrary constant.

The symmetry generator X_4 yields the similarity reduction which be obtained by solving the characteristic system of first order ordinary differential equations

$$\frac{dx}{x} = \frac{dt}{3t} = \frac{du}{-u} = \frac{dv}{-v} \,. \tag{148}$$

Integration of these ordinary differential equations yields the similarity reduction

$$u = t^{\frac{1}{3}} f(\zeta), \quad v = t^{-1/3} g(\zeta), \quad \zeta = xt^{-1/3} \tag{149}$$

and $W(\zeta)=f(\zeta)+ig(\zeta)$ satisfies complex ordinary differential equation

$$-3W'''+(\zeta W)'+18|W|^2W'=0, \qquad ' = \frac{d}{d\zeta} \tag{150}$$

while the generator X_3 does not yield any similarity reduction.

The following list summarizes the one parameter groups of point transformations, the form of invariant solutions and similarity reductions corresponding to the generators X_1, X_2, X_3 and X_4 :

Generator Point Trans. Invariant Soln. Similarity Reduction

$$x^* = x+\varepsilon$$

$$X_1 : t^* = t \qquad W(t); \qquad W'=0 \tag{151}$$

$$\omega^* = \omega$$

$$x^* = x$$

$$X_2 : t^* = t+\varepsilon \qquad W(x); \qquad W'''-|W|^2W'=0 \tag{152}$$

$$\omega^* = \omega$$

$$x^* = x$$

$$X_3 : t^* = t \qquad \text{no invariant solution} \tag{153}$$

$$\omega^* = \omega e^{ic}$$

$$x^* = \varepsilon x$$

$$X_4 : t^* = \varepsilon^3 t \qquad W\left(xt^{-1/3}\right); \; -3W'''+(\zeta W)'+18|W|^2W'=0; \tag{154}$$

$$\omega^* = \omega/\varepsilon$$

while

$$x^* = x+\frac{1}{c}\varepsilon$$

$$X_1+CX_2 : t^* = t+\varepsilon \quad W(x-Ct); \quad -W'''+CW'+6|W|^2W'=0 \tag{155}$$

$$\omega^* = \omega$$

Painleve Analysis for the Similarity Reductions of the CMKdV-II Equation

To apply the Painleve analysis the similarity reduction

$$-3W'''+(\zeta W)'+18|W|^2W'=0 \tag{156}$$

of the CMKdV-II equation we first separate the real and imaginary parts.

By the substitution $W = \omega_1 + i\omega_2$ we get a real nonlinear third order system of ODE's

$$(\zeta\omega_1)' + 18(\omega_1^2 + \omega_2^2)\omega_1' - 3\omega_1''' = 0 ,$$

$$(\zeta\omega_2)' + 18(\omega_1^2 + \omega_2^2)\omega_2' - 3\omega_2''' = 0 . \tag{157}$$

Now we substitute

$$\omega_1 = \sum_{j=0}^{\infty} a_j \zeta^{j-1} , \tag{158}$$

$$\omega_2 = \sum_{j=0}^{\infty} b_j \zeta^{j-1} , \tag{159}$$

in (157), and arranging terms with respect to the assending powers of ζ we find that the resonances are at -1, 0, 1, 3, 4 and 5 and it has been shown that the compatibility conditions are all satisfied for the system (157).

Therefore the similarity reduction (156) has a general solution with at most pole type moving singularities. Hence it has the Painleve property. Indeed in the special case $\omega_1 = \omega_2 = F$ the system (157) reduces to the single equation

$$F''' = (\zeta F)' + 12F^2F' \tag{160}$$

and integrating this equation once one obtains the second Painleve equation

$$F'' = \zeta F + 4F^3 + \gamma . \tag{161}$$

The similarity reduction

$$-W''' + CW' + 6|W|^2 W' = 0 \tag{162}$$

of the CMKdV-II equation has the same dominant behaviour as the reduction (157) and it has been shown that this reduction also has the Painleve property.

REFERENCES

[1] R. Conte and M. Musette: Painleve analysis and Backlund transformation in the Kuramoto-Sivashinsky equation, J. Phys. A: Math. Gen. 22 (1989) 169-177.

[2] E. Hille: Ordinary Differential Equations in the Complex Plane, John Wiley, New York, 1960.

[3] S. Lie: Vorlesungen Uber Differentialgleichungen mit Bekannten Infinitesimalen Transformtionen, Teuber, Leipzig, 1891. (Printed again by Chelsea, New York 1967).

[4] N.H. Ibragimov: Lie Group Analysis of Differential Equations, CRC Press, London 1994.

[5] A.A. Mohammad and M. Can: Painleve analysis and infinite Lie symmetries of the complex modified Korteweg-de vries equation, J. Phys. A: Math. Gen. 28 (1995) 3223.

[6] F. Schwarz: Symmetries of differential equations: From Lie to computer algebra, Siam Review, 30(3) (1988) 450-481.

[7] W.H. Steeb and N. Euler: 1988 Nonlinear Evolution Equations and Painleve Test, World Scientific, Singapore 1988.

[8] W. Strampp: Symmetries and Painleve property, Progress of Theoretical Phys. 76 (4) (1986) 802-809.

[9] M.T. Weiss and G. Carnevale: The painleve for partial differential equations, J. Math. Phys. 24(1983) 522-526.

[10] J. Weiss: The Painleve property for partial differential equations. II: Backlund transformation, Lax pairs, and Schwarzian derivative, J. Math. Phys. 24(6) (1983) 1405.

[11] J. Weiss: On classes of integrable systems and the Painleve property, J. Math. Phys. 25 (1984) 13-24.

[12] J. Weiss: The Sine-Grodon equations: complete and partial integrability, J. Math. Phys. 25 (7) (1984) 2226-2235.

[13] J. Weiss: The Painleve property and Backlund transformations for the sequence of Boussinesq equations, J. Math. Phys. 26(2) (1985) 258-269.

[14] S. Wolfram: Mathematica, Addison-Wesley, California, 1991.

Journal of Natural & Physical Sciences, Vol. 19 (2) (2005) 136-147

APPROXIMATE TREATMENT OF BLAST WAVES IN A PERFECTLY CONDUCTING NON-IDEAL GAS

J.P. Vishwakarma* and Sateesh N. Pandey*

(Received 28.07.05, Revised 22.01.06)

ABSTRACT

We obtain the trajectory and related quantities such as the velocity of the leading edge of free or driven spherical blast wave in a non-ideal gas using a simple approximation technique. The gas is assumed to have infinite electrical conductivity and to be permeated by an idealized, spatially decreasing magnetic field. It is found that the values of ε (the ratio of the effective total pressure in the blast wave and the total pressure just behind the shock) are independent of the ratio of specific heats of the gas γ and the parameter of non-idealness of the gas δ in the non-magnetic case; but they dependent on as γ as well as on δ in the magnetogasdynamic case. Also, an increase in the value of δ or in the strength of the ambient magnetic field causes an increase in the shock velocity.

Keywords : Blast waves, Magnetogasdynamics, Non-ideal gas, Spatially decreasing magnetic field, Simple approximation technique.

Subject Classification : PACS. 47.40,-X Compressible flows; Shock and detonation phenomena - 47.65, + a Magnetohydrodynamics and electrohydrodynamics.

INTRODUCTION

The theory of blast waves and related flows are of considerable physical interest: for example the theory of sonic booms, high altitude nuclear detonation, supernova explosions and sudden expansion of corona into interplanetary space. In the latter context, blast wave conceivably driven by solar flares are observed to propagate into the interplanetary medium [7]. Many investigators [8,11,15], have already considered the blast wave problem in a perfect gas and obtained numerical solutions by using similarity method. The problem of blast waves is also solved by analytical methods (see, for example, [2,9,16,17,20,21]) based on well defined approximations. Sachdev [17] extended the Brinkley-Kirkwood theory [3] and obtained analytical solutions which is valid from the source of explosion to the distances far from it, both when the medium is uniform and non-uniform. Verma and Vishwakarma [20] extended the Laumbach-Probstein method in magnetogas dynamics and applied to solve an explosion problem.

*Department of Mathematics and Statistics, D.D.U. Gorakhpur University, Gorakhpur - 273009, India

When the flow of a gas takes place at high temperatures the assumption that the gas is ideal is no more valid. Anisimov and Spiner [1] have studied a problem of point explosion in a non-ideal gas by taking the equation of state in a simplified form, which describes the behaviour of the medium satisfactorily at low density. Ranga Rao and Purohit [12] have studied the self-similar flows of a non-ideal gas driven by an expanding piston and obtained approximate analytic and numerical solutions by taking the equation of state suggested by Anisimov and Spinar [1]. Roberts and Wu [13,14] have used an equivalent equation of state to study the shock wave theory of sonoluminescence.

The purpose of the present work is to obtain trajectory and related quantities such as the velocity of the leading edge of a free or driven spherical blast wave in a non-ideal gas [1] using a simple approximation technique [4,22]. The medium is assumed to have infinite electrical conductivity and to be permeated by an idealised spatially decreasing magnetic field. Effects of the non-idealness of the gas and the magnetic field are obtained on the shock strength and shock velocity.

GOVERNING EQUATIONS AND SOLUTION

According to the paper of Anisimov and Spiner [1], we start with the equation of state in the form.

$$p = \rho R^* T(1 + \bar{b}\rho), \tag{2.1}$$

We consider a blast wave, headed by a strong spherical shock, produced by energy ejection into a perfectly conducting non-ideal gas at a rate $dE(t)/dt$. The initial density ρ_0 of the gas is assumed to be constant. The initial magnetic field distribution h is assumed to be an idealized field such that the lines of force lie on hemispheres whose centre is the point of explosion [4,17], the intensity is assumed to be

$$h_o = h_c r^{-w_1} \tag{2.2}$$

and directed tangential to the advancing shock front, where h_c and w_1 are constants, and r is the radial distance from the point of explosion.

The internal energy e per unit mass of the non-ideal gas is given by [10,18].

$$e = \frac{p}{(\gamma-1)\rho(1+\bar{b}\rho)} \tag{2.3}$$

Which implies that

$$C_p - C_V = \frac{T(\partial\rho/\partial T)_V}{(\partial T/\partial\rho)_p} = R^* \tag{2.4}$$

where $b^2\rho^2$ is neglected; C_p, C_v are the specific heats at constant pressure and constant volume processess; V,t are the specific volume and time, respectively; and $\gamma = C_p/C_v$.

Jump conditions for a strong shock moving in a perfectly conducting non-ideal gas at a rest, are [13,19]

$$u_1 = (1-\beta)V \tag{2.5}$$
$$\rho_1 = (1-\beta)\rho_0 V^2 \tag{2.6}$$
$$\rho_1 = \rho_0/\beta \tag{2.7}$$
$$h_1 = h_0/\beta \tag{2.8}$$

where $V = \frac{dR}{dt}$ is the shock velocity, R the shock radius, u the fluid velocity, h the magnetic field, and

$$\beta^3(\gamma+1) - \beta^2(\gamma+1-\delta) + \beta\{2(\gamma-1)M_A^{-2} - \delta\} + 2\delta M_A^{-2} = 0 \tag{2.9}$$

with
$$\delta = \bar{b}\rho_0(\gamma-1). \tag{2.10}$$

For given values of δ,γ and M_A,the value of β $(0 < \beta < 1)$ can be obtained by solving the equation (2.9), where $M_A = V\rho_0^{1/2}/h_0$ is the Alfven Mach number. In equations (2.5) to (2.8), the quantities with suffices '0' and '1' denote the values of those quantities just in front and just behind of the shock, respectively.

If however, the energy ejection $E=E(t)$ is continuous over a time scale comparable with the expansion time of interest R/V, the flow somewhat downstream of the shock may terminate with a tangential discontinuity, at $r = R_p(t)$ say; physically, at $R_p(t)$ the gas is acted upon by a 'piston' (consisting of a medium generally different) which transfers to it part α of the power continuously delivered by the source, so that $E = \alpha E_{source}$ [4].

For a spherical blast, the energy balance is given by

$$E(t) = 4\pi\int_{\max[0,R_p]}^{R}\left[\frac{\rho u^2}{2} + \frac{p}{(\gamma-1)(1+b\rho)} + \frac{h^2}{2}\right]r^2\,dr$$

$$= N\frac{MV^2}{2} \tag{2.11}$$

with

$$N = \frac{3(1-\beta)^2}{\beta}\int_{\max[0,\frac{R_p}{R}]}^{1}\left|\frac{\rho u^2}{\rho_1 u_1^2}+\frac{2\beta}{(1-\beta)(\gamma-1)(1+b\rho)}\frac{\rho}{\rho_1}+\frac{h^2}{\rho_1 u_1^2}\right|\xi^2 d\xi; \tag{2.12}$$

here equations (2.5), (2.6) and (2.7) have been used; and

$$M = \frac{4\pi R^3 \rho_0}{3} \tag{2.13}$$

is the mass initially contained within the radius R and now constituting the flow.

We shall consider [6]

$$E(t) = E_0 t^s, \tag{2.14}$$

where E_0 and s are constants. Then it can be shown that self-similar solution [19,22], exists only when $w_1 = (3-s)/(2+s)$ and when the flow has settled down to a self-similar behaviour, N becomes a constant shape-factor. Considering h_c and $\frac{E_0}{\rho_0}$ as two independent dimensional constants with dimensions $M^{1/2}L_{(2w_1-1)/2}T^{-1}$ and $L^5T^{-(2+s)}$, respectively, the similarity variable ξ is obtained as

$$\xi = \left(\frac{E0}{\rho_0}\right)^{-1/5} r t^{-\left[\frac{2+s}{5}\right]} \tag{2.15}$$

The shock position must correspond to a constant value of ξ, say ξ_1, so that

$$R(t) = \xi_1\left[\frac{E0}{\rho_0}\right]^{1/5} t^{\left[\frac{2+s}{5}\right]} \tag{2.16}$$

Also, equation (2.11) with $V = \frac{dR}{dt}$, can be used as a simple differential equation to determine the shock position in terms of the constant N as

$$R(t) = \left[\left(\frac{5}{2+s}\right)^2 \frac{3}{2\pi N}\frac{E0}{\rho_0}\right]^{1/5} t^{\left[\frac{2+s}{5}\right]} \tag{2.17}$$

Comparing (2.16) and (2.17), we get

$$\xi_1 = \left[\left(\frac{5}{2+s}\right)^2 \frac{3}{2\pi N}\right]^{1/5} \tag{2.18}$$

Therefore, the shock velocity $V(R)$ is given by

$$V(R) = (\xi_1)^{\left[\frac{5}{2+s}\right]}\left(\frac{2+s}{5}\right)\left(\frac{E0}{\rho 0}\right)^{1/2(2+s)} R^{\left[\frac{s}{2+s}\right]} \tag{2.19}$$

For decaying shock $s < 3$. It now remains to compute the value of N.

We compute N in a closed algebric form using the approximations proposed by Chernyi [5] and Laumbach and Probstein [9]. First, we may take the advantage of the notion that most of the mass of the blast must be confined to a shell of effective thicknesss $\Lambda R < R$ adjoining the shock front; infact, mass conservation in its crudest form $4\pi R^2 \Lambda R \rho_1 = M$ imposes the condition

$$\Lambda R/R = \beta/3 \tag{2.20}$$

Moreover, the velocity field must vanish at the centre by symmetry; hence the kinetic energy is even more confined outward, i.e. kinetic energy of the blast wave is approximately equal to $\frac{1}{2} M u_1^2$. Also, the thermal energy density (and hence, the internal energy density) must be important inside the shell when $s = 0$; in fact, a high temperature, through low-density gas must have resulted near the centre from the higher rate of entropy generation when the velocity of the shock was higher; the effective total pressure inside the shell, hence is conveniently expressed as $p^* \approx \in p_1^* (\in \leq 1)$, where $p^* = p + \frac{h^2}{2}$, finally since most of the mass of the blast is confined to a shell of small thickness adjoining the shock front, the density ρ is constant in the shell and is equal to ρ_1; and hence, due to frozen-in-field condition the magnetic field h is also more confined near the shock front and is constant in the shell being equal to h_1. Following these guidelines the energy balance may be approximated as

$$E(t) \approx \frac{M u_1^2}{2} + \frac{\in p_1^*}{(\gamma-1)(1+\bar{b}\rho_1)} \frac{4\pi R^3}{3} + \left\{ \frac{(\gamma-2)+(\gamma-1)\bar{b}\rho_1}{(\gamma-1)(1+\bar{b}\rho_1)} \right\} h_1^2 \frac{2\pi R^3}{3}$$

when $s = 0$, with

$$N = \frac{\beta(1-\beta)}{(\gamma+1)\beta+\delta} \left[(1-\beta)(\gamma-1) + (1-\beta)\frac{\delta}{\beta} + 2\in_1 + \frac{\{(\gamma-2)\beta+\delta\}}{(1-\beta)} \frac{M_A^{-2}}{\beta^3} \right] \tag{2.21}$$

where

$$\in_1 = \in \left[1 + \frac{M_A^{-2}}{2\beta^2(1-\beta)} \right]$$

The expression for N may be improved as follows. Considering the magnetic field equation [20]

$$h_0 r_0 dr_0 = h r dr \tag{2.22}$$

analogous to Lagrangian continuity equation

$$\rho_0 r_0^2 dr_0 = \rho r^2 dr \tag{2.23}$$

we have

$$\int_{\max[0,R_p]}^{R} \frac{h^2}{2} r^2 dr = \int_0^R \frac{h_0^2 r_0^2}{2} \left(\frac{\partial r}{\partial r_0}\right)^{-1} dr_0,$$

where the term $\left(\frac{\partial r}{\partial r_0}\right)$ may be approximated by its value at the shock, from continuity equation (2.23) and strong shock, from condition (2.7) [9]. The energy balance, therefore, may be approximated as,

$$E(t) \approx \frac{Mu_1^2}{2} + \frac{4\pi \in p_1^*}{(\gamma-1)(1+\bar{b}\rho_1)} \frac{R^3}{3} + \left\{\frac{(\gamma-2)+(\gamma-1)\bar{b}\rho_1}{(\gamma-1)(1+\bar{b}\rho_1)}\right\} \beta h_1^2 \frac{2\pi R^3}{(3-2w_1)}$$

when $s = 0$, with

$$N = \frac{\beta(1-\beta)}{[(\gamma-1)\beta+\delta]}\left[(\gamma-1)(1-\beta) + \frac{\delta}{\beta}(1-\beta) + 2 \in_1 + \frac{\{(\gamma-2)\beta+\delta}{(1-\beta)(3-2w_1)} \frac{3M_A^{-2}}{\beta^2}\right] \tag{2.24}$$

When a piston is present, we expect that, from the shock to the advancing piston at R_p (t), $u \approx u_1$ *holds, since* $\frac{\Delta R}{R} = \frac{R-R_p}{R}$ = constant in a self-similar flows; also the relevant internal energy is confined within the shell $\Delta R = (R - R_p)$. The energy balance now assumes the form

$$E(t) \approx \frac{Mu_1^2}{2} + \frac{\in p_1^* 4\pi R^2 \Lambda R}{(\gamma-1)(1+\bar{b}\rho_1)} + \left\{\frac{(\gamma-2)+(\gamma-1)\bar{b}\rho_1}{(\gamma-1)(1+\bar{b}\rho_1)}\right\} \frac{2\pi\beta h_1^2 R^3}{(3-2w_1)}$$

when $s > 0$, with

$$N = \frac{\beta(1-\beta)}{[(\gamma-1)\beta+\delta]}\left[(\gamma-1)(1-\beta) + \frac{\delta}{\beta}(1-\beta) + 2 \in_1 \beta + \frac{\{(\gamma-2)\beta+\delta\}}{\beta^2(1-\beta)(3-2w_1)} 3M_A^{-2}\right]. \tag{2.25}$$

The value of $\in$ may be computed requiring that energy and overall momentum conservation be consistent. The latter reads in the shell approximation

$$\frac{d}{dt}(Mu_1) = 4\pi R^2 \in p_1^*$$

and integrates to

$$R(t) \alpha t^{\frac{1}{[3(1-\epsilon)+1]}}$$

The consistency requires that

$$\epsilon = \frac{3+4s}{3(2+s)}\left[1+\frac{M_A^{-2}}{2\beta^2(1-\beta)}\right]^{-1}, \tag{2.26}$$

so that from equations (2.24) and (2.25) we have, respectively,

$$N = \frac{\beta(1-\beta)}{[(\gamma-1)\beta+\delta]}\left[(\gamma-1)(1-\beta)+\frac{\delta}{\beta}(1-\beta)+1+\frac{[(\gamma-2)\beta+\delta]}{(1-\beta)(3-2w_1)}\frac{3M_A^{-2}}{\beta^2}\right], (s=0) \tag{2.27}$$

and

$$N=\frac{\beta(1-\beta)}{[(\gamma-1)\beta+\delta]}\left[(\gamma-1)(1-\beta)+\frac{\delta}{\beta}(1-\beta)+2\beta\frac{(3+4s)}{3(2+s)}+\frac{[(\gamma-2)\beta+\delta]}{\beta^2(1-\beta)(3-2w_1)}3M_A^{-2}\right], \quad (s>0) \tag{2.28}$$

The expression for N may be improved, further, as follows. When $s = 0$ the decay of ρ (r) and h (r) from the front inward may be expected to follow the power-laws $\rho = \rho_1(\frac{r}{R})^x$ and $h = h_1(\frac{r}{R})^{x_1}$, respectively. The exponents x and x_1 may be computed by using mass conservation in the form $4\pi\int_0^R \rho(r)r^2dr = M$ and the integral $\int_0^R hrdr = \int_0^R h_0 r_o dr_o$ of the magnetic field equation (2.22); the results are

$$x = \frac{3(1-\beta)}{\beta} \text{ and } x_1 = \left[\frac{(2-w_1)}{\beta} - 2\right]$$

The law $\rho = \rho_1(\frac{r}{R})^x$ can not be used in the middle term under the integral sign in (2.12), as N is a constant shape factor for the self-similar flow. For this term, ρ may be apprioximated by $\rho \approx k\rho_1$, and k may be determined by using the integral

$$\int_0^R \rho r^2 dr = \int_0^R \rho_0 r^2 dr_0$$

of the Lagrangian equation of continuity (2.23), which gives $k = \beta$. Also the velocity decreases at least as $u = u_1(\frac{r}{R})$. Hence the corresponding N is

$$N = \frac{3}{\beta}\left[\left\{\frac{\beta(1-\beta)^2}{3}(1+\frac{2}{3}\beta)^{-1}\right\} + \frac{\beta(1-\beta)}{3\{(\gamma-1)+\delta\}} + \frac{\{\beta(\gamma+\delta)-(\beta+1)\}}{\{(\gamma-1)+\delta\}}\frac{M_A^{-2}}{2(2-w_1)}\left(1-\frac{\beta}{2(2-w_1)}\right)^{-1}\right], \quad (s=0) \tag{2.29}$$

RESULTS AND DISCUSSION

In the table 1, the values of β, ε, N and ξ_1, calculated from equations (2.9), (2.26), (2.28) (or (2.29)) and (2.18) are given for $\gamma = 1.4$; $s = 0, 1$; $\delta = 0, 0.025, 0.05$; and $M_A^{-2} = 0, 0.01$. Figures 1 and 2 show that variation of the shock velocity $V/(\frac{E_0}{\rho_0})^{\frac{1}{2+s}}$ with shock position R, respectively for $s = 0$ and $s = 1$. $\delta = 0$ corresponds to the case of a perfect gas, and $M_A^{-2} = 0$ to the non-magnetic case.

It is found that the values of $\in$ (the ratio of the effective total pressure in the blast wave and the total pressure just behind the shock) are independent of γ and δ in the non-magnetic case; but they depend on γ as well as on δ in the magnetogasdynamic case (see (2.26). Table 1 shows that the effect of an increase in M_A^{-2} (i.e. in the strength of ambient magnetic field) is to decrease, both $\in$ and β, i.e. to increase the shock strength. On the other hand the effect of an increase in the parameter of non-idealness of the gas δ is found to increase β, i.e. to decrease the shock strength.

Figures 1 and 2 show that an increase in δ, the parameter of non-idealness of the gas, produces an increase in the shock velocity in both the cases, when a piston is present ($s > 0$) or when it is not present ($s = 0$). An increase in the ambient magnetic field, also, causes an increase in the shock velocity.

$s = 0$

δ	M_A^{-2}	β	$\in$	N	ξ_1
0	0	0.16666	0.5	2.70792	1.01971
0	0.01	0.14342	0.38948	2.23546	1.05958
0.025	0	0.20666	0.5	2.41962	1.04293
0.025	0.01	0.18802	0.42583	1.98377	1.08519
0.05	0	0.23462	0.5	2.20722	1.06228
0.05	0.01	0.21736	0.44044	1.80957	1.10534

$s = 1$

δ	M_A^{-2}	β	$\in$	N	ξ_1
0	0	0.16666	0.77777	1.23450	1.01454
0	0.01	0.14342	0.60585	1.02320	1.05336
0.025	0	0.20666	0.77777	1.11895	1.03468
0.025	0.01	0.18802	0.66240	1.02114	1.05379
0.05	0	0.23462	0.77777	1.04145	1.04964
0.05	0.01	0.21736	0.68512	0.98393	1.06164

Table. 1. Values of β, $\in$, N and ξ_1 for $\gamma = 1.4$ and $s = 0, 1$

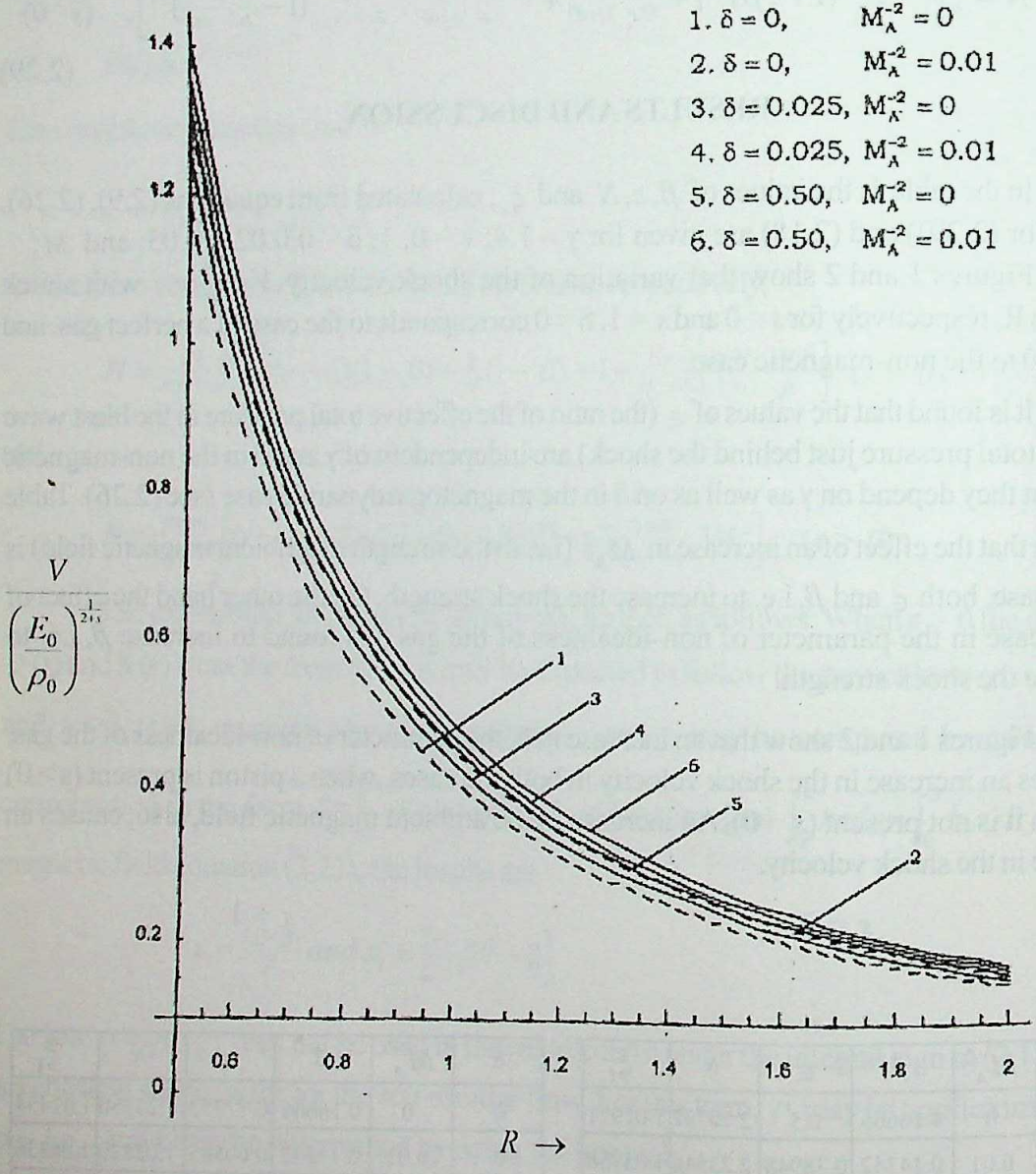

Fig. 1. Variation of shock velocity with shock radius for $s = 0$

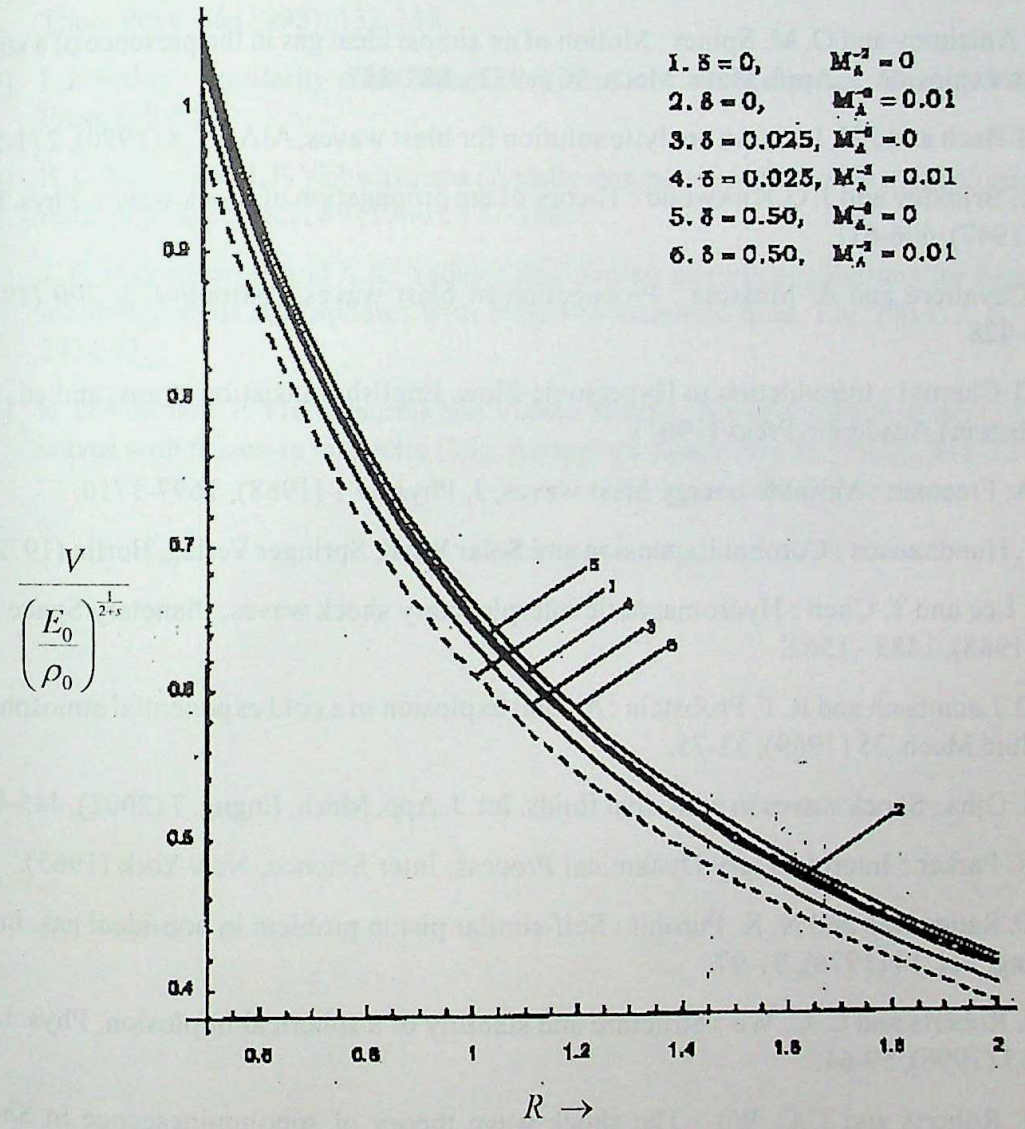

Fig. 2. Variation of shock velocity with shock radius for $s = 1$

REFRENCES

[1] S. I. Anisimov and O. M. Spiner : Motion of an almost ideal gas in the presence of a strong point explosion, J. Appl. Math. Mech. 36 (1972), 883-887.

[2] G. G. Bach and J.H. Lee : An analytic solution for blast waves, AIAA J. 8 (1970), 271-275.

[3] S. R. Brinkley and J. G. Kirkwood : Theory of the propagation of shock waves, Phys. Rev. 71 (1947), 606-611.

[4] A. Cavaliere and A. Messina : Propagation of blast waves, Astrophys. J. 209 (1976), 424-428.

[5] G. G. Chernyi : Introduction to Hypersonic Flow, English translation (trans. and ed. R.F. Probstein) Academic Press (1961).

[6] R. A. Freeman : Variable-energy blast waves, J. Phys. D 1 (1968), 1697-1710.

[7] A. J. Hundhausen : Coronal Expansion and Solar Wind, Springer Verlag, Berlin (1972).

[8] T.S. Lee and T. Chen : Hydromagnetic interplanetary shock waves, Planetary Space Sci. 16 (1968), 1483 - 1502.

[9] D. D. Laumbach and R. F. Probstein : A point explosion in a cold exponential atmosphere, J. Fluid Mech. 35 (1969), 53-75.

[10] S. N. Ojha : Shock waves in non-ideal fluids, Int. J. App. Mech. Engng. 7 (2002), 445-464.

[11] E. N. Parker : Interplanetary Dynamical Process; Inter Science, New York (1963).

[12] M. P. Ranga Rao and N. K. Purohit : Self-similar piston problem in non-ideal gas, Int. J. Engng. Sci. 14 (1976), 91-97.

[13] P. H. Roberts and C. C. Wu : Structure and stability of a spherical implosion, Phys. Lett. A 213 (1996), 59-64.

[14] P. H. Roberts and C.C. Wu : The shock wave theory of sonoluminescence in Shock Focussing effect in Medical Science and Sonoluminescence (Eds. R. C. Srivastava, D. Leutloff, K. Takayama, H. Gronig), Springer - Verlag (2003).

[15] D. Summers : An idealised model of a magnetohydrodynamic spherical blast wave applied to a flare-produced shock in the solar wind, Astron. Astrophys. 45 (1975), 151-158.

[16] A. Sakurai : Blast wave theory, in Basic Development in Fluid Dynamics (ed. M. Holt), Academic Press, New York (1965).

[17] P. L. Sachdev : Propagation of a blast wave in uniform or non-uniform media : a uniformly valid analytic solution, J. Fluid Mech. 52 (1972), 369 - 378.

[18] R. A. Singh and J. B. Singh : Analysis of diverging shock waves in non-ideal gas, Ind. J. Theo. Phys. 46 (1998), 133-138.

[19] L.I. Sedov : Similarity and Dimensional Methods in Mechanics, Chapter IV, Academic Press (1959).

[20] B. G. Verma and J. P. Vishwakarma : Axially symmetric explosion in magnetogasdynamics, Astrophys space Sci., 69 (1980), 177-188.

[21] J. P. Vishwakarma and A.K. Yadav : Self-similar analytical solutions for blast waves in inhomogeneous atmospheres with frozen-in-magnetic field, Eur. Phys. J. B. 34 (2003), 247-253.

[22] B. G. Verma, J. P. Vishwakarma and Vishnu Sharan : Approximate treatment of ideal blast waves with frozen-in magnetic field, Astrophys. Space Sci. 81 (1982), 315-321.

Journal of Natural & Physical Sciences, Vol. 19 (2) (2005) 148-155

A NEW APPROACH TO SUPERIOR JULIA SET

Manish Kumar* and Mamta Rani**

(Received 08.03.06)

ABSTRACT

Julia sets and recently invented Superior Julia sets have been studied through Picard and Superior iterations respectively. The objective of this paper is to introduce general superior iteration in the study of Julia sets.

Mathematics subject classifications (2000): 37C25, 40G25, 92D25

Key words and Phrases: Superior Julia set, General superior Julia set, General superior escape criterion, Filled general superior Julia set

INTRODUCTION

Julia sets are named after the Gaston Julia, who did much of his fundamental work on the dynamics of complex functions [12] in 1917. The subject didn't gain much interest, until in the 1970s, Mandelbrot generated Julia sets on a computer. Initially it has been generated for quadratic functions. In 1988, Barnsley [1] applied the Picard iteration method to compute Julia sets for higher degree of polynomials. Recently, Devaney [6] has generated Julia sets for rational maps. Its beauty, intricacies and application has attracted mathematical and graphcial scientists (see, for instacne, Barnsley [1], Beardon [2], Blanchard [3], Branner [4], Devaney [5]- [6], Devaney *et al.* [7]-[11], Kigami [13], Norton [15], Peitgen *et al.* [16]-[17], Pickover [18], Rani [19], Rani *et al.* [20], Roth [21], and references thereof.

By simplest definition, for a polynomial, f, the filled Julia set FJ_f is the collection of points whose orbits are bounded under the Picard iteration (also called function iteration) by f. The boundary of the filled Julia set is the Julia set J_f (see also Remarks 1 and 2 below). The complement of Julia set is Fatou set F_f (see Devaney [6] and Roth [21]).

*Department of Computer Applications, Shri Ramswaroop Memorial College of Engg. & Management, U.P. Technical University, Lucknow 226018. Email: mani_kr_2000@yahoo.com

** Department of Computer Science & Engg., Galgotia's College of Engineering & Technology, Ghaziabad, Mailing address: 21, Govind Nagar, Rishikesh 249201, Email: vedicmri@sancharnet.in

Recently Rani and Kumar [20] (see also [19]) have introduced superior iterations in the study of Julia set for complex-valued polynomials. In this paper, we continue their work and study filled superior Julia sets on a more general setting for quadratics, cubics and biquadratics.

PRELIMINARIES

In all that follows, X will denote the set of complex numbers.
Let $f: X \to X$. For a point $x_0 \in X$, construct a sequence $\{x_n\}$ in X as follows:
$x_n = \beta_n f(x_{n-1}) + (1-\beta_n) x_{n-1}$, $n = 1, 2, ...n$
where $0 \leq \beta_n \leq 1$ and, $\{\beta_n\}$ is convergent to β away from 0.

The sequence $\{x_n\}$ constructed above and denoted by $GSO\ (f, x_0, \beta_n)$ will be called the general superior orbit for $f: X \to X$ with the initial choice x_0. The general superior orbit $GSO\ (f, x_0, \beta_n)$ with $\beta_n = \beta$, denoted by $SO\ (f, x_0, \beta_n)$ is called the superior orbit [20].

Remark 1. The GSO (f, x_0, β_n) is the Picard orbit when $\beta_n = 1$, $n = 1, 2, ...$

The sequence $\{x_n\}$, essentially due to W.R. Mann [14], was introduced in nonlinear analysis, However, the same is generally called the superior orbit in discrete dynamics (see, for instance, [19], [20]).

In all that follows $Q_{m,c}(z)$ will stand for the complex-valued polynomial $z^m + c$ for some value of c, where $m > 1$ is a positive integer.

By definition, the filled general superior Julia set is the set of points whose orbits are bounded under the general superior iteration of the function $Q_{m,c}(z)$, where $\{\beta_n\}$ converges to a non-zero number between 0 and 1. The general superior Julia (briefly denoted by *GSJ*) set for $Q_{m,c}(z)$ is the boundary of the filled general superior Julia set. The filled general suprior Julia set for the function $Q_{m,c}(z)$ will be denoted by *FGSJ*.

The general superior escape criterion for the function $Q_{m,c}(z) = z^m + c$ is given by $\max \{|c|, (2/\beta_n)^{1/m-1}\}$, where $0 < \beta_n \leq 1$, $n = 1, 2, ..., m > 1$ and a positive integer, and c is a complex parameter (see [20]). Since $\{\beta_n\}$ converges to β, the escape criterion will remain the same as discussed for the filled superior Julia set in [20]. For the sake of completeness, we list the following escape criterions.

(i) Escape criterion for $Q_{2,c}(z) = z^2 + c$ is max $\{|c|, (2/\beta)\}$;
(ii) Escape criterion for $Q_{3,c}(z) = z^3 + c$ is max $\{|c|, (2/\beta)^{1/2}\}$;
(iii) Escape criterion for $Q_{4,c}(z) = z^4 + c$ is max $\{|c|, (2/\beta)^{1/3}\}$.

Remark 2. The filled general superior Julia set becomes the filled Julia set when we take $\beta_n = 1$.

GENERATION OF *FGSJ* SET

For generating the filled general superior Julia set for a polynomial, we have developed an algorithm based on the discussion in [19]. The algorithm can be converted into a program using *C++* or any other language. We generate some striking pictures of *FGSJ* sets for quadrtic, cubic and biquadratic polynomials. We also calculate the number of pixels in the figures, width and height of figures for the sake of comparison. In all the figures that follow, black color will show the *FGSJ* set and the other colours show those points, which escape after certain number of iterations.

GENERATION OF *FGSJ* SET FOR QUADRATICS

We begin with an outline of filled general superior Julia sets for the quadratics $Q_{2,c}(z) = z^2 + c$, where the sequence of parametre $\{\beta_n\}$ converges to β, $0 < \beta < 1$.

Fig. 1 corresponds to $(\beta_n, c) = (0.8 + 1/\log(10^n), -1.354)$ with $n = 2$. The combination of $(\beta_n, c) = (0.8 + 1/\log(10^n), -1.354)$ with $n = 25$ produced Fig. 2. Fig 3 is generated for the same value of c with $\beta_n = (0.8 + 1/\log(10^n)$ and $n = 100$. Fig. 4 is produced with $(\beta_n, c) = (0.8, -1.354)$. Hence the sequence $\{\beta_n\}$ converges to 0.8. We observe that Fig. 3 appears to be much closer to Fig. 4 than Figs. 2 and 1. Fig. 5 is drawn for $(\beta_n, c) = (0.4 + 1/\log(10^n), -0.5 + 1.6i)$ with $n = 2$. The choice $(\beta_n, c) = (0.4 + 1/\log(10^n), -0.5 + 1.6i)$ with $n = 25$ generates Fig.6, while $(\beta_n, c) = (0.4 + 1/\log(10^n), -0.5 + 1.6i)$ with $n = 100$ gives Fig. 7. Fig. 8 is generated with the choice $(\beta_n, c) = (0.4, -0.5 + 1.6i)$ which appears to be closest with Fig. 7 amongst Fig. 5, 6 and 7. Similarly we generate various figures for different values of β_n and c. The basic purpose is to notice the emerging pattern through convergence of the objects.

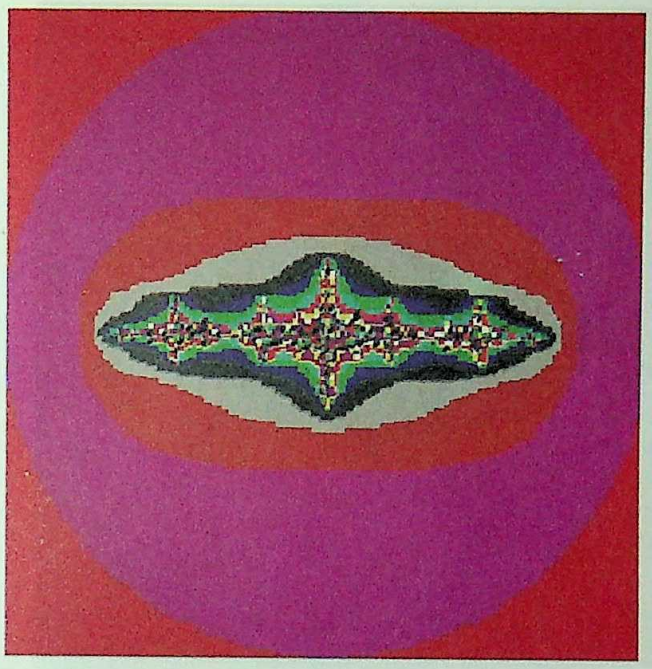

Fig. 1. Filled general superior Julia set for $z^2 + c$ with $(\beta_n, c) = (0.8 + 1/log(10^n), -1.354)$ and $n = 2$

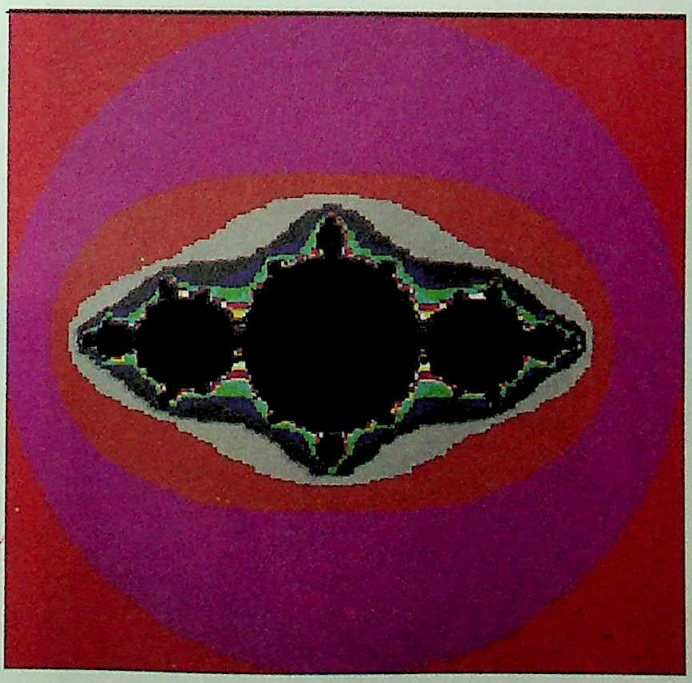

Fig. 2. Filled general superior Julia set for $z^2 + c$ with $(\beta_n, c) = (0.8 + 1/log(10^n), -1.354)$ and $n = 25$

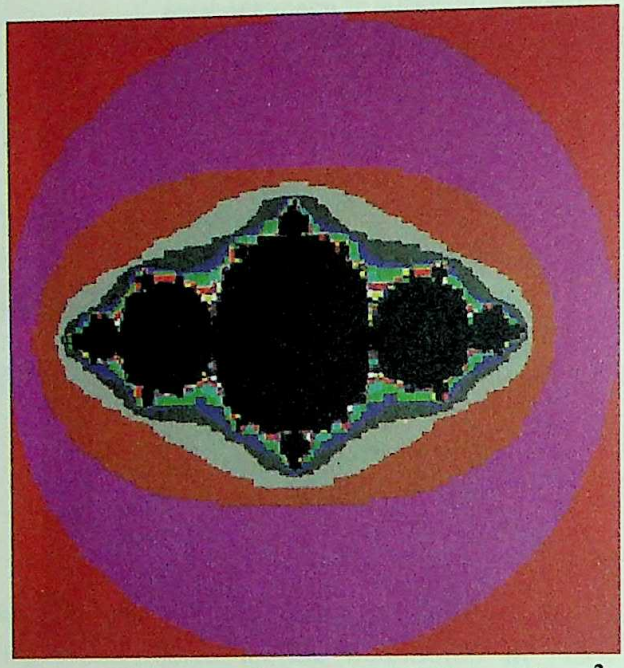

Fig. 3. Filled general superior Julia set for $z^2 + c$ with $(\beta_n, c) = (0.8 + 1/log(10^n), -1.354)$ and $n = 100$

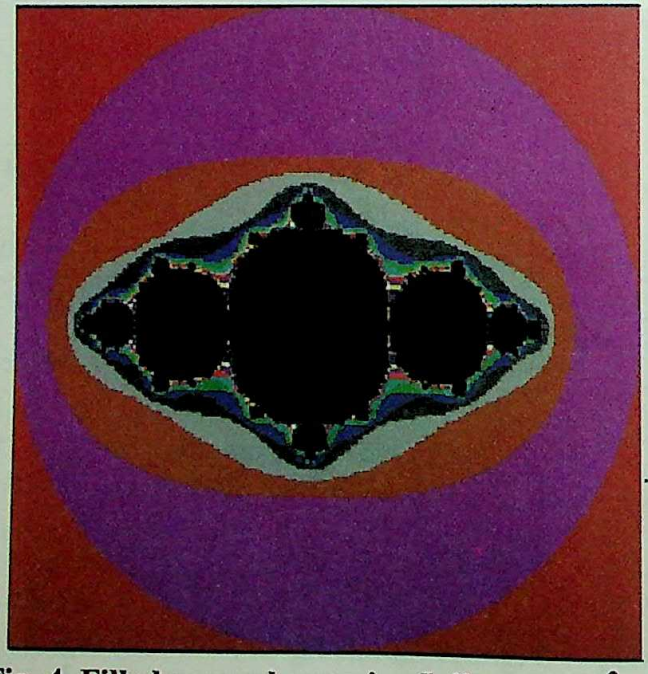

Fig. 4. Filled general superior Julia set for $z^2 + c$ with $(\beta_n, c) = (0.8, -1.354)$

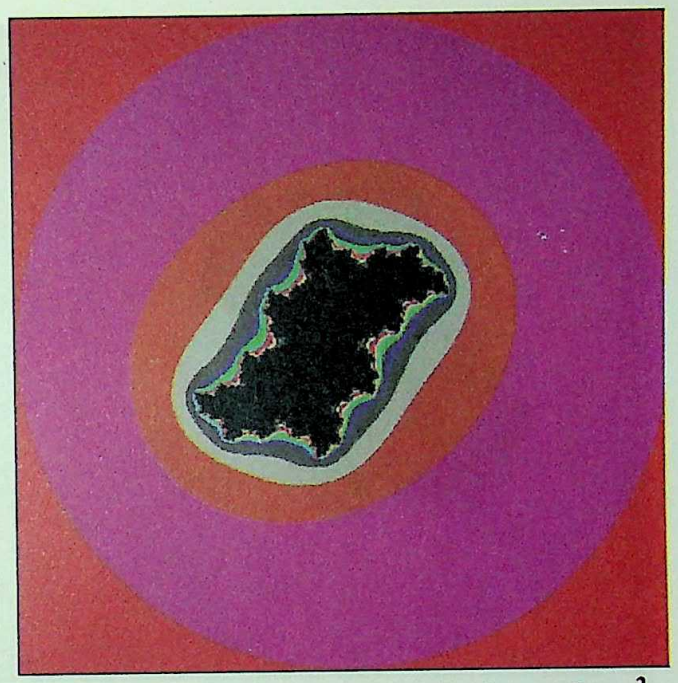

Fig. 5. Filled general superior Julia set for $z^2 + c$ with $(\beta_n, c) = (0.4 + 1/log(10^n), -0.5 + 1.6i)$ and $n = 2$

Fig. 6. Filled general superior Julia set for $z^2 + c$ with $(\beta_n, c) = (0.4 + 1/log(10^n), -0.5 + 1.6i)$ and $n = 25$

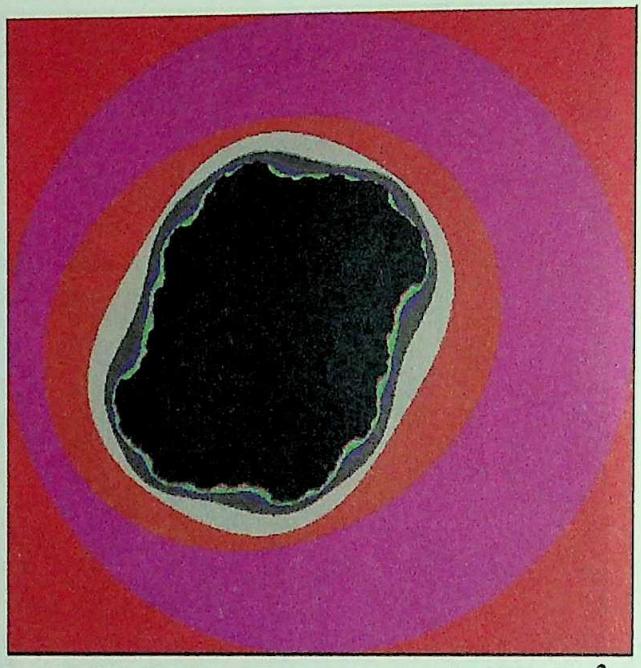

Fig. 7. Filled general superior Julia set for $z^2 + c$ with $(\beta_n, c) = (0.4 + 1/log(10^n), -0.5 + 1.6i)$ and $n = 100$

Fig. 8. Filled general superior Julia set for $z^2 + c$ with $(\beta_n, c) = (0.4, -0.5 + 1.6i)$

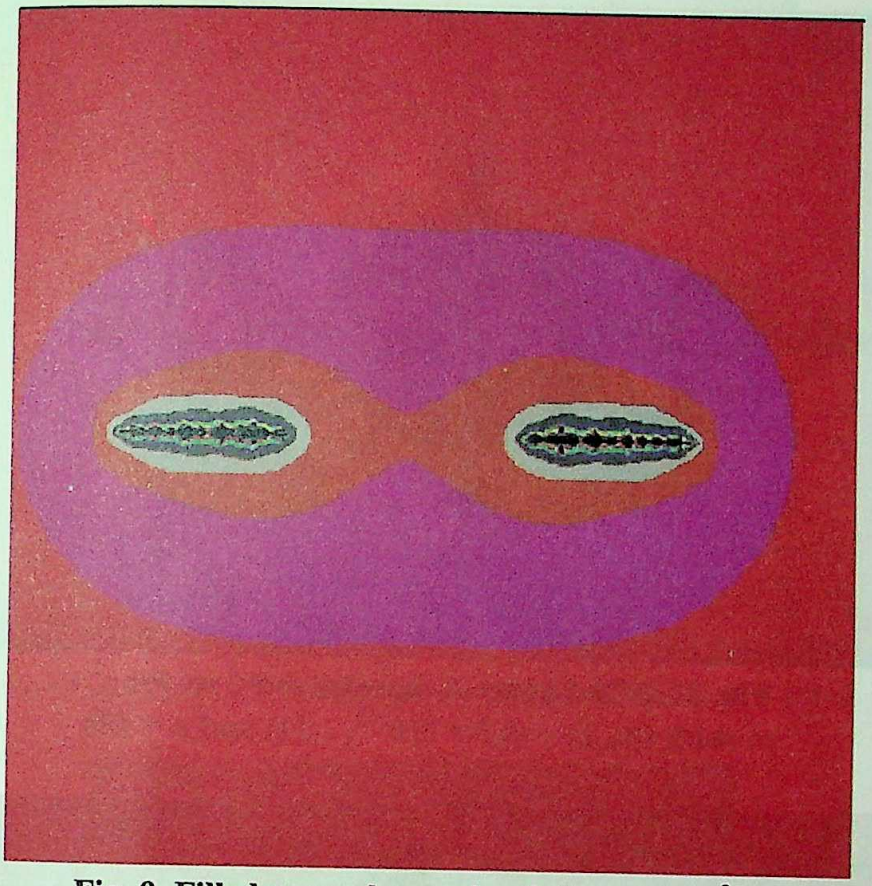

Fig. 9. Filled general superior Julia set for $z^2 + c$ with $(\beta_n, c) = (0.3 + 1/2^{n+1}, -13)$ and $n = 2$

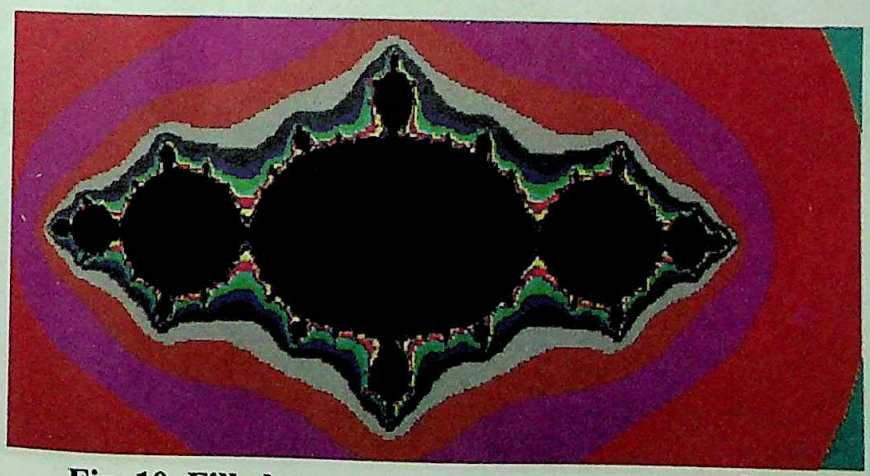

Fig. 10. Filled general superior Julia set for $z^2 + c$ with $(\beta_n, c) = (0.3 + 1/2^{n+1}, -13)$ and $n = 25$

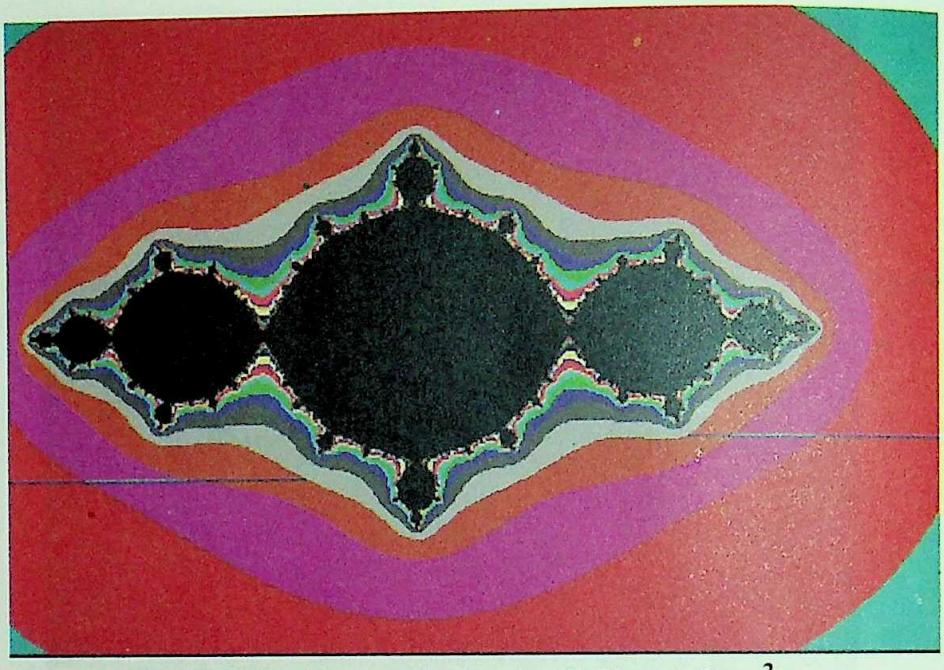

Fig. 11. Filled general superior Julia set for $z^2 + c$ with $(\beta_n, c) = (0.3 + 1/2^{n+1}, -13)$ and $n = 100$

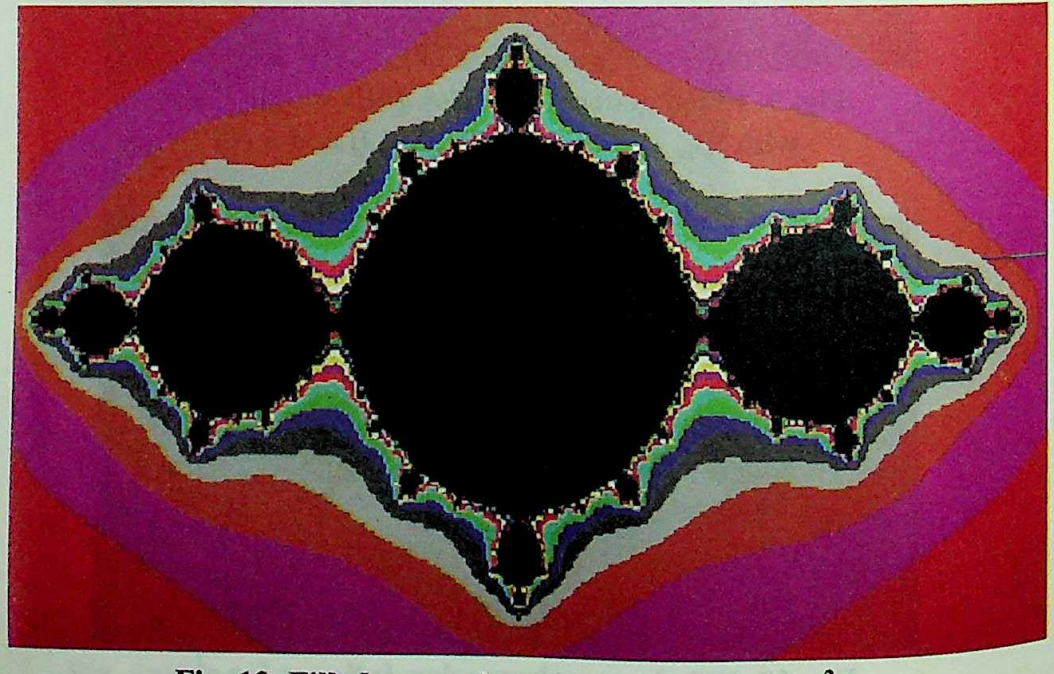

Fig. 12. Filled general superior Julia set for $z^2 + c$ with $(\beta_n, c) = (0.3 + 1/2^{n+1}, -13)$

Fig. 13. Filled general superior Julia set for $z^3 + az + b$ with $(\beta_n, a, b) = (0.5 + 1/log(10^n), -1.97 + 1.88i, 0)$ and $n = 2$

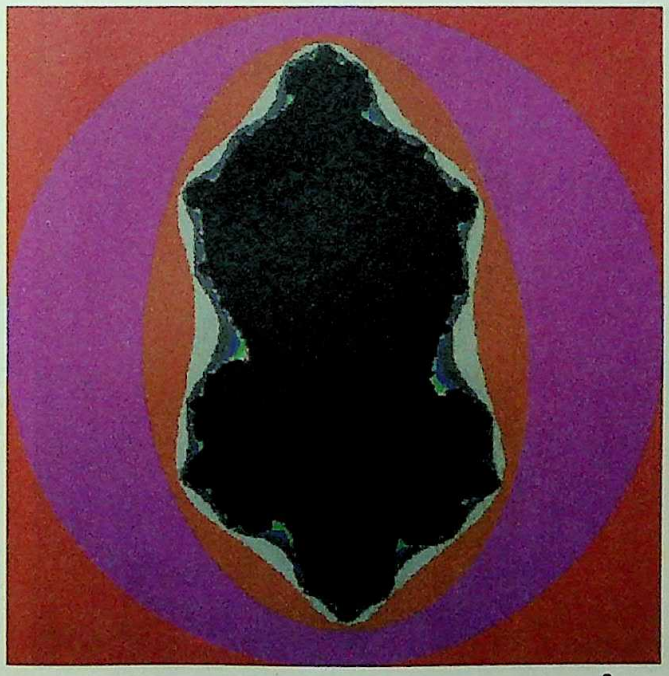

Fig. 14. Filled general superior Julia set for $z^3 + az + b$ with $(\beta_n, a, b) = (0.5 + 1/log(10^n), -1.97 + 1.88i, 0)$ and $n = 25$

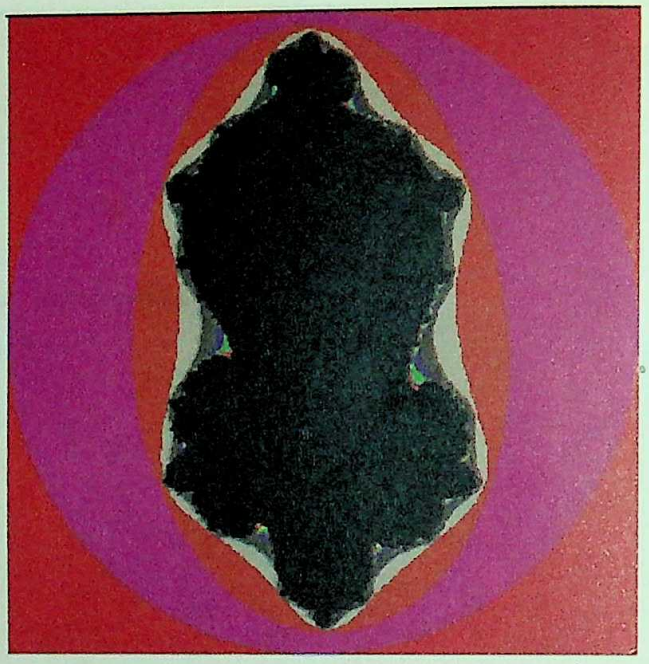

Fig. 15. Filled general superior Julia set for $z^3 + az + b$ with $(\beta_n, a, b) = (0.5 + 1/log(10^n), -1.97 + 1.88i, 0)$ and $n = 100$

Fig. 16. Filled general superior Julia set for $z^3 + az + b$ with $(\beta_n, a, b) = (0.5, -1.97 + 1.88i, 0)$

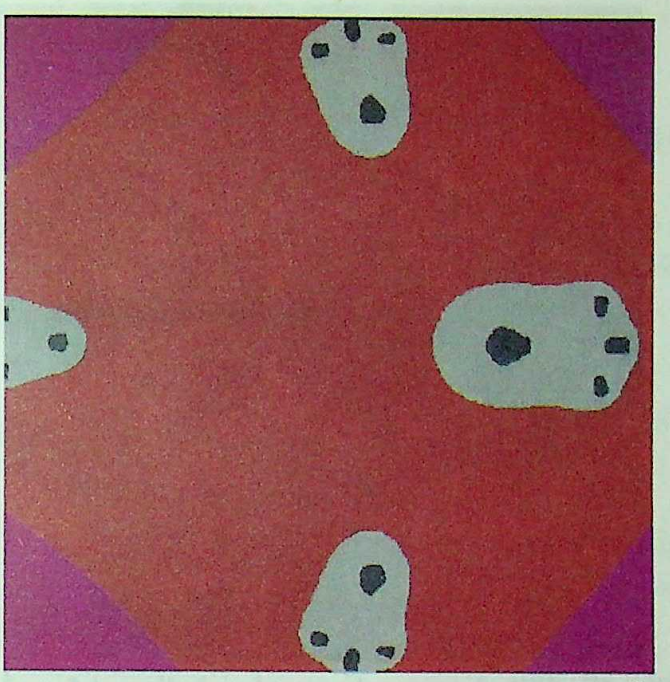

Fig. 17. Filled general superior Julia set for $z^4 + c$ with $(\beta_n, c) = (0.1 + 1/log(10^n), -9.8)$ and $n = 2$

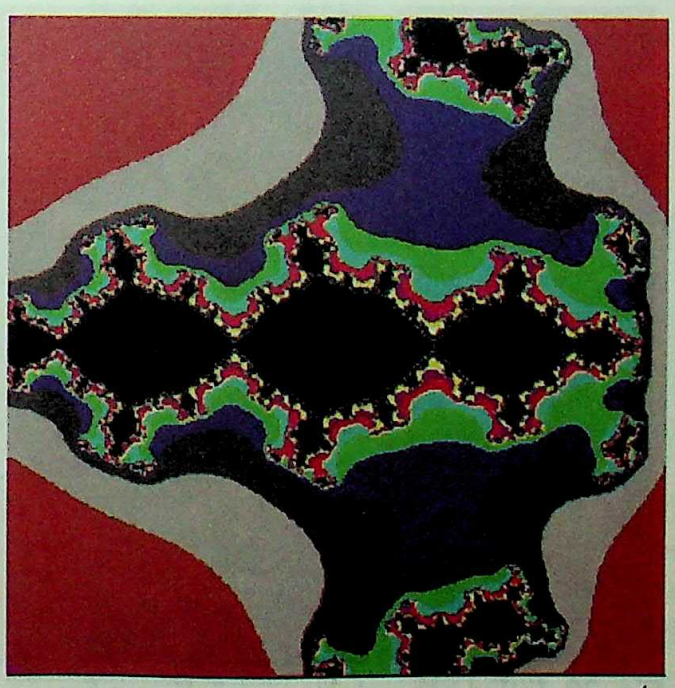

Fig. 18. Filled general superior Julia set for $z^4 + c$ with $(\beta_n, c) = (0.1 + 1/log(10^n), -9.8)$ and $n = 25$

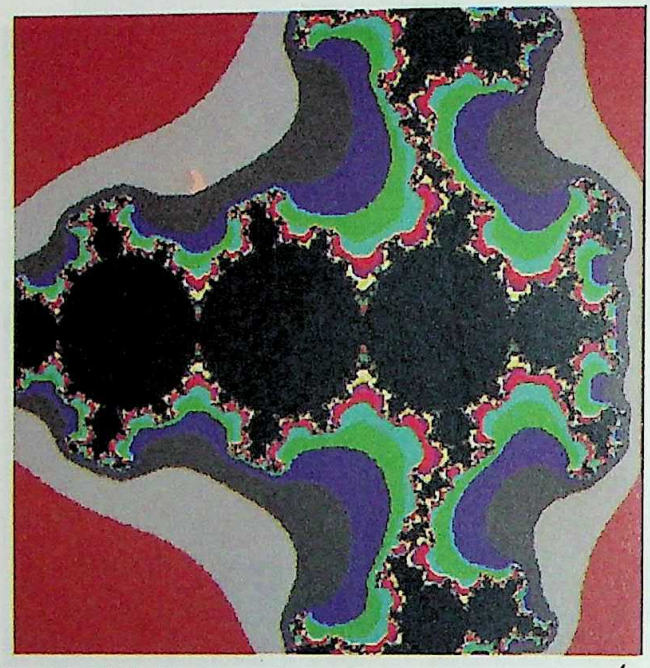

Fig. 19. Filled general superior Julia set for $z^4 + c$ with $(\beta_n, c) = (0.1 + 1/log(10^n), -9.8)$ and $n = 100$

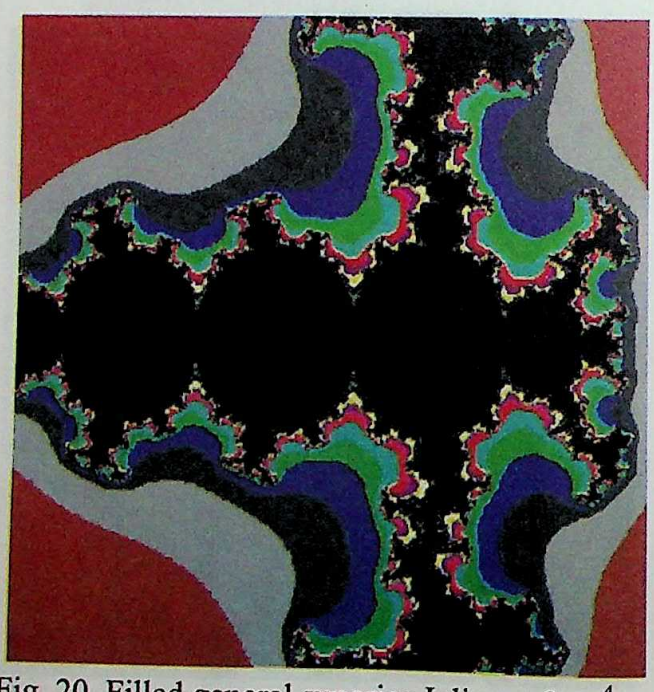

Fig. 20. Filled general superior Julia set for $z^4 + c$ with $(\beta_n, c) = (0.1, -9.8)$

GENERATION OF *FGSJ* SET FOR CUBICS

In this subsection we generate filled general superior Julia sets for the cubic $Q_{a,b}(z) = z^3 + az + b$, where a, b are coplex parameters. The superior escape criterion for the cubic $Q_{a,b}(z)$ is given by max $\{|b|, (|a| + 2/\beta)^{1/2}\}$ (see [19]).

Fig. 13 corresponds to $(\beta_n, a, b) = (0.5 + (1/log(10^n), -1.97 + 1.88i, 0)$ with $n = 2$. The combination of $(\beta_n, a, b) = (0.5 + 1/\log(10^n), -1.97 + 1.88i, 0)$ with $n = 25$ produces Fig. 14. Fig. 15 is generated for the same values of a, b with $\beta_n = 0.1 + 1/log(10^n)$ and $n = 100$. Fig. 16 is generated for $(\beta_n, a, b) = (0.5, -1.97 + 1.88i, 0)$. Here the sequence $\{\beta_n\}$ converges to 0.5. Notice that the figures drawn are comparatively closer to Fig. 16 as the number of iterations increase. Notice that of Figures 15 and 16 appear almost similar.

GENERATION OF *FGSJ* SET FOR BIQUADRATICS

In this subsection, we generate filled general superior Julia sets for $Q_{4, c}(z) = z^4 + c$.

Fig. 17 corresponds to $(\beta_n, c) = (0.1 + 1/log(10^n), -9.8)$ with $n = 2$. The choice $(\beta_n, c) = (0.1 + 1/log(10^n), -9.8)$ with $n = 25$ gives Fig. 18, which is entirely different from Fig. 1. Fig. 17 is produced for the same value of c with $(\beta_n, c) = 0.1 + 1/log(10^n)$ with $n = 100$. Fig. 20 is drawn for $(\beta_n, c) = (0.1, -9.8)$. According to our choice, the sequence $\{\beta_n\}$ converges to 0.1.

COMPARISON

We offer a comparison between filled superior Julia sets (with β constant) and filled general superior Julia sets ($\beta_n \rightarrow \beta$) for the quadratics. For the sake of comparison, the parameters we choose, are the number of pixels in figures, height and width. Height and width of the figures are calculated as difference between maximum and minimum y co-ordinate and x coordinate respectively. It is natural to anticipate that height and width depend on the value of the parameters β as it changes the size of the grid under consideration.

Tables for comparison

In our tables, we fix up c and choose β_n, and the computation is made for some related values of $\beta'_n s$. The final entry in each table corresponds to the corresponding value of β, where $\beta n \to \beta$ as n gets large.

Table 1 : (c = -1.354)

β_n	n	no. of pixels	height (unit)	width (unit)
$0.8 + 1/log(10^n)$	2	10060	1.23	3.45
$0.8 + 1/log(10^n)$	25	18954	2.01	3.68
$0.8 + 1/log(10^n)$	100	20036	2.08	3.73
.		.	.	.
.		.	.	.
.		.	.	.
0.8		20400	2.11	3.76

Table 2: (c = -0.5 + 1.6i)

β_n	n	no. of pixels	height (unit)	width (unit)
$0.4 + 1/log(10^n)$	2	2151	2.45	3.29
$0.4 + 1/log(10^n)$	25	10083	3.00	3.59
$0.4 + 1/log(10^n)$	100	11167	3.07	3.65
.		.	.	.
.		.	.	.
.		.	.	.
0.4		11444	3.10	3.69

Table 3: (c = 0.4 - 2.9i)

β_n	n	no. of pixels	height (unit)	width (unit)
$0.5 + 1/log(10^n)$	2	4340	4.22	4.04
$0.5+ 1/log(10^n)$	25	17459	5.42	4.90
$0.5+ 1/log(10^n)$	100	19469	5.62	5.07
.		.	.	.
.		.	.	.
.		.	.	.
0.5		20170	5.67	5.17

Analogous tables may be prepared for cubics and biquadratics for different values of β_n and c.

CONCLUDING REMARKS

Observe that the figure generated with $\beta_n = 0.8 + 1/\log(10^n)$ and $n = 100$ (cf. Fig. 3) is much closer or almost similar in shape with Fig. 4 in comparison to those generated with $\beta_n = 0.8 + 1/\log(10^n)$ & $n = 25$ and $\beta_n = 0.8 + 1/\log(10^n)$ & $n = 2$. We further observe that the number of pixels inside Fig. 3 and the corresponding height and width obtained, are much closer to the filled superior Julia set ($\beta_n = 0.8$) than other values of β_n taken in Figs. 1 and 2 (see Table 1).

On the basis of the above experimental analysis, we find that when β_n tends to β, the figure corresponding to β_n becomes closer to the figure involving β. This merely means that the figure involving β_n is closer to the figure involving β when $\beta_n \to \beta$ as n becomes large. This kind of phenomenon has been found for cubics and biquadratics as well, although we have not depicted analogous tables of observations for the reason of space. Finally, the authors conjecture similar patterns for other functions.

ACKNOWLEDGEMENT

The authors thank Professor S. L. Singh for his valuable suggestions to improve upon the original typescript.

REFERENCES

[1] M.F. Barnsley: Fractal modelling of real world images, in The Science of Fractal Images (Edited by H. O. Peitgen and D. Saupe), Springer-Verlag, New York, 1988.

[2] A.F. Beardon: Iteration of Rational Functions, Complex Analytic Dynamical Systems, Springer-Verlag, New York, 1991.

[3] Egbert J.W. Boers: Using L-systems as graph grammar: G2Lsystems, Technical Report 95-30, Dep. of Computer Science, Leiden University, Leiden, Netherlands, Oct 1995.

[4] B. Branner and J. Hubbard: The iteration of cubic polynomials, Part I, Acta. Math. 66 (1988), 143-206.

[5] R.L. Devaney: A First Course in Chaotic Dynamical Systems: Theory and Experiment, Addison-Wesley, 1992.

[6] R.L. Devaney: Cantor and Sierpinski, Julia and Fatou: Complex Topology Meets Complex Dynamics, Notices Amer. Math. Soc. 51(2004), 9-15.

[7] R.L. Devaney, K. Josi_c and Y. Shapiro: Singular perturbations of quadratic maps, Intl. J. Bifurcacations and Chaos, 14 (2004), 161- 169.

[8] R.L. Devaney and D.M. Look: Buried Sierpinski curve Julia sets, Discrete and Continuous Dynamic System 13 (2005), 1035- 1046.

[9] R.L. Devaney and D.M. Look: Criterion for Sierpinski curve Julia set for rational maps, To appear in Topology proceedings.

[10] R.L. Devaney, D.M. Look and D. Uminsky: The escape trichotomy for singularly perturbed rational maps, Indiana University Mathematics Journal 54 (2005), 1621-1634.

[11] R.L. Devaney, M.M. Rocha and S. Siegmund: Rational maps with generalized Sierpinski gasket Julia sets, Preprint, 2003.

[12] G. Julia: M´emoire Sur L'iteration des Fonctions Rationnelles, Journal de Math. Pure et Appl. 8 (1918) 47-245.

[13] Jun Kigami: Analysis on Fractals, Cambridge Univ. Press, Cambridge, 2001.

[14] W.R. Mann: Mean value methods in iteration, Proc. Amer. Math. Soc. 4 (1953), 506-510.

[15] V.A. Norton: Julia sets in quaternions, Computers and Graphics 13, 2 (1989) 267-278.

[16] H.O. Peitgen, H. Jürgens and D. Saupe: The Language of Fractals, Scientific American (August 1990), 40-47.

[17] H.O. Peitgen, H. Jürgens and D. Saupe: Chaos and Fractals, Springer-Verlag, New York, Inc., 1992.

[18] C.A. Pickover: Fractal Horizons: The Future Use of Fractals, New York: St. Martin's Press, 1996.

[19] M. Rani: Iterative procedure in Fractals and Chaos, Ph. D. Thesis, Gurukala Kangri University, Haridwar, 2002.

[20] M. Rani and V. Kumar: Superior Julia set, J. Korean Soc. Math. Educ. Ser. D 8(4) (2004), 261-277.

[21] A. Kimberly: Roth, Julia Sets that are Full of Holes, preprint, 2002.

Journal of Natural & Physical Sciences, Vol. 19 (2) (2005) 156-161

BPR IN ORDER CONFIRMATION PROCESS

Ashok Kumar* and Priti Sharma*

(Received 20.04.2006 Revised 05.09.2006)

ABSTRACT

Re-engineering is the most important technique today. As the world economy is moving towards a boardless market, efforts to implement re-engineering has become more and more important. The radical organizational changes have become the need of today. Business process Re-engineering (BPR) is a new management tool which stands for innovative manager for organizing work for the satisfaction of customers. In the business process, customer is the main source. In this paper an attempt is made to use BPR in order confirmation process for an industry. A model has been formed for it. The effects of this techniques have also been discussed on order confirmation process for an industry. We have also studied the characteristcs and furute prospects of BPR in industry.

Keywords and phrases: Business process Re-engineering (BPR), Characteristics of BPR.

INTRODUCTION

Re-engineering is most important technique in today's world. The use of Business process Re-engineering for effecting radical organizational change has become more prevalent in recent years.

In a simple way BPR (Business process Re-engineering) means starting all over. i.e. abandoning along established procedures and looking a fresh at the work required to create company's product or services and deliver value to the customer.

The term BPR was first defined by Micheal Hammer in this seminal article Re-engineering work: don't automate; obliterate which appeared in 1990 in Harvard Business Review (Hammer - 1990).

According to Hammer and Champy, Business Process Re-engineering is "THE FUNDAMENTAL RETHINKING AND RADICAL REDESIGN OF BUSINESS PROCESS TO ACHIEVE DRAMATIC IMPROVEMENT IN CRITICAL AND CONTEMPORARY MEASURES OF PERFORMANCE SUCH AS COST, QUALITY, SERVICE AND SPEED."

The term business process RE-engineering was coined in Massachuetts institute of Technology's (MIT) research program management in the 1990s, which ran from 1984 to 1989. During this project, researchers observed, as illustrated by Davenport, "successful

* Department of Computer Science and Applications, Kurukshetra University, Kurukshetra.

organizations were using IT systems in ways quite different from the traditional automation of clerical and operational tasks", (Davenport, 1993).

Due to introduction of the concept of BPR in the industry process of product cost and delivery the reconciliation is minimized. This paper sketches a new process for order confirmation process to help support business process re-engineering.

ORDER CONFIRMATION PROCESS

Before Re-engineering

In order confirmation process a customer wants a product, its cost, and also the date of delivery. Firstly, we shall duscuss a process before Re-engineering.

In re-engineering process, work is sequenced in terms of what needs to follow. For example, in a manufacturing company, it requires five steps to go from receipt of customer order to the delivery of the product.

- The first step is to determine customer requirements and then enquire marketing executive.
- Second step is to enquire the product cost and its delivery date with comments.
- The third step is to convey to an engineering executive and computing a scheduling system.
- The fourth is to receive a process plan and its feasibility date.
- The fifth is for accounting executive and then delivering a product.

Every manufacturing organization has to perform the above steps.

After Re-engineering :

Re-engineering process is minimized.

- The first step is to know the customer's requirements and also to take the details from a customer service representative.
- The second and third steps, mentioned above, are combined and treated as second step. In this step, enquiry about product with comments is taken from engineering executive and a chart for computing scheduling system is prepared.
- The fourth and fifth steps. mentioned above, are combined and act as third step. In this step, the process have been completed and the product is delivered to the customer.

Order Confirmation Process
Before Re-engineering

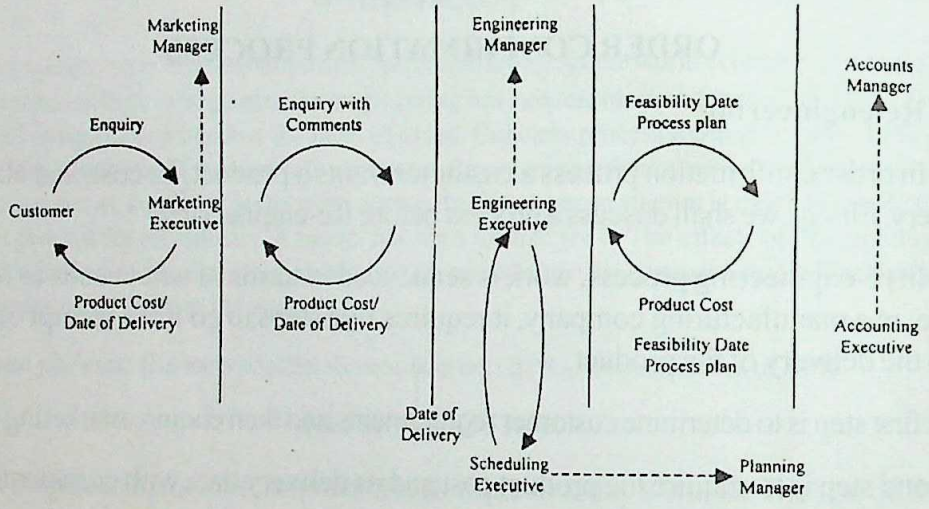

Order Confirmation Process
After Re-engineering

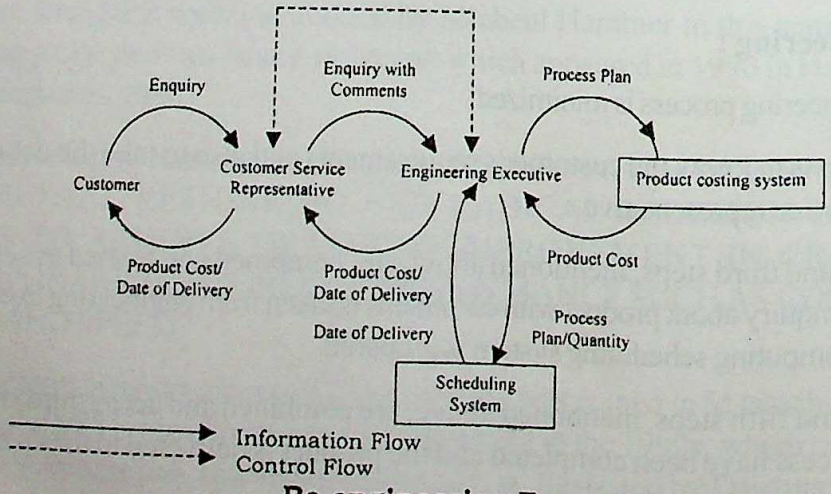

Re-engineering Example :

Effects of BPR on order Confirmation Process:

Here we hall study the effects of BPR on order confirmation process.

- It reduced the company's time to fulfill a customer's order.
- Another form of non-value adding work that re-engineered process minimize is reconciliation. They do it by cutting back the number of external contact points that a process has.
- By reducing the enhances, consistent data requiring reconciliation, will be received.

CHARACTERISTICS OF RE-ENGINEERING BUSINESS PROCESS

In the service industry the use of IT to automate existing business process had often fallen short of the expected results (Hackett; 1990; Hammer, 1990).

A Typical Business process shows following characteristics:

Breadth and Depth

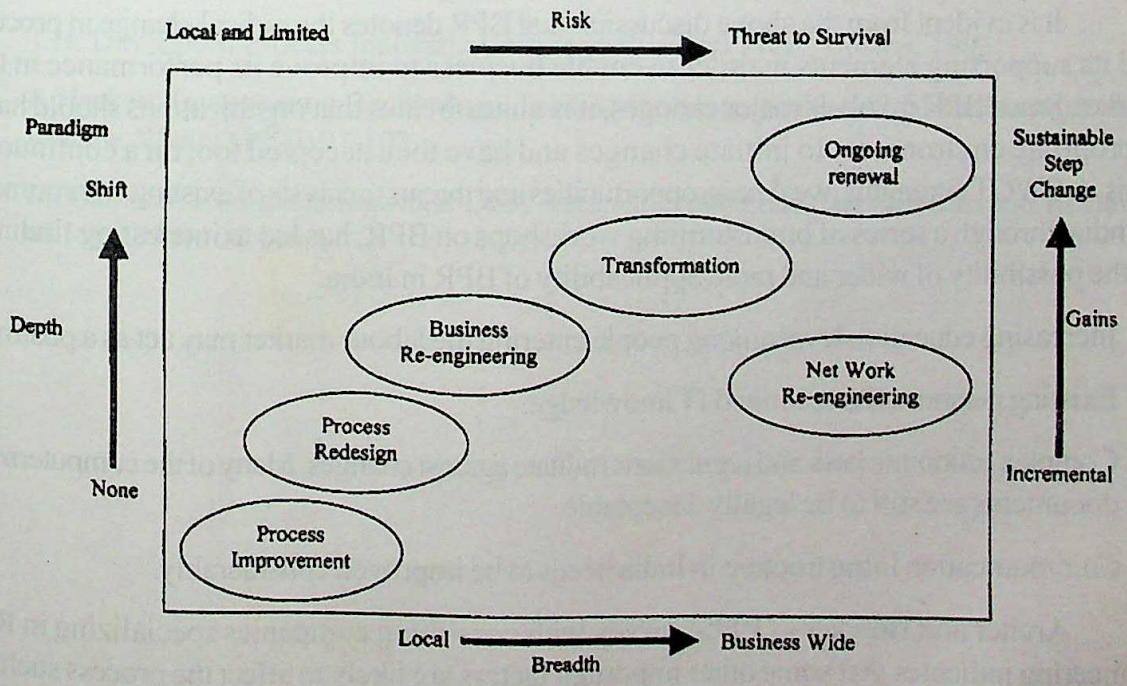

Breadth-Depthwise Levels of BPR

Breadth refers to scope. A process can be narrowly defined as a single activity within a single function or (i.e. work process) or broadly defined as the entire business system for the business unit (i.e. total business process) Depth of a process refers to linkage with other aspects of an organization like roles and responsibilities, measurements and incentives, organizational structure, information technology, shared values and skills.

- **Several Jobs are combined into one**
- **The steps in the process are performed in a natural order**
- **Process have multiple versions**
- **Workers make Decisions**
- **Work is performed where it makes the most sense**
- **Checks and controls are reduced**
- **Case manager provides a single point of contract**
- **Hybrid Centralized/Decentralized operations are prevalent**

FUTURE SCOPE OF BRP

It is evident from the above discussion that BPR denotes the radical change in process and its supporting elements in order to enable business to improve its performance in the market. Since BPR involves major changes, it is quite obvious that organizations should have appropriate environment to initiate changes and have then accepted too, on a continuous basis. A SWOT (strengths, weakness, opportunities and threats) analysis of existing environment in India, through a series of brainstorming workshops on BPR, has led to interesting findings on the possibility of wider and rapid applicability of BPR in India.

- Increasing education level among people entering the labour market may act as a positive.
- Existing personnel have limited IT knowledge.
- Complex economic laws and regulations militate against changes. Many of the computerized documents are still to be legally acceptable.
- Communication infrastructure in India needs to be improved considerably.

Archer and Bowker's (1995) survey with consulting companies specializing in Re-engineering indicates that some other important factors are likely to affect the process such as lack of communications of a clear vision of the project, lack of staff participation and ownership, lack of involvement from staff at different levels, future to install a re-engineering culture, and

lack of project organization and planning.

Given all the above factors, the future prospects of BPR are very bright.

CONCLUSION

Business process re-engineering is a new management tool. It will result in dramatic improvements in higher profit, greater customer satisfaction, lower expenses, consolidated activities, and increased productivity. Change has become both pervasive and persistent.

An organization strives to keep up with ever-changing demands and market needs. An order confirmation process help to minimize the reconciliation. Combining smaller process sub-tasks and sub-activities into larger, integrating units and packages Indian organizations could initiate appropriate steps.

ACKNOWLEDGEMENTS

The author are thankful to the learned referee for his wise suggestions.

REFRENCES

[1] R. Archer and P. Bowker: BPR Consulting : An Evaluation of the methods Employed, Business Process Re-Engineering & Management, 1 (2) (1995) 28-46.

[2] T.H. Davenport: Process Innovation, Harvard Business Press, Boston, 1993.

[3] P. Hackett: Investment in Technology. The Service Sector Sinkhole?, Sloan Management Review, Winter (1990) 97-103.

[4] M. Hammer: Reengineering work: Don't Automatic, obliterate, Harvard Business Review, 68 (4) (1990) 104-114.

NUMERICAL SOLUTION OF STEADY FLOW OF A VISCOELASTIC FLUID BETWEEN COAXIAL ROTATING POROUS DISCS WITH UNIFORM SUCTION OR INJECTION FOR HIGH REYNOLDS NUMBERS

Anjali Pant* and Manoj Kumar**

(Received 31.07.2006)

ABSTRACT

A numerical study of steady flow of an incompressible fluid between two rotating discs with uniform suction or injection is presented. By using a proper transformation of variables the partial differential equations of the flow are transformed to ordinary differential equations. Solutions are obtained for high values of Reynolds numbers using iterative scheme.

Keywords and phrases: Visco-elastic fluid, Reynolds number.

AMS subject classification : Primary : 76U05, Secondary : 76M20

INTRODUCTION

A number of approaches have been tried to investigate the rheological behavior of the so-called Viscoelastic fluids i.e. fluids which when sheared demonstrate elastic properties besides viscous ones. The computation of flow of Viscoelastic fluids has been on the leading edge of research in non-Newtonian fluid mechanics during last few years. The constitutive equation of even the simplest of Viscoelastic fluids, such as the second order fluids are such that the momentum equations give rise to boundary value problems in which the order of the system of differential equations is greater than the number of boundary conditions.

Flows induced by rotating discs are of considerable fundamental interest because of the richness of the physical phenomenon they encompass. These flows have technical applications in many areas, such as rotating machinery, lubrication, viscometry and crystal growth process. The flow of a classical viscous fluid between a pair of infinite coaxial rotating discs has been studied by several authors due to its both theoretical and practical interest and that the problem offers the possibility on exact solution to the Navier-Stokes equations. Karman [8] was the first to give the solution to the Navier-Stokes equation for the flow of a Newtonian fluid in the vicinity of an infinitely large rotating discs. Batchelor [2] and Stewartson [13] to calculate the steady flow between two coaxial infinite rotating discs.

*Department of Mathematics, Govt. Polytechnic, Nainital.
**Department of Mathematics, G.B. Pant Univ. of Ag. & Tech. Pantnagar.

The flow of a viscous incompressible fluid contained between two parallel discs which at time t are spaced a distance $h(1-\alpha t)^{1/2}$ apart has been studied by Hamza and MacDonald (1984), where h and α^{-1} denote a representative length and time. The flow near a rotating porous disc with uniform suction or injection has been studies by Attia [1]. Ibrahim [7] considered the steady flow of viscoelastic fluid between the two rotating discs for small value of Reynolds numbers by using regular perturbation method. The present study is based on the iterative method for high value of Reynolds numbers.

EQUATION OF MOTION

There are numerous models of viscoelastic fluids suggested in the literature. The computation of flow of these fluids is at best a complicated affair, therefore, in order to get some insight into their flow behaviour, and it is preferable to restrict to a model with minimum number of parameters in the constitutive equations. Accordingly we have chosen the model of Walters' B' fluid for our steady as it involves only non-Newtonian parameters. The equation of motion for a Walter's B' fluid

$$\rho\left(\frac{\partial \underline{V}}{\partial} + (\underline{V}\bullet\underline{\nabla})\underline{V}\right) = -\underline{\nabla}P + \eta_o\nabla^2\underline{V} - K_0\left[\frac{\partial}{\partial}\nabla^2\underline{V} + 2(\underline{V}\bullet\underline{\nabla})\nabla^2\underline{V} - \nabla^2(\underline{V}\bullet\underline{\nabla})\underline{V}\right] \tag{1}$$

$$(\underline{V}\bullet\underline{\nabla}) = 0$$

where V being the velocity.

Let us consider the steady flow of a Walters B' fluid filling the space between two infinite parallel discs. Choosing a cylindrical polar coordinate system (r, θ, z), let the lower in the plane $z = 0$ rotate with a constant angular velocity $S\Omega$ while the upper disc at $z = d$ has angular velocity Ω Let u, v and w represent the velocity compoment in the increasing the direction of r, θ and z respectively.

The boundary conditions of the problem are :

$$u = 0,\ V = rs\Omega, \qquad w = w_0 \text{ at } z = 0$$

$$u = 0,\ V = r\Omega, \qquad w = w_0 \text{ at } z = d \tag{2}$$

METHOD OF SOLUTION

In order to solve the problem under consideration, the equations (1) - (2) have to be writen in cylindrical polar coordinate system. This leads to a set of three non-linear partial differential equations. In order to obtain their solution, we first transform them to a set of ordinary non-linear differential equaions by making use of the transformation Bhatnagar [3] as :

$$u = -\frac{1}{2} r\Omega H', \quad V = r\Omega H(\eta), \qquad w = d\Omega H(\eta) \tag{3}$$

where $\eta = z/d$ and prime denotes differentiation with respect to η.

Substituting equation (3) into the equation of motion (2), the equation in the θ–direction transforms to:

$$G'' + RH'G - RHG' + KR(2H'G - HG'''-H''G') = 0 \tag{4}$$

while the elimination of the pressure between the equations in the radial direction r and axial direction z leads to:

$$H'''' + KR(H'H''''+2H''H''' + 8\, G'G'' - HH'''') - RHH''' - 4GG' = 0 \tag{5}$$

where

1. $R = \dfrac{\Omega d^2}{V}$ (Reynolds number) and

2. $K = \dfrac{K_o}{\rho d^2}$ (viscoelastic parameter)

The transformations (3) applied to the boundary conditions (2) which give

$$G(0) = S, \qquad G(1) = 1,$$
$$H(0) = a, \qquad H(1) = a,$$
$$H'(0) = 0, \qquad H'(1) = 0. \tag{6}$$

In the above equations, S is the ratio of the angular velocities of the two discs, respectively located at $z = 0$ (angular velocity $S\Omega$) and $z = d$ (angular velocity Ω) and "a" is the suction or injection parameter, which takes negative values for suction and positive values for injection, where

$$a = \frac{w_0}{\Omega d}. \tag{7}$$

Equations (4) and (5) are highly non-linear in G and H, which are functions of η. The first, second, third, fourth and fifth order derivatives can be given by finite-difference approximation and the resulting equations are solved by Newton-Raphson iterative method.

RESULTS AND DISCUSSION

The variation of function $H(\eta)$ which characterizes the axial component of velocity, with distance η have been depicted by Figures 1,2 and 3 choosing the fluid to be visco-elastic.

The calculations show the magnitude of H is maximum for $S = 0$ as shown Fig 1. Also $H > 0$ near the lower disc means that the flow is directed towards the axis of the two discs and the corresponding value of H must be positive, i.e. the fluid flow towards the upper disc.

Fig. 2 represents the variation of H with R for $S = -1$. It has been observed and concluded that at $S = -1$, $a = 0$ and $K = 0.1$ the axial velocity decreases first with an increase in Reynolds number and start increasing thereafter middle of the discs at $\eta = 0.5$. The condition of recirculation occurs at the lower disc at point $\eta=0$ το $\eta=0.5$ and attains maximum at $\eta=0.25$ and from point $\eta=0.5$ to $\eta=1.0$ the set of values shows the normal study of circulation and attains maximum at $\eta=0.75$.

The Fig. 3 depicts the variation of axial velocity H with K for a Newtonian fluid and a non-Newtonian fluid. For Newtonian fluid the behavior of fluid between the two discs is normal but for non-Newtonian fluids the condition of recirculation takes place at the upper discs. With the increase in visco-elastic parameter the behavior of the fluid becomes turbulent near the upper discs.

The variation of function $G(\eta)$, which characterize the transverse component of velocity, has been depicted from the figures 4,5,6.

Fig. 4 shows that the transverse velocity decreases with the increase in Reynolds number. From Fig. 5 it has been observed and concluded that for fixed value of $S = 0$, $R = 0.2$ and $a = 1$ transverse velocity G varies with visco - elastic parameter K and larger recirculation takes place at the lower disc as compared to the upper disc.

Fig. 6 shows that for injection condition the flow of the visco-elastic the two discs are normal. But as soon as the suction prameter increases the behavior of the fluid between the two discs becomes turbulent and larger recirculation takes place near the upper disc as compared to the lower disc.

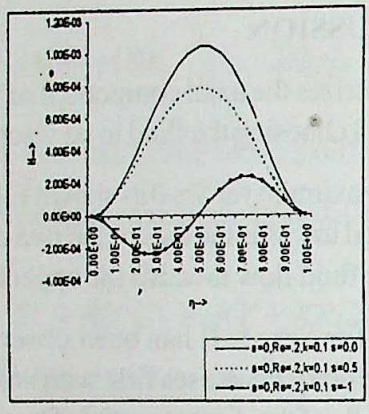

Fig. 1

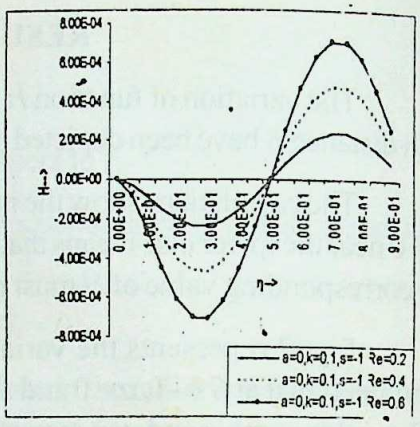

Fig. 2

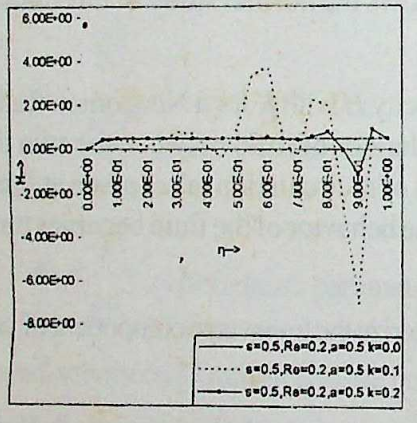

Fig. 3

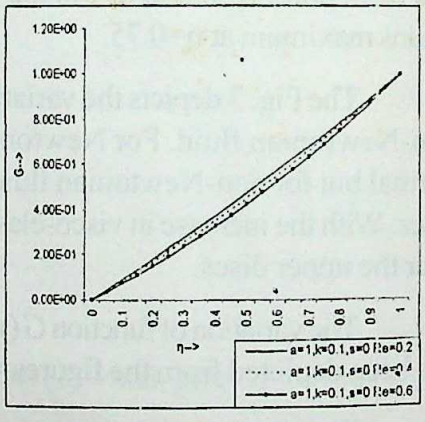

Fig. 4

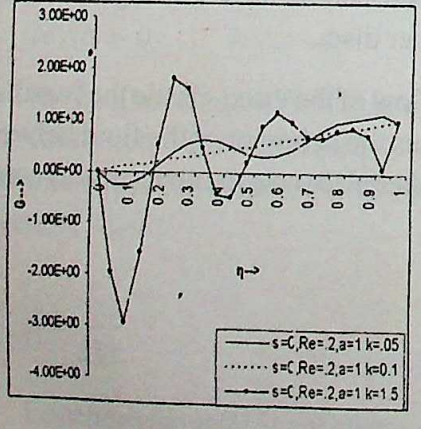

Fig. 5

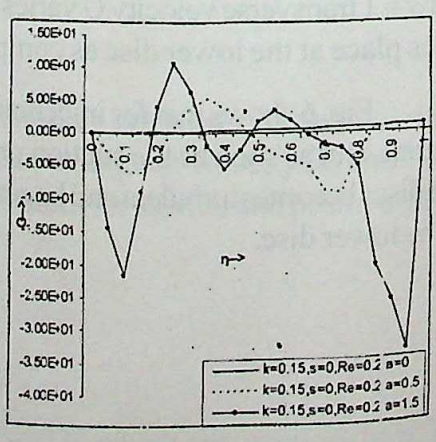

Fig. 6

REFRENCES

[1] H.A. Attia: Unsteady MHD flow near a rotating porous disks with uniform suction or injection, J. Fluid Mech. 23 (1998)283.

[2] G.K. Batchelor: Note on a class of solutions of the Navier-Stokes equations representing steady rotationally-symmetric flow, Quart. J.Mech. Appl. Math. 4 (1951) 29.

[3] P.L. Bhatnagar: Flow between torsionally oscillating infinite plane disks in the presence of uniform magnetic field normal to the disks, Ind. J. Maths. 3 (1961) 27.

[4] R.K. Bhatnagar: Non-Newtonian fluid flow between coaxial rotating disks: effect of an externally applied magnetic field, Mat. Aplic. Com.2 (1962).

[5] T.M. El-Mistikawy, H.A. Attia, and A.A. Megahed: The rotating disks flow in the presence of weak magnetic field, Proc. 4th Conf. on Theoretical and Applied Mechanics, Cairo, Egypt, 5-7 November. 69 (1991).

[6] E.A. Hamza and D.A. MacDonald: A similar flow between two rotating disks, Quart. J. Mech. Appl. Math. (1984).

[7] F.N. Ibrahim, A.H. Essawy, M.R. Hedar, and T.O. Gad: Flow of a viscoelastic fluid between coaxial rotating porous disks with uniform suction and injection, Bull. Cal. Math. Soc. 96 (2004) 241.

[8] T.V. Karman: Laminare and Turbulente Reibung, Zeit. Angew Math. Mech. 1 (1921) 233.

[9] M. Kubicek, M. Holodniok and V. Hlavacek: Calculation of flow between two rotating coaxial disks by differentiation with respect to an actual parameter, Comp. Fluids, 4 (1976) 59.

[10] N.D. Nguyen, J.P. Ribault and P. Florent: Multiple solution for flow between coaxial disks, J. Fluid Mech. 68 (1975) 309.

[11] S.M. Roberts. and J.S. Shipman: Computation of the flow between rotating and stationary disk, J. Fluid Mech. 73 (1975) 35.

[12] A.C. Srivastava: Flow of a non-Newtonian fluid at small Reynolds number between two infinite discs, Quart. J. Mech. App. Math. 2 (1961) 353.

[13] K. Stewartson: On the flow between two rotating coaxial disks, Proc. Camb. Phil. Soc. 49 (1953) 333.

RADIATION DUE TO STEPPED LEADER IN HIGHER FREQUENCY RANGE DURING GROUND DISCHARGE

P P Pathak* and Shelly Rajput*

(Received 13.01.2006, Revised 10.09.2006)

The stepped leader and return strokes are well known to emit the radiation in LF to VHF and microwave region[1]. In present paper the magnitude of electromagnetic radiation (in HF - VHF range) during stepped leader have been calculated and compared with the observed radiation. For this electric field radiated by corona steamers is integrated theoretically throughout the stepped leader channel.

Key Words: Stepped leader, Corona steamer, Electromagnetic radiation.

INTRODUCTION

The usual cloud-to-ground lightning discharge is initiated by a negatively charged stepped leader that propagated from cloud to ground. During cloud discharge and ground discharge, electromagnetic radiations are emitted which cover a wide frequency range from ELF to ultra violet region. Even before the actual discharge some, radiation is observed due to pre-discharge breakdown known as preliminary breakdown, though the radiation is only in VHF range. In VLF range the observed power is accounted for the radiation from a variable dipole constituted by the propagating lightning channel and its image in the finitely conducting ground [4,5]. In ELF region the emitted power is accounted by lateral corona current flowing towards return stroke channel within the stepped leader sheath[6,7]. The UHF power attributed to the Bremsstrahlung radiation arising due to acceleration or deceleration of electrons in their orbit around the ions or that of atom due to coulomb field interaction in the lightning channel [8,9]. The physical process behind the radiation in the microwave region above UHF are not yet explained., The mechanism applicable in ELF,VLF and UHF regions [4,9] are not applicable or they do not give sufficient radiation in LF to VHF region. The stepped leader and return stroke are known to emit the radiation in LF to VHF and microwave region[1]. Mechanism responsible for this radiation is also not known. To the authors knowledge no work has been done on the mechanism for radiation in this region[12]. In this paper an attempt is made to explain the magnitude of observed radiation in some of these frequency ranges during stepped leader by corona streamer mechanism[1,3].

THEORY

It is known that the cloud-to-ground lightning consists of mainly two types of strokes. It starts with stepped leader i.e. column of partially ionized channel of radius of few meters

*Department of Physics, Gurukula'Kangri University, Haridwar - 249404

propagating from cloud to ground. On reaching near ground this leader triggers return stroke i.e. a fast moving fully ionized thin column of radius of about a centimeter. We assume the stepped leader to consist of a number of positive corona streamers propagating simultaneously. All such streamers give away radiations. Radiation from single streamer is calculated by Pathak[3] and Bhardwaj[1]. Propagation of streamer for time t in z-direction produces a dipole moment (see Ref.1)

$$\vec{M} = \frac{Q_0 v_s^3 t^3}{4} \hat{k} \tag{1}$$

where, v_s is the velocity of corona streamer and Q_0 is the initial charge on the streamer tip or head. The radiated field at a distance r from a dipole is given by

$$\xi = \frac{1}{4\pi\varepsilon_0 c^2 r} \frac{d^2 M}{dt^2} \tag{2}$$

where c is speed of light. Now from Equation (1)

$$\frac{d^2 M}{dt^2} = \frac{3}{2} Q_0 v_s^3 t \tag{3}$$

on substituting equation (3) in equation (2), one gets

$$\xi = \frac{1}{4\pi\varepsilon_0 c^2 r} \frac{3}{2} Q_0 v_s^3 t \tag{4}$$

If number density of corona streamers is n, the expression of electric field at a distance D from foot of the channel due to a disc of thickness dx at height $(H - x)$ of the channel from ground is given by

$$dE = \pi a^2 dx n \xi = \frac{1}{4\pi\varepsilon_0 c^2} \frac{3}{2} \frac{n \pi a^2 v_s^3 t dx}{\sqrt{(H-x)^2 + D^2}} \tag{5}$$

where, a is the radius of leader channel. Electric field due to whole channel is the integral of equation (5) with $dx = v\,dt$, v being the velocity of stepped leader, i.e.

$$E = \frac{1}{4\pi\varepsilon_0 C^2}\ \frac{3}{2}\ n\pi a^2 v_s^3 t Q_0 v \int_0^t \frac{tdt}{\sqrt{(H-x)^2 + D^2}} \qquad (6)$$

$$= E_0 I$$

where,

$$E_0 = \frac{1}{4\pi\varepsilon_0 c^2}\ \frac{3}{2}\ n\pi\ a^2 v_s^3 Q_0 v$$

and $$I = \int_0^t \frac{tdt}{\sqrt{(H-x)^2 + D^2}}$$

On solving the above integral,

$$I = \frac{1}{v^2}\left[\sqrt{(H-vt)^2 + D^2} - \sqrt{H^2 + D^2}\right] - \frac{H}{v^2}\left[\ln\left\{(H-vt) + \sqrt{(H-vt)^2 + D^2}\right\} - \ln(H + \sqrt{H^2 + D^2}\right]$$

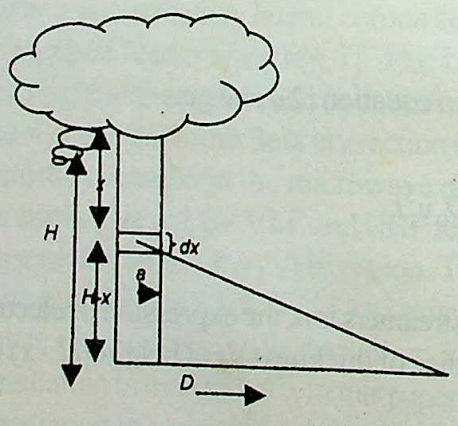

Fig. 1: A drawing defining the factor used in computing the electric field of a stepped leader.

CALCULATION AND RESULTS

We idealize a section of the stepped ieader channel of height H [of range 3 to 4 km] as a straight vertical line above perfectly conducting plane (the earth) as shown in Fig.I. The

radius of leader channel is of few meters in the range 1 to 10m. An average value (i.e. most frequently observed value) of 3 m can be taken for calculations. The stepped leader moves downward in a series of discontinuous luminous steps that range in length from 10 to 200 m [an average value of 50 m can be taken for calculations] and that are separated by pause time of 40 to 100 μsec. Longer pause time are generally followed by longer steps. It was observed that there is mean time of 50 μsec between steps far above the ground. The step luminosity is of the order of 1 μsec or less. A fully developed stepped leader lowers up to 10 or more coulombs negative cloud charge towards ground in tens of milliseconds. Schonland et. al.[10] and Schonland[11] concluded that the propagating velocity v exceeds 5×10^7 m/s. We have calculated the electric field of leader steps for a discharge over 50 km distant, which is denoted by D in above formulation. The velocity of corona streamer is about 5×10^5 m/s (see Ref. 2). The initial charge on the tip of streamer (Q_0), is taken 4.61×10^{-7} C (seeRef.1).

With these values the electric field from stepped leader of 4 km height at a distance of 50 km is calculated. As the observations of Weidman and Krider[13] are in frequency (f) domain, we need to convert our results also in frequency domain. For this an expression of E in time (t) domain is needed. To get such an expression the values of electric field are first plotted with time. While plotting these values the pause time of the steps is added to obtain the real time after start of stepped leader. Though this is not the time of propagation of leader which is simply total length of leader up to that instant divided by velocity. The values of $E(t)$ are fitted to a parabolic curve $A + Bt + ct^2$ and the values of constants A, B and C are evaluated. We found that the value of constant C is zero.

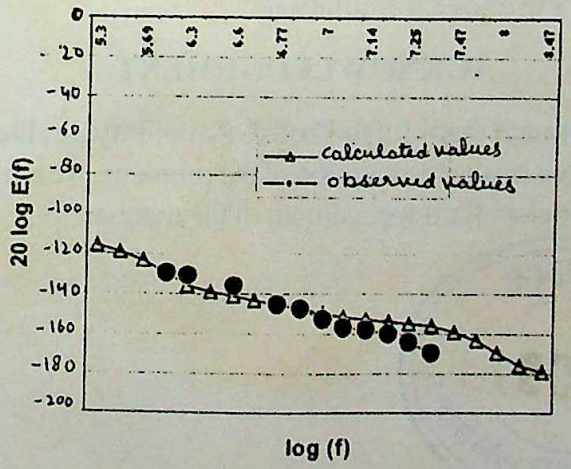

Fig. 2: The graph showing observed values and computed values of electric field radiated during stepped leader at a distance of 50 km.

Then by Fourier transform $E(t)$ is converted to $E(f)$ and 20 log $E(f)$ is evaluated and plotted with log (f). Observed values of Weidman and Krider[13] are also plotted along with calculated values for comparison in Fig.2. Though the observations are available in the range 1-20 MHz, the calculations are made from 200 kHz to 300 MHz just to show the variation of emitted field for wider range.

DISCUSSION

As mentioned above the variation of computed electric field of radiation on the basis of positive corona streamer in higher frequency range from leader channel is shown in Fig. 2 along with the observed field of Weidman and Krider[13]. It is clear that there is very good agreement between them .The fields were calculated for discharge during stepped leader at a distance of 50 km as the observations of Weidman and Krider[13] are at same distance. The height of leader channel is taken as 4 km. As the cloud-to-ground lightning is more frequent in convective clouds, which generally occur at the heights of many kilometers varying from 2 km to 10 km or more. The average value 4 km is taken for the calculations. The average value of radius of leader channel is taken as 3 m. We further considered that the stepped leader moves downward in a series of discontinuous luminous steps of average value of length 50 m. There is a mean pause time of 50 μsec between steps. The stepped leader consist of a number of positive corona streamer propagating simultaneously, all these corona streamers gives radiations. For number of corona streamer Bhardwaj[1] has concluded values in the range of 30 - 35 m^{-3} during preliminary breakdown. But during stepped leader it is expected to be much more. A value of 50 is taken for these calculations .The average value of the velocity of corona streamer taken for calculations is 5×10^5 m/s (Ref. 1). The velocity of stepped leader is 5×10^7 m/s (Ref. 1) , denoted by v in above formulation.

ACKNOWLEDGEMENT

Authors are very much thankful to Prof. J. Rai of Physics Department IIT Roorkee For many fruitful discussions on the formulation of the problem. We are also thankful to learned referee for his valuable criticism for improvement of the manuscript.